Consistency and observational consequences of loop quantum cosmology

Linda Linsefors

Communauté
UNIVERSITÉ Grenoble Alpes

THÈSE

Pour obtenir le grade de

DOCTEUR DE L'UNIVERSIT ´E DE GRENOBLE

Spécialité : **Physique théorique**

Arrêté ministériel : 25 mai 2016

Présentée par

Linda Linsefors

Thèse dirigée par **Aurélien Barrau**

préparée au sein
Laboratoire de Physique Subatomique et de Cosmologie

et de **l'école doctorale de physique**

Consistency and observational consequences of Loop Quantum Cosmology

Thèse soutenue publiquement le 22 Juin 2016,
devant le jury composé de :

Richard Taillet
Professeur, Université Savoie Mont-Blanc, Président du jury
Philippe Brax
Directeur de recherches, CEA, Rapporteur
Alejandro Perez
Professeur, Université Aix-Marseille, Rapporteur
Aurélien Barrau
Professeur, Université Grenoble-Alpes, Directeur de thèse

Contents

Acknowledgements

Most of all, I want to thank my supervisor Aurélien Barrau. Firstly because Aurélien offered me the position that made this work possible, but even more than that, because Aurélien is the kindest person I know. He has put up with my not-so-tactful ways of saying things during our many physics discussions. In addition to that he has also acted as my translator, helped me navigate though all sorts of French bureaucracy, and taught me not to take all of the rules too seriously.

Lots of thanks to Thomas Cailleteau, my predecessor of a sort. Thomas left our little group in Grenoble only weeks after I arrived. But during this short time he introduced me to the basis of LQC and most of the deformed algebra approach. Later we did some nice work together.

Also thanks to the rest of my collaborators Boris Bolliet, Julien Grain, Jakub Mielczarek and Susanne Schander. You have all taught me different things. When Boris fist arrived at the lab, he challenged me on everything, this was both taxing and stimulating for me. I remember Julien explaining the quantum origin of cosmic perturbation when he was visiting. At the end of my stay in Grenoble Jakub was giving classes to the rest of our group, which I really enjoyed. Getting lectures are such a luxury as a PhD student, and I am sorry that I missed the end of if.

Thanks to everyone in Choresace, the contact improvisation group in Grenoble. Some of my best moments during this time have been in the dance with you. In the dance we all speak the same language. Extra thanks to my friend Myriam, for hugs and comfort in hard times, for hugs and smiles in good times.

Thanks to Lunar who has twice given me a home in Grenoble. First by introducing me to his friend's collocation when they had a spot open, and again, sometime later, inviting me to live at his collocation.

Thanks to David and Riia because you were there for me, on the other side of Internet, when I was newly arrived in a new city full of strangers. Extra thanks to Riia for giving me courage over the phone just before my first conference talk, and for proofreading this manuscript.

Thanks Laurent for a brief time of climbing, hiking and dancing. You are missed.

Thanks Egil for convincing me that I can do other things than theoretical physics research, and for proving this by teaching me computer programming. I don't yet know if I will stay in research or not. But thanks to you I get to choose.

Thanks to both Mats and Hjalmar who both, at different occasions, took me in when I needed to get away and take a break from France.

Lots of thanks to Markus, my fantastic boyfriend. During the time I have been writing this manuscript Markus has been taking care of me. Research is all fun and play, but writing is hard work. I could not have done this alone.

Introduction

Trying to reconcile quantum mechanics and general relativity is probably one of the greatest challenge for physics. Since the first articles of Einstein this question has been identified as an important challenge for theoretical physics. There are many reasons for a quantum gravity theory to be necessary. Even more important than unification, the best reason might be consistency. We have very good reasons to believe that the center of black holes and the big bang are both highly quantum and deeply relativistic. It therefore seems quite inevitable to have a theory where both aspects are taken into account. Other paths can be considered, like emergent gravity, but they are not yet very well developed.

Building a quantum theory of gravity is very difficult for many reasons. Some are technical. For example, gravity is perturbatively non-renormalizable. To make predictions with the theory, one would need to measure infinitely many parameters. Some are more conceptual. For example, time is an external parameter in quantum mechanics although, in a sense, it just does not exist in general relativity (or at least is somehow equivalent to space).

There are however several attempts to quantize gravity. The most popular one is string theory. This is obviously an interesting path. If successful this might provide a "theory of everything" (which does not mean the end of physics). But it relies on heavy hypotheses (supersymmetry, extra-dimensions) that are still lacking any experimental support. In addition, the phenomenology of string theory is not well defined and it is hard to make clear predictions for observables.

An interesting other approach is asymptotic safety. The most important ingredient is the existence of a nontrivial fixed point of the renormalization group flow which controls the behavior of the coupling constants in the ultraviolet regime and make physical quantities free of divergences.

Causal dynamical triangulation is a model that does not assume any pre-existing dimensional space, but rather attempts to show how the spacetime fabric evolves. Although there seems to exist a dimensional reduction around the Planck scale, the theory leads to a four dimension spacetime at large scales.

In this thesis we focus on a specific approach called loop quantum gravity (LQG). Loop quantum gravity is a non-perturbative and background invariant quantization of general relativity. It gathers a growing community all over the world. The theory is, of course, not perfect and still requires a lot of work but it seems to provide a consistent and promising framework. It can be written either in a canonical way – the traditional loop quantum gravity approach – or in a covariant way – the so-called spin-foam formalism.

As for all tentative quantum gravity theories, the link with experiments or observations is the main missing part. This is what this thesis is devoted to. We focus on the cosmological sector

of the theory. Even when the cosmological symmetries are taken into account, it is still very difficult to derive the resulting loop quantum cosmology (LQC) model from the full LQG theory. Quite a lot of non-trivial hypotheses are required. We have considered in this manuscript one of the two main approaches to this problem: *deformed algebra*. This is basically a view in which the emphasis is put on the consistency of the theory. The most robust result of loop quantum cosmology, whatever the specific approach, is the existence of a bounce that replaces the big bang.

We have considered several different aspects of LQC. First, we have shown that the theory not only predicts inflation if the proper matter content is assumed (which is somehow obvious because of the energy scale of the bounce) but also predicts the duration of inflation. Second, we have studied in detail the consequences of anisotropies in a bouncing universe and generalized the previous results on inflation to the Bianchi-I framework. Third, we have studied the theoretical structure of the algebra of constraints and the resulting gauge-invariant equations of motion, in particular when the two main quantum corrections from LQG are taken into account. This leads an interesting possible "change of signature" of spacetime at high energy density. Fourth, we have investigated many possible consequences in the cosmological microwave background (CMB) of the previously studied model, in particular depending on how the "change of signature" is interpreted and implemented. Fifth, we have compared our results with those from the other main approach to loop quantum cosmology, *dressed metric*, and shown the existence of some universal features. Finally, we have built an original model of cyclic universe in this framework with a key role played by the thermodynamical properties of de-Sitter space.

Loop quantum cosmology might be the best way to test LQG ideas. However, it has not succeeded yet in leading to perfectly clear predictions that could be tested in the forthcoming years. Some work is still needed ...

Part I

Quantum Gravity to Loop Quantum Cosmology

Chapter 1

Loop Quantum Gravity

Loop Quantum Gravity (LQG) is an attempt to solve the problem of quantum gravity.

1.1 Why quantum gravity?

There are two major reasons for quantum gravity. The first reason is that the best understanding we have of matter requires quantum physics. Let us consider Einstein's equations:

$$R_{\mu\nu} - \frac{1}{2}Rg_{\mu\nu} + \Lambda g_{\mu\nu} = \frac{8\pi G}{c^4}T_{\mu\nu}. \tag{1.1}$$

Our current best description of the right hand side (matter) is a quantum description. However, it is not mathematically possible for a classical field to have a quantum source, therefore the left hand side (gravity) has to be quantized too. This is mostly a theoretical problem. Due to the weakness of gravity, circumstances have to be very extreme for both gravitational effects and quantum effects to be relevant in the same phenomenon. This leads us to the second main reason for quantum gravity.

General relativity predicts singularities. Singularity theorems prove, under quite general assumptions, that Einstein's equations have singularities both for black holes and for the expanding universe. In the universe we believe that we live in, the two types of singularities, the big bang and the center of black holes, seem to exist. There is also the possibility of a big crunch, which is just like a time-reversed big bang, however, observations seem to indicate otherwise. It should be noticed that if we take Einstein's theory literally there should be many singularities around as there are lot of black holes (if only a dozen are identified within our galaxy, a full number around ten million is a good guess).

Why are singularities a problem? Firstly, we know from history of science that if one gets an infinite result in the calculation, something is probably wrong, *e.g.* classical particles are singularities and the classical calculation of the heat radiation leads to an infinite result. Both these problems were solved by quantum physics. Secondly, geometrical singularities cause problems with information.

Most of the information that reaches the center of a black hole gets smashed by the singularity. Even if the event horizon somehow disappears (*e.g.* trough the process of Hawking evaporation), the information is still irretrievable because it literally does not exist any more. This has to do with the fact that a geodesic that reaches the singularity has no continuation. This information loss seems out of place in a universe where information is otherwise always conserved.

In cosmology, there is the important problem of initial conditions. A good cosmological theory must not only include relevant dynamics, but also the initial condition for the universe, or some probability distribution of initial conditions. This is a problem since there is an infinite amount of information to specify. The big bang singularity, as one might think, does not provide complete initial conditions for the Universe. In fact the singularity makes the problem worse. The singularity does not only *not* provide complete initial conditions for the Universe, but it also make any attempt to define them, ill-defined. It is mathematically impossible to define the initial conditions of the Universe at the moment of the singularity.

To sum up: The main reason for quantum gravity is that, for technical reasons, we believe that if some aspects of physics is quantized, everything has to be quantized. A positive side effect of this is that quantum gravity will probably modify strong gravity effects, and in doing so hopefully remove the singularities of GR. This is a good thing since singularities are usually a sign of error in the theory, and also they mess up information flow.

1.2 What is LQG?

The philosophy of LQG is to take seriously the geometrical nature of GR. The gravitational force is the effect on matter of the curvature of spacetime. The theory of gravity is a theory of dynamical geometry. Therefore LQG is an attempt to quantify geometry.

There are at the moment two major branches of development of LQG: The canonical approach and spin-foams.

1.3 Reformulation of gravity

For later quantization we need a separate time variable. To get this we split space-time into time and space using the Arnowitt-Deser-Misner (ADM) decomposition. In this formulation, the line element is

$$\begin{aligned} ds^2 &= g_{\mu\nu}dx^\mu dx^\nu \\ &= -\left(Ndx^0\right)^2 + q_{ab}\left(N^a dx^0 + dx^a\right)\left(N^b dx^0 + dx^b\right), \end{aligned} \tag{1.2}$$

where N and N^a are called the shift and laps functions, and q_{ab} is the spatial 3 dimensional metric. This leads to the following relations for the metric and inverse metric:

$$g_{\mu\nu} = \begin{bmatrix} -N^2 + N^a N_b & N_b \\ N_a & q_{ab}, \end{bmatrix} \tag{1.3}$$

$$g^{\mu\nu} = \begin{bmatrix} -1/N^2 & N_b/N^2 \\ N_a/N^2 & q^{ab}N^a N^b/N^2, \end{bmatrix} \tag{1.4}$$

A simple interpretation of the shift and laps is the following. Let us consider a constant time slice Σ_{x^0} and pick up a point A_1 on it. Let us then consider the normal at that point. It intersects an other constant-time slice $\Sigma_{x^0+dx^0}$ at A_2. The proper distance is given by $dt = Ndx^0$, which defines the meaning of the laps, N. However the normal vector will take the spatial coordinates x^i on Σ_{x^0} to some new coordinates on $\Sigma_{x^0+dx^0}$. Let A_3 be the point on $\Sigma_{x^0+dx^0}$ with the same coordinates that A_1 on Σ_{x^0}. The vector from A_2 to A_3 is N_i defines the meaning of the shift, N^a.

Further, from the spatial 3D metric, we construct the co-triads.

$$q_{ab}(x) =: \delta_{ij}e^i_a(x)e^j_b(x). \tag{1.5}$$

The triads provide a local internal orthogonal frame, which we denote by indices $i, j, k, \ldots$. However this leads to a local rotational invariance

$$e^i_a(x) \to R^i{}_j(x) e^j_a, \tag{1.6}$$

where $R^i{}_j(x)$ is an arbitrary rotation matrix.

From the triads, we define the densitised triads

$$E^a_i := \sqrt{\det(q)} e^a_i = \sqrt{\det(q)}\, \delta_{ij} q^{ab} e^j_b, \tag{1.7}$$

and the Ashtekar connection

$$A^i_a := \Gamma^i_a + \gamma K^i_a, \tag{1.8}$$

where K^i_a is the extrinsic curvature

$$K_{ab} = \frac{1}{2N} \left(\partial_0 q_{ab} - D_a N_b - D_b N_b \right), \tag{1.9}$$

$$K^i_a = K_{ab} e^b_j \delta^{ij}, \tag{1.10}$$

and Γ^i_a is the spin connection,

$$\Gamma^i_a = \frac{1}{2} \epsilon^{ijk} e^b_k \left(\partial_b e^j_a - \partial_a e^j_b + e^c_j e^l_a \partial_b e^l_c \right), \tag{1.11}$$

γ being the Barbero-Immirzi parameter, which is a free constant in this formulation. The value of γ has no consequence in classical gravity, however it does make a difference in the quantum theory as we shall see.

E^a_i and A^i_a are together called the Ashtekar variables, and they form a canonically conjugate pair:

$$\left\{ A^j_b(x), E^a_i(y) \right\} = \kappa\gamma\, \delta^a_b \delta^j_i \delta(x - y). \tag{1.12}$$

The Einstein-Hilbert action can be re-formulated with those variables and presented in a Hamiltonan formalism. By doing so one can strait-forwardly get the gravitational Hamiltonian:

$$\mathcal{H}_G = \frac{1}{2\kappa} \int dx^3 \left(N\mathcal{C} + N^a C_a \right), \tag{1.13}$$

where the laps N and the shift N^a act as Lagrangian multipliers for the two constraints, the Hamiltonian constraint

$$\mathcal{C} = \frac{E^a_i E^b_j}{\sqrt{|\det E|}} \epsilon^{ij}{}_k \left[F^k_{ab} - (1 + \gamma^2) \epsilon^k{}_{lm} K^l_a K^m_b \right] = 0, \tag{1.14}$$

and the diffeomorphism constraint

$$\mathcal{C}_a = F^i_{ab} E^b_i = 0, \tag{1.15}$$

where F^i_{ab} is the connection field strength

$$F^i_{ab} = \partial_a A^i_b - \partial_b A^i_a + \epsilon^i_{jk} A^j_a A^k_b. \tag{1.16}$$

Note that at this point K^i_a should be seen as functions of A^i_a and E^a_i:

$$K^i_a = \frac{1}{\gamma} \left[A^i_a - \Gamma^i_a(E) \right]. \tag{1.17}$$

However, in introducing the triads, we have introduced an additional gauge, *i.e.* the rotational invariance of the local internal frame. To insure this symmetry, an extra constraint is needed. This is called the Gauss constraint:

$$\mathcal{G}_i = \partial_a E^a_i + \epsilon_{ij}{}^k \Gamma^j_a E^a_k = 0. \tag{1.18}$$

We add the Gauss constraint to the Hamiltonian together with an additional Lagrangian multiplier, λ^i

$$\mathcal{H}_G = \frac{1}{2\kappa} \int dx^3 \left(N\mathcal{C} + N^a \mathcal{C}_a + \lambda^i \mathcal{G}_i \right). \tag{1.19}$$

1.4 Canonical LQG

The canonical formulation of LQG is the traditional way to formulate this theory and it based on the Ashtekar variables just described, E^a_i and A^i_a, and the Hamiltonian Eq. (1.19).

The conjugate pair of variables used in LQG are not Ashtekar variables themselves, but fluxes and holonomies of those variables. This formulation is chosen for two reasons. First, in any field theory one needs to smear the variables to get rid of Dirac functions and the holonomy precisely allows one to do that without introducing a background metric. Second, because this is reminiscent of Wilson loops and this is consistent with the usual way to measure curvature in GR, by circulating a vector along a closed curve. The fluxes are defined as

$$F^f_S = \int_S d^2x \, n_a E^a_i f^i \tag{1.20}$$

where S is any surface, f^i is any function defined on S and n_a is the normal to S. The holonomies are defined as

$$h_l = \mathcal{P} \exp \int_l A^i_a \tau_i dx^a, \tag{1.21}$$

where $\mathcal{P}$ is the path order operator, l is any curve and $\tau_i = \frac{i}{2}\sigma_i$ where σ_i are the Pauli matrices. In the definition of the theory, only closed holonomies are allowed, however it is useful to have the definition above, also include open holonomies.

As explained in [1], the Poisson algebra of holonomies and fluxes is well-defined and one can look for representations in a Hilbert space. Diffeomorphism invariance is also required, which means there must be a unitary action of the diffeomorphism group on the representation by moving edges and surfaces in space. Under this condition, there is a unique representation which defines the kinematical Hilbert space.

The Hilbert space can be constructed in the representation where states are functionals of connections. This can be done by using holonomies as kind of "creation operators" starting with a "ground state" which does not depend on connections. Multiplying by holonomies creates states which do depend on connections but only along the edges entering the process.

The spatial geometry can be derived from fluxes of the densitized triad. Since these are now momenta, they are represented by derivative operators with respect to values of connections on the flux surface. States as constructed above depend on the connection only along edges of graphs such that the flux operator is non-vanishing only if there are intersection points between its surface and the graph in the state it acts on. In addition, the contribution from each intersection point can be seen as analogous to an angular momentum operator. The spectrum depends on the value of the Immirzi parameter. As angular momentum operators do not commute, flux operators do not commute in general.

Two points are worth emphasizing. Firstly, flux operators have discrete spectrums and, secondly, holonomies of connections are well-defined operators. It is, however, not possible to obtain operators for connection components or their integrations directly but only in the exponentiated form. These are direct consequences of the background independent quantization.

1.5 Spin Foams

There is an alternative formulation of LQG called *spin foam*, which is a covariant formulation. Following [2], we might say that the spin-networks Hilbert space is essentially nothing other than the conventional Hilbert space of $SU(2)$ lattice Yang-Mills theory, which admits an interpretation as a description of quantized geometries (this is the "spin-geometry" theorem by Roger Penrose generalizing an earlier theorem by Hermann Minkowski).

The approach tries to make sense of the usual definition of the formal "sum over 4-geometries"

$$Z \sim \int Dg \;\; e^{\frac{i}{\hbar}\int R\sqrt{g}\, d^4x}, \tag{1.22}$$

which is usually very hard to use for any concrete prediction.

In the simpler context of three Euclidean spacetime dimensions, the Ponzano-Regge approach addresses this problem by fixing a triangulation Δ of spacetime, assigning half integers, or spins, j_f to each segment f of Δ and defining a partition function. A similarity has been discovered between a four dimensional version of the Ponzano-Regge amplitude and the amplitude that defines the covariant dynamics of LQG:

$$Z = \sum_{j_f, i_e} \prod_f (2j_f + 1) \prod_v A_v(j_e, i_v), \tag{1.23}$$

where the spins are associated with the faces of a decomposition Δ of spacetime (or "foam"), *i.e.* are $SU(2)$ quantum numbers associated to 3-cells, called intertwiners, v labels the 4-cells and $A_v(j_e, i_v)$ is a simple generalization of the $\{6j\}$ symbol, which involves both $SU(2)$ and $SL(2, C)$. Importantly, in the semiclassical limit, (1.23) approaches (1.22): $A_v(j_e, i_v)$ approaches the exponential of the Regge action, which in turns leads to the action of GR. In this sense, (1.23) is a discretization of the path integral for quantum gravity. In addition, (1.23) is UV finite and IR finite (with a cosmological constant).

The Hilbert space of LQG has a lot in common with the one of lattice QCD. It is basically defined as follows. For each graph Γ, we consider a "graph space"

$$\mathcal{H}_\Gamma = L_2[SU(2)^L / SU(2)^N] \tag{1.24}$$

which looks like the Hilbert space of an $SU(2)$ lattice gauge theory.

Then we define an equivalence relation $\sim$ as follows: two states are equivalent if they can be mapped into each other by the group of the automorphisms of Γ. Let us define

$$\tilde{\mathcal{H}}_\Gamma = \mathcal{H}_\Gamma / \sim . \tag{1.25}$$

The full Hilbert space of quantum gravity is finally obtained by

$$\mathcal{H} = \lim_{\Gamma \to \infty} \tilde{\mathcal{H}}_\Gamma. \tag{1.26}$$

States in $\mathcal{H}_\Gamma$ can be understood as formed by N quanta, with N being the number of nodes of the graph. Each node is of the graph is a quanta of space, just like a particle in QED, that is a quantum of electromagnetic field.

Interpreting $\mathcal{H}$ as describing quanta of space follows from a theorem due to Roger Penrose: each Hilbert space $\mathcal{H}_\Gamma$ has an interpretation as a space of quantum metrics.

The momentum operator on the Hilbert space of a particle $L_2[R]$ is the derivative operator $\vec{p} = -i\nabla = -i\frac{d}{d\vec{x}}$. The equivalent "momentum" operator on $L_2[SU(2)]$ is also a derivative operator. There is one of these for each link, that we call $\vec{L}_l$.

Thanks to gauge invariance, we have

$$C_n = \sum_{l \in n} \vec{L}_l = 0 \tag{1.27}$$

at each node n. One cas write a gauge invariant operator:

$$G_{ll'} = \vec{L}_l \cdot \vec{L}_{l'} \tag{1.28}$$

where $s(l) = s(l') = n$. The diagonal components of $G_{ll'}$ are $A_l^2 = G_{ll}$.

The operator $G_{ll'}$ coincides with Penrose's metric operator. Penrose spin-geometry theorem precisely states that the operator $G_{ll'}$ can be interpreted as defining angles in three dimensional space, at each node. The theorem states that these angles obey the usual relations of angles in three dimensional space. In addition to the volume operator A_l, a volume operator can be defined:

$$V_n = \frac{\sqrt{2}}{3} \sqrt{|\vec{L}_{l_1} \cdot (\vec{L}_{l_2} \times \vec{L}_{l_3})|}; \tag{1.29}$$

(here given in the specific case of a tetrahedron).

The full set of $SU(2)$ invariant operators $G_{ll'}$ do not commute, but the Area and Volume operators A_l and V_n do commute. They form a complete set of commuting observables in $\mathcal{H}_\Gamma$, in the sense of Dirac. The orthonormal basis that diagonalizes these operators is called the *spin-network* basis.

1.6 Testing LQG

We expect to see the effects of quantum gravity when gravity is extremely strong, *i.e.* at extremely strong space time curvature, close to the Planck scale. Though it is possible that there are testable effects at lower curvature, we do not consider these situations here. We know of two situations of extreme gravity, both resulting in singularities according to classical GR, as discussed in Section 1.1. These are the early stages of the universe and in the center of a black hole. We have reason to suspect that classical GR fails here, and quantum gravity effects might be visible.

The goal of Loop Quantum Cosmology (LQC) is to calculate and predict measurable effects of quantum gravity by applying ideas from LQG to the early history of our Universe.

Chapter 2

Homogeneous Loop Quantum Cosmology

From observations, we know that the observable part of the universe is homogeneous on large scales. The universe is therefore well described by perturbation on an homogenous background. This is even more true in the past, since gravity will cause inhomogeneities to grow over time. In cosmology the observables are almost exclusively the perturbations, since these are the the seeds for stars and galaxies, and also the most of the information in the cosmic background radiation. In cosmological phenomenology, perturbations should therefore be the most important to study. However, the dynamics of the perturbations is determined by the evolution of the homogenous background, on which they live. We shall therefore start with modeling a completely homogenous universe.

The Universe also seems extremely flat and isotropic. The relative importance of the curvature of the Universe increases over time during radiation or dust dominated expansion but decreases during exponential expansion *e.g.* during cosmic inflation. It is therefore safe to assume that the Universe had negligible curvature at the end of inflation, however the universe could have had significant curvature before the inflation. The relative importance of the anisotropies of the Universe always decreases faster than anything else during expansion. It is therefore not safe to assume isotropy in the very early Universe.

However, for simplicity, we will nonetheless start with a simple model: a completely flat, isotropic, and homogenous universe. These assumptions will be relaxed later. In this chapter we will limit ourselves to the metric

$$ds^2 = \left(N dx^0\right)^2 + \left[a(x^0)\right]^2 \delta_{ab} dx^a dx^b, \tag{2.1}$$

combined with a homogenous matter content, and try to derive the resulting dynamics based on LQG. We will very closely follow the steps taken in constructing LQG, by first reformulating cosmology in suitable variables and then modify the Hamiltonian to include holonomy corrections.

A comment on notations: we use x^0 for coordinate time, and will later on use t for proper time. We could just choose these to be the same by choosing $N = 1$ to start with. However, we will keep N because it is sometimes convenient to use other time variables. Conformal time $\tau = at$ is probably the most commonly used time variable in the literature. By keeping N general, the relation between different choices of time variables becomes clearer.

2.1 Reformulation

For simplicity, we choose triads so that the internal frame lines up with the coordinates, *i.e.* $e^i_a \propto \delta^i_a$. This is possible since the coordinates are already orthogonal. Thus we have

$$e^i_a(x) = a\delta^i_a, \tag{2.2}$$

$$e^a_i(x) = \frac{1}{a}\delta^a_i \tag{2.3}$$

From Eqs. (1.7) - (1.10) we then find:

$$E^a_i(x) = p\delta^a_i, \tag{2.4}$$

$$A^i_a(x) = c\delta^i_a, \tag{2.5}$$

where

$$|p| = a^2, \tag{2.6}$$

$$c = \gamma\dot{a}. \tag{2.7}$$

Dots correspond to a derivative with respect to cosmic time, t, with $dt = Ndx^0$ and $\dot{a} = \frac{1}{N}\frac{da}{dx^0}$.

p can, in principle, be negative which leads to some technical complications, however this turns out not to be important in the end. Therefore we will assume non-negative p throughout this thesis.

Next, we want to express the gravitational Hamiltonian, Eq. (1.19), as a function of p and c. We first notice that both the diffeomorphism constraint, $\mathcal{C}_a$, and the Gauss constraint, $\mathcal{G}_i$, are identically zero. However since we have assumed homogeneity, the remaining Hamiltonian density is a constant over space, which causes the integral in Eq. (1.19) to diverge when integrating over an infinite volume. Therefore, we have to restrict the integral to a finite volume. This is what we call the *fiducial cell*, Σ, which is a fixed body in coordinate space. Because we have assumed homogeneity, it is not a problem to study only a limited part of space, because everything else will be just the same. However, we have to check that the final dynamics does not depend on the specifics of the fiducial cell since this has been arbitrarily introduced. We use V_0 and V do denote the coordinate and physical volumes of Σ:

$$V_0 = \int_\Sigma d^3x, \tag{2.8}$$

$$V = \int_\Sigma \det(q_{ab})\, d^3x = V_0 a^3 = V_0 p^{3/2}. \tag{2.9}$$

The total gravitational Hamiltonian over this is directly derived from Eq. (1.19) to be

$$\mathcal{H}_G = \frac{1}{2\kappa}\int_\Sigma dx^3 N\mathcal{C} = -\frac{3NV_0}{\kappa\gamma^2}\sqrt{p}\, c^2. \tag{2.10}$$

Here c and p are the canonical conjugate pair with Poisson bracket

$$\{c, p\} = \frac{\kappa\gamma}{3V_0}, \tag{2.11}$$

which is inherited from the Poisson bracket of E^j_i and A^b_j, Eq. (1.12).

We combine this with the matter Hamiltonian

$$\mathcal{H}_m = \int_\Sigma N \det(q_{ab})\rho\, dx^3 = NV\rho = NV_0 p^{3/2}\rho, \tag{2.12}$$

where ρ is the energy density. According to our simplified model, ρ is a constant over space, but can vary in time.

Combining $\mathcal{H}_G$ and $\mathcal{H}_m$, we form the total Hamiltonian:

$$\mathcal{H} = \mathcal{H}_G + \mathcal{H}_m = NV_0 \left(-\frac{3}{\kappa\gamma^2}\sqrt{p}\, c^2 + p^{3/2}\rho \right). \tag{2.13}$$

We can now see that the total Hamiltonian constraint $\mathcal{H} = 0$ is exactly the Friedman equation

$$H^2 = \left(\frac{\dot{a}}{a}\right)^2 = \frac{c^2}{\gamma^2 p} = \frac{\kappa}{3}\rho, \tag{2.14}$$

where the first equality comes from the definition of the Hubble factor, $H := \frac{\dot{a}}{a}$, the second from Eqs. (2.6) - (2.7), and the last one from $\mathcal{H} = 0$.

So far, everything behaves exactly as in classical cosmology. This is because so far, we have only reformulated the theory. In the next step, we will modify it.

2.2 Loop modification

Just as in full LQG, the Hamiltonian needs to be reformulated in terms of fluxes and of holonomies.

Following Eq. (2.4) the flux becomes

$$\begin{aligned} F_S^f &= \int_S d^2x\, n_a E_i^a f^i \\ &= p \int_S d^2x\, n_a f^a, \end{aligned} \tag{2.15}$$

which, given S and f, is just a constant times p. By choosing S and f appropriately we can choose this constant to be one. Therefore we can just use p as it is in the Hamiltonian, with our reformulation or modification.

The holomomies are not so straight-forward because of the exponential function. The simple holonomy one can make is along a straight line l_k in the direction of the k^{th} coordinate.

$$\begin{aligned} h_{l_k} &= \mathcal{P} \exp \int_{l_k} A_a^i \tau_i dx^a \\ &= e^{|l_k| c\, \tau_k} \\ &= \cos\left(\frac{1}{2}|l_k|c\right) + 2\sin\left(\frac{1}{2}|l_k|c\right)\tau_k, \end{aligned} \tag{2.16}$$

where $|l_k|$ is the coordinate length of l_k. The simplest closed holonomy we can make is along a square $\square_{ij}$ with sides that are lined up with two of the coordinate directions, i and j.

$$\begin{aligned} h_{\square_{ij}} &= h_{l_i} h_{l_j} h_{l_i}^{-1} h_{l_j}^{-1} \\ &= \left[\cos\left(\frac{1}{2}|l|c\right) + 2\sin\left(\frac{1}{2}|l|c\right)\tau_i\right]\left[\cos\left(\frac{1}{2}|l|c\right) + 2\sin\left(\frac{1}{2}|l|c\right)\tau_j\right] \\ &\quad \times \left[\cos\left(\frac{1}{2}|l|c\right) - 2\sin\left(\frac{1}{2}|l|c\right)\tau_i\right]\left[\cos\left(\frac{1}{2}|l|c\right) - 2\sin\left(\frac{1}{2}|l|c\right)\tau_j\right] \\ &= \cos\left(\frac{1}{2}|l|c\right)^4 \end{aligned}$$

$$
\begin{aligned}
&+2\cos\left(\frac{1}{2}|l|c\right)^3 \sin\left(\frac{1}{2}|l|c\right)(\tau_i+\tau_j-\tau_i-\tau_j)\\
&+4\cos\left(\frac{1}{2}|l|c\right)^2 \sin\left(\frac{1}{2}|l|c\right)^2 (\tau_i\tau_j-\tau_i\tau_i-\tau_i\tau_j-\tau_j\tau_i-\tau_j\tau_j+\tau_i\tau_j)\\
&+8\cos\left(\frac{1}{2}|l|c\right)\sin\left(\frac{1}{2}|l|c\right)^3 (\tau_j\tau_i\tau_j+\tau_i\tau_i\tau_j-\tau_i\tau_j\tau_j-\tau_i\tau_j\tau_i)\\
&+16\sin\left(\frac{1}{2}|l|c\right)^4 \tau_i\tau_j\tau_i\tau_j\\
=\;& \cos\left(\frac{1}{2}|l|c\right)^4\\
&+4\cos\left(\frac{1}{2}|l|c\right)^2 \sin\left(\frac{1}{2}|l|c\right)^2 \left(\tau_i\tau_j-\tau_j\tau_i+\frac{1}{2}\right)\\
&+4\cos\left(\frac{1}{2}|l|c\right)\sin\left(\frac{1}{2}|l|c\right)^3 (\tau_i-\tau_j)\\
&-\sin\left(\frac{1}{2}|l|c\right)^4\\
=\;& 1-2\sin\left(\frac{1}{2}|l|c\right)^4+\sin\left(|l|c\right)^2(\tau_i\tau_j-\tau_j\tau_i)\\
&+4\cos\left(\frac{1}{2}|l|c\right)\sin\left(\frac{1}{2}|l|c\right)^3 (\tau_i-\tau_j)\,,
\end{aligned}
\tag{2.17}
$$

where l_i and l_j are the sides of the square, and $|l|=|l_i|=|l_j|$ are the coordinate lengths of the sides of the square.

It is natural to write the connection field strength F^k_{ab} in terms of the limit of a closed loop

$$
\begin{aligned}
F^k_{ab} &= -2\lim_{|l|\to 0}\frac{\mathrm{tr}\left[\tau_k\left(h_{\Box_{ab}}-1\right)\right]}{|l|^2} \qquad (2.18)\\
&= \lim_{|l|\to 0}\left[\frac{\sin(|l|c)^2}{|l|^2}\epsilon^k_{ab}+\frac{4}{|l|^2}\cos\left(\frac{1}{2}|l|c\right)\sin\left(\frac{1}{2}|l|c\right)^3\left(\delta^k_i-\delta^k_j\right)\right].
\end{aligned}
$$

However, the second term vanish when combined with the rest of the Hamiltonian, therefore we get effectively

$$
F^k_{ab}=\lim_{|l|\to 0}\frac{\sin(|l|c)^2}{|l|^2}\epsilon^k_{ab}. \tag{2.19}
$$

In LQC the area operator have a minimum non zero value. Therefore, we should not let $|l|$ go to zero but stop at a minimum value $\bar{\mu}$. We should therefore use $\frac{\sin(\bar{\mu}c)^2}{\bar{\mu}^2}\epsilon^k_{ab}$ rather than F^k_{ab} to express curvature in the Hamiltonian. This corresponds to the replacement

$$
c^2\to\frac{\sin(\bar{\mu}c)^2}{\bar{\mu}^2} \tag{2.20}
$$

in Eq. (2.10) and the associated modified Hamiltonian is

$$
\mathcal{H}=-\frac{3NV_0}{\kappa\gamma^2}\sqrt{p}\left(\frac{\sin(\bar{\mu}c)}{\bar{\mu}}\right)^2+NV_0p^{3/2}\rho. \tag{2.21}
$$

So what then exactly should $\bar{\mu}$ be? Can it be a constant? The answer is no. $\bar{\mu}$ is a length in coordinate space, setting it to a constant, would lead to a physics that is not coordinate independent[1]. If one follows this path, one ends up with a Friedmann equation that depends directly on the scale factor, which is unphysical. Instead we can choose $\bar{\mu}$ to be the coordinate length of a fixed physical length. The translation between the coordinate length and physical length is given by multiplication by the scale factor, $a = \sqrt{p}$, therefore

$$\bar{\mu} = \frac{\lambda}{\sqrt{p}}, \tag{2.22}$$

for some physical length λ. Lambda could be seen as a parameter of the theory, but more commonly λ is chosen as the square root of the minimal area gap of LQG, that is

$$\lambda = \sqrt{[\text{minimum area gap}]}. \tag{2.23}$$

Our final expression for the modified Hamiltonian, taking into account Eq. (2.22), is

$$\mathcal{H} = NV_0 p^{3/2} \left(\frac{3}{\kappa\gamma^2\lambda^2} \sin(\bar{\mu}c)^2 + \rho \right). \tag{2.24}$$

2.3 Effective equations

Even with our quantization, Eq. (2.24) is not the same as Eq. (2.13). It might therefore be interesting to see what dynamics we get from Eq. (2.24) if we treat it classically. In a classical theory, the result is independent of the canonical variables we choose to work with, so for simplicity we will use just c and p.

In this section we will simply use Eq. (2.24) and the Poisson bracket

$$\{c, p\} = \frac{\kappa\gamma}{3V_0}. \tag{2.25}$$

We actually do not need to involve the dynamics of the matter for now.

From the Hamiltonan constraint, $\mathcal{H} = 0$, we get that

$$\sin(\bar{\mu}c)^2 = \frac{\kappa\gamma^2\lambda^2}{3}\rho. \tag{2.26}$$

Next, we calculate the proper time derivative of p:

$$\begin{aligned} \dot{p} &= \frac{1}{N}\{p, \mathcal{H}\} \\ &= -\frac{\kappa\gamma}{3NV_0}\frac{\partial\mathcal{H}}{\partial c} \\ &= \frac{2p}{\gamma\lambda}\sin(\bar{\mu}c)\cos(\bar{\mu}c). \end{aligned} \tag{2.27}$$

The factor $\frac{1}{N}$ comes from translating from derivative of coordinate time x^0 to derivative with respect to proper time t. Given that $p = a^2$, Eq. (2.6), we can now calculate the Hubble factor

$$H = \frac{\dot{p}}{2p} = \frac{1}{\gamma\lambda}\sin(\bar{\mu}c)\cos(\bar{\mu}c), \tag{2.28}$$

[1] Not everyone agree that this coordinate is necessary, see for example [3].

and the square

$$\begin{aligned} H^2 &= \frac{1}{\gamma^2\lambda^2}\sin(\bar{\mu}c)^2\cos(\bar{\mu}c)^2 \\ &= \frac{1}{\gamma^2\lambda^2}\sin(\bar{\mu}c)^2\left(1-\sin(\bar{\mu}c)^2\right) \\ &= \frac{\kappa}{3}\rho\left(1-\frac{\kappa\gamma^2\lambda^2}{3}\rho\right). \end{aligned} \tag{2.29}$$

This above result is usually expressed as

$$H^2 = \frac{\kappa}{3}\rho\left(1-\frac{\rho}{\rho_c}\right). \tag{2.30}$$

This is the LQC-modified Friedmann equation, which is (one of) the key result of LQC. The ρ_c term is the critical density, which is the maximal density of the system:

$$\rho_c = \frac{3}{\kappa\gamma^2\lambda^2}. \tag{2.31}$$

A universe that starts out contracting will bounce at $\rho = \rho_c$ and after that it starts expanding (see [4]). Note that Eq. (2.30) does not predict an oscillating universe since there is nothing in this theory that turns an expanding universe into a contracting one. One can construct an oscillating model by combining LQC which some other theory or hypothesis that leads to this (in particular a positively curved universe), but by itself LQC does not necessarily leads to a cyclic universe. In the case of our own universe, the current acceleration of the expansion leaves little hope for a future bounce.

2.4 Quantization

To perform the quantum calculations, we need to find some suitable representations where the operators $\widehat{p^{3/2}}$ and $\widehat{e^{\pm i\frac{1}{2}\bar{\mu}c}}$ are well defined and have the correct commutation relation. Just looking at Eq. (2.24), one might think that we want the operator $\widehat{e^{\pm i\bar{\mu}c}}$, or even possible $\widehat{\sin(\bar{\mu}c)^2}$. However, looking back at the holonomies, Eq. (2.16), and remembering that $|l_k| \to \bar{\mu}$, we realize that $\widehat{e^{\pm i\frac{1}{2}\bar{\mu}c}}$ is the most natural operator.

We find the desired commutation relation from the classical Poisson bracket

$$\left[\widehat{e^{\pm i\frac{1}{2}\bar{\mu}c}}, \widehat{p^{3/2}}\right] = i\widehat{\left\{e^{\pm i\frac{1}{2}\bar{\mu}c}, p^{3/2}\right\}} \tag{2.32}$$

Calculating the Poisson bracket

$$\begin{aligned} i\left\{e^{\pm i\frac{1}{2}\bar{\mu}c}, p^{3/2}\right\} &= i\sum_{n=0}^{\infty}\frac{\left(\pm i\frac{1}{2}\mu\right)^n}{n!}\left\{c^n, p^{3/2}\right\} \\ &= i\sum_{n=0}^{\infty}\frac{\left(\pm i\frac{1}{2}\lambda p^{-1/2}\right)^n}{n!}\frac{\kappa\gamma}{3V_0}nc^{n-1}\frac{3}{2}p^{1/2} \\ &= i\left(\pm i\frac{1}{2}\lambda\right)\frac{\kappa\gamma}{3V_0}\frac{3}{2}e^{\pm i\frac{1}{2}\bar{\mu}c} \\ &= \mp\frac{\kappa\gamma\lambda}{4V_0}e^{\pm i\frac{1}{2}\bar{\mu}c} \end{aligned} \tag{2.33}$$

gives us

$$\left[\widehat{e^{\pm i\frac{1}{2}\bar{\mu}c}}, \widehat{p^{3/2}}\right] = \mp\frac{\kappa\gamma\lambda}{4V_0}\widehat{e^{\pm i\frac{1}{2}\bar{\mu}c}} \tag{2.34}$$

There is a very suitable representation for this system. Let the Hilbert space be $L^2(\mathbb{R}, dv)$ and the operators

$$\widehat{e^{\pm i\frac{1}{2}\bar{\mu}c}} = e^{\mp\frac{d}{dv}} \tag{2.35}$$

$$\widehat{p^{3/2}} = \frac{\kappa\gamma\lambda}{4V_0}v \tag{2.36}$$

We can also define the volume operator for the volume of the financial cell

$$\hat{V} = V_0\widehat{p^{3/2}} = \frac{\kappa\gamma\lambda}{4}v \tag{2.37}$$

Expressing the Hamiltonian in these operators, it is possible to calculate the evolution of a homogenous universe in a fully quantized setting. This has been done [5] and the result was that highly peaked quantum states followed exactly the trajectories of the effective theory described in the previous section.

We should not find it surprising to find this nice agreement between the quantum and effective theory. Consider the commutator Eq. (2.34). The commutator is proportional to $1/V_0$ where V_0 is the coordinate volume of the fiducial cell that was introduced in Section 2.1. Since V_0 can be made arbitrary large, this means that the quantum theory can me made arbitrary classical, and this in turn means that we should expect classical and quantum theories to agree. [6]

Because of this consistency between the classical effective theory and the quantum theory, there is often no need to work in a more complicated setting for the quantum theory. For this reason, we will from now on use the effective theory to describe the homogenous part of LQC, with the exception of Section 3.2.

Chapter 3

Non-homogenous Loop Quantum Cosmology

The input from LQG in LQC is all included in the modified Hamiltonian Eq. (2.24). This can then be used to derive the modified Friedman equation, Eq. (2.30), or be quantized as in Section 2.4. Or be used as a background for adding perturbations, as we shall do in this section. However no approach to this task takes any further input from LQG than what is already described in the previous chapter. Any underlying theory that produces Eq. (2.30) can be used to motivate LQC.

As mentioned in the previous chapter, what we are really interested in, in cosmology, are perturbations, because this is what can be observed. In LQC, there are two competing approaches to this task. All the papers presented in this thesis are based on the deformed algebra approach, but for completeness, we will also review the dressed metric approach.

Throughout this manuscript we keep the number of bibliographic references to a minimum as they are already given in the reproduced articles.

3.1 Deformed Algebra approach

The motivation for the deformed algebra approach is grounded in trying to avoid as much as possible quantization techniques that require gauge fixing before quantization. In some cases, gauge fixing before quantization can indeed be assumed to be harmless, but the situation considered in gravity is different. First, the constraints are more complicated functions than, say, the Gauss constraint of Yang–Mills theories. It is therefore more likely that the constraints receive significant quantum corrections. If the constraints are deeply corrected, the gauge transformations they generate are not of the classical form. Gauge fixing before quantization is then inconsistent, because one would fix the gauge according to transformations which subsequently will be heavily modified. Secondly, in the considered case the dynamics is part of the gauge system. A consistent theory must therefore quantize gauge transformations and the dynamics at the same time: one cannot fix one part (the gauge) in order to derive the second part (the dynamics) in an unrestricted way.

In classical GR we have:

$$\{D[M^a], D[N^a]\} \approx 0, \tag{3.1}$$
$$\{D[M^a], S[N]\} \approx 0, \tag{3.2}$$
$$\{S[M], S[N]\} \approx 0 \tag{3.3}$$

where S and D are the smeared Hamiltionan and diffeomorphism constraints,

$$S[N] = \int dx^3 N\mathcal{C}, \tag{3.4}$$
$$D[N^a] = \int dx^3 N^a \mathcal{C}_a, \tag{3.5}$$

and $\approx$ means equal on the constraint surface $D = S = 0$. More precisely this means that all the above Poisson brackets have to be proportional to one of the smeared constraints itself. This is called a closed algebra and has to be be true also in the loop modified version of the theory. The idea is to close the algebra on a perturbative level before quantising the perturbations.

For the deformed algebra approach, we start from the classical perturbed Hamiltonian and replace the zeroth order expression (i.e. the homogenious background) with the expression from homogenous LQC, Eq. (2.24). When only the zeroth order expression is modified, the constraints does not form a closed algebra. The next step is to modify the first and second order corrections in such a way that Eqs. (3.1) - (3.3) holds true once again, up till second order of perturbation. In this, we also require the classical limit, i.e. the classical expression for all constraints must be recovered in the limit $\bar{\mu} \to 0$.

Impressively, these conditions fix most of the ambiguities of the introduced quantum corrections. There is a small amount of freedom which is discussed in the paper in Section 5, but for now we will use the simplest solution. We find that anomaly-free algebra of effective constraints is deformed compared to the classical algebra of constraints by:

$$\left\{D^Q[M^a], D^Q[N^a]\right\} = D^Q[M^b\partial_b N^a - N^b\partial_b M^a], \tag{3.6}$$
$$\left\{D^Q[M^a], S^Q[N]\right\} = S^Q[M^a\partial_a N - N\partial_a M^a], \tag{3.7}$$
$$\left\{S^Q[M], S^Q[N]\right\} = \mathbf{\Omega} D^Q\left[q^{ab}(M\partial_b N - N\partial_b M)\right], \tag{3.8}$$

where D^Q and S^Q are the new modified diffeomorphism and the scalar constraints. The new physics is encoded in $\mathbf{\Omega}$ which depends on the background phase-space variables, $\mathbf{\Omega} = \cos(2\gamma\bar{\mu}\bar{k}) = 1 - 2\rho/\rho_c$. Importantly, the structure of space-time seems to become – at least at the effective level – Euclidean around the bounce. This possibly important effect will be discussed later. It is quite impressive that the long and intricate calculations associated with the anomaly freedom lead to this very simple and elegant algebraic structure.

Moreover, the set of effective constraints can be used to generate the gauge transformations required to derive the effective gauge-invariant variables for the cosmological perturbations. The evolutions are generated by the second-order effective Hamiltonian. Those perturbations are finally quantized *à la* Fock using the techniques developed for quantum fields in curved spaces in a quite standard way. In this deformed algebra approach, the mode functions describing the dynamics of the scalar and tensor modes (in terms of Mukhanov-Sasaki variables) are solutions of

$$v"_{\mathrm{S(T)},k} + \left[\mathbf{\Omega}k^2 - \frac{z"_{\mathrm{S(T)}}}{z_{\mathrm{S(T)}}}\right] v_{\mathrm{S(T)},k} = 0, \tag{3.9}$$

with $z_{\rm S} = (a\bar{\varphi}')/\mathcal{H}$ and $z_{\rm T} = a/\sqrt{\mathbf{\Omega}}$. Those functions encode the impact of the effective background on the perturbations and the spectrums they generate will be shown in this manuscript.

In the deformed algebra approach, only the background dynamics is taken from LQG and not much is really quantum. But the subtle consistency is ensured by construction. This is a kind of embedding of general relativity in a more general framework. If no care is taken, the vector of evolution generically becomes, when effective quantum corrections are implemented, non-parallel to the sub-manifold of constraints and the theory will likely become inconsistent. This is precisely what is avoided here.

3.2 Dressed Metric approach

The dressed metric approach [7, 8, 9] relies on a minisuperspace strategy where the homogeneous and isotropic degrees of freedom and the inhomogoneous degrees of freedom (considered as perturbations) are all quantized. The homogeneous part relies on the loop quantization and the inhomogeneous part is obtained by a Fock quantization on a *quantum* background. The gauge-invariant inhomogeneous degrees of freedom are given by a set of Mukhanov-Sasaki variables obtained from the linearized classical constraints. The second order Hamiltonian (restricted to the square of the first order perturbations) is promoted to be an operator and the quantization is performed using techniques suitable for the quantization of a test field evolving in a quantum background, as derived by Ashtekar and Lewandowski [10]. The Hilbert space is described by the tensor product $\Psi(\nu, v_{\rm S(T)}, \varphi) = \Psi_{\rm FLRW}(\nu, \bar{\varphi}) \otimes \Psi_{\rm pert}(v_{\rm S}, v_{\rm T}, \bar{\varphi})$ where ν stands for the homogeneous and isotropic degrees of freedom and $v_{\rm S(T)}$ stands for the degrees of freedom associated with perturbations. The main point is that the Schrödinger equation for the perturbations was shown to be formally identical to the Schrödinger equation for the quantized perturbations evolving in a classical background but using a *dressed* metric encoding the quantum nature of the background (for tensor modes):

$$i\hbar\partial_{\bar{\varphi}}\Psi_{\rm pert} = \frac{1}{2}\int \frac{d^3k}{(2\pi)^3}\left\{\frac{32\pi G}{\tilde{p}_\varphi}\left|\hat{\pi}_{{\rm T},\vec{k}}\right|^2\Psi_{\rm pert} + \frac{k^2}{32\pi G}\frac{\tilde{a}^4(\bar{\varphi})}{\tilde{p}_\varphi}\left|\hat{v}_{{\rm T},\vec{k}}\right|^2\Psi_{\rm pert}\right\}, \tag{3.10}$$

with

$$(\tilde{p}_\varphi)^{-1} = \left\langle \hat{H}^{-1}_{\rm FLRW}\right\rangle \quad \text{and} \quad \tilde{a}^4 = \frac{\left\langle \hat{H}^{-1/2}_{\rm FLRW}\hat{a}^4(\bar{\varphi})\hat{H}^{-1/2}_{\rm FLRW}\right\rangle}{\left\langle \hat{H}^{-1}_{\rm FLRW}\right\rangle}. \tag{3.11}$$

In this equation, $(\hat{v}_{{\rm T},\vec{k}}, \hat{\pi}_{{\rm T},\vec{k}})$ are the configuration and momentum operators of the perturbations while $\hat{H}_{\rm FLRW}$ is the Hamiltonian operator of the isotropic and homogeneous background. This is the key result of Agullo, Ashtekar and Nelson: although the approach is fully quantum in its structure, the net result is quite similar to the usual classical situation. The dressed metric is in principle *neither* equal to the classical metric *nor* equal to the metric traced by the peak of the sharply peaked background state one often uses to describe the dynamics. (In principle this formalism can also be used with non-sharply peaked states.) This can finally be translated into a Fock quantization for which the mode functions (providing the evolution of scalar and tensor perturbations in a quantum background, here expressed in the spatial Fourier space) are

solutions of

$$Q"_k + 2\left(\frac{\tilde{a}'}{\tilde{a}}\right)Q'_k + \left(k^2 + \tilde{U}\right)Q_k = 0, \tag{3.12}$$

$$h"_k + 2\left(\frac{\tilde{a}'}{\tilde{a}}\right)h'_k + k^2 h_k = 0. \tag{3.13}$$

The gauge-invariant variable Q_k is related to the Mukhanov-Sasaki variables for scalar modes via $Q_k = v_{\mathrm{S},k}/a$, and, $\tilde{U}$ is a dressed potential-like term given by

$$\tilde{U}(\bar{\varphi}) = \frac{\left\langle \hat{H}^{-1/2}_{\mathrm{FLRW}}\hat{a}^2(\bar{\varphi})\hat{U}(\bar{\varphi})\hat{a}^2(\bar{\varphi})\hat{H}^{-1/2}_{\mathrm{FLRW}}\right\rangle}{\left\langle \hat{H}^{-1/2}_{\mathrm{FLRW}}\hat{a}^4(\bar{\varphi})\hat{H}^{-1/2}_{\mathrm{FLRW}}\right\rangle}, \tag{3.14}$$

the quantum counterpart of

$$U(\bar{\varphi}) = a^2\left(fV(\bar{\varphi}) - 2\sqrt{f}\partial_{\bar{\varphi}}V + \partial^2_{\bar{\varphi}}V\right), \tag{3.15}$$

with $f = 24\pi G(\dot{\bar{\varphi}}^2/\rho)$, the fraction of kinetic energy in the scalar field.

This approach is very interesting in that it really deals with quantum fields on a quantum geometry. From that point of view, it is arguably "better" than the deformed algebra approach. However, what can be questioned is the *consistency* of this framework. In general relativity, there is in principle an infinite number of dynamical evolution laws, all written with respect to different choices of coordinates. They are all equivalent one to another because of the symmetries of the classical theory and it is legitimate to pick up an arbitrary choice, depending of the requirements of the considered study. In the dressed metric approach, one is implicitly using several such choices, referred to as a background gauge. The mode dynamics is then written in terms of coordinate-invariant combinations of metric and matter perturbations. Only after these specific steps does one obtain a clear dynamics for background variables and perturbations, all written in a Hamiltonian way. Classically, that result does not depend on the coordinate choice and the procedure is valid. But as some degrees of freedom are here quantized, the equations should be modified by quantum corrections of different kinds – as shown by the deformed algebra study–, and nothing still guaranties that the results do not depend on the arbitrary choices made before. This basically means that the theory may not be covariant or anomaly-free.

Part II

Consistency and observational consequences of LQC

Chapter 4

Duration of inflation in LQC

In this chapter, we focus on the homogeneous Universe. This is the best controlled situation as all the different approaches to LQC currently studied do agree on the behavior or the background. Both by analytical and by numerical methods, it has been shown that the resolution of the Big Bang singularity is a very robust feature of LQC [11] and that the modified Friedmann equation with a quadratic correction captures the main features of the evolution of sharply peaked states (and even of non-gaussian states [12]). All the physical quantities are bounded from above and no divergence does occur. This is the Big Bounce picture.

It is however important to go beyond this generic statement and to study in more details what happens after the bounce. This is interesting in itself but also because this will play a key role in the calculation of the observable consequences of LQC at the level of perturbations by setting the size of relevant modes at the bounce time corresponding to physical wave-numbers probed by current astronomical observations. In this study we focus on the specific case of a single massive scalar field assumed to be the dominant content of the Universe in its high density stage. Although slightly disfavored by the last Planck results this is still an excellent benchmark model.

This question has already been studied by Ashtekar and Sloan [13] but they decided to set initial conditions at the bounce which is arguably the worst possible choice as the Universe is here "more quantum" than at any other stage. Here, we take causal evolution seriously and put initial conditions in the remote past. This is clearly more consistent at the level of an intuitive interpretation but this is also technically better motivated as the universe is then "less quantum". This later argument will be even more important for perturbations. In addition the evolution of the horizon is such that the vacuum is well defined.

By following this strategy, we explicitly show that the phase of the scalar field in the contracting branch is the natural parameter on which one should assume a flat probability distribution. We have checked that this distribution is preserved over time, as long as we are sufficiently far into the past before the bounce. Varying this phase, it is possible to investigate how the duration of inflation varies and how probable each outcome is. The main result of this study is that the fraction of potential energy at the bounce time (or equivalently the value of the field) is far from being random and exhibits a very highly peaked value. This value determines the subsequent duration of inflation which is peaked around 140 e-folds, which is compatible with observations.

It is sometimes claimed to be a great success of LQC that slow-roll inflation is practically a certainty. This statement is highly misleading. LQC only leads to inflation if the inflation field is put in by hand. Moreover, if a contracting universe is dominated by a suitable inflaton field, slow-roll inflation is a very strong attractor. If the initial conditions are set at a high enough density (e.g. at the bounce) slow-roll inflation is practically inevitable, but the duration of inflation can still be highly uncertain. It is therefore very interesting that the duration of inflation is now predicted with high precision, and that it is far from the maximum one.

We also used these calculations to set an upper limit on the Immirzi parameter. If this latter is too big, the energy scale at the bounce is not high enough and one does not have enough inflation to be compatible with observations.

However, it is worth keeping in mind that all of these results are found using one specific inflation potential. We suspect that the duration of inflation could be predicted in a similar way using an alternative potential, but the resulting numbers of e-folds could be very different. This remains to be tested.

PHYSICAL REVIEW D **87,** 123509 (2013)

Duration of inflation and conditions at the bounce as a prediction of effective isotropic loop quantum cosmology

Linda Linsefors* and Aurelien Barrau†

Laboratoire de Physique Subatomique et de Cosmologie, UJF, INPG, CNRS, IN2P3 53, Avenue des Martyrs, 38026 Grenoble Cedex, France

(Received 2 January 2013; published 10 June 2013)

Loop quantum cosmology with a scalar field is known to be closely linked with an inflationary phase. In this article, we study probabilistic predictions for the duration of slow-roll inflation, by assuming a minimalist massive scalar field as the main content of the Universe. The phase of the field in its ''prebounce'' oscillatory state is taken as a natural random parameter. We find that the probability for a given number of inflationary e-folds is quite sharply peaked around 145, which is consistent with the most favored minimum values. In this precise sense, a satisfactory inflation is therefore a clear prediction of loop gravity. In addition, we derive an original and stringent upper limit on the Barbero-Immirzi parameter. The general picture of inflation, superinflation, deflation, and superdeflation is also much clarified in the framework of bouncing cosmologies.

DOI: 10.1103/PhysRevD.87.123509 PACS numbers: 98.80.Qc, 04.60.Pp, 98.80.Cq

I. INTRODUCTION

Loop quantum gravity (LQG) is a tentative nonperturbative and background-independent quantization of general relativity. It uses Ashtekar variables, namely, SU(2) valued connections and conjugate densitized triads. The quantization is obtained through holonomies of the connections and fluxes of the densitized triads (see, e.g., Ref. [1] for an introduction). Basically, loop quantum cosmology (LQC) is the symmetry reduced version of LQG. In LQC, the big bang is generically replaced by a big bounce due to huge repulsive quantum geometrical effects (see, e.g., Ref. [2] for a review).

Trying to confront LQG with the real world is a key issue. It is not currently possible to compute the cosmological dynamics from the full quantum theory (interesting attempts have recently been presented in Ref. [3], in particular, for perturbations). As in most works on the subject, we will therefore deal with effective equations that are believed to capture the main quantum effects. Many studies have been devoted to the computation of power spectra and their subsequent comparison with observations (see, e.g., Ref. [4]). Here, we do not follow this track but, in the spirit of Ref. [5], focus instead on only the homogenous part of the Universe, and the probability corresponding to different durations of inflation, within the loop gravity framework.

Two main LQG corrections are expected when dealing with a semiclassical approach, as will be the case in this study. The first one comes from the fact that loop quantization is based on holonomies, i.e., exponentials of the connection rather than direct connection components. The second one arises for inverse powers of the densitized triad, which, when quantized, becomes an operator with zero in its discrete spectrum, thus lacking a direct inverse. As the status of ''inverse volume'' corrections is not fully clear, due to the fiducial volume cell dependence, this work focuses on the holonomy term, which has a major influence on the background equations.

This paper is organized as follows: In Sec. II we present the equations that are the starting point of this paper. In Sec. III we explain the different phases of evolution that these equations give rise to. The calculations used in this section can be found in the Appendix. In Sec. IV we calculate the probability distribution of different solutions and, in particular, the probability distribution of the number of e-folds of slow-roll inflation. In Sec. V we derive an analytical expression for the most probable value of the number of e-folds of slow-roll inflation. In Sec. VI we use the above results to constrain the critical density and the Barbero-Immirzi parameter.

This study is complementary to the ones performed in Ref. [5], where the probability distribution was assumed to be flat and defined at the bounce (the first attempts in this direction were performed in Ref. [6]). Here, we make a very different assumption: the phase of the field oscillating in the remote past is considered to be the most natural random variable. As shown in Ref. [7] the choice of what is a natural measure, and therefore the outcome of these kinds of calculations, can depend heavily on when one decides to define the initial conditions. Here, we take seriously the meaning of an ''initial'' condition in a Universe that extends in the past beyond the bounce. We do not use any heavy machinery and rely only on very minimalistic hypotheses. Nor do we assume different conditions at the bounce, as in Ref. [5], but instead derive them explicitly as predictions of the model.

In the end, we show that, if the critical density is assumed to be a free parameter, a stringent upper limit on the Barbero-Immirzi parameter, γ, that is, the free

*linsefors@lpsc.in2p3.fr
†Aurelien.Barrau@cern.ch

parameter of loop gravity, can be obtained. This is especially important if, as suggested in Ref. [8], the entropy of black holes can be recovered for any γ, therefore leaving its value mostly unconstrained.

The emphasis of this study is put on LQC, as this model provides a well-defined framework, with known and controlled equations of motion. Most results are, however, probably quite generic to bouncing models.

II. FRAMEWORK

The holonomy-corrected LQC-modified Friedman equation reads as

$$H^2 = \frac{\kappa}{3}\rho\left(1 - \frac{\rho}{\rho_c}\right). \tag{1}$$

Here, we assumed that the Universe is kinetic energy dominated around the bounce so that higher-order terms can be neglected [9]. We will see later from the prediction of Sec. IV that this is self-consistent.

The main content of the Universe is assumed to be a massive scalar field ϕ with mass m fulfilling

$$\ddot{\phi} + 3H\dot{\phi} + m^2\phi = 0. \tag{2}$$

This is both the most common and the best motivated (as a scalar can account effectively for many kinds of other fundamental contents) choice, allowing for easy comparisons with works carried out in standard cosmology.

We use the critical density, i.e., density at the bounce, given by [2] $\rho_c = \sqrt{3}m_{\mathrm{Pl}}^4/(32\pi^2\gamma^3) \simeq 0.41 m_{\mathrm{Pl}}^4$, where $\kappa = 8\pi G$ and $\gamma = 0.2375$ (except in Secs. IV and V, where ρ_c is considered as a free parameter). We use the mass of the scalar field $m = 1.21 \times 10^{-6}$ as is favored by observations [10] (except in Sec. V, where m can be taken as a free parameter).

We define the fractions of potential and kinetic energy, normalized to the maximum energy density,

$$x := \frac{m\phi}{\sqrt{2\rho_c}} \quad \text{and} \quad y := \frac{\dot{\phi}}{\sqrt{2\rho_c}}, \tag{3}$$

so that

$$\rho = \rho_c(x^2 + y^2). \tag{4}$$

The equations of motion for x, y, and ρ are

$$\dot{x} = my, \qquad \dot{y} = -mx - 3Hy, \tag{5}$$

$$\dot{\rho} = -6H\rho_c y^2. \tag{6}$$

III. PHASES OF THE LQC BOUNCING UNIVERSE

Using Eq. (1) and Eqs. (4)–(6), the evolution of the Universe can be generically described by five phases:

(A) Prebounce oscillations
(B) Slow-roll deflation
(C) Superdeflation, bounce, and superinflation
(D) Slow-roll inflation
(E) Post-bounce oscillations

Examples of plots of x for different solutions are given in Fig. 1. They are good indicators of what is happening since one can see here very clearly the differences between the phases of evolution.

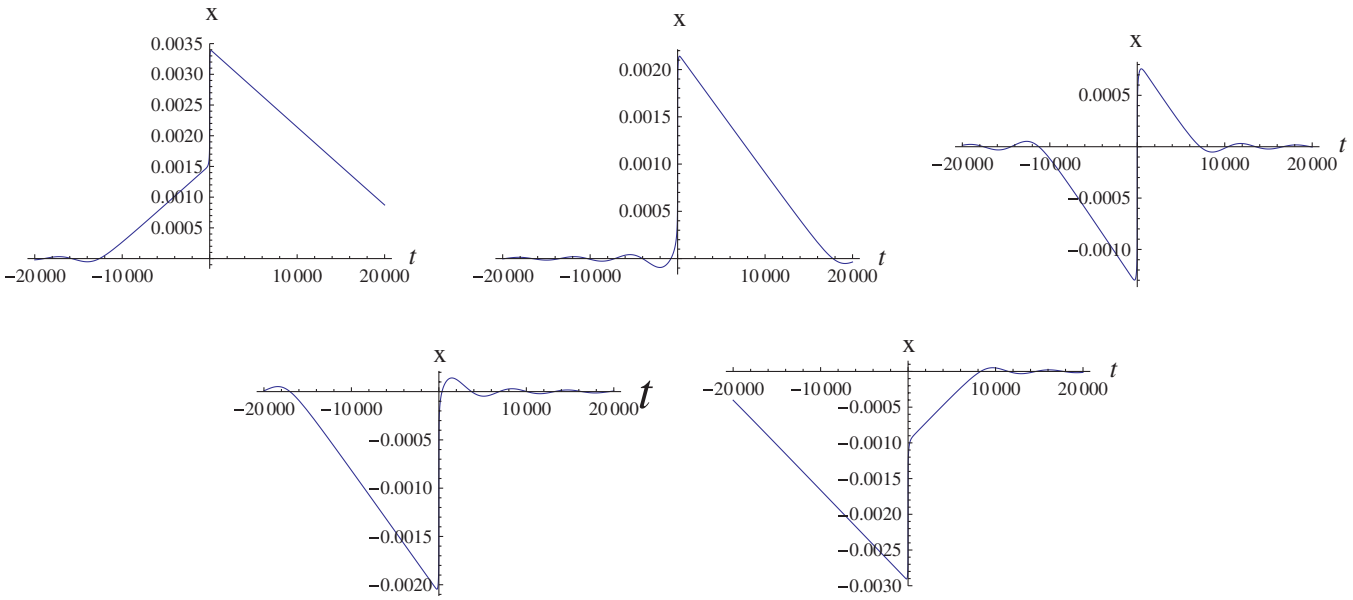

FIG. 1 (color online). Examples of evolutions of x as a function of time for different solutions. The linear increase (decrease) of $|x|$ is the slow-roll deflation (inflation) phase, and the almost vertical increase or decrease of x is the superdeflation, bounce, and superinflation phase. A solution with no deflation at all like in the upper middle plot is by far the most probable. The mass of the scalar field used here is $m = 10^{-3}$, but the features remain true for any mass.

We assume that ρ_c is large enough so that $\rho \ll \rho_c$ is always the last of the relevant conditions to be violated before the bounce and the first one to be restored after the bounce. This is in agreement with result from numerical simulations. In the following equations, t is always the cosmic time, but it will be shifted between solutions for the different phases; for convenience reasons, the convention for the origin of time is not always the same. The exact origin of time is irrelevant for the underlying physics.

The calculations behind the results in this section are presented in the Appendix.

A. Prebounce oscillations

This phase is characterized by the fact that x and y are oscillating with vanishing mean values and growing amplitudes. In this study, we naturally assume this phase to be the initial state of the bouncing Universe. This is of course a hypothesis that can be questioned. The conditions for prebounce oscillations are

$$\rho \ll \rho_c, \qquad H < 0, \qquad H^2 \ll m^2. \tag{7}$$

The evolution in this phase can be approximated by

$$\rho = \rho_0\left(1 - \frac{1}{2}\sqrt{3\kappa\rho_0}\left(t + \frac{1}{2m}\sin(2mt + 2\delta)\right)\right)^{-2}, \tag{8}$$

$$x = \sqrt{\frac{\rho}{\rho_c}}\sin(mt + \delta), \qquad y = \sqrt{\frac{\rho}{\rho_c}}\cos(mt + \delta). \tag{9}$$

This is stable until ρ grows large enough to violate the last condition.

B. Slow-roll deflation

Slow-roll deflation is characterized by an almost constant y and a linearly growing $|x|$. The probability of slow-roll deflation is small, since it occurs only if the relation between x and y is very specific at the end of the phase of prebounce oscillations. The conditions for slow-roll deflation are

$$\rho \ll \rho_c, \qquad H < 0, \qquad H^2 \gg m^2, \qquad x^2 \gg y^2. \tag{10}$$

In this phase, the equation of motion for y can be approximated by

$$\dot{y} = \sqrt{3\kappa\rho_c}|x|\left(y - \mathrm{sign}(x)\frac{m}{\sqrt{3\kappa\rho_c}}\right). \tag{11}$$

The value $y = \mathrm{sign}(x)\frac{m}{\sqrt{3\kappa\rho_c}}$ is an unstable stationary point. The variable y will evolve away from $\mathrm{sign}(x)\frac{m}{\sqrt{3\kappa\rho_c}}$. However, if y starts out very close to $\mathrm{sign}(x)\frac{m}{\sqrt{3\kappa\rho_c}}$, then $\dot{y} \approx 0$ for a while, and this leads to slow-roll deflation. Slow-roll deflation is in this sense unstable.

C. Superdeflation, bounce, and superinflation

This phase is characterized by a large $|y|$ and a rapidly growing or decreasing x (y, and therefore $\dot{x}$, do not change sign during this phase). Superdeflation starts directly after post-bounce oscillations or after slow-roll deflation. The conditions for this phase are

$$H^2 \gg m^2, \qquad y^2 \gg x^2. \tag{12}$$

The evolution can be approximated by

$$\rho = \rho_c(1 + 3\kappa\rho_c t^2)^{-1}, \qquad y = \pm(1 + 3\kappa\rho_c t^2)^{-1/2}, \tag{13}$$

$$x = x_B \pm \frac{m}{\sqrt{3\kappa\rho_c}}\,\mathrm{arcsinh}\left(\sqrt{3\kappa\rho_c}\,t\right), \tag{14}$$

where $t = 0$ at the bounce for Eqs. (13) and (14). This phase is stable for $H < 0$ but unstable for $H > 0$ since, in the later case, $|y|$ is decreasing rapidly and will eventually violate the second condition of Eqs. (12).

D. Slow-roll inflation

Slow-roll inflation happens if the second condition of Eqs. (12) is broken before the first one. The conditions for slow-roll inflation are

$$\rho \ll \rho_c, \qquad H > 0, \qquad H^2 \gg m^2, \qquad x^2 \gg y^2. \tag{15}$$

In this phase, the equation of motion for y can be approximated by

$$\dot{y} = -\sqrt{3\kappa\rho_c}|x|\left(y + \mathrm{sign}(x)\frac{m}{\sqrt{3\kappa\rho_c}}\right), \tag{16}$$

which should be compared with Eq. (11). In this case, $y = -\mathrm{sign}(x)\frac{m}{\sqrt{3\kappa\rho_c}}$ is an attractor; therefore, slow-roll inflation is stable until one of the two last conditions is violated, which occurs at approximately the same value of x for both conditions [11].

E. Post-bounce oscillations

The conditions for post-bounce oscillations are

$$\rho \ll \rho_c, \qquad H > 0, \qquad H^2 \ll m^2. \tag{17}$$

The evolutions in this phase—corresponding to reheating—can be approximated by

$$\rho = \rho_0\left(1 + \frac{1}{2}\sqrt{3\kappa\rho_0}\left(t + \frac{1}{2m}\sin(2mt + 2\delta)\right)\right)^{-2}, \tag{18}$$

together with Eqs. (9).

IV. NUMERICAL PREDICTIONS

In this section, we calculate the probability density function for x_B, the square root of the fraction of potential energy at the bounce, and N, the number of e-folds of slow-roll

inflation. This is done by first finding the most natural initial probability distribution and then evolving it numerically.

We believe that it is most natural and consistent with the big bounce model to set the initial probability distribution in the prebounce oscillation phase. The evolution of the Universe in this phase is described by Eqs. (8) and (9), with parameters ρ_0 and δ. However, the transformation

$$\rho_0 \rightarrow \rho_1 \tag{19}$$

corresponds to

$$\begin{aligned} \delta &\rightarrow \delta - \frac{2m}{\sqrt{3\kappa\rho_1}}\left(1 - \sqrt{\frac{\rho_1}{\rho_0}}\right), \\ t &\rightarrow t + \frac{2}{\sqrt{3\kappa\rho_1}}\left(1 - \sqrt{\frac{\rho_1}{\rho_0}}\right), \end{aligned} \tag{20}$$

and does not therefore generate new solutions. This allows us to take δ as the only parameter.

In addition of being the obviously expected distribution for any oscillatory process of this kind, a flat probability for δ will be preserved over time within the prebounce oscillation phase [under the assumptions given by Eq. (7)], making it a very natural choice for initial conditions. By "preserved over time," it is meant here that it is preserved by transformations described by Eqs. (19) and (20). This is not a trivial point as any other probability distribution would be distorted over time, meaning that the final result in the full numerical analysis would depend on the choice of ρ_0. It can be noticed that time itself is not a relevant parameter in the numerical analysis: the time it takes for the Universe to evolve from its initial state to the bounce is determined by ρ_0.

Starting with a flat probability distribution for δ, and choosing ρ_0 so that the solution is initially well approximated by Eqs. (8) and (9), the probability for different values of x_B can be calculated numerically using the full set of Eqs. (1), (4), and (5). At the bounce, the solutions can be parametrized by x_B and sign(y); however, only the relative sign is physical. We therefore project the result down to the physically relevant parameters by considering sign(y_B)x_B. The value of sign(y_B)x_B as a function of δ and the resulting probability distribution are shown in Fig. 2.

In previous works, sign(y_B)x_B was taken as unknown [5]. However, here, we show that it is sharply peaked around 3.55×10^{-6} (this values scales with m as $m \log(\frac{1}{m})$, where we assumed that $m \ll 1$ in Planck units). The most likely solutions are exactly those that have no slow-roll deflation. In the tails of the probability spectrum, there are solutions with some slow-roll deflation, but the probability density decreases very rapidly with the length of slow-roll deflation. This result is also expected from the arguments given in Sec. III.

Our result is not symmetric under a time reversal transformation. This is not surprising as we broke the time

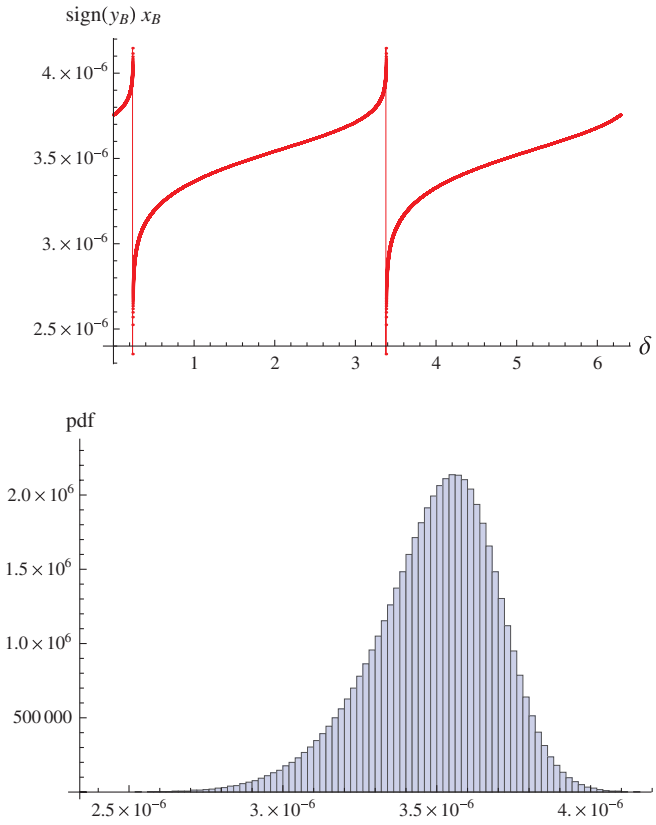

FIG. 2 (color online). sign(y_B)x_B as a function of δ (upper plot) and its probability distribution (lower plot).

symmetry of the model by choosing initial conditions outside of the bounce. There is here a clear causal evolution from the past to the future. However, given the same prior (initial) distribution for the post-bounce oscillation phase and evolving backward, one would of course find that these results hold for the probability of prebounce deflation.

This result also shows that the bounce is strongly kinetic energy dominated, leading to backreaction effects that can be safely neglected [9]. The model is therefore self-consistent.

Slow-roll inflation starts when $|x| = x_{\max}$ where $x_{\max} \doteq \max_{t>t_B}(|x|)$, which is related to the length of slow-roll inflation by $N = \frac{\kappa\rho_c}{2}(\frac{x_{\max}}{m})^2 \simeq 5.1(\frac{x_{\max}}{m})^2$, where N is the number of e-folds during slow-roll inflation. The probability density for N is given in Fig. 3, showing that the model leads to a slow-roll inflation of about 145 e-folds. This becomes an important and clear prediction of effective LQC; inflation and its duration are not arbitrary in the model.

This prediction is in agreement with observations that require a slow-roll inflation longer than 65 e-folds. Strictly, no fine-tuning was required to obtain this result.

The old and well-known "measure problem" in cosmology is basically related to the way ignorance should be described. Ignorance means a flat probability distribution function over some natural measure, and the question is the

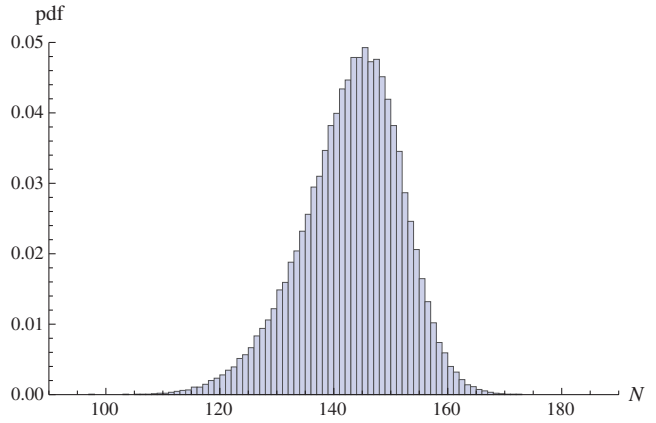

FIG. 3 (color online). Probability density of the number of e-folds of slow-roll inflation.

following: what should this measure be? In the minisuperspace (homogeneous, isotropic, and flat) approximation used in this study, the relevant problem is not related with the existence of infinitely many degrees of freedom or with divergent integrals but with the way to chose the significant measure with respect to which the probability distribution is flat. If we assume no knowledge of quantum gravity, it might be a reasonable assumption to chose the "time of ignorance" at the Planck density and search for a natural measure of the parameters at that time. However, in this study, we assume that, through the bounce, the Universe is well described by Eqs. (1) and (2). In this approach, our ignorance starts when the mater content begins to be well approximated by the (effective) scalar field (assuming, e.g., that the prebounce oscillation phase is created by some inverse reheating process). As we know neither the details of this process "which might very well be purely random" nor the density at which this occurs, we translate this ignorance as a flat probability distribution for the most natural parameter of this phase. In addition, even if we somehow gain knowledge of the physics governing the "inverse reheating," and even if this this theory predicts a nonflat probability distribution for δ, unless this probability distribution is extremely peaked around the specific value that gives significant slow-roll deflation, our result will hold.

V. ANALYTICAL PREDICTIONS

A raw analytical estimate for N can be obtained by assuming that the phase of superdeflation, bounce, and superinflation starts at $H = -m$ with $x = 0$ and ends at $H = m$. One then finds that

$$x_{\max} = \frac{2m}{\sqrt{3\kappa\rho_c}} \ln\left(\frac{2}{m}\sqrt{\frac{\kappa}{3}\rho_c}\right), \tag{21}$$

where we have used $\operatorname{arcsinh}(\frac{1}{m}\sqrt{\frac{\kappa}{3}\rho_c}) \approx \ln(\frac{2}{m}\sqrt{\frac{\kappa}{3}\rho_c})$. This approximation agrees very well with numerical result as can bee seen in Fig. 4. From this, we get the number of e-folds of slow-roll inflation as

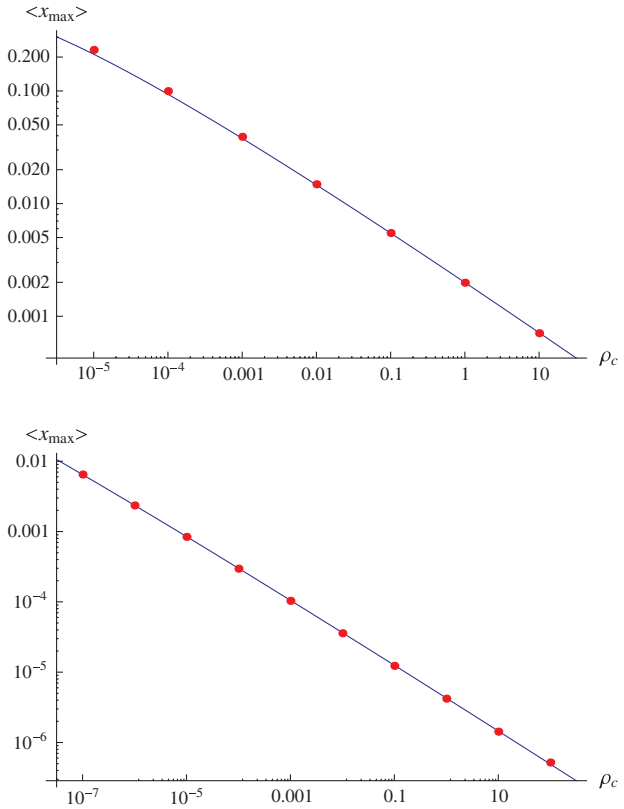

FIG. 4 (color online). Analytical approximation of $x_{\max}$ as a function of ρ_c (blue line) and mean values of numerical simulations (red dots) for $m = 10^{-3}$ (upper plot) and $m = 1.21 \times 10^{-6}$ (lower plot).

$$N = \frac{2}{3} \ln\left(\frac{2}{m}\sqrt{\frac{\kappa}{3}\rho_c}\right)^2. \tag{22}$$

VI. CONSTRAINTS

So far, we have used the standard value of ρ_c, with a Barbero-Immirzi parameter γ assumed to be known from black hole entropy (see, e.g., Ref. [12]) in our numerical investigation. By instead taking ρ_c as a free parameter, we

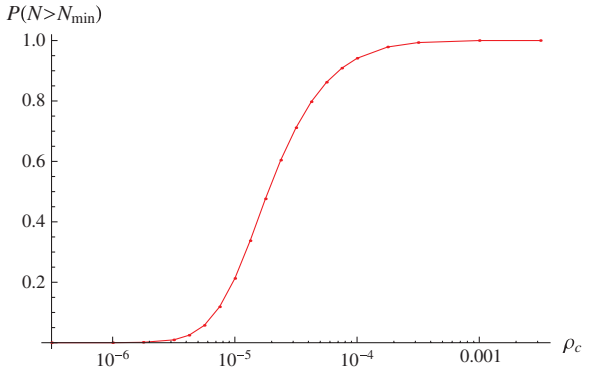

FIG. 5 (color online). Probability for having more than 65 e-folds of slow-roll inflation, $P(N > 65)$, as a function of ρ_c.

TABLE I. Lower bound on ρ_c and upper bound on γ, for different minimum required probabilities of a slow-roll inflation longer than 65 e-folds.

$P(N > 65)$	ρ_c	γ
0.5	1.9×10^{-5}	6.6
0.05	5.4×10^{-6}	10.1
0.01	3.2×10^{-6}	11.9

can constrain ρ_c and γ. Previous attempts to constrain ρ_c (see Ref. [13]) from cosmological data were based on $x_{\max} < 1$. However, we have shown that, in all realistic cases, $x_{\max}$ is much more limited than that.

We can derive an upper limit on γ by requiring a large enough probability for a long enough slow-roll inflation. This is again done by assuming the (natural) prior probability distribution in the prebounce phase that was described previously. Figure 5 shows $P(N > 65)$ as a function of ρ_c, and Table I gives the constraints on ρ_c and γ for different required minimum probabilities for $N > 65$. One can also perform an analytical calculation using Eq. (22), leading to $\rho_c > 1.6 \times 10^{-5}$.

The main results of this analysis are that $\gamma < 10.1$ at 95% confidence level and $\gamma < 11.9$ at 99% confidence level. This is much more stringent than previous cosmological constraints [13]: $\gamma < 1100$. As the value of γ derived form black holes is still controversial, this new bound is clearly meaningful.

VII. CONCLUSION

This article establishes a prediction regarding the duration of slow-roll inflation based on holonomy-corrected effective LQC together with a single massive scalar field. The preferred value is $N = 145$ e-folds. Values lower than 110 or greeter than 170 are highly improbable. In addition, the value of x_B, the square root of the fraction of potential energy at the bounce, is no longer unknown but is shown to be very close to 3.5×10^{-6}. Finally, the Barbero-Immirzi parameter is now bounded to be smaller than 10–12 (depending on the confidence level), which is, by far, the best cosmological constraint.

This work should be developed by including other types of matter, by taking into account inverse volume correction, and, in the long run, by trying to use the full LQG theory.

ACKNOWLEDGMENTS

This work was supported by the Labex ENIGMASS.

APPENDIX: DERIVATION OF EVOLUTIONS IN THE DIFFERENT PHASES

In this Appendix, we present the calculations behind the results in Sec. III.

1. Oscillations

These calculations apply to both pre- and post-bounce oscillations.

The first condition of Eqs. (7) and (17) ensure that we can approximate Eq. (1) by

$$H = \pm\sqrt{\frac{\kappa}{3}\rho}. \tag{A1}$$

In addition, the last condition of Eqs. (7) and (17) ensures that we can approximate x and y by oscillating functions with frequency m and varying amplitudes. This, together with Eq. (4), gives Eq. (9). From this, Eq. (6) can be simplified to

$$\dot{\rho} = \mp 2\sqrt{3\kappa}\cos^2(mt + \delta)\rho^{3/2}, \tag{A2}$$

which can be integrated to give Eqs. (8) and (18).

2. Slow roll

These calculations apply to both slow-roll deflation and slow-roll inflation.

The last condition of Eqs. (10) and (15) ensures that we can approximate Eq. (4) by

$$\rho = \rho_c x^2. \tag{A3}$$

This, together with Eq. (1), with the first condition of Eq. (10), and with Eq. (15), gives

$$H = \pm\sqrt{\frac{\kappa}{3}\rho_c}|x|, \tag{A4}$$

so that the second part of Eq. (5) becomes Eq. (11) or Eq. (16).

3. Superdeflation, bounce, and superinflation

Without approximations, Eq. (1) can be written as

$$H = \pm\sqrt{\frac{\kappa}{3}\rho\left(1 - \frac{\rho}{\rho_c}\right)}. \tag{A5}$$

The second condition of Eq. (12) ensures that we can approximate Eq. (4) by

$$\rho = \rho_c y^2. \tag{A6}$$

Using the two above equations, Eq. (6) can be simplified to

$$\dot{\rho} = \mp 2\sqrt{3\kappa\left(1 - \frac{\rho}{\rho_c}\right)}\rho^{3/2}, \tag{A7}$$

which can be integrated to give Eq. (13). It is true both before and after the bounce. Integrating the first part of Eq. (5), using the second part of Eq. (13), gives Eq. (14).

[1] P. Dona and S. Speziale, arXiv:1007.0402; A. Perez, arXiv:gr-qc/0409061; R. Gambini and J. Pullin, *A First Course in Loop Quantum Gravity* (Oxford University Press, New York, 2011); C. Rovelli, Proc. Sci. QGQGS2011 (2011) 003; *Quantum Gravity* (Cambridge University Press, Cambridge, England, 2004); Living Rev. Relativity **1**, 1 (1998); L. Smolin, arXiv:hep-th/0408048; T. Thiemann, Lect. Notes Phys. **631**, 41 (2003); *Modern Canonical Quantum General Relativity* (Cambridge University Press, Cambridge, England, 2007).

[2] A. Ashtekar, M. Bojowald, and J. Lewandowski, Adv. Theor. Math. Phys. **7**, 233 (2003); A. Ashtekar, Gen. Relativ. Gravit. **41**, 707 (2009); A. Ashtekar and P. Singh, Classical Quantum Gravity **28**, 213001 (2011); M. Bojowald, Living Rev. Relativity **11**, 4 (2008); Classical Quantum Gravity **29**, 213001 (2012); K. Banerjee, G. Calcagni, and M. Martn-Benito, SIGMA **8**, 016 (2012); G. Calcagni, Ann. Phys. (Berlin) **525**, 323 (2013); I. Agullo and A. Corichi, arXiv:1302.3833.

[3] I. Agullo, A. Ashtekar, and W. Nelson, Classical Quantum Gravity **30**, 085014 (2013).

[4] J. Mielczarek, J. Cosmol. Astropart. Phys. 11 (2008) 011; J. Grain and A. Barrau, Phys. Rev. Lett. **102**, 081301 (2009); J. Mielczarek, Phys. Rev. D **79**, 123520 (2009); M. Bojowald, G. M. Hossain, M. Kagan, and S. Shankaranarayanan, Phys. Rev. D **79**, 043505 (2009); J. Mielczarek, T. Cailleteau, J. Grain, and A. Barrau, Phys. Rev. D **81**, 104049 (2010); J. Grain, A. Barrau, T. Cailleteau, and J. Mielczarek, Phys. Rev. D **82**, 123520 (2010); M. Bojowald and G. Calcagni, J. Cosmol. Astropart. Phys. 03 (2011) 032; M. Bojowald, G. Calcagni, and S. Tsujikawa, Phys. Rev. Lett. **107**, 211302 (2011); E. Wilson-Ewing, Classical Quantum Gravity **29**, 085005 (2012); L. Linsefos, T. Cailleteau, A. Barrau, and J. Grain, arXiv:1212.2852.

[5] A. Ashtekar and D. Sloan, Phys. Lett. B **694**, 108 (2010); Gen. Relativ. Gravit. **43**, 3619 (2011).

[6] C. Germani, W. Nelson, and M. Sakellariadou, Phys. Rev. D **76**, 043529 (2007).

[7] A. Corichi and A. Karami, Phys. Rev. D **83**, 104006 (2011).

[8] E. Bianchi, arXiv:1204.5122.

[9] M. Bojowald, Phys. Rev. Lett. **100**, 221301 (2008).

[10] A. Linde, Prog. Theor. Phys. Suppl. **163**, 295 (2006).

[11] The slow roll parameters are $\epsilon = \eta = \frac{m^2}{\kappa\rho_c x^2}$.

[12] A. Ashtekar, J. Baez, A. Corichi, and K. Krasnov, Phys. Rev. Lett. **80**, 904 (1998).

[13] J. Mielczarek, M. Kamionka, A. Kurek, and M. Szydlowski, J. Cosmol. Astropart. Phys. 07 (2010) 004.

Chapter 5

Perturbations in LQC

5.1 Anomaly freedom

Having checked that the background behavior in LQC is correct, the next obvious step is to consider perturbations. This is the key ingredient to confront the model with observations. Precision measurements from the Planck experiment make CMB prediction especially crucial. In this thesis we have focused on the deformed algebra approach described in Section 3.1.

In previous works, the Poisson bracket structure with holonomy corrections has been derived. However, there is a second possible correction that was neglected. It is due to the fact that the quantized densitized triad has a discrete spectrum, with the value zero in its spectrum. Such an operator does not allow the existence of a well-defined inverse, but an operator providing the inverse as the classical limit can nevertheless be defined, this is the Thiemman trick. When one departs from the classical regime, quantum corrections arise and their form can be guessed or parametrized sufficiently generally for phenomenological investigations. The algebra structure for such inverse-volume corrections was also derived. In the work presented here, for the first time, we explicitly address the question of the algebraic structure with both holonomy and inverse-volume corrections.

The procedure consists in calculating all the Poisson brackets and registering all the anomalies that appear, that is terms not proportional to another constraint. Then we fixed as many of the free parameters as possible, by requiring the anomalies to vanish and the classical limit to be correct. Although some freedom still remains the conclusion shows that a solution does exist. In this paper, we also find previously missed solutions for the situation with only holonomy corrections.

IOP Publishing Classical and Quantum Gravity
Class. Quantum Grav. **31** (2014) 125011 (35pp) doi:10.1088/0264-9381/31/12/125011

Anomaly-free perturbations with inverse-volume and holonomy corrections in loop quantum cosmology

Thomas Cailleteau[1], **Linda Linsefors**[2] **and Aurelien Barrau**[2,3]

[1] Institute for Gravitation and the Cosmos, Pennsylvania State University, University Park, PA 16802, USA
[2] Laboratoire de Physique Subatomique et de Cosmologie, UJF, INPG, CNRS, IN2P3 53, avenue des Martyrs, F-38026 Grenoble cedex, France
[3] Institut des Hautes Etudes Scientifiques, 35 route de Chartres, F-91440 Bures-sur-Yvette, France

E-mail: thomas@gravity.psu.edu, linsefors@lpsc.in2p3.fr and Aurelien.Barrau@cern.ch

Received 19 July 2013, revised 10 March 2014
Accepted for publication 11 March 2014
Published 2 June 2014

Abstract
This paper addresses the issue of the closure of the algebra of constraints for generic (cosmological) perturbations when taking into account simultaneously the two main corrections of effective loop quantum cosmology, namely the holonomy and the inverse-volume terms. Previous works on either the holonomy or the inverse-volume case are reviewed and generalized. In the inverse-volume case, we point out new possibilities. An anomaly-free solution including both corrections is found for perturbations, and the corresponding equations of motion are derived.

Keywords: loop quantum cosmology, loop quantum gravity, closure of algebra, anomaly resolution, cosmological perturbations, inverse-volume correction, holonomy correction
PACS numbers: 04.60.−m, 98.80.Qc

1. Introduction

Loop quantum gravity (LQG) is a tentative theory of quantum geometry that builds on both Einstein gravity and quantum physics without any fundamental new principle. Reviews can be found in [1]. Loop quantum cosmology (LQC) is basically the symmetry reduced version of LQG (see [2] for general introductions to LQC). At this stage a rigorous derivation of

LQC from the full mother theory is not yet possible. Rather, LQC mostly imports the main techniques of LQG in the cosmological sector. It relies on a kinematical Hilbert space that is different than in the Wheeler–DeWitt case. This so-called polymeric quantization has been shown to be unique when diffeomorphism invariance is rigorously imposed [3]. In this space, in order for the quantum version of the constraints to be well defined, an operator is associated not with the connection, but only with its holonomy. The basic variables of LQC are therefore the holonomy of the connection and its conjugate variable, the flux of the densitized triads.

At the effective level, it is believed that LQC can be modeled by two main corrections. In this framework, we restrain our study to an isotropic and homogeneous universe, considering neither possible backreaction effects [4], nor higher derivatives terms in the constraints via momentum terms [5] . Consequently, the quantum corrections studied here are the simplest homogeneous and isotropic corrections one can use. The inverse-volume correction [6] (or inverse-triad if one relaxes the isotropy hypothesis) provides natural cut-off functions of divergences for factors containing inverse components of densitized triads, arising from spatial discreteness. The holonomy correction [7] is instead associated with higher powers of intrinsic and extrinsic spatial curvature components stemming from the appearance of holonomies of the Ashtekar connection.

Here, we focus on the well known problem of the consistency of the effective theory of perturbations around an homogeneous and isotropic universe. By consistency, we mean that the evolution produced by the model should be consistent with the theory itself. This basically translates into the requirement that the Poisson bracket between two constraints should be proportional to another constraint. The coefficient of proportionality being a function of the fundamental variables, this makes the situation slightly more subtle than in usual field theories dealing with simple structure constants. Another important point is that the closure of the algebra of constraints [8] should even be considered off-shell [9].

To some extent, this paper is more technical than physical. The physical consequences will need more work to be fully explored. The aim of this work is not to describe all the steps of the derivations, but rather to give hints on the way it has been done. More information can also be found in the references given. Here, we first re-address the case of inverse-volume corrections. Previous results are revised. Then a reminder on the holonomy-corrected algebra is presented. Finally, the inverse-volume and holonomy case is studied and solved.

2. LQC perturbations

In the canonical formulation of general relativity, the Hamiltonian is a sum of three constraints:

$$H[N^i, N^a, N] = \frac{1}{2\kappa}\int_\Sigma \mathrm{d}^3x(N^iC_i + N^aC_a + NC) \approx 0,$$

where $\kappa = 8\pi G$, (N^i, N^a, N) are Lagrange multipliers, C_i is the Gauss constraint, C_a is the diffeomorphism constraint, and C is the scalar constraint. The sign '$\approx$' means in this context equality on the surface of constraints. The smeared constraints, whose expressions will be given later, are defined so that $H[N^i, N^a, N] = G[N^i] + D[N^a] + H[N]$:

$$\mathcal{C}_1 = G[N^i] = \frac{1}{2\kappa}\int_\Sigma \mathrm{d}^3x\, N^iC_i, \tag{2.1}$$

$$\mathcal{C}_2 = D[N^a] = \frac{1}{2\kappa}\int_\Sigma \mathrm{d}^3x\, N^aC_a, \tag{2.2}$$

$$\mathcal{C}_3 = H[N] = \frac{1}{2\kappa}\int_\Sigma \mathrm{d}^3x\, NC. \tag{2.3}$$

The full Hamiltonian is a total constraint which is vanishing for all multiplier functions (N^i, N^a, N).

As $H[N^i, N^a, N] \approx 0$ at any times, the time derivative of the Hamiltonian constraint is also weakly vanishing, $\dot{H}[N^i, N^a, N] \approx 0$. Due to the Hamilton equation $\dot{f} = \{f, H[M^i, M^a, M]\}$, one has

$$\{H[N^i, N^a, N], H[M^i, M^a, M]\} \approx 0. \tag{2.4}$$

Because of the linearity of the Poisson brackets, it is straightforward to find that the condition (2.4) is fulfilled if the smeared constraints belong to a first class algebra

$$\{\mathcal{C}_I, \mathcal{C}_J\} = f^K{}_{IJ}\big(A^j_b, E^a_i\big)\mathcal{C}_K, \tag{2.5}$$

also called 'algebra of deformation'. In equation (2.5), the $f^K{}_{IJ}(A^j_b, E^a_i)$ are structure functions which, in general, depend on the phase space (Ashtekar) variables (A^j_b, E^a_i). The algebra of constraints is fulfilled at the classical level due to general covariance. To prevent the system from escaping the surface of constraints, leading to an unphysical behavior, the algebra must also be closed at the quantum level. In addition, as stated in the introduction and as pointed out in [10], the algebra of quantum constraints should be strongly closed (that is should close *off-shell*). This means that the relation (2.5) should hold in the whole kinematical phase space, and not only on the surface of constraints. This should remain true after promoting the constraints to quantum operators.

In effective LQC, the constraints are quantum-modified and the corresponding Poisson algebra might not be closed:

$$\big\{\mathcal{C}^Q_I, \mathcal{C}^Q_J\big\} = f^K{}_{IJ}\big(A^j_b, E^a_i\big)\mathcal{C}^Q_K + \mathcal{A}_{IJ}, \tag{2.6}$$

where $\mathcal{A}_{IJ}$ stands for the anomaly term which can appear due to the quantum modifications. For consistency (closure of algebra), $\mathcal{A}_{IJ}$ is required to vanish. The condition $\mathcal{A}_{IJ} = 0$ induces some restrictions on the form of the quantum corrections. More importantly this requires the addition of counterterms that should vanish at the classical limit.

The question of the construction of an anomaly-free algebra of constraints is especially interesting to address in inhomogeneous LQC. Perturbations around the cosmological background are indeed responsible for structure formation in the Universe and are a promising way to try to test the theory. In the case of a flat FLRW background, the Ashtekar variables can be decomposed as

$$A^i_a = \gamma\bar{k}\delta^i_a + \delta A^i_a \quad \text{and} \quad E^a_i = \bar{p}\delta^a_i + \delta E^a_i, \tag{2.7}$$

where $\bar{k}$ and $\bar{p}$ parametrize the background phase space, and γ is the so-called Barbero–Immirzi parameter. The issue of anomaly freedom for the algebra of cosmological perturbations was extensively studied for inverse-volume corrections. It was shown that this requirement can be fulfilled for first order perturbations. This was derived for scalar [9, 11], vector [12] and tensor perturbations [13]. Based on the anomaly-free scalar perturbations, predictions for the power spectrum of cosmological perturbations were also performed [14]. This gave a chance to put constraints on some parameters of the model using observations of the cosmic microwave background (CMB) radiation [15]. The closure for holonomy-corrected vector modes was obtained in [16] and for holonomy-corrected scalar modes in [17] and [18]. Interestingly, it was pointed out that the requirement of consistency for scalar modes also modifies the algebra of tensor modes [19], leading to a possible effective change from hyperbolic to elliptic regime around the bounce with this deformed algebra [20]. It was also found recently that

under a change of variables, the usual non-deformed algebra of general relativity could be recovered [21].

The aim of this paper is to address the issue of anomaly freedom when both holonomy and inverse-volume corrections are included. Our path is not the only possible one. In [22], several criticisms were formulated. However it seems to us that, at this stage, this deformed algebra approach (see [20] for a review) is suitable enough to capture the main features of the full theory at an effective level [23].

3. Inverse-volume case

Whenever inverse powers of densitized triads components, that would classically diverge at singularities, appear, an effective quantum correction, called 'inverse-volume', is expected. A comprehensive treatment was performed in [9]. However, to prepare for the simultaneous treatment of both holonomy and inverse-volume terms, we re-visit and generalize this issue. In [9], where only inverse-volume corrections were studied, the authors basically considered only linear terms in the anomalies. However, in the case of holonomy corrections, it has been shown [17] that a more rigorous treatment can be done by solving the exact nonlinear anomalies. Therefore, in the following, even for the inverse-volume term alone, the anomalies will not be approximated and their nonlinear properties will be used to derive the general expressions for the counterterms. This is consistent with the holonomy case.

In the *semi-classical limit*, where quantum corrections are small, the inverse-volume correction can be expressed as [24]

$$\gamma_0(\bar{p}) = 1 + \frac{\lambda}{\bar{p}^n}, \tag{3.1}$$

where n is assumed to be positive. This is a meaningful assumption as long as one considers scales of inhomogeneities that are larger than the scale of discreteness. In the following, we will however try to find the expression of the counterterms whatever the behavior of the inverse-volume correction. We will therefore assume no particular expression and see that in order to close the algebra, this correction will have to fulfil some differential equations in agreement with what was obtained at the semi-classical limit.

In order to extract and resolve the anomalies, we will first express the modified constraints and add counterterms α_i and β_i in their expressions. We are here interested in the linear theory of perturbations, so the constraints will be considered up to the second order in perturbations only. Moreover, it has been shown previously [19] that the case of scalar perturbations is the more general one. For this reason we will focus on this one.

In LQG, the diffeomorphism constraints are expected not to be modified by the quantum corrections. In the gravitational sector, this leads to:

$$D_G[N^c] = \int \frac{\mathrm{d}^3x}{\kappa} \delta N^c \big[\bar{p}\partial_c \delta K^d_d - \bar{p}\partial_d \delta K^d_c - \bar{k}\partial_d \delta E^d_c\big], \tag{3.2}$$

where spatial and internal indices are set identically for clarity only, i.e. $\delta K^d_d \doteq \delta K^i_a \delta^a_i$ as they would not play any role in this study. The Hamiltonian constraint reads as

$$H^Q_G[N] = \frac{1}{2\kappa} \int \mathrm{d}^3x (\bar{N} + \delta N)(\gamma_0 + \gamma^{(1)} + \gamma^{(2)})\big[\mathcal{H}^{(0)}_G + \mathcal{H}^{(1)}_G + \mathcal{H}^{(2)}_G\big]. \tag{3.3}$$

Here, γ_0 is the homogeneous and isotropic part of the inverse-volume correction whereas $\gamma^{(1)}$ and $\gamma^{(2)}$ are the inhomogeneous parts, at first and second order in δE and δK. In the classical limit: $\gamma_0 = 1$, $\gamma^{(1)} = \gamma^{(2)} = 0$.

The zeroth, first and second orders of the gravitational Hamiltonian densities are:

$$\mathcal{H}_G^{(0)} = -6\sqrt{\bar{p}}\bar{k}^2, \tag{3.4}$$

$$\mathcal{H}_G^{(1)} = -4\sqrt{\bar{p}}(\bar{k}+\alpha_1)\delta K_d^d - \frac{1}{\sqrt{\bar{p}}}(\bar{k}^2+\alpha_2)\delta E_d^d + \frac{2}{\sqrt{\bar{p}}}(1+\alpha_3)\partial_c\partial^d\delta E_d^c, \tag{3.5}$$

$$\begin{aligned}\mathcal{H}_G^{(2)} = {}& \sqrt{\bar{p}}(1+\alpha_4)\delta K_c^d\delta K_d^c - \sqrt{\bar{p}}(1+\alpha_5)\big(\delta K_d^d\big)^2 \\ & -\frac{2}{\sqrt{\bar{p}}}(\bar{k}+\alpha_6)\delta E_d^c\delta K_c^d - \frac{1}{2\bar{p}^{\frac{3}{2}}}(\bar{k}^2+\alpha_7)\delta E_d^c\delta E_c^d \\ & + \frac{1}{4\bar{p}^{\frac{3}{2}}}(\bar{k}^2+\alpha_8)\big(\delta E_d^d\big)^2 - \frac{\delta^{jk}}{2\bar{p}^{\frac{3}{2}}}(1+\alpha_9)\big(\partial_c\delta E_j^c\big)\big(\partial_d\delta E_k^d\big).\end{aligned} \tag{3.6}$$

The very same approach should be applied to the matter sector. We assume throughout the paper that the matter consists of a single scalar field with a potential $V(\phi)$. It is interesting to notice that the approach used here leads to the same counterterms, whatever the chosen shape of the potential.

The diffeomorphism constraint is

$$D_m[N^c] = \int \mathrm{d}^3x\delta N^c\bar{\pi}\,\partial_c\delta\varphi, \tag{3.7}$$

and the Hamiltonian is

$$\begin{aligned}H_m[N] = {}& \int \mathrm{d}^3x\bar{N}\big[\nu_0\mathcal{H}_\pi^{(0)} + \mathcal{H}_\varphi^{(0)}\big] + \int \mathrm{d}^3x\delta N\big[\nu^{(1)}\mathcal{H}_\pi^{(0)} + \nu_0\mathcal{H}_\pi^{(1)} + \mathcal{H}_\varphi^{(1)}\big] \\ & + \int \mathrm{d}^3x\bar{N}\big[\nu^{(2)}\mathcal{H}_\pi^{(0)} + \nu^{(1)}\mathcal{H}_\pi^{(1)} + \nu_0\mathcal{H}_\pi^{(2)} + \sigma_0\mathcal{H}_\nabla^{(2)} + \mathcal{H}_\varphi^{(2)}\big].\end{aligned} \tag{3.8}$$

The ν and σ terms play roles similar to the ones of the γ terms in the gravitational sector. The different parts of the matter Hamiltonian read as:

$$\mathcal{H}_\pi^{(0)} = \frac{\bar{\pi}^2}{2\bar{p}^{\frac{3}{2}}}, \quad \mathcal{H}_\nabla^{(0)} = 0, \quad \mathcal{H}_\varphi^{(0)} = \bar{p}^{\frac{3}{2}}V, \tag{3.9}$$

$$\mathcal{H}_\pi^{(1)} = \frac{\bar{\pi}}{\bar{p}^{\frac{3}{2}}}(1+\beta_1)\delta\pi - \frac{\bar{\pi}^2}{2\bar{p}^{\frac{3}{2}}}(1+\beta_2)\frac{\delta E_d^d}{2\bar{p}}, \tag{3.10}$$

$$\mathcal{H}_\nabla^{(1)} = 0, \tag{3.11}$$

$$\mathcal{H}_\varphi^{(1)} = \bar{p}^{\frac{3}{2}}\partial_\varphi V(1+\beta_3)\delta\varphi + \bar{p}^{\frac{3}{2}}V(1+\beta_4)\frac{\delta E_d^d}{2\bar{p}}, \tag{3.12}$$

$$\begin{aligned}\mathcal{H}_\pi^{(2)} = {}& \frac{1}{2\bar{p}^{\frac{3}{2}}}(1+\beta_5)(\delta\pi)^2 - \frac{\bar{\pi}}{\bar{p}^{\frac{3}{2}}}(1+\beta_6)\delta\pi\frac{\delta E_d^d}{2\bar{p}} \\ & + \frac{\bar{\pi}^2}{2\bar{p}^{\frac{3}{2}}}(1+\beta_7)\frac{\big(\delta E_d^d\big)^2}{8\bar{p}^2} + \frac{\bar{\pi}^2}{2\bar{p}^{\frac{3}{2}}}(1+\beta_8)\frac{\delta E_d^c\delta E_c^d}{4\bar{p}^2},\end{aligned} \tag{3.13}$$

$$\mathcal{H}_\nabla^{(2)} = \frac{\sqrt{\bar{p}}}{2}(1+\beta_9)\partial_a\delta\varphi\partial^a\delta\varphi, \tag{3.14}$$

$$\mathcal{H}_{\varphi}^{(2)} = \frac{\bar{p}^{\frac{3}{2}}}{2}\partial_{\varphi\varphi}V(1+\beta_{10})(\delta\varphi)^2 + \bar{p}^{\frac{3}{2}}\partial_{\varphi}V(1+\beta_{11})\delta\varphi\frac{\delta E_d^d}{2\bar{p}}$$
$$+\bar{p}^{\frac{3}{2}}V(1+\beta_{12})\frac{\left(\delta E_d^d\right)^2}{8\bar{p}^2} - \bar{p}^{\frac{3}{2}}V(1+\beta_{13})\frac{\delta E_d^c\delta E_c^d}{4\bar{p}^2}. \tag{3.15}$$

The counterterms α_i and β_i are function of the homogeneous background. In the spirit of LQG where matter fields live on top of the gravitational field, we assume that both the gravitational counterterms and the matter ones do not depend on the matter fields themselves but only on $\bar{k}$ and $\bar{p}$. This assumption can be questioned but is reasonable at this stage of development of LQC. In the following, we will therefore consider

$$\alpha_i = \alpha_i[\bar{p},\bar{k}], \tag{3.16}$$

$$\beta_i = \beta_i[\bar{p},\bar{k}], \tag{3.17}$$

where $i \in N$ labels the counterterms and is not related to the indices of the variables described above.

In this work, we have considered that it should be also the case for the inverse-volume correction (this will also remain true for the holonomy correction), whose dependence should only be in terms of the gravitational variables, namely $\bar{k}$ and $\bar{p}$. It is therefore decomposed according to:

$$\gamma_0 = \gamma_0[\bar{p},\bar{k}], \tag{3.18}$$

$$\gamma^{(1)} = \gamma_1\delta E_d^d + \gamma_2\delta K_d^d, \tag{3.19}$$

$$\gamma^{(2)} = \gamma_3\delta E_d^c\delta E_c^d + \gamma_4\left(\delta E_d^d\right)^2 + \gamma_5\delta K_d^c\delta K_c^d + \gamma_6\left(\delta K_d^d\right)^2 + \gamma_7\delta E_d^c\delta K_c^d + \gamma_8\delta E_d^d\delta K_c^c, \tag{3.20}$$

and

$$\nu_0 = \nu_0[\bar{p},\bar{k}], \tag{3.21}$$

$$\nu^{(1)} = \nu_1\delta E_d^d + \nu_2\delta K_d^d, \tag{3.22}$$

$$\nu^{(2)} = \nu_3\delta E_d^c\delta E_c^d + \nu_4\left(\delta E_d^d\right)^2 + \nu_5\delta K_d^c\delta K_c^d + \nu_6\left(\delta K_d^d\right)^2 + \nu_7\delta E_d^c\delta K_c^d + \nu_8\delta E_d^d\delta K_c^c, \tag{3.23}$$

where all $\gamma_i = \gamma_i[\bar{p},\bar{k}]$ and $\nu_i = \nu_i[\bar{p},\bar{k}]$.

This parametrization can however be much simplified: it can be shown easily that, after replacing the former expressions in the constraint densities, γ_3, γ_4, γ_5, γ_6, γ_7, ν_1, ν_3, and ν_4 can be absorbed into the counterterms. This setting will have no physical consequences, only technical ones. In the case where the holonomy correction was considered with scalar perturbations [17], some unknown parameters were introduced in the definition of the correction, but after some calculations it was demonstrated that the correct counterterms will anyway compensate for these parameters, leading to physical results not depending on them. The very same thing happens here. We will therefore choose $\gamma_3 = \gamma_4 = \gamma_5 = \gamma_6 = \gamma_7 = \nu_1 = \nu_3 = \nu_4 = 0$ without loss of generality.

We should also notice that σ_0 appears only once together with $(1+\beta_9)$ in equation (3.8). This means that only the combination $\sigma_0(1+\beta_9)$ is of physical importance and not the individual factors. Because of this, we can absorb the fraction $\frac{\sigma_0}{\nu_0}$ into $(1+\beta_9)$, that is we can choose $\sigma_0 = \nu_0$ in equation (3.8).

3.1. Classical limit

When trying to close the algebra, it is mandatory to ensure that the classical limit is correct. This means that, when taking the limit

$$\bar{p} \to \infty, \tag{3.24}$$

the final expressions for the constraints should reduce to the classical ones. Inverse-volume corrections are indeed assumed to be important only for small volumes, i.e. for small $\bar{p} = \bar{a}^2$, where $\bar{a}$ is the scale factor of the homogeneous part of the metric.

The interpretation of this limit is not without problems. One can simply rescale $\bar{a}$, and therefore $\bar{p}$, by a change of coordinates which is pure gauge. But such a gauge transformation will also affect the other quantities. Roughly speaking, if one decides to apply this change of coordinate, some of the quantities among the observables will remain unchanged, scale invariant, when taking the limit $\bar{p} \to \infty$, but some others will be consequently diluted. In fact, the universe can tend to a Minkowski space just by such a transformation. We do not expect quantum effects in Minkowski space. We therefore assume that, at the classical limit, $\forall n \in N$

$$\gamma_0, \nu_0, \sigma_0 \to 1, \tag{3.25}$$

$$\gamma^{(1)}, \gamma^{(2)}, \nu^{(1)}, \nu^{(2)} \to 0, \tag{3.26}$$

$$\forall \gamma, \nu, \sigma, \quad \partial^n\gamma, \partial^n\nu, \partial^n\sigma \to 0, \tag{3.27}$$

and demand that

$$\alpha_i \to 0, \tag{3.28}$$

$$\beta_i \to 0, \tag{3.29}$$

$$\forall \alpha, \beta, \quad \partial^n\alpha, \partial^n\beta \to 0, \tag{3.30}$$

when $\bar{p} \to \infty$.

3.2. Calculation of the Poisson brackets

This section is devoted to the calculation of the different Poisson brackets involved in the final algebra. In order to maintain some clarity in the paper, we define:

$$\Lambda_\gamma = \frac{\bar{p}}{\gamma_0}\frac{\partial\gamma_0}{\partial\bar{p}}, \tag{3.31}$$

$$\Lambda_\nu = \frac{\bar{p}}{\nu_0}\frac{\partial\nu_0}{\partial\bar{p}}. \tag{3.32}$$

3.2.1. $\{H_G[N], D_G[N^c]\}$. After some calculations, the Poisson bracket can be decomposed as a sum of independent terms

$$\{H_G[N], D_G[N^c]\} = -H_G[\delta N^c \partial_c \delta N] \tag{3.33}$$

$$+ \gamma_0 \frac{\bar{N}}{\sqrt{\bar{p}}}\left(\bar{k}\alpha_4 + \alpha_6 - \frac{\bar{k}^2}{\gamma_0}\frac{\partial\gamma_0}{\partial\bar{k}}\right) D_G[N^c] \tag{3.34}$$

$$-\int \frac{\mathrm{d}^3x}{\kappa}\sqrt{\bar{p}}\gamma_0(\delta N\partial_c\delta N^c)\mathcal{A}_1 \tag{3.35}$$

$$+\int \frac{\mathrm{d}^3x}{\kappa}\bar{k}\sqrt{\bar{p}}\gamma_0\bar{N}\big(\delta N^c\partial_c\delta K_d^d\big)\mathcal{A}_2 \tag{3.36}$$

$$-\int \frac{\mathrm{d}^3x}{2\kappa}\frac{\bar{N}}{\sqrt{\bar{p}}}\gamma_0(\partial_c\delta N^c)\big(\delta E_d^d\big)\mathcal{A}_3 \tag{3.37}$$

$$+\int \frac{\mathrm{d}^3x}{2\kappa}\frac{\bar{N}}{\sqrt{\bar{p}}}\gamma_0(\partial_d\delta N^c)\big(\delta E_c^d\big)\mathcal{A}_4 \tag{3.38}$$

$$+\int \frac{\mathrm{d}^3x}{\kappa}\sqrt{\bar{p}}\bar{N}(\partial_d\delta N^d)\big(\partial^a\partial_c\delta E_a^c\big)\mathcal{A}_5 \tag{3.39}$$

$$+2\int \frac{\mathrm{d}^3x}{\kappa}\sqrt{\bar{p}}\gamma_0(\partial_c\partial^d\delta N)\big(\partial_d\delta N^c-(\partial_a\delta N^a)\delta_d^c\big)(1+\alpha_3) \tag{3.40}$$

$$+\int \frac{\mathrm{d}^3x}{\kappa}\sqrt{\bar{p}}\gamma_0\big(\partial_d\delta N^c-(\partial_a\delta N^a)\delta_d^c\big)\big(\partial^d\partial_a\delta E_c^a\big)(1+\alpha_9). \tag{3.41}$$

From this expression it can be noticed that:

- Equation (3.33) is simply the classical, anomaly-free, expression.
- Equation (3.34) is proportional to the gravitational diffeomorphism constraint which is an element of the algebra. However, it is not expected at the classical level and could be interpreted as an anomaly. Nevertheless, only the full algebra (taking also into account matter) is physically relevant. If the matter Poisson brackets exhibit a similar term with the matter diffeomorphism constraint, it might then not be an anomaly. At this stage, this term should be kept.
- $\mathcal{A}_1$, $\mathcal{A}_2$, $\mathcal{A}_3$, $\mathcal{A}_4$ and $\mathcal{A}_5$ are anomalies that must vanish. In other words, to close this part of the algebra we must have

$$\mathcal{A}_1=\mathcal{A}_2=\mathcal{A}_3=\mathcal{A}_4=\mathcal{A}_5=0. \tag{3.42}$$

- By integrating by part and due to the commutation property of the derivatives, it can be easily shown that equations (3.40) and (3.41) vanish for any values of α_3 and α_9. This is true here for the scalar perturbations, but it remains correct for any kind of perturbations [19].
- Moreover,

$$\mathcal{A}_5=(1+\alpha_3)\left(2\gamma_1+\frac{\bar{k}}{\bar{p}}\gamma_2\right) \tag{3.43}$$

exhibits the term $(1+\alpha_3)$. However, we cannot demand that $(1+\alpha_3)=0$ as this would violate the classical limit. Therefore, we must have

$$\gamma_1=-\frac{\bar{k}}{2\bar{p}}\gamma_2, \tag{3.44}$$

in order to cancel the anomaly.

After using equation (3.44), the remaining anomalies lead to:

$$\mathcal{A}_1 = 2\bar{k}\alpha_1 + \alpha_2, \tag{3.45}$$

$$\mathcal{A}_2 = \alpha_5 - \alpha_4 + \frac{1}{\gamma_0}\left[\left(3\bar{k} + 2\alpha_1 + \frac{\alpha_2}{\bar{k}}\right)\gamma_2 + 6\bar{k}\bar{p}\gamma_8\right], \tag{3.46}$$

$$\mathcal{A}_3 = \alpha_7 - \alpha_8 + \frac{1}{\gamma_0}[-(3\bar{k}^3 + 2\bar{k}^2\alpha_1 + \bar{k}\alpha_2)\gamma_2 + 6\bar{k}^3\bar{p}\gamma_8], \tag{3.47}$$

$$\mathcal{A}_4 = -2\bar{k}^2\alpha_4 - 4\bar{k}\alpha_6 + \alpha_7 + 2\bar{k}^2\Lambda_\gamma + \frac{2\bar{k}^3}{\gamma_0}\frac{\partial\gamma_0}{\partial\bar{k}}. \tag{3.48}$$

3.2.2. $\{H_G[N_1], H_G[N_2]\}$. The computation of this Poisson bracket leads to:

$$\{H_G[N_1], H_G[N_2]\} = \gamma_0^2(1+\alpha_3)(1+\alpha_4)D_G\left[\frac{\bar{N}}{\bar{p}}\partial^c(\delta N_2 - \delta N_1)\right] \tag{3.49}$$

$$+ \int \frac{\mathrm{d}^3x}{\kappa}\gamma_0^2\bar{N}\Delta(\delta N_2 - \delta N_1)\left(\delta K_d^d\right)\mathcal{A}_6 \tag{3.50}$$

$$+ \int \frac{\mathrm{d}^3x}{2\kappa}\gamma_0^2\bar{N}(\delta N_2 - \delta N_1)\left(\delta K_d^d\right)\mathcal{A}_7 \tag{3.51}$$

$$+ \int \frac{\mathrm{d}^3x}{2\kappa}\gamma_0^2\frac{\bar{N}}{\bar{p}}(\delta N_2 - \delta N_1)\left(\partial_c\partial^d\delta E_d^c\right)\mathcal{A}_8 \tag{3.52}$$

$$+ \int \frac{\mathrm{d}^3x}{4\kappa}\gamma_0^2\frac{\bar{N}}{\bar{p}}(\delta N_2 - \delta N_1)\left(\delta E_d^d\right)\mathcal{A}_9 \tag{3.53}$$

$$+ \int \frac{\mathrm{d}^3x}{2\kappa}\gamma_0\frac{\bar{N}}{\bar{p}}(\delta N_2 - \delta N_1)\left(\partial_c\partial^c\delta E_d^d\right)\mathcal{A}_{10} \tag{3.54}$$

$$+ \int \frac{\mathrm{d}^3x}{\kappa}\gamma_0\frac{\bar{N}}{\bar{p}}\Delta(\delta N_2 - \delta N_1)\left(\partial_c\partial^d\delta E_d^c\right)\mathcal{A}_{11}, \tag{3.55}$$

where Δ corresponds to the Laplacian (that is $\Delta X = \partial_c\partial^c X$).

From this expression one can notice that:

- Equation (3.49) is proportional to the gravitational diffeomorphism constraint, as it should be classically. However, the factor in front of the constraint now depends on the counterterms α_3 and α_4.
- We get a new set of anomalies that must vanish.

Two of the anomalies are

$$\mathcal{A}_{10} = -(1+\alpha_3)[(\bar{k}^2 + \alpha_2)\gamma_2 + 6\bar{k}^2\bar{p}\gamma_8], \tag{3.56}$$

$$\mathcal{A}_{11} = (1+\alpha_3)^2\gamma_2. \tag{3.57}$$

Together with equation (3.44), canceling these anomalies leads to

$$\gamma_1 = \gamma_2 = \gamma_8 = 0, \tag{3.58}$$

which consequently allows one to simplify the remaining anomalies such that:

$$\mathcal{A}_6 = (1+\alpha_3)(\alpha_5-\alpha_4), \tag{3.59}$$

$$\mathcal{A}_7 = -\bar{k}^2\alpha_4 + 3\bar{k}^2\alpha_5 + \alpha_2(2-\alpha_4+3\alpha_5) - 4\alpha_6(\bar{k}+\alpha_1) + 4\bar{k}\Lambda_\gamma(\bar{k}+2\alpha_1) \\ -2\bar{k}^2\frac{\partial\alpha_1}{\partial\bar{k}}(1+2\Lambda_\gamma) + 4\bar{k}\bar{p}\frac{\partial\alpha_1}{\partial\bar{p}}\left(2+\frac{\bar{k}}{\gamma_0}\frac{\partial\gamma_0}{\partial\bar{k}}\right), \tag{3.60}$$

$$\mathcal{A}_8 = -2(\bar{k}\alpha_4+\alpha_6) + 2\bar{k}\alpha_9 + 2\alpha_1(1+\alpha_9) - 4\bar{k}\Lambda_\gamma - 2\alpha_3(\bar{k}+\bar{k}\alpha_4+\alpha_6+2\bar{k}\Lambda_\gamma) \\ +\bar{k}^2\frac{\partial\alpha_3}{\partial\bar{k}}(1+2\Lambda_\gamma) - 2\bar{k}\bar{p}\frac{\partial\alpha_3}{\partial\bar{p}}\left(2+\frac{\bar{k}}{\gamma_0}\frac{\partial\gamma_0}{\partial\bar{k}}\right) + 2\frac{\bar{k}^2}{\gamma_0}\frac{\partial\gamma_0}{\partial\bar{k}}(1+\alpha_3) \tag{3.61}$$

and

$$\mathcal{A}_9 = 2(\bar{k}^2+\alpha_2)\alpha_6 + 2\alpha_1(\bar{k}^2-2\alpha_7+3\alpha_8) + 2\bar{k}(3\alpha_8-2\alpha_7+2\alpha_2\Lambda_\gamma) \\ -\bar{k}^2\frac{\partial\alpha_2}{\partial\bar{k}}(1+2\Lambda_\gamma) + 2\bar{k}\bar{p}\frac{\partial\alpha_2}{\partial\bar{p}}\left(2+\frac{\bar{k}}{\gamma_0}\frac{\partial\gamma_0}{\partial\bar{k}}\right) - 2\frac{\bar{k}^2}{\gamma_0}\frac{\partial\gamma_0}{\partial\bar{k}}(\bar{k}^2+\alpha_2). \tag{3.62}$$

3.2.3. $\{H_G[N], D_m[N^a]\}$. This Poisson bracket vanishes:

$$\{H_G[N], D_m[N^a]\} = 0, \tag{3.63}$$

and as a result of this

$$\{H_G[N], D_{\rm tot}[N^a]\} = \{H_G[N], D_G[N^a]\}. \tag{3.64}$$

3.2.4. $\{H_m[N], D_{\rm tot}[N^a]\}$. This Poisson bracket is given by:

$$\{H_m[N], D_{\rm tot}[N^a]\} = -H_m[\delta N^c\partial_c\delta N] \tag{3.65}$$

$$+\int {\rm d}^3x(\delta N\partial_c\delta N^c)(V\bar{p}^{\frac{3}{2}})\mathcal{A}_{12} \tag{3.66}$$

$$+\int {\rm d}^3x(\delta N\partial_c\delta N^c)\left(\frac{\nu_0\bar{\pi}^2}{2\bar{p}^{\frac{3}{2}}}\right)\mathcal{A}_{13} \tag{3.67}$$

$$+\int {\rm d}^3x\bar{N}(\partial_c\delta N^c)(V'\bar{p}^{\frac{3}{2}}\delta\varphi)\mathcal{A}_{14} \tag{3.68}$$

$$+\int {\rm d}^3x\bar{N}(\partial_c\delta N^c)\left(\frac{\nu_0\bar{\pi}}{\bar{p}^{\frac{3}{2}}}\delta\pi\right)\mathcal{A}_{15} \tag{3.69}$$

$$-\int {\rm d}^3x\bar{N}\left(\delta N^c\partial_d\delta E^d_c\right)\left(\frac{1}{2}V\sqrt{\bar{p}}\right)\mathcal{A}_{16} \tag{3.70}$$

$$+\int {\rm d}^3x\bar{N}\left(\delta N^c\partial_d\delta E^d_c\right)\left(\frac{\nu_0\bar{\pi}^2}{12\bar{p}^{\frac{5}{2}}}\right)\mathcal{A}_{17} \tag{3.71}$$

$$-\int {\rm d}^3x\bar{N}\left(\delta N^c\partial_c\delta E^d_d\right)\left(\frac{1}{2}V\sqrt{\bar{p}}\right)\mathcal{A}_{18} \tag{3.72}$$

$$+\int \mathrm{d}^3x\bar{N}\left(\delta N^c\partial_c\delta E^d_d\right)\left(\frac{\nu_0\bar{\pi}^2}{4\bar{p}^{\frac{5}{2}}}\right)\mathcal{A}_{19} \tag{3.73}$$

$$+\int \mathrm{d}^3x\bar{N}\left(\delta N^c\partial_d\delta K^d_c\right)\left(\frac{\bar{\pi}^2}{6\bar{p}^{\frac{3}{2}}}\right)\mathcal{A}_{20} \tag{3.74}$$

$$+\int \mathrm{d}^3x\bar{N}\left(\delta N^c\partial_c\delta K^d_d\right)\left(\frac{\bar{\pi}^2}{6\bar{p}^{\frac{3}{2}}}\right)\mathcal{A}_{21}. \tag{3.75}$$

In this case:

- As for equations (3.33), equation (3.65) is what is expected classically. Because only the total algebra is physically relevant, it should be noticed that $\{H_{\mathrm{tot}}, D_{\mathrm{tot}}\}$ will also be proportional to H_{tot}, as expected.
- Moreover, one can see that, after comparing with $\{H_G[N], D_G[N^c]\}$, there is no term proportional to the matter diffeomorphism constraint, in a similar way as the one in equation (3.34) for the gravitational sector. Therefore, one can conclude, as previously stated, that equation (3.34) corresponds also to an anomaly, $\mathcal{A}_{22}$, whose expression is given in the following.

The new anomalies are then:

$$\mathcal{A}_{12} = \beta_4, \tag{3.76}$$

$$\mathcal{A}_{13} = 2\beta_1 - \beta_2 + 2\bar{k}\frac{\nu_2}{\nu_0}, \tag{3.77}$$

$$\mathcal{A}_{14} = \beta_{11}, \tag{3.78}$$

$$\mathcal{A}_{15} = \beta_5 - \beta_6 + \bar{k}\frac{\nu_2}{\nu_0}(1+\beta_1), \tag{3.79}$$

$$\mathcal{A}_{16} = \beta_{13}, \tag{3.80}$$

$$\mathcal{A}_{17} = 3\beta_8 + 2\Lambda_\nu - 6\bar{k}\bar{p}\frac{\nu_7}{\nu_0}, \tag{3.81}$$

$$\mathcal{A}_{18} = \beta_{12} - \beta_{13} \tag{3.82}$$

$$\mathcal{A}_{19} = 2\beta_6 - \beta_7 - \beta_8 + \bar{k}\frac{\nu_2}{\nu_0}(1+\beta_2) - 2\bar{k}\bar{p}\frac{\nu_8}{\nu_0}, \tag{3.83}$$

$$\mathcal{A}_{20} = -6\bar{k}\nu_5 + 3\bar{p}\nu_7 - \frac{\partial\nu_0}{\partial\bar{k}}, \tag{3.84}$$

$$\mathcal{A}_{21} = 3(-1-2\beta_1+\beta_3)\nu_2 - 6\bar{k}\nu_6 - 3\bar{p}(\nu_7+2\nu_8) + \frac{\partial\nu_0}{\partial\bar{k}}, \tag{3.85}$$

$$\mathcal{A}_{22} = \bar{k}\alpha_4 + \alpha_6 - \frac{\bar{k}^2}{\gamma_0}\frac{\partial\gamma_0}{\partial\bar{k}}. \tag{3.86}$$

3.2.5. $\{H_m[N_1], H_m[N_2]\}$. This Poisson bracket is given by:

$$\{H_m[N_1], H_m[N_2]\} = v_0^2(1+\beta_1)(1+\beta_9)D_m\left[\frac{\bar{N}}{\bar{p}}\partial^a(\delta N_2 - \delta N_1)\right] \tag{3.87}$$

$$+\int \mathrm{d}^3x\bar{N}(\delta N_2 - \delta N_1)(\delta\varphi)(V''v_0\bar{\pi})\mathcal{A}_{23} \tag{3.88}$$

$$+\int \mathrm{d}^3x\bar{N}(\delta N_2 - \delta N_1)(\delta\varphi)\left(-\frac{\kappa}{2}VV'\bar{p}^2\right)\mathcal{A}_{24} \tag{3.89}$$

$$+\int \mathrm{d}^3x\bar{N}(\delta N_2 - \delta N_1)(\delta\varphi)\left(\frac{\kappa}{12p}v_0V'\bar{\pi}^2\right)\mathcal{A}_{25} \tag{3.90}$$

$$+\int \mathrm{d}^3x\bar{N}(\delta N_2 - \delta N_1)(\delta\pi)(v_0V')\mathcal{A}_{26} \tag{3.91}$$

$$+\int \mathrm{d}^3x\bar{N}(\delta N_2 - \delta N_1)(\delta\pi)\left(\frac{\kappa}{2\bar{p}}v_0V\bar{\pi}\right)\mathcal{A}_{27} \tag{3.92}$$

$$+\int \mathrm{d}^3x\bar{N}(\delta N_2 - \delta N_1)(\delta\pi)\left(-\kappa\frac{v_0}{12\bar{p}^4}\bar{\pi}^3\right)\mathcal{A}_{28} \tag{3.93}$$

$$+\int \mathrm{d}^3x\bar{N}(\delta N_2 - \delta N_1)\left(\delta E_d^d\right)\left(\frac{\kappa}{4}V^2\bar{p}\right)\mathcal{A}_{29} \tag{3.94}$$

$$+\int \mathrm{d}^3x\bar{N}(\delta N_2 - \delta N_1)\left(\delta E_d^d\right)\left(\frac{v_0}{2\bar{p}}V\bar{\pi}\right)\mathcal{A}_{30} \tag{3.95}$$

$$+\int \mathrm{d}^3x\bar{N}(\delta N_2 - \delta N_1)\left(\delta E_d^d\right)\left(\frac{\kappa v_0}{16\bar{p}^2}m^2\bar{\pi}^2\bar{\varphi}^2\right)\mathcal{A}_{31} \tag{3.96}$$

$$+\int \mathrm{d}^3x\bar{N}(\delta N_2 - \delta N_1)\left(\delta E_d^d\right)\left(\frac{\kappa v_0^2}{48\bar{p}^5}\bar{\pi}^4\right)\mathcal{A}_{32} \tag{3.97}$$

$$+\int \mathrm{d}^3x\bar{N}(\delta N_2 - \delta N_1)\left(\delta K_d^d\right)\left(\frac{\kappa}{3\bar{p}}V\bar{\pi}^2\right)\mathcal{A}_{33} \tag{3.98}$$

$$+\int \mathrm{d}^3x\bar{N}(\delta N_2 - \delta N_1)\left(\delta K_d^d\right)(V'\bar{\pi})\mathcal{A}_{34} \tag{3.99}$$

$$+\int \mathrm{d}^3x\bar{N}(\delta N_2 - \delta N_1)\left(\delta K_d^d\right)\left(\frac{\kappa}{24\bar{p}^4}\bar{\pi}^4\right)\mathcal{A}_{35}. \tag{3.100}$$

It should be noticed that:

- equation (3.87) is equivalent to equation (3.49) but with a different factor in front. In order to get them compatible, we can re-express equation (3.87) as

$$v_0^2(1+\beta_1)(1+\beta_9)D_m = \gamma_0^2(1+\alpha_3)(1+\alpha_4)D_m + \mathcal{A}_{36}\,D_m, \tag{3.101}$$

where we have introduced a new anomaly $\mathcal{A}_{36}$.

The anomalies from this Poisson bracket are then given by:

$$\mathcal{A}_{23} = -\beta_3 + \beta_{10} + \beta_1 + \beta_1\beta_{10}, \tag{3.102}$$

$$\mathcal{A}_{24} = \frac{\partial \beta_3}{\partial \bar{k}}, \tag{3.103}$$

$$\mathcal{A}_{25} = (3 - 2\Lambda_\nu)\frac{\partial \beta_3}{\partial \bar{k}} + \frac{1}{\nu_0}\frac{\partial \nu_0}{\partial \bar{k}}\left(3(1+\beta_3) + 2\bar{p}\frac{\partial \beta_3}{\partial \bar{p}}\right) - 9\frac{\nu_2}{\nu_0}(1+\beta_{11}), \tag{3.104}$$

$$\mathcal{A}_{26} = \beta_1 - \beta_5 - \beta_3 - \beta_3\beta_5, \tag{3.105}$$

$$\mathcal{A}_{27} = -\frac{\partial \beta_1}{\partial \bar{k}} + 3\frac{\nu_2}{\nu_0}(1+\beta_1)(1+\beta_4) - (1+\beta_1)\frac{1}{\nu_0}\frac{\partial \nu_0}{\partial \bar{k}} \tag{3.106}$$

$$\mathcal{A}_{28} = (-3 + 2\Lambda_\nu)\frac{\partial \beta_1}{\partial \bar{k}} - \frac{2p}{\nu_0}\frac{\partial \nu_0}{\partial \bar{k}}\frac{\partial \beta_1}{\partial \bar{p}} + 9\frac{\nu_2}{\nu_0}(\beta_1 + \beta_2 + \beta_1\beta_2 - \beta_6), \tag{3.107}$$

$$\mathcal{A}_{29} = -\frac{\partial \beta_4}{\partial \bar{k}}, \tag{3.108}$$

$$\mathcal{A}_{30} = \beta_1 - \beta_2 + \beta_3 - \beta_4 + (1+\beta_3)\beta_6 + (1+\beta_1)\beta_{11}, \tag{3.109}$$

$$\begin{aligned}\mathcal{A}_{31} = {} & \frac{\partial \beta_2}{\partial \bar{k}} + \left(1 + \frac{2p}{3\nu_0}\frac{\partial \nu_0}{\partial \bar{p}}\right)\frac{\partial \beta_4}{\partial \bar{k}} + \frac{1}{3\nu_0}\frac{\partial \nu_0}{\partial \bar{k}}\left(4 + 3\beta_2 + \beta_4 + 2\bar{p}\frac{\partial \beta_4}{\partial \bar{p}}\right) \\ & + \frac{\nu_2}{\nu_0}(-4 - 3\beta_2 - 3\beta_4 - 3\beta_2\beta_4 - 3\beta_{12} + 2\beta_{13}) + \frac{2\bar{p}}{\nu_0}(\nu_7 + 3\nu_8)(1+\beta_4),\end{aligned} \tag{3.110}$$

$$\begin{aligned}\mathcal{A}_{32} = {} & (3 - 2\Lambda_\nu)\frac{\partial \beta_2}{\partial \bar{k}} + \frac{1}{2\nu_0}\frac{\partial \nu_0}{\partial \bar{k}}\left(1 + \beta_2 + \bar{p}\frac{\partial \beta_2}{\partial \bar{p}}\right) + \frac{3\nu_2}{\nu_0}\left(-2 + 6\beta_2 + 3\beta_2^2 - 3\beta_7 - 2\beta_8\right) \\ & - \frac{6\bar{p}}{\nu_0}(\nu_7 + 3\nu_8)(1+\beta_2),\end{aligned} \tag{3.111}$$

$$\mathcal{A}_{33} = (2\nu_5 + 6\nu_6)(1+\beta_4) - \frac{\partial \nu_2}{\partial \bar{k}}, \tag{3.112}$$

$$\mathcal{A}_{34} = -\nu_2(\beta_1 + \beta_2 + \beta_1\beta_2), \tag{3.113}$$

$$\begin{aligned}\mathcal{A}_{35} = {} & 9\nu_2^2(1+\beta_1) - 6\nu_0(\nu_5 + 3\nu_6)(1+\beta_2) - 6\nu_2\bar{p}(\nu_7 + 3\nu_8) \\ & + \left(-3\nu_2 + 2\bar{p}\frac{\partial \nu_2}{\partial \bar{p}}\right)\frac{\partial \nu_0}{\partial \bar{k}} + (3 - 2\Lambda_\nu)\nu_0\frac{\partial \nu_2}{\partial \bar{k}},\end{aligned} \tag{3.114}$$

and

$$\mathcal{A}_{36} = \gamma_0^2(1+\alpha_3)(1+\alpha_4) - \nu_0^2(1+\beta_1)(1+\beta_9). \tag{3.115}$$

3.2.6. $\{H_G[N_1], H_m[N_2]\} - (N_1 \leftrightarrow N_2)$. This Poisson bracket reads as:

$$\{H_G[N_1], H_m[N_2]\} - (N_1 \leftrightarrow N_2) = \int \mathrm{d}^3x\bar{N}(\delta N_2 - \delta N_1)(\delta\pi)\left(-\frac{\gamma_0}{2\bar{p}^2}\bar{\pi}\nu_0\right)\mathcal{A}_{37} \tag{3.116}$$

$$+ \int \mathrm{d}^3x\bar{N}\Delta(\delta N_2 - \delta N_1)(\delta\pi)\left(\frac{\gamma_0}{\bar{p}^2}\bar{\pi}\right)\mathcal{A}_{38} \tag{3.117}$$

$$+ \int \mathrm{d}^3x\bar{N}(\delta N_2 - \delta N_1)(\delta\varphi)\left(\frac{\gamma_0}{2}V'\bar{p}\right)\mathcal{A}_{39} \tag{3.118}$$

$$+ \int \mathrm{d}^3x\bar{N}(\delta N_2 - \delta N_1)\left(\delta K_d^d\right)\left(\frac{\gamma_0}{12\bar{p}^2}\nu_0\bar{\pi}^2\right)\mathcal{A}_{40} \tag{3.119}$$

$$+ \int \mathrm{d}^3x\bar{N}(\delta N_2 - \delta N_1)\left(\delta K_d^d\right)\left(\frac{\gamma_0}{2}\bar{p}V\right)\mathcal{A}_{41} \tag{3.120}$$

$$+ \int \mathrm{d}^3x\bar{N}(\delta N_2 - \delta N_1)\left(\delta E_d^d\right)\left(\frac{\gamma_0}{12\bar{p}^3}\frac{\nu_0}{2}\bar{\pi}^2\right)\mathcal{A}_{42} \tag{3.121}$$

$$+ \int \mathrm{d}^3x\bar{N}(\delta N_2 - \delta N_1)\left(\delta E_d^d\right)\left(\frac{\gamma_0}{4}V\right)\mathcal{A}_{43} \tag{3.122}$$

$$+ \int \mathrm{d}^3x\bar{N}(\delta N_2 - \delta N_1)\left(\partial_c\partial^d\delta E_d^c\right)\left(\frac{\gamma_0}{12\bar{p}^3}\bar{\pi}^2\right)\mathcal{A}_{44} \tag{3.123}$$

$$+ \int \mathrm{d}^3x\bar{N}(\delta N_2 - \delta N_1)\left(\partial_c\partial^d\delta E_d^c\right)\left(\frac{\gamma_0}{2}V\right)\mathcal{A}_{45} \tag{3.124}$$

$$- \int \mathrm{d}^3x\bar{N}(\delta N_2 - \delta N_1)\left(\Delta\delta E_d^d\right)\left(\frac{\gamma_0}{4\bar{p}^3}\bar{\pi}^2\right)\mathcal{A}_{46} \tag{3.125}$$

$$+ \int \mathrm{d}^3x\bar{N}(\delta N_2 - \delta N_1)\left(\partial_c\partial^d\delta K_d^c\right)\left(\frac{\gamma_0}{\bar{p}^2}\bar{\pi}^2\right)\mathcal{A}_{47} \tag{3.126}$$

$$+ \int \mathrm{d}^3x\bar{N}(\delta N_2 - \delta N_1)\left(\Delta\delta K_d^d\right)\left(\frac{\gamma_0}{\bar{p}^2}\bar{\pi}^2\right)\mathcal{A}_{48}. \tag{3.127}$$

After using equation (3.58), we find that

$$\mathcal{A}_{38} = (1+\alpha_3)(1+\beta_1)\nu_2, \tag{3.128}$$

$$\mathcal{A}_{46} = (1+\alpha_3)(1+\beta_2)\nu_2, \tag{3.129}$$

$$\mathcal{A}_{47} = (1+\alpha_3)\nu_5, \tag{3.130}$$

$$\mathcal{A}_{48} = (1+\alpha_3)\nu_6. \tag{3.131}$$

Demanding that the above anomalies do vanish, while respecting the classical limit, leads to:

$$\nu_2 = \nu_5 = \nu_6 = 0. \tag{3.132}$$

Using equations (3.58) and (3.132) leads to the remaining anomalies:

$$\mathcal{A}_{37} = 6\alpha_1 - 6\bar{k}\beta_1 + 6(\bar{k}+\alpha_1)\beta_6 - \bar{k}^2(1+2\Lambda_\gamma)\frac{\partial\beta_1}{\partial\bar{k}} + 2\bar{k}\bar{p}\frac{\partial\beta_1}{\partial\bar{p}}\left(2+\frac{\bar{k}}{\gamma_0}\frac{\partial\gamma_0}{\partial\bar{k}}\right) + (1+\beta_1)\left(4\bar{k}\Lambda_\nu - \frac{\bar{k}^2}{\gamma_0}(3-2\Lambda_\nu)\frac{\partial\gamma_0}{\partial\bar{k}}\right) - \frac{\bar{k}^2}{\nu_0}\frac{\partial\nu_0}{\partial\bar{k}}(1+\beta_1)(1+2\Lambda_\gamma), \tag{3.133}$$

$$\mathcal{A}_{39} = 6(\bar{k}+\alpha_1)(1+\beta_{11}) + \bar{k}^2(1+2\Lambda_\gamma)\frac{\partial\beta_3}{\partial\bar{k}} - \bar{k}\left(2+\frac{\bar{k}}{\gamma_0}\frac{\partial\gamma_0}{\partial\bar{k}}\right)\left(3(1+\beta_3)+2\bar{p}\frac{\partial\beta_3}{\partial\bar{p}}\right), \tag{3.134}$$

$$\mathcal{A}_{40} = 6\beta_2 + (9\alpha_5 - 3\alpha_4)(1+\beta_2) + 4\Lambda_\nu + \left(\frac{(4\Lambda_\nu - 6)}{\gamma_0}\frac{\partial\gamma_0}{\partial\bar{k}} + \frac{12\bar{p}}{\nu_0}(\nu_7+3\nu_8) - \frac{2+4\Lambda_\gamma}{\nu_0}\right)(\bar{k}+\alpha_1) + (4\Lambda_\nu - 6)\frac{\partial\alpha_1}{\partial\bar{k}} - \frac{4\bar{p}}{\nu_0}\frac{\partial\nu_0}{\partial\bar{k}}\frac{\partial\alpha_1}{\partial\bar{p}}, \tag{3.135}$$

$$\mathcal{A}_{41} = -2\beta_4 + (\alpha_4 - 3\alpha_5)(1+\beta_4) + 2\frac{\partial\alpha_1}{\partial\bar{k}} + \frac{2}{\gamma_0}(\bar{k}+\alpha_1)\frac{\partial\gamma_0}{\partial\bar{k}}, \tag{3.136}$$

$$\mathcal{A}_{42} = -3\bar{k}^2\frac{\partial\beta_2}{\partial\bar{k}}(1+2\Lambda_\gamma) + 6(\bar{k}+\alpha_1)(5+3\beta_7+2\beta_8) + 6(\bar{k}+\alpha_6)(1+\beta_2) + 3\bar{k}\left(2+\frac{\bar{k}}{\gamma_0}\frac{\partial\gamma_0}{\partial\bar{k}}\right)\left((1+\beta_2)(-5+2\Lambda_\nu) + 2\bar{p}\frac{\partial\beta_2}{\partial\bar{p}}\right) + \frac{(-3+2\Lambda_\nu)}{\gamma_0}\frac{\partial}{\partial\bar{k}}(\gamma_0(\alpha_2+\bar{k}^2)) - \frac{6\bar{p}}{\nu_0}(\nu_7+3\nu_8)(\bar{k}^3+\alpha_2) - \frac{1}{\nu_0}\frac{\partial\nu_0}{\partial\bar{k}}\left(2k^2 - \alpha_2 + 3k^2\beta_2 + 2p\frac{\partial\alpha_2}{\partial\bar{p}}\right) - \frac{2\Lambda_\gamma}{\nu_0}\frac{\partial\nu_0}{\partial\bar{k}}(4k^2+\alpha_2+3k^2\beta_2), \tag{3.137}$$

$$\mathcal{A}_{43} = -2(\bar{k}+\alpha_6)(1+\beta_4) + (\bar{k}+\alpha_1)(-4\beta_{13}+6\beta_{12}+2) - \bar{k}\left(2+\frac{\bar{k}}{\gamma_0}\frac{\partial\gamma_0}{\partial\bar{k}}\right)\left(\beta_4 + 2\bar{p}\frac{\partial\beta_4}{\partial\bar{p}}\right) + \bar{k}^2\frac{\partial\beta_4}{\partial\bar{k}}(1+2\Lambda_\gamma) + \frac{1}{\gamma_0}\frac{\partial}{\partial\bar{k}}(\gamma_0\alpha_2), \tag{3.138}$$

$$\mathcal{A}_{44} = \frac{\nu_0(3-2\Lambda_\nu)}{\gamma_0}\frac{\partial}{\partial\bar{k}}\gamma_0(1+\alpha_3) + \frac{\partial\nu_0}{\partial\bar{k}}\left((2\Lambda_\gamma - 1)(1+\alpha_3) + 2p\frac{\partial\alpha_3}{\partial\bar{p}}\right) + 6p(\nu_7+\nu_8)(1+\alpha_3), \tag{3.139}$$

and

$$\mathcal{A}_{45} = -\frac{1}{\gamma_0}\frac{\partial}{\partial\bar{k}}\gamma_0(1+\alpha_3). \tag{3.140}$$

3.2.7. $\{D_{\text{tot}}[N^a], D_{\text{tot}}[N^b]\}$. Finally,

$$\{D_{\text{tot}}[N^a], D_{\text{tot}}[N^b]\} = 0. \tag{3.141}$$

3.3. Solution after canceling the anomalies

After solving the anomalies, it can be found that:

$$\gamma_1 = \gamma_2 = \gamma_8 = 0, \tag{3.142}$$

$$\nu_2 = \nu_3 = \nu_5 = \nu_6 = \nu_7 = \nu_8 = 0. \tag{3.143}$$

As pointed out before, the remaining γ_i, ν_i, $i \neq 0$, can safely be absorbed into the counterterms α_i and β_i. This leads to an interesting situation: only the corrections expressed with the homogeneous background corrections will affect the algebra and therefore the equations of motion. In other words, the whole effect of the corrections in this work is obtained only by the zeroth order. Nevertheless, this may not be true anymore when the higher order derivatives will be taken into account.

We also find that

$$\frac{\partial \nu_0}{\partial \bar{k}} = 0, \tag{3.144}$$

that is, ν has to depend only on $\bar{p}$.

In order to clarify the equations in the following, we will use the convention

$$\Gamma_{\bar{k}} = \frac{\bar{k}}{\gamma_0}\frac{\partial \gamma_0}{\partial \bar{k}}, \tag{3.145}$$

$$\Gamma_{\bar{k},2} = \frac{\bar{k}^2}{\gamma_0}\frac{\partial^2 \gamma_0}{\partial \bar{k}^2}, \tag{3.146}$$

$$\Sigma_{\bar{p}} = \frac{9 - 9\Lambda_\nu + 2\Lambda_\nu^2 + 2p\frac{\mathrm{d}\Lambda_\nu}{\mathrm{d}\bar{p}}}{2\nu_0(3-\Lambda_\nu)^2}. \tag{3.147}$$

It should be noticed that, because of equation (3.144), $\Sigma_{\bar{p}}$ only depends on $\bar{p}$. In the classical limit $\Gamma_{\bar{k}}, \Gamma_{\bar{k},2} \to 0$ and $\Sigma_{\bar{p}} \to \frac{1}{2}$.

After having solved all the previous anomalies without any ambiguity, the 'final' expressions for the counterterms are now given by:

$$\alpha_1 = \bar{k}(-1 + (2 + \Gamma_{\bar{k}})\Sigma_{\bar{p}}), \tag{3.148}$$

$$\alpha_2 = -2\bar{k}^2(-1 + (2 + \Gamma_{\bar{k}})\Sigma_{\bar{p}}), \tag{3.149}$$

$$\alpha_3 = -1 + \frac{f_1[\bar{p}]}{\gamma_0}, \tag{3.150}$$

$$\alpha_4 = -1 + (2 + 4\Gamma_{\bar{k}} + \Gamma_{\bar{k},2})\Sigma_{\bar{p}}, \tag{3.151}$$

$$\alpha_5 = -1 + (2 + 4\Gamma_{\bar{k}} + \Gamma_{\bar{k},2})\Sigma_{\bar{p}}, \tag{3.152}$$

$$\alpha_6 = \bar{k}(1 + \Gamma_{\bar{k}} - (2 + 4\Gamma_{\bar{k}} + \Gamma_{\bar{k},2})\Sigma_{\bar{p}}), \tag{3.153}$$

$$\alpha_7 = 2\bar{k}^2(1 - \Lambda_\gamma + \Gamma_{\bar{k}} - (2 + 4\Gamma_{\bar{k}} + \Gamma_{\bar{k},2})\Sigma_{\bar{p}}), \tag{3.154}$$

$$\alpha_8 = 2\bar{k}^2(1 - \Lambda_\gamma + \Gamma_{\bar{k}} - (2 + 4\Gamma_{\bar{k}} + \Gamma_{\bar{k},2})\Sigma_{\bar{p}}), \tag{3.155}$$

$$\alpha_9 = -1 + \frac{1}{2\gamma_0 \Sigma_{\bar{p}}} \left(f_1[\bar{p}] + 2\bar{p} \frac{\mathrm{d}f_1[\bar{p}]}{\mathrm{d}\bar{p}} \right), \tag{3.156}$$

and

$$\beta_1 = -\frac{\Lambda_\nu}{3}, \tag{3.157}$$

$$\beta_2 = -2\frac{\Lambda_\nu}{3} \tag{3.158}$$

$$\beta_3 = -1 + \frac{3}{\nu_0(3 - \Lambda_\nu)} \tag{3.159}$$

$$\beta_4 = 0, \tag{3.160}$$

$$\beta_5 = -1 + \frac{\nu_0(3 - \Lambda_\nu)^2}{9}, \tag{3.161}$$

$$\beta_6 = -1 + \frac{\nu_0(3 - \Lambda_\nu)^2}{9}, \tag{3.162}$$

$$\beta_7 = \frac{2(3 - \Lambda_\nu)(3(\nu_0 - 1) - \Lambda_\nu \nu_0)}{9}, \tag{3.163}$$

$$\beta_8 = -2\frac{\Lambda_\nu}{3}, \tag{3.164}$$

$$\beta_9 = -1 + \frac{3\gamma_0(2 + 4\Gamma_{\bar{k}} + \Gamma_{\bar{k},2})\Sigma_{\bar{p}}}{\nu_0^2(3 - \Lambda_\nu)} f_1[\bar{p}], \tag{3.165}$$

$$\beta_{10} = -1 + \frac{9}{\nu_0(3 - \Lambda_\nu)^2}, \tag{3.166}$$

$$\beta_{11} = 0, \tag{3.167}$$

$$\beta_{12} = 0, \tag{3.168}$$

$$\beta_{13} = 0, \tag{3.169}$$

where $f_1[\bar{p}]$ is an unknown function of $\bar{p}$. In order for all the counterterms to vanish at the classical limit, we require that $f_1[\bar{p}]$ tends towards 1 and its derivatives towards 0 in this limit.

Some preliminary comments can be made at this stage:

- Firstly, if we consider the different total Poisson brackets, we have now:

$$\left\{ D_{\mathrm{tot}}\left[N_1^c\right], D_{\mathrm{tot}}\left[N_2^d\right] \right\} = 0, \tag{3.170}$$

$$\{H_{\mathrm{tot}}[N], D_{\mathrm{tot}}[N^c]\} = -H_{\mathrm{tot}}[\delta N^c \partial_c \delta N], \tag{3.171}$$

$$\{H_{\mathrm{tot}}[N_1], H_{\mathrm{tot}}[N_2]\} = \Omega D_{\mathrm{tot}}\left[\frac{\bar{N}}{\bar{p}} \partial^c (\delta N_2 - \delta N_1) \right], \tag{3.172}$$

where Ω corresponds to the structure function of the modified algebra, given theoretically by

$$\Omega = \gamma_0^2(1+\alpha_3)(1+\alpha_4) \tag{3.173}$$

$$= \nu_0^2(1+\beta_1)(1+\beta_9). \tag{3.174}$$

After using the solutions for the counterterms, we find that in the case of the inverse-volume corrections, Ω can be expressed as

$$\begin{aligned}\Omega &= \gamma_0(2+4\Gamma_{\bar{k}}+\Gamma_{\bar{k},2})\Sigma_{\bar{p}}f_1[\bar{p}]\\ &= \left(\frac{\partial^2}{\partial\bar{k}^2}(\bar{k}^2\gamma_0)\right)\Sigma_{\bar{p}}f_1[\bar{p}].\end{aligned} \tag{3.175}$$

So far, nothing conclusive can be said about the evolution of the structure function with respect to the evolution of the universe. One would need the full theory. Nevertheless, it can be seen here that, as for the holonomy correction, the general expression of Ω has a possible dependence on $\bar{k}$ or $\bar{p}$ and it is possible that when both corrections will be taken into account simultaneously, a compatible structure function will emerge from the formalism. This would allow one to study a cosmological scenario which could be close to, or consistent with, the one derived from LQG. Moreover, in this case, it will be interesting to compare the results with what was predicted in [22].

- Secondly, after having derived the counterterms in equations (3.142)–(3.169), one additional equation remains: one can notice that $\mathcal{A}_5$ and $\mathcal{A}_7$ appear to be equivalent up to a factor $-k$:

$$\mathcal{A}_7 \equiv -\bar{k}\mathcal{A}_5 = 0, \tag{3.176}$$

and requiring that these two anomalies vanish generates a differential equation relating γ_0 to ν_0, which after some reformulation, becomes:

$$\bar{p}\frac{\partial}{\partial\bar{p}}\ln\left[\gamma_0(2+\Gamma_k)\Sigma_{\bar{p}}^2\right] = \bar{k}\frac{(1-\Lambda_\gamma)}{(2+\Gamma_{\bar{k}})}\frac{\partial}{\partial\bar{k}}\ln\left[\frac{1-\Lambda_\gamma}{\gamma_0(2+\Gamma_{\bar{k}})^2}\right]. \tag{3.177}$$

This equation can be regarded as an extra constraint on the expression of the inverse-volume corrections, as it has to be fulfilled in order for the total algebra to be closed. Moreover, in order to solve it, one needs either an additional assumption, or the expression from the full theory. In the next section, we will play with the dependence of γ_0 as the required extra assumption and see what the approach has to say.

3.4. Solution after further assumptions

So far in this study the only thing that determines the behavior of the inverse-volume corrections is equation (3.177), which is a result of the closure of the algebra, and the fact that we require appropriate conditions on γ_0 and ν_0 in the classical limit ($\gamma_0 \to 1$ and $\nu_0 \to 1$). These constraints are not enough to fully determine the shape of the inverse-volume corrections, therefore further inputs must come from the full theory. Nevertheless, it can be interesting to make some assumptions and see what they do imply. In this section, we will first make some assumptions on the dependence of γ_0 on $\bar{k}$ and $\bar{p}$ and see what are the consequences on Ω, and then, reverse the logic.

3.4.1. Case where $\gamma_0 = \gamma_0[\bar{p}]$ only. In most of the literature, the inverse-volume corrections are assumed to depend only on $\bar{p}$. In this case, equation (3.177) reduces to

$$\gamma_0 \Sigma_{\bar{p}}^2 = \text{constant}. \tag{3.178}$$

Since $\gamma_0 \to 1$ and $\Sigma_{\bar{p}} \to \frac{1}{2}$ in the classical limit, we must have

$$\Sigma_{\bar{p}} = \frac{1}{2\sqrt{\gamma_0}}, \tag{3.179}$$

which, after using the definition of $\Sigma_{\bar{p}}$ given by equation (3.147), leads to a differential equation relating γ_0 with ν_0 (both depending only on $\bar{p}$) such that

$$9 - 9\Lambda_\nu + 2\Lambda_\nu^2 - \frac{\nu_0(3-\Lambda_\nu)^2}{\sqrt{\gamma_0}} + 2p\frac{\mathrm{d}\Lambda_\nu}{\mathrm{d}\bar{p}} = 0. \tag{3.180}$$

This equation is complicated and requires to know at least the expression for one correction to be solved. Nevertheless, solving all the anomalies leads to:

$$\alpha_1 = \bar{k}\left(-1 + \frac{1}{\sqrt{\gamma_0}}\right), \tag{3.181}$$

$$\alpha_2 = 2\bar{k}^2\left(1 - \frac{1}{\sqrt{\gamma_0}}\right), \tag{3.182}$$

$$\alpha_3 = -1 + \frac{f_1[\bar{p}]}{\gamma_0}, \tag{3.183}$$

$$\alpha_4 = -1 + \frac{1}{\sqrt{\gamma_0}}, \tag{3.184}$$

$$\alpha_5 = -1 + \frac{1}{\sqrt{\gamma_0}}, \tag{3.185}$$

$$\alpha_6 = \bar{k}\left(1 - \frac{1}{\sqrt{\gamma_0}}\right), \tag{3.186}$$

$$\alpha_7 = 2\bar{k}^2\left(1 - \frac{1}{\sqrt{\gamma_0}} - \Lambda_\gamma\right), \tag{3.187}$$

$$\alpha_8 = 2\bar{k}^2\left(1 - \frac{1}{\sqrt{\gamma_0}} - \Lambda_\gamma\right), \tag{3.188}$$

$$\alpha_9 = -1 + \frac{1}{\sqrt{\gamma_0}}\left(f_1[\bar{p}] + 2\bar{p}\frac{\mathrm{d}f_1[\bar{p}]}{\mathrm{d}\bar{p}}\right), \tag{3.189}$$

and

$$\beta_9 = -1 + \frac{3\sqrt{\gamma_0}}{\nu_0^2(3-\Lambda_\nu)} f_1[\bar{p}], \tag{3.190}$$

the other β_i remaining unchanged. It can be also noticed that in this case, equation (3.175) becomes:

$$\Omega = f_1[p] \times \sqrt{\gamma_0}. \tag{3.191}$$

So far, nothing has been assumed on the shape of $f_1[p]$ except that it has to go to 1 at the classical limit. In this case, one could assume correctly that $f_1[p] = \frac{1}{\sqrt{\gamma_0}}$ such that $\Omega = 1$ and $\alpha_3 = -1 + \frac{1}{\gamma_0^{\frac{3}{2}}}$.

This case is interesting because it shows that even when dealing with some perturbed and quantum-corrected constraints, the algebra remains closed and one recovers the usual spacetime of general relativity, a consequence which was not expected when considering the previous results derived with the holonomy correction alone.

3.4.2. Case where $\gamma_0 = \gamma_0\left[\frac{\bar{k}}{\sqrt{\bar{p}}}\right]$. After applying corrections, such as the inverse-volume or holonomy corrections, the resulting physical observable (i.e. the Hubble parameter) are generally not independent of a rescaling of the scale factor. This is a problem since rescaling the scale factor is a gauge choice and therefore not physical. But in the $\bar{\mu}$-scheme for holonomy corrections and $\gamma_0 = \gamma_0[\frac{\bar{k}}{\sqrt{\bar{p}}}]$ for the inverse-volume corrections, the physics becomes invariant under this rescaling. This is why we here consider this case: $\gamma_0 = \gamma_0\left[\frac{\bar{k}}{\sqrt{\bar{p}}}\right]$.

In this section, a prime will denote derivative with respect to the argument $\frac{\bar{k}}{\sqrt{\bar{p}}}$,

$$\gamma_0' := \frac{\mathrm{d}\gamma_0\left[\frac{\bar{k}}{\sqrt{\bar{p}}}\right]}{\mathrm{d}\frac{\bar{k}}{\sqrt{\bar{p}}}}. \tag{3.192}$$

Interesting consequences arise in this example. Indeed, in this case equation (3.177) reduces to

$$\Sigma_{\bar{p}} = \tfrac{1}{2}. \tag{3.193}$$

The obtained counterterms are:

$$\alpha_1 = \frac{k^2\gamma_0'}{2\sqrt{\bar{p}}\gamma_0}, \tag{3.194}$$

$$\alpha_2 = -\frac{k^3\gamma_0'}{\sqrt{\bar{p}}\gamma_0}, \tag{3.195}$$

$$\alpha_3 = -1 + \frac{f_1[\bar{p}]}{\gamma_0}, \tag{3.196}$$

$$\alpha_4 = \frac{k(4\sqrt{\bar{p}}\gamma_0' + k\gamma_0'')}{2\bar{p}\gamma_0}, \tag{3.197}$$

$$\alpha_5 = \frac{k(4\sqrt{\bar{p}}\gamma_0' + k\gamma_0'')}{2\bar{p}\gamma_0}, \tag{3.198}$$

$$\alpha_6 = \frac{k^2(2\sqrt{\bar{p}}\gamma_0' + k\gamma_0'')}{2\bar{p}\gamma_0}, \tag{3.199}$$

$$\alpha_7 = -\frac{k^3(\sqrt{\bar{p}}\gamma_0' + k\gamma_0'')}{\bar{p}\gamma_0}, \tag{3.200}$$

$$\alpha_8 = -\frac{k^3(\sqrt{\bar{p}}\gamma_0' + k\gamma_0'')}{\bar{p}\gamma_0}, \tag{3.201}$$

$$\alpha_9 = -1 + \frac{1}{\gamma_0}\left(f_1[\bar{p}] + 2\bar{p}\frac{\mathrm{d}f_1[\bar{p}]}{\mathrm{d}\bar{p}}\right). \tag{3.202}$$

The expression for the β_i terms are much more complicated and are not given here. Nevertheless, the structure function remains simple and becomes

$$\Omega = \left(\gamma_0 + 2\frac{\bar{k}}{\sqrt{\bar{p}}}\gamma_0' + \frac{1}{2}\left(\frac{\bar{k}}{\sqrt{\bar{p}}}\right)^2\gamma_0''\right) f_1[\bar{p}]. \tag{3.203}$$

In this example, $\Omega = \Omega\left[\frac{\bar{k}}{\sqrt{\bar{p}}}\right]$ if and only if $f_1 \equiv 1$.

As a toy model, one can also assume that $f_1 \equiv 1 \equiv \Omega$ and solve directly the corresponding differential equation: the solution is given by

$$\gamma_0 = 1 + D_1 \frac{\sqrt{\bar{p}}}{\bar{k}} + D_2 \frac{\bar{p}}{\bar{k}^2}, \tag{3.204}$$

and one can see that it blows up at the classical limit, for any constants $D_i \neq 0$. If $D_1 = D_2 = 0$, then the above expression remains finite, however there will be no inverse-volume correction in the gravitational sector, which is not a good solution.

Nevertheless, the interesting part comes from equation (3.193) leading to an equation similar to equation (3.180), whose solution is given by

$$\nu_0 = 2\frac{\bar{p}^3}{C_1^2}\left(\frac{C_1}{p^{3/2}} - \ln\left[1 + \frac{C_1}{p^{3/2}}\right]\right), \tag{3.205}$$

where C_1 is an unknown constant. In the calculations, the classical limits have been respected, such that $\lim_{p\to\infty} \nu_0 = 1$. Moreover, it should be noticed that

$$\nu_0 = \lim_{C_1\to 0} 2\frac{\bar{p}^3}{C_1^2}\left(\frac{C_1}{p^{3/2}} - \ln\left[1 + \frac{C_1}{p^{3/2}}\right]\right) = 1 \tag{3.206}$$

is also solution. Surprisingly, when one tries to plot these expressions for a large range of given values of C_1, one sees that the evolution of ν_0 corresponds exactly to the evolution expected for an inverse-volume correction, namely an evolution similar to the one given by equation (3.1). From this perspective, it can be understood that assuming that the inverse-volume depends also on the connection is consistent and leads to a good behavior, at least for the correction in the matter sector.

The results obtained here could suggest that with a quite similar dependence for γ_0 on $\bar{k}$, it would be possible to have also a good expression for ν_0 and, more importantly, a good expression for γ_0 with $\Omega = 1$ in the classical limit.

3.4.3. General case where $\Omega = \Omega[\bar{p}]$. So far, we have seen two examples where specific dependencies of γ_0 on $\bar{k}$ and $\bar{p}$ were assumed. In this section, we would like to generalize the approach by studying only Ω and see the consequences of the following assumptions on the inverse-volume correction. We have considered one case where if $\gamma_0 = \gamma_0\left[\frac{\bar{k}}{\sqrt{\bar{p}}}\right]$, then $\Omega = \Omega\left[\frac{\bar{k}}{\sqrt{\bar{p}}}\right]$ if and only if $f_1 = 1$, and another one where $\Omega = 1$.

Moreover, everything following from $\Omega = \Omega[\bar{p}]$ follows for $\Omega = 1$ and we will now assume only $\Omega = \Omega[\bar{p}]$. Doing this, one can firstly notice that equation (3.175) can be reformulated as

$$\frac{\partial^2}{\partial \bar{k}^2}(\bar{k}^2\gamma_0) = \frac{\Omega}{\Sigma_{\bar{p}} f_1[\bar{p}]}. \tag{3.207}$$

If we demand that Ω depends only on $\bar{p}$ and not on $\bar{k}$ as assumed here, we obtain under the condition that γ_0 and $\Sigma_{\bar{p}}$ fulfils also equation (3.177), the general solution

$$\gamma_0 = \frac{\Omega}{2\Sigma_{\bar{p}} f_1[\bar{p}]} + \frac{f_2[p]}{\bar{k}} + \frac{f_3[p]}{\bar{k}^2}, \tag{3.208}$$

where $f_2[p]$ and $f_3[p]$ are functions of $\bar{p}$, going to 0 if one assumes $\gamma_0 = \gamma_0[\bar{p}]$. After some assumptions and manipulations, it is easy to see that the solutions previously derived, corresponding to equations (3.191) and (3.204) can be recovered from equation (3.208).

Looking at the expression in equation (3.208), one can worry about the behavior of the inverse-volume correction when $\bar{k} \to 0$, that is, about the possibility that the correction is diverging at low curvature. The important point is that the correction derived here should not

to be considered alone, but rather with the gravitational Hamiltonian constraint density which include a $\bar{k}^2$ in the numerator. As a consequence, one deals finally with this $\bar{k}^2$ coming from the density and the terms $\frac{1}{\bar{k}}$ and $\frac{1}{\bar{k}^2}$ coming from the correction, such that on the one hand, only the Hamiltonian constraints are well defined for every $\bar{k}$, and consequently, on the other hand, the Friedmann equation is indeed modified but finite.

Roughly speaking, the Friedmann equation would have in this case an expression similar to

$$\left(c_1[\bar{p}]\frac{\bar{k}^2}{\bar{p}} + c_2[p]\bar{k} + c_3[p]\right) = \frac{\kappa}{3}\rho, \tag{3.209}$$

where

$$\rho = \frac{\nu_0}{2}\frac{\bar{\pi}^2}{\bar{p}^3} + V(\varphi). \tag{3.210}$$

One can analyze this situation in the simplest toy model where, for instance $c_2[\bar{p}] = 0$ and $H = c_1[\bar{p}]\bar{k}$: in this case, the former equation leads to

$$H^2 = c_1[\bar{p}]\left(\frac{\kappa}{3}\rho[\bar{p}] - c_3[p]\right), \tag{3.211}$$

where a bounce is possible when $\frac{\kappa}{3}\rho[\bar{p}] = c_3[p]$. Of course, this is just a preliminary idea of a possible consequence of the inverse-volume correction, and one should go through the full equations.

Another comment could be made: the goal of effective LQC is to obtain some constraints which would be as close as possible to the one derived from the full theory. Considering the holonomy correction, it can be shown that the constraints used in [18], built somehow as in LQG but however considering Lagrange multipliers depending also on the phase space variables, lead after a Taylor expansion around the background, exactly to the one derived in [17], which pioneered the approach depicted here. One could wonder if it is also the case in this study. The answer is not known yet, the inverse-volume correction having not been considered in the first case, as was the holonomy correction. To do so, one could at least notice that during the derivation of the counterterms, it is possible to see from equations (3.102) and (3.174) that β_9 and β_{10} which, with β_3, are expressed in the potential φ part of the matter densities, are proportional to $\frac{1}{1+\beta_1}$, while the others β_i (including β_1) found in the momentum π part of the matter densities are mostly proportional to $\frac{1}{1+\beta_3}$. One can then wonder in which way β_9 and β_{10}, related to β_3 in the derivation of the perturbed constraints, are intertwined with β_1, while the other counterterms, related to β_1 in the derivation of the perturbed constraints, are related to β_3. One can therefore wonder how this particular property in the expressions of the β_i counterterms could emerge from the not Taylor-expanded constraint.

Finally, it is possible to see here that this result works also for $\Omega = 1$ and one can generalize the comments presented for $\gamma_0 = \gamma_0[\bar{p}]$: having a perturbed and quantum-corrected constraint whose corrections depend possibly on both the connection and the flux of densitized triad does not necessarily lead to a deformed algebra as suggested in some previous work.

3.5. Summary of the inverse-volume case

The situation for the inverse-volume correction can be summarized as follows:

- It is possible to close the algebra under the assumptions of this work.
- All the counterterms and higher order inverse-volume corrections can be determined as functions of the zeroth order inverse-volume corrections and of the unknown functions $f_1[\bar{k}]$ and $\Sigma_{\bar{p}}$.

- One can constrain the zeroth order inverse-volume corrections through $\frac{\partial \nu_0}{\partial \bar{k}} = 0$ and equation (3.177).
- All the counterterms have correct classical limits, as required by construction.
- The case $\gamma_0 = \gamma_0\left[\frac{\bar{k}}{\sqrt{\bar{p}}}\right]$ leads to simplified expressions for the counterterms, and also to a consistent solution for ν_0 given by equation (3.205).
- Assuming $\Omega = \Omega[\bar{p}]$ leads to a general expression for γ_0 given by equation (3.208), but also a modified Friedmann equation, equation (3.211), with a possible bounce (depending on the value of $\bar{p}$).
- More importantly, it is possible to consider the presence of quantum corrections in effective LQC without having to deform the algebra, namely $\Omega = 1$ is allowed but with a modified Friedmann equation compatible with a bounce.

4. Holonomy case—reminder

In order to understand better what happens when both corrections are taken into account, it is useful to recall briefly the main results obtained with the holonomy corrections.

In [17], an anomaly-free algebra was constructed for holonomy-corrected constraints. It was then demonstrated that the $\bar{\mu}$-scheme is recovered, that is $\omega = -\frac{1}{2}$ in equation (4.9), and the function structure was given by $\Omega = \cos(2\bar{\mu}\gamma\bar{k})$. The fact that it can change its sign could be interpreted as a change from an hyperbolic to an elliptic regime around the bounce, or as a change of signature of the metric from $(-,+,+,+)$ in the Lorentzian phase (where $\{H,H\} = +D$ in our convention) to $(+,+,+,+)$ in the Euclidean phase (where $\{H,H\} = -D$). As Ω enters directly the equation of motion of the perturbations, this would lead to a radical change in the resulting spectrum (see [25] and [26] for an analysis of the spectrum). The surface $\Omega = 0$ may also be interpreted as an 'asymptotic silence' surface where initial conditions would have to be set [27]. The debate is not closed on this point. We simply try here to push the effective approach as far as possible to investigate its consequences.

4.1. Constraints

The constraints with holonomy corrections read as:

$$D_G[N^c] = \int \frac{\mathrm{d}^3x}{\kappa}\delta N^c\left[\bar{p}\partial_c\delta K_d^d - \partial_d\delta K_c^d - \bar{k}\partial_d\delta E_c^d\right], \tag{4.1}$$

$$H_G[N] = \frac{1}{2\kappa}\int \mathrm{d}^3x(\bar{N}+\delta N)\times\left[\mathcal{H}_G^{(0)} + \mathcal{H}_G^{(1)} + \mathcal{H}_G^{(2)}\right], \tag{4.2}$$

$$D_m[N^c] = \int \mathrm{d}^3x\delta N^c\bar{\pi}\,\partial_c\delta\varphi, \tag{4.3}$$

$$H_m^Q[N] = \int \mathrm{d}^3x\bar{N}\times\left[\mathcal{H}_\pi^{(0)} + \mathcal{H}_\varphi^{(0)} + \mathcal{H}_\pi^{(2)} + \mathcal{H}_\nabla^{(2)} + \mathcal{H}_\varphi^{(2)}\right] + \int \mathrm{d}^3x\delta N\times\left[\mathcal{H}_\pi^{(1)} + \mathcal{H}_\varphi^{(1)}\right], \tag{4.4}$$

with

$$\mathcal{H}_G^{(0)} = -6\sqrt{\bar{p}}(\mathbb{K}[1])^2, \tag{4.5}$$

$$\mathcal{H}_G^{(1)} = -4\sqrt{\bar{p}}(\mathbb{K}[s_1]+\alpha_1)\delta K_d^d - \frac{1}{\sqrt{\bar{p}}}(\mathbb{K}[1]^2+\alpha_2)\delta E_d^d + \frac{2}{\sqrt{\bar{p}}}(1+\alpha_3)\partial_c\partial^d\delta E_d^c, \tag{4.6}$$

$$\mathcal{H}_G^{(2)} = \sqrt{\bar{p}}(1+\alpha_4)\delta K_c^d \delta K_d^c - \sqrt{\bar{p}}(1+\alpha_5)(\delta K_d^d)^2 - \frac{2}{\sqrt{\bar{p}}}(\mathbb{K}[s_2]+\alpha_6)\delta E_d^c \delta K_c^d$$
$$-\frac{1}{2\bar{p}^{3/2}}(\mathbb{K}[1]^2+\alpha_7)\delta E_d^c \delta E_c^d + \frac{1}{4\bar{p}^{3/2}}(\mathbb{K}[1]^2+\alpha_8)\left(\delta E_d^d\right)^2$$
$$-\frac{1}{2\bar{p}^{3/2}}(1+\alpha_9)\delta^{jk}\left(\partial_c \delta E_j^c\right)\left(\partial_d \delta E_k^d\right), \tag{4.7}$$

where we have set

$$\forall n \neq 0, \qquad \mathbb{K}[n] = \frac{\sin[n\mu\gamma\bar{k}]}{n\mu\gamma}, \tag{4.8}$$

and $\mathbb{K}[n] = \bar{k}$ for $n = 0$. The $\mathbb{K}[s_i]$ are the holonomy-corrected versions of the single $\bar{k}$ in the constraint, with s_i an unknown parameter: this parametrization comes from the fact that when one quantizes using the holonomies, the field strength of the connection, initially appearing as $\bar{k}^2$, becomes exactly $\mathbb{K}[1]^2$. Therefore, all the terms in the constraints that are in $\bar{k}^2$ will be replaced by $\mathbb{K}[1]^2$, and because we do not know exactly the general correspondence $\bar{k} \to \mathbb{K}[s_i]$, except when for squared terms, we will let s_i be unknown integers.

In our approach, the integers s_i are set by hand without any requirements except the one that at the end, for a specific value (or not) of s_i, the algebra should be closed [13]. However, it should be mentioned that there exists another approach trying rather to extract the effects of the quantum modifications directly from the quantum formalism by using an hybrid formalism: the Hybrid quantization [28]. In this other approach, generally, the quantization procedure is adapted by setting the value of the integer s_i, determining the step of displacement of the holonomies, as a result of the necessity to respect the superselection sectors of LQC.

Nevertheless, it has been noticed in previous works, as explained in the former section, that one of the effects of the counterterms as used here and also added by hand, is to remove the terms depending on the parameters s_i such that at the end, no dependence on these integers remains. This effect will be shown below.

We assume that

$$\mu \propto \bar{p}^{\omega}, \tag{4.9}$$

for some constant $-\frac{1}{2} \leqslant \omega \leqslant 0$. The case $\omega = -\frac{1}{2}$ is the so-called $\bar{\mu}$-scheme, whereas $\omega = 0$ corresponds to the μ_0-scheme.

$\mathcal{H}_\pi^{(0)}$, $\mathcal{H}_\varphi^{(0)}$, $\mathcal{H}_\pi^{(1)}$, $\mathcal{H}_\varphi^{(1)}$, $\mathcal{H}_\pi^{(2)}$, $\mathcal{H}_\nabla^{(2)}$ and $\mathcal{H}_\varphi^{(2)}$ are not affected by the holonomy corrections[5] and are therefore given by equations (3.9)–(3.15).

4.2. Counterterms

The associated counterterms are:

$$\alpha_1 = \mathbb{K}[2] - \mathbb{K}[s_1], \tag{4.10}$$

$$\alpha_2 = 2(\mathbb{K}[1]^2 - \bar{k}\mathbb{K}[2]), \tag{4.11}$$

$$\frac{\partial \alpha_3}{\partial \bar{k}} = 0, \tag{4.12}$$

$$\alpha_4 = -1 + \cos(2\bar{k}\gamma\bar{\mu}), \tag{4.13}$$

$$\alpha_5 = -1 + \cos(2\bar{k}\gamma\bar{\mu}), \tag{4.14}$$

[5] Which is not true when one considers the polymer quantization approach [29].

$$\alpha_6 = -\bar{k}\cos(2\bar{k}\gamma\bar{\mu}) + 2\mathbb{K}[2] - \mathbb{K}[s_2], \tag{4.15}$$

$$\alpha_7 = -2\bar{k}^2\cos(2\bar{k}\gamma\bar{\mu}) - 4\mathbb{K}[1]^2 + 6\bar{k}\mathbb{K}[2], \tag{4.16}$$

$$\alpha_8 = -2\bar{k}^2\cos(2\bar{k}\gamma\bar{\mu}) - 4\mathbb{K}[1]^2 + 6\bar{k}\mathbb{K}[2], \tag{4.17}$$

$$\alpha_9 = \alpha_3 + 2\bar{p}\frac{\mathrm{d}\alpha_3}{\mathrm{d}\bar{p}}. \tag{4.18}$$

Because of equation (4.12), α_3 is an unknown function of $\bar{p}$.

$$\beta_i = 0 \quad \text{for} \quad i \neq 9, \tag{4.19}$$

$$\beta_9 = -1 + \cos(2\bar{k}\gamma\bar{\mu})(1 + \alpha_3). \tag{4.20}$$

We find that

$$\Omega = \cos(2\bar{k}\gamma\bar{\mu})(1 + \alpha_3). \tag{4.21}$$

If one chooses $\alpha_3 = 0$, then necessarily $\alpha_9 = 0$, and the previous results [17] are recovered, i.e. a possible change from an hyperbolic to an elliptic regime and/or an asymptotic silence scenario. Moreover, and this has not been underlined before, one can also keep α_3 and α_9. As an heuristic example, let us consider the specific case $\alpha_9 = 0$. This leads to

$$\alpha_3 = \frac{\text{constant}}{\sqrt{\bar{p}}}, \tag{4.22}$$

and different cases must be considered:

- *constant* $= 0$, this has been extensively studied in [17].
- *constant* > 0, this is basically similar but with a modified dynamics. The Euclidean phase is dynamically shifted. The Ω term can be negative and even smaller than -1.
- *constant* < 0. When adjusting the value of the constant in a tuned way, this can lead to an evolution without the Euclidean phase. However, the asymptotic silence surface remains.

Numerical investigations have shown that the corresponding power spectrum of tensor perturbations does not depend heavily on the value of the *constant*. The shapes of the different power spectra are quite equivalent to the case $\alpha_3 = \alpha_9 = 0$. Too much freedom is however still remaining and more constraints are required to fully fix the dynamics.

5. Inverse-volume and holonomy corrections considered simultaneously

In the previous sections, the anomalies appearing when one considers either the holonomy or the inverse-volume correction alone were described. In this section, both terms are considered simultaneously and the resulting algebra is studied.

5.1. Constraints

The constraints considered in this section are equations (3.2), (3.3), (3.7) and (3.8) but with $\mathcal{H}^{(0)}$, $\mathcal{H}^{(1)}$ and $\mathcal{H}^{(2)}$ given by equations (4.5)–(4.7). The matter Hamiltonian does not depend on the Ashtekar connection and is therefore not subject to holonomy corrections, except for β_9.

For the same reasons as explained before, we are allowed to choose $\gamma_3 = \gamma_4 = \gamma_5 = \gamma_6 = \gamma_7 = \nu_1 = \nu_3 = \nu_4 = 0$ and $\sigma_0 = \nu_0$ without any loss of generality.

5.2. μ-scheme

In Section 4 we have recalled the results of [17] where μ was assumed to depend on $\bar{k}$ according to $\mu \propto \bar{p}^{\omega}$. In that case it was shown that we must have $\omega = -\frac{1}{2}$.

This time, we will try to be one step more general. We assume that μ is an unknown function of $\bar{k}$ and define

$$\omega := \frac{\bar{p}}{\mu}\frac{\mathrm{d}\mu}{\mathrm{d}\bar{p}}. \tag{5.1}$$

This definition is a generalization, and therefore is in agreement with the one previously used, $\mu \propto \bar{p}^{\omega}$.

Since μ is an unknown function of $\bar{p}$, so is ω. However, we still expect $-\frac{1}{2} \leqslant \omega \leqslant 0$, for the same reasons as before.

5.3. Solution after closing the algebra

The Poisson brackets will have the same shape as in the inverse-volume case, but with some modifications in the expressions of the anomalies, because of the holonomy corrections. However, no new anomaly arises, and the calculations are very similar.

Again, we find

$$\gamma_1 = \gamma_2 = \gamma_8 = 0, \tag{5.2}$$

$$\nu_2 = \nu_3 = \nu_5 = \nu_6 = \nu_7 = \nu_8 = 0, \tag{5.3}$$

and

$$\frac{\partial \nu_0}{\partial \bar{k}} = 0. \tag{5.4}$$

As before, in order to simplify the equations, we define:

$$\Gamma_{\bar{k}[1]} := \frac{\mathbb{K}[1]}{\gamma_0}\frac{\partial \gamma_0}{\partial \bar{k}}, \tag{5.5}$$

$$\Gamma_{\bar{k}[2]} := \frac{\mathbb{K}[2]}{\gamma_0}\frac{\partial \gamma_0}{\partial \bar{k}}, \tag{5.6}$$

$$\Gamma_{\bar{k}[1],2} := \frac{\mathbb{K}[1]^2}{\gamma_0}\frac{\partial^2 \gamma_0}{\partial \bar{k}^2}. \tag{5.7}$$

The counterterms for the gravity sector are given by:

$$\alpha_1 = -\mathbb{K}[s_1] + (2\mathbb{K}[2] + \mathbb{K}[1]\Gamma_{\bar{k}[1]})\Sigma_{\bar{p}}, \tag{5.8}$$

$$\alpha_2 = 2\mathbb{K}[1]^2 - 2\bar{k}(2\mathbb{K}[2] + \mathbb{K}[1]\Gamma_{\bar{k}[1]})\Sigma_{\bar{p}}, \tag{5.9}$$

$$\alpha_3 = -1 + \frac{f_1[\bar{p}]}{\gamma_0}, \tag{5.10}$$

$$\alpha_4 = -1 + (2\cos(2\gamma\mu\bar{k}) + 4\Gamma_{\bar{k}[2]} + \Gamma_{\bar{k}[1],2})\Sigma_{\bar{p}}, \tag{5.11}$$

$$\alpha_5 = -1 + (2\cos(2\gamma\mu\bar{k}) + 4\Gamma_{\bar{k}[2]} + \Gamma_{\bar{k}[1],2})\Sigma_{\bar{p}}, \tag{5.12}$$

$$\alpha_6 = -\mathbb{K}[s_2] + 2\mathbb{K}[2] + \mathbb{K}[1]\Gamma_{\bar{k}[1]} - \bar{k}(2\cos(2\gamma\mu\bar{k}) + 4\Gamma_{\bar{k}[2]} + \Gamma_{\bar{k}[1],2})\Sigma_{\bar{p}}, \tag{5.13}$$

$$\alpha_7 = 6\bar{k}\mathbb{K}[2] - \mathbb{K}[1]^2(4+2\Lambda_\gamma) + 2\bar{k}\mathbb{K}[1]\Gamma_{\bar{k}[1]} + 2(1+2\omega)(\mathbb{K}[1]^2 - \bar{k}\mathbb{K}[2]) \\ -2\bar{k}^2(2\cos(2\gamma\mu\bar{k}) + 4\Gamma_{\bar{k}[2]} + \Gamma_{\bar{k}[1],2})\Sigma_{\bar{p}}, \tag{5.14}$$

$$\alpha_8 = 6\bar{k}\mathbb{K}[2] - \mathbb{K}[1]^2(4+2\Lambda_\gamma) + 2\bar{k}\mathbb{K}[1]\Gamma_{\bar{k}[1]} + 2(1+2\omega)(\mathbb{K}[1]^2 - \bar{k}\mathbb{K}[2]) \\ -2\bar{k}^2(2\cos(2\gamma\mu\bar{k}) + 4\Gamma_{\bar{k}[2]} + \Gamma_{\bar{k}[1],2})\Sigma_{\bar{p}}, \tag{5.15}$$

$$\alpha_9 = -1 + \frac{1}{2\gamma_0\Sigma_{\bar{p}}}\left(f_1[\bar{p}] + 2\bar{p}\frac{\mathrm{d}f_1[\bar{p}]}{\mathrm{d}\bar{p}}\right). \tag{5.16}$$

For the matter sector, without assumptions, the results are the same as for the inverse-volume case, except for β_9 which reads here as

$$\beta_9 = -1 + \frac{3\gamma_0}{\nu_0^2}\frac{(2\cos(2\gamma\mu\bar{k}) + 4\Gamma_{\bar{k}[2]} + \Gamma_{\bar{k}[1],2})}{(3-\Lambda_\nu)}\Sigma_{\bar{p}}f_1[\bar{p}]. \tag{5.17}$$

All the counterterms have the correct (i.e. vanishing) classical limit.

The structure function of the algebra is now given by

$$\Omega = \gamma_0(2\cos(2\gamma\mu\bar{k}) + 4\Gamma_{\bar{k}[2]} + \Gamma_{\bar{k}[1],2})\Sigma_{\bar{p}}f_1[\bar{p}] \\ = \left(\frac{\partial^2}{\partial\bar{k}^2}(\gamma_0\mathbb{K}[1]^2)\right)\Sigma_{\bar{p}}f_1[\bar{p}]. \tag{5.18}$$

When both corrections are taken in to account, equation (3.176) can be expressed as:

$$-\frac{\partial}{\partial\bar{k}}\frac{\frac{\partial}{\partial\bar{p}}\left(\frac{\gamma_0}{\bar{p}}\mathbb{K}[1]^2\right)}{\frac{\partial}{\partial\bar{k}}\left(\frac{\gamma_0}{\bar{p}}\mathbb{K}[1]^2\right)} = \frac{\partial}{\partial\bar{p}}\ln(\sqrt{\bar{p}}\,\Sigma_{\bar{p}}), \tag{5.19}$$

which can be shown to be equivalent to equation (3.177) when $\mathbb{K}[i] \to \bar{k}$ ($\mu \to 0$).

If $\gamma_0 = \nu_0 = 1$ then equation (5.19) reduces to $\omega = -\frac{1}{2}$, and we recover the $\bar{\mu}$-scheme which was found as the solution in the holonomy case.

5.4. Solutions after further assumptions

5.4.1. Case where $\gamma_0 = \gamma_0[\bar{p}]$. If we assume that γ_0 is only a function of $\bar{p}$ and not of $\bar{k}$, equation (5.19) becomes:

$$\frac{\Lambda_\gamma - 1 - 2\omega}{\cos(\gamma\bar{\mu}\bar{k})} = (3\Lambda_\gamma - 1 - 2\omega) + 4\bar{p}\frac{\partial}{\partial\bar{p}}\ln(\Sigma_{\bar{p}}). \tag{5.20}$$

The right hand side of the above equation is clearly $\bar{k}$-independent, therefore the left hand side must be so too. Nevertheless, this is only the case if

$$\Lambda_\gamma = 1 + 2\omega, \tag{5.21}$$

and consequently

$$\bar{p}\frac{\partial}{\partial\bar{p}}\ln(\Sigma_{\bar{p}}) = -\frac{1}{2}\Lambda_\gamma. \tag{5.22}$$

Equations (5.21) and (5.22) have the solutions

$$\mu \propto \sqrt{\frac{\gamma_0}{\bar{p}}}, \tag{5.23}$$

$$\Sigma_{\bar{p}} = \frac{1}{2\sqrt{\gamma_0}}, \tag{5.24}$$

when the correct classical limit has been taken in to account.

From this, we see that if the inverse-volume corrections are unaffected by the holonomy corrections, then the holonomy corrections will be affected by the inverse-volume corrections. Therefore we should conclude that either the inverse-volume corrections are affected by the holonomy corrections, or the holonomy corrections are affected by the inverse-volume corrections.

5.4.2. Case where $\omega = -\frac{1}{2}$ *and* $\gamma_0 = \gamma_0\left[\frac{\bar{k}}{\sqrt{\bar{p}}}\right]$. In the case where $\omega = -\frac{1}{2}$ and $\gamma_0 = \gamma_0\left[\frac{\bar{k}}{\sqrt{\bar{p}}}\right]$, $\frac{\gamma_0}{\bar{p}}\mathbb{K}[1]^2$ is now a function of $\frac{\bar{k}}{\sqrt{\bar{p}}}$. Equation (5.19) reduces thus to $\Sigma_{\bar{p}} = \frac{1}{2}$ which is exactly the result obtained previously, without considering the holonomy corrections, leading ν_0 to evolve as in equation (3.205).

The structure function is now given by

$$\Omega = \left(\gamma_0 \cos(2\gamma\bar{\mu}\bar{k}) + 2\frac{\mathbb{K}[2]}{\sqrt{\bar{p}}}\gamma_0' + \frac{1}{2}\frac{\mathbb{K}[1]^2}{\bar{p}}\gamma_0''\right) f_1[\bar{p}]. \tag{5.25}$$

In this case, $\Omega = \Omega\left[\frac{\bar{k}}{\sqrt{\bar{p}}}\right]$ if and only if $f_1[\bar{p}] \equiv 1$.

5.4.3. Case where $\Omega = \Omega[\bar{p}]$. In the same way as before, if Ω does not depend on $\bar{k}$, then equation (5.18) can be solved for γ_0 giving in the considered case:

$$\gamma_0 = \frac{1}{\mathbb{K}[1]^2}\left(\frac{\bar{k}^2\Omega}{2\Sigma_{\bar{p}}f_1[\bar{p}]} + \bar{k}f_2[\bar{p}] + f_3[\bar{p}]\right). \tag{5.26}$$

It is interesting to notice that the expression of the correction has a really similar shape as the one given by equation (3.208) for the inverse-volume correction. Moreover, as said previously, in order to understand the action of the correction and its characteristics on the related phenomenology, it is necessary to consider it with the constraints densities. An interesting consequences arises: in the gravitational constraint density, the term in the numerator is now given by $\mathbb{K}[1]^2$ which cancels exactly the same term in the correction, and only the terms in $\bar{k}$ remains. In other words, after including this correction in the constraint, the final constraint will have exactly the same expression as the one derived previously for the inverse-volume correction only. Therefore, this case is not interesting, the holonomy correction being cancelled by the inverse-volume correction, even if the idea of the bounce remains. One can consequently assume that the interesting cases are obtained in a similar way as when the holonomy correction was considered, that is to say when the structure function Ω depends not only on $\bar{p}$, but also on $\bar{k}$. This question is left opened for further investigations.

5.5. Some remarks on the case where both corrections are taken into account

We have shown that the full algebra can be closed and that either the inverse-volume correction has to depend on the holonomy one, or vice versa.

It should also be noticed that equations (4.2) and (4.3) of [30] read respectively

$$E_k^j = \frac{2}{\kappa^2}\int \epsilon_{\mathrm{krs}}\epsilon^{abc}\left\{A_b^r, V(R)\right\}\left\{A_c^s, V(R)\right\}n_a^S, \tag{5.27}$$

and

$$E_k^j \sim \mathrm{Tr}[h\{h^{-1}, V\}\tau_k h\{h^{-1}, V\}]. \tag{5.28}$$

Considering the quantum version of the previous equation, one can hope to gain a better understanding of the most general inverse-volume correction and its interplay with the holonomy correction. This is however beyond the scope of this paper.

6. Gauge-invariant variables and equations of motion

In order to understand better the consequences of the counterterms presented in this work, it is interesting to study the modifications they induce on the equations of motion for the cosmological perturbations. This section is therefore dedicated to the derivation of the generic equations of motion, for scalar and tensor modes, by first expressing them with the general expressions for the counterterms, and then by replacing in the final equations these expressions by the ones found in the previous sections. In the following, only some details will be given as one can simply follow what has been done in [11] and [31] for instance. However a reader having a specific model in mind will be able to compute to the end the corresponding equations of motion.

As in [19], one can write the general perturbation of the densitized triad as

$$\delta E^a_i = \bar{p}\big[-2\psi\delta^a_i + \big(\delta^a_i\partial^d\partial_d - \partial^a\partial_i\big)E - c_1\partial^a F_i - c_2\partial_i F^a - \tfrac{1}{2}h^a_i\big], \tag{6.1}$$

where the first two terms ψ and E correspond to the scalar modes, F_i and F^a to the vector modes, and h^a_i to the tensor modes. One will also have to deal with the perturbations of the matter content, which are related to the perturbations of the metric by the Einstein equations.

Moreover, expressing the perturbations of the metric as in the previous equation (choosing a specific gauge) will also constrain the lapse function δN and the shift vector δN^a. The form of the metric in the case of vector and tensor modes implies that the variation of the lapse is zero: $\delta N = 0$. For vector modes, the variation of the shift corresponds to one of the two degrees of freedom: $\delta N^a = S^a$, while for the tensors modes, $\delta N^a = 0$. One can then notice that for the tensor modes, due to the vanishing of the perturbations of the lapse function and of the shift vector, the first order in the constraints densities will never be considered.

Vector modes are transverse, and tensor modes are transverse and traceless. These conditions constrain δE^a_i and δK^i_a. In particular, the vanishing trace implies

$$\delta^i_a\delta E^a_i = \delta^a_i\delta K^i_a = 0, \tag{6.2}$$

which, when one considers the case of the tensor or vector perturbations, leads to a simplification of the expressions of the constraints, the terms proportional to the traces above vanishing. Moreover, for the tensor modes, the transverseness, i.e. vanishing divergence, implies also

$$\partial^i\delta E^a_i = \partial_a\delta E^a_i = 0. \tag{6.3}$$

The more general case is therefore given by the one for the scalar perturbations, no term disappearing due to the properties of the perturbations, with consequently a contribution of all orders of the constraints densities. In this case, we have

$$\delta N = \bar{N}\phi \qquad \text{and} \qquad \delta N^a = \partial^a B, \tag{6.4}$$

where $\bar{N}$ is the unperturbed part of the lapse $N = \bar{N} + \delta N$, and ϕ and B are the other degrees of freedom for the scalar perturbations in the metric: considering only the metric, only two of these degrees of freedom are physically relevant which, with the Einstein equations, reduce to one when considering also the perturbations of the matter content, the remaining true physical degree of freedom is the Mukhanov–Sasaki variable, v, as explained later.

6.1. Background equation of motion

Because we neglect the backreaction of the perturbations on the background, its homogeneous part on which the perturbations live, is not affected by the next orders from which the previous counterterms have been derived. However it will be affected by the zeroth order

of the inverse-volume and holonomy corrections. In this section, we give the equations of motion for the background, namely the Friedmann and Klein–Gordon equations, when both corrections are considered simultaneously. One can recover the decoupled equations by taking the corresponding limits.

The Friedmann equation, partially derived first in [32], is given by

$$H^2 = \frac{\kappa}{3}\gamma_0\rho\left(1 - \frac{\rho}{\rho_c\gamma_0} + \Gamma_{\bar{k}[2]} + \frac{1}{4}\Gamma^2_{\bar{k}[1]}\right), \tag{6.5}$$

where

$$\rho := \frac{1}{2\nu_0}\left(\frac{\mathrm{d}\bar{\varphi}}{\mathrm{d}t}\right)^2 + V(\bar{\varphi}), \quad \rho_c := \frac{\kappa}{3\gamma^2\mu^2\bar{p}}, \tag{6.6}$$

and the Klein–Gordon equation for the matter field by

$$\frac{\mathrm{d}^2\bar{\varphi}}{\mathrm{d}t^2} + (3 - 2\Lambda_\nu)H\frac{\mathrm{d}\bar{\varphi}}{\mathrm{d}t} + \nu_0 V'(\bar{\varphi}) = 0. \tag{6.7}$$

Here, H is the Hubble factor in cosmic time t.

6.2. Tensor variables and equations of motion

In this section, we derive the corresponding equations of motion for the tensor variables $h_{\mu\nu}$ which are gauge-invariant. The two degrees of freedom will be called in the following $h = h_\times = h_+$. We consider here the case where both corrections are taken into account simultaneously. To make the expression clearer, we will firstly not fix the counterterms.

After some algebra following [13], one obtains the expression of δK^i_a,

$$\gamma_0(1+\alpha_4)\delta K^i_a = \tfrac{1}{2}(\dot{h} + h\gamma_0(2\mathbb{K}[2] - \mathbb{K}[s_2] - \alpha_6)), \tag{6.8}$$

whose equation of motion leads to the equation of motion for the tensor perturbations:

$$\begin{aligned}
0 = \ddot{h} + \dot{h}\left(\frac{\partial}{\partial\bar{k}}(\gamma_0\mathbb{K}[1]^2) - \frac{1}{\gamma_0(1+\alpha_4)}\frac{\mathrm{d}}{\mathrm{d}\eta}(\gamma_0(1+\alpha_4))\right) - \gamma_0^2(1+\alpha_4)(1+\alpha_9)\partial_i\partial^i h \\
+h\Bigg[\gamma_0(\mathbb{K}[s_2]+\alpha_6)\left(\frac{\partial}{\partial\bar{k}}(\gamma_0\mathbb{K}[1]^2) - \gamma_0(\mathbb{K}[s_2]+\alpha_6)\right) \\
+\frac{\mathrm{d}}{\mathrm{d}\eta}\left(\frac{\partial}{\partial\bar{k}}(\gamma_0\mathbb{K}[1]^2) - \gamma_0(\mathbb{K}[s_2]+\alpha_6)\right) \\
-\left(\frac{\partial}{\partial\bar{k}}(\gamma_0\mathbb{K}[1]^2) - \gamma_0(\mathbb{K}[s_2]+\alpha_6)\right)\frac{\frac{\mathrm{d}}{\mathrm{d}\eta}(\gamma_0(1+\alpha_4))}{\gamma_0(1+\alpha_4)} \\
-\frac{1}{2}\gamma_0^2(1+\alpha_4)(\mathbb{K}[1]^2+\alpha_7) \\
+\frac{\kappa}{2}\gamma_0(1+\alpha_4)\left((1+\beta_8)\frac{\bar{\nu}\bar{\pi}^2}{2\bar{p}^2} - \bar{p}V(1+\beta_{13})\right)\Bigg].
\end{aligned} \tag{6.9}$$

In the above equation we have used $\gamma_i = \nu_i = 0$ for $i \neq 0$, and also $\frac{\mathrm{d}\nu_0}{\mathrm{d}\bar{k}} = 0$, but left the counterterms α_j and β_j general.

Surprisingly, when the expression of the counterterms derived previously are inserted into the former equation, one can derive a really simpler expression

$$0 = h'' + h'\left(2\mathscr{H}\left(1 + \frac{2\bar{p}}{f_1[\bar{p}]}\frac{\mathrm{d}f_1[\bar{p}]}{\mathrm{d}\bar{p}}\right) - \frac{\Omega'}{\Omega}\right) - \frac{\Omega}{2\Sigma_{\bar{p}}}\left(1 + \frac{2\bar{p}}{f_1[\bar{p}]}\frac{\mathrm{d}f_1[\bar{p}]}{\mathrm{d}\bar{p}}\right)\nabla^2 h, \tag{6.10}$$

where the prime refers here to the conformal time η, $\mathscr{H}$ is the conformal Hubble factor $\mathscr{H} = \frac{a'}{a} = \frac{\bar{p}'}{2\bar{p}}$, and Ω is given in the general case by equation (5.18). When one considers

only the inverse-volume correction, Ω is given by equation (3.175) whereas for the holonomy correction it is given by equation (4.21) with also $f_1[\bar{p}] \to (1+\alpha_3)$ (the dependence on α_3 was missed in previous works, since α_3 was there assumed to be zero). The equation of motion can also be simplified when one considers $\Omega = 1$, as for instance in equation (3.191).

Moreover, it is interesting to notice that the tensor perturbations propagate with the speed c_t given by

$$c_t^2 = \frac{\Omega}{2\Sigma_{\bar{p}}}\left(1 + \frac{2\bar{p}}{f_1[\bar{p}]}\frac{\mathrm{d}f_1[\bar{p}]}{\mathrm{d}\bar{p}}\right). \tag{6.11}$$

In conclusion, we can see that there is no term proportional to h, which is usually expected at the classical limit, but also when the holonomy correction only is considered. In order to investigate the consequences of the inverse-volume correction, for instance, a possible study could be performed with $\Omega = 1$ and equation (3.191), such that the expression of the inverse-volume correction could be expressed as equation (3.1). This work, with the help of [26], could be compared with what has been derived in [15]. This is nevertheless left for future investigation.

6.3. Scalar variables and equations of motion

In this section, the scalar gauge-invariant variables and their equations of motion are derived for a general expression of the counterterms. The procedure, conventions and notations used here are described in details in [31], based on [33], but some steps will be recalled briefly in the following (the reader interested in the way the equations are derived is invited to read the previously cited articles).

The calculations are quite tedious in some cases. To simplify, we first assume that the gauge-invariant variable has the 'minimal required shape' Q related to the Mukhanov–Sasaki variable v: for instance, classically, $Q = \frac{v}{\sqrt{\bar{p}}} = \delta\varphi - \frac{\dot{\bar{\varphi}}}{\sqrt{\bar{p}}\mathcal{H}}\psi$ where $\delta\varphi$ and ψ are respectively the first order perturbations for the matter (a single Klein–Gordon field $\bar{\varphi}$) and for the metric, with $\mathcal{H}$ the conformal Hubble parameter described previously. As in [31], for simplicity, the calculation of the Hamiltonian giving the equations of motion for the gauge-invariant variables will be first done using the variable Q, and then the usual Mukhanov–Sasaki action will be rederived for the variable v. As shown in the following, in order to switch from the Hamiltonian to the Lagrangian, the second Mukhanov–Sasaki variable z will have to fulfil classically the relation

$$\frac{\ddot{z}}{z} + \Gamma - k^2 - \left(\frac{1}{\sqrt{\bar{p}}}\frac{\mathrm{d}(\sqrt{\bar{p}})}{\mathrm{d}\eta}\right)^2 - \frac{\mathrm{d}}{\mathrm{d}\eta}\left(\frac{1}{\sqrt{\bar{p}}}\frac{\mathrm{d}(\sqrt{\bar{p}})}{\mathrm{d}\eta}\right) = 0, \tag{6.12}$$

where Γ corresponds to the effective mass of Q in the Hamiltonian and k^2 is the eigenvalue of the Laplacian operator after a Fourier transform. It should be noticed that contrarily to the background variables where the Hamiltonian is in fact a constraint, for the gauge-invariant variable it corresponds to a true Hamiltonian.

In this procedure, in order to perform a change of variables from the different perturbations to the gauge-invariant ones, as Q or v, one defines a symmetric matrix A_{ij}, which by definition allows Q and v to commute with the constraints as shown in [31], and whose components will affect the effective mass Γ of the gauge-invariant variables. The important components, A_{00} and A_{01}, can be calculated and are given by:

$$A_{00} = -\frac{\bar{p}}{2\nu_0(1+\beta_5)}\left(\frac{\dot{\bar{\varphi}}^2}{\nu_0}\frac{(1+\alpha_4)(1+\beta_1)}{(\mathbb{K}[s_1]+\alpha_1)}\right), \tag{6.13}$$

and

$$A_{01} = -\frac{1}{2\bar{p}\gamma_0(\mathbb{K}[s_1]+\alpha_1)}[A_{00}(1+\beta_1)\dot{\bar{\varphi}} + \bar{p}^2(1+\beta_3)\partial_\varphi V],$$

such that Γ is

$$\Gamma = f(A_{ij}, \bar{p}, \bar{k}, \ldots)(\alpha_4-\alpha_5) + \frac{\dot{A}_{00}}{\bar{p}} + \frac{3}{2}\gamma_0(1+\alpha_4)\left(\frac{\dot{\bar{\varphi}}}{\nu_0}\right)^2 - 2\gamma_0(1+\alpha_4)\frac{\dot{\bar{\varphi}}}{\nu_0}A_{01}$$
$$+\nu_0(1+\beta_5)\left(\frac{A_{00}}{\bar{p}}\right)^2 + \nu_0(1+\beta_9)k^2 + \bar{p}(1+\beta_{10})\partial_{\varphi\varphi}V. \tag{6.14}$$

Due to the modification of the constraints with the counterterms, we need to redefine v such that at the end

$$v = \sqrt{\frac{\bar{p}}{\chi}}Q = \sqrt{\frac{\bar{p}}{\chi}}\left(\delta\varphi + \frac{\dot{\bar{\varphi}}}{\gamma_0}\frac{(1+\beta_1)}{(\mathbb{K}[s_1]+\alpha_1)}\Psi\right), \tag{6.15}$$

where

$$\begin{aligned}\chi &= \nu_0(1+\beta_5)\\ &= \frac{\nu_0^2(3-\Lambda_v)^2}{9}.\end{aligned} \tag{6.16}$$

The Hamiltonian for Q is then given by

$$H^S_{GI} = \int \frac{\mathrm{d}^3k}{2}\left[\left(\sqrt{\frac{\chi}{\bar{p}}}P\right)^2 + (\chi\Gamma)\left(\sqrt{\frac{\bar{p}}{\chi}}Q\right)^2\right]. \tag{6.17}$$

With the definition of v given in equation (6.15), it is possible to obtain the usual Mukhanov–Sasaki action

$$\mathcal{S} = \int \mathrm{d}\eta \int \mathrm{d}^3k \frac{1}{2}\left[\dot{v}^2 + \left(-c_s^2k^2 + \frac{\ddot{z}}{z}\right)v^2\right], \tag{6.18}$$

such that z has to fulfil a similar equation than equation (6.12), now modified due to the counterterms:

$$0 = \frac{\ddot{z}}{z} + \chi\Gamma - \nu_0(1+\beta_9)\chi k^2 - \left(\left(\sqrt{\frac{\bar{p}}{\chi}}\right)^{-1}\frac{\mathrm{d}}{\mathrm{d}\eta}\left(\sqrt{\frac{\bar{p}}{\chi}}\right)\right)^2$$
$$-\frac{\mathrm{d}}{\mathrm{d}\eta}\left(\left(\sqrt{\frac{\bar{p}}{\chi}}\right)^{-1}\frac{\mathrm{d}}{\mathrm{d}\eta}\left(\sqrt{\frac{\bar{p}}{\chi}}\right)\right) = 0. \tag{6.19}$$

Previous works have suggested that z would have in fact the following expression:

$$\begin{aligned}z &= \sqrt{\frac{\bar{p}}{\chi}}\frac{\dot{\bar{\varphi}}}{\gamma_0}\frac{(1+\beta_1)}{(\mathbb{K}[s_1]+\alpha_1)}\\ &= \frac{\sqrt{\bar{p}}\dot{\bar{\varphi}}}{\nu_0\gamma_0(2\mathbb{K}[2]+\mathbb{K}[1]\Gamma_{\bar{k}[1]})\Sigma_{\bar{p}}}\end{aligned} \tag{6.20}$$

but at this stage, due to some unknown relations and to the difficulties of the calculations, this expression remains only an assumption, which works classically and in the case of the holonomy correction.

The speed of propagation for the scalars is in general given by

$$c_s^2 = \nu_0(1+\beta_9)\chi = \frac{\nu_0(3-\Lambda_\nu)}{3}\Omega \tag{6.21}$$

and it is interesting to notice that this expression of c_s is different from the one c_t derived for the tensor perturbations. This could be explained by the fact that c_t depends on α_9 in equation (6.9), and it was shown in [19] that the corresponding term in the Hamiltonian constraint is in fact different when one considers the tensor perturbations. Therefore, the expression obtained here for α_9 was in fact specific to the scalar perturbations and could be different for the tensor perturbations. Nevertheless, due to the properties of the tensor perturbations, the algebra for these kind of perturbations corresponds to the homogeneous one, where $\{H, H\} = 0$, and it is not possible to derive an expression for the counterterms, which remain unknown if one considers the approach only for these perturbations. In order to solve this problem, one could also assume that $c_s = c_t$ and see what are the consequences on the phenomenology induced by the previous modifications (in a similar way as the case where only the holonomy corrections were considered, where $c_s = c_t = \Omega$ if and only if $\alpha_3 = 0$, and whose spectrum was derived in [25]). This is also left for future works.

When one considers the holonomy correction only, the variables are then given by:

$$\chi = 1, \qquad z = \sqrt{\bar{p}}\frac{\dot{\bar{\varphi}}}{\mathbb{K}[2]}, \quad \text{and} \quad c_s^2 = \Omega, \tag{6.22}$$

as found in [17]. However, due to the unknown expressions, when the inverse-volume corrections are considered, we will not derive here the expressions of the equation of motion with the specific counterterms given previously, the expression being too complicated and not useful. Nevertheless, the reader who would have a specific set of counterterms will be able to derive without any ambiguities the corresponding equation of motion for the scalar perturbations and check that what has been said previously will work also in this case.

7. Conclusions

In this work, we have tried to sum-up all that is currently known on the issue of the closure of the algebra in effective LQC and to address the question of a full resolution taking into account both corrections simultaneously. To this aim, we have generalized the previously derived results for the inverse-volume corrections. We have also found new solutions, that were missed in previous works, for the holonomy case.

We have found that in all three cases (holonomy, inverse-volume, and holonomy + inverse-volume) it is possible, under the assumptions of this paper, to close the algebra of constraints. Further, we have calculated the explicit counterterms required for this closure. These counterterms are functions of the zeroth order corrections and of an unknown function of integration ($f_1[\bar{p}]$ in the case of inverse-volume or inverse-volume + holonomy, and α_3 in the case of holonomy only).

An interesting result is that the final form of the constraints does only depend on the zeroth order of the corrections and not on higher order terms.

We have found some equations constraining the form of the corrections. This includes (not exhaustively):

- In both the inverse-volume and inverse-volume + holonomy cases:

$$\frac{\partial \nu_0}{\partial \bar{k}} = 0. \tag{7.1}$$

- In the case with only holonomy corrections:

$$\mu \propto \frac{1}{\sqrt{\bar{p}}}. \tag{7.2}$$

- In the case of both corrections simultaneously:

$$\frac{\partial \gamma_0}{\partial \bar{k}} \neq 0 \qquad \text{or} \qquad \mu \propto \sqrt{\frac{\gamma_0}{\bar{p}}}. \tag{7.3}$$

The inverse-volume corrections are constrained but far from being fully determined by the closure of the algebra. This is normal, and the final input is expected to come from the full theory.

We have found that the final algebra is modified when compared with the classical one, by a factor Ω given by

$$\Omega = \left(\frac{\partial^2}{\partial \bar{k}^2} (\gamma_0 \mathbb{K}[1]^2) \right) \Sigma_{\bar{p}} f_1[\bar{p}], \tag{7.4}$$

in the case of both corrections. The inverse-volume case is given by $\bar{\mu} \to 0$ or $\mathbb{K}[n] \to \bar{k}$ and the only holonomy case is given by $\gamma \to 1$, $\Sigma_{\bar{p}} \to \frac{1}{2}$ and $f_1[\bar{p}] \to (1 + \alpha_3)$.

If the holonomy corrections are included (with or without inverse-volume corrections), then a modification of the algebra should be unavoidable, that is, there is no solution such that $\Omega = 1$ which does not completely cancels the holonomy corrections. Surprisingly, a bounce might still be possible whenever the inverse-volume corrections are considered.

In the case of only inverse-volume corrections, the solution $\Omega = 1$ is not excluded, showing an interesting example of an unmodified algebra with nevertheless some modifications of the constraints, in tension with a naive interpretation of the Hojman–Kuchar–Teitelboim theorem [34].

Moreover, the equations of motion for the tensor and scalar perturbations have been derived in the general case, but a full example when both corrections are considered simultaneously is still awaited. Some toy models could also be studied, leading to some open new perspectives for phenomenology.

To conclude, the simplest case for the constraints has been considered so far, and the next steps could be either to include backreaction or higher derivatives in the expressions of the constraints.

Acknowledgments

The authors would like to thank Martin Bojowald, Norbert Bordendofer but also the referees for their improvement of this paper, by their careful readings and comments. TC was supported by the NSF grant PHY-1205388. LL is supported by the Labex ENIGMASS.

References

[1] Barrau A, Cailleteau T, Grain J and Mielczarek J 2014 *Class. Quantum Grav.* **31** 053001
Dona P and Speziale S 2010 arXiv:1007.0402V1
Perez A 2004 arXiv:gr-qc/0409061v3
Gambini R and Pullin J 2011 *A First Course in Loop Quantum Gravity* (Oxford: Oxford University Press)
Rovelli C 2011 *PoS* **QGQGS 2011** 003
Rovelli C 2004 *Quantum Gravity* (Cambridge: Cambridge University Press)
Rovelli C 1998 *Living Rev. Rel.* **1** 1
Smolin L 2004 arXiv:hep-th/0408048v3

Thiemann T 2003 *Lect. Notes Phys.* **631** 41
Thiemann T 2007 *Modern Canonical Quantum General Relativity* (Cambridge: Cambridge University Press)
[2] Ashtekar A, Bojowald M and Lewandowski J 2003 *Adv. Theor. Math. Phys.* **7** 233
Ashtekar A 2009 *Gen. Rel. Grav.* **41** 707
Ashtekar A and Singh P 2011 *Class. Quantum Grav.* **28** 213001
Bojowald M 2008 *Living Rev. Rel.* **11** 4
Bojowald M 2012 *Class. Quantum Grav.* **29** 213001
Banerjee K, Calcagni G and Martin-Benito M 2012 *SIGMA* **8** 016
Calcagni G 2013 *Ann. Phys.* **525** 323
Agullo I and Corichi A 2013 arXiv:1302.3833 [gr-qc]
[3] Ashtekar A and Campiglia M 2012 *Class. Quantum Grav.* **29** 242001
[4] Bojowald M, Brizuela D, Hernandez H H, Koop M J and Morales-Tecotl H A 2011 *Phys. Rev.* D **84** 043514
[5] Bojowald M and Skirzewski A 2006 *Rev. Math. Phys.* **18** 713–45
Bojowald M and Skirzewski A 2007 *Int. J. Geom. Methods Mod. Phys.* **4** 25–52
Bojowald M, Brahma S and Nelson E 2012 *Phys. Rev.* D **86** 105004
[6] Thiemann T 1998 *Class. Quantum Grav.* **15** 839
Rovelli C and Smollin L 1994 *Phys. Rev. Lett.* **72** 446
[7] Thiemann T 1998 *Class. Quantum Grav.* **15** 1281
[8] Dirac P M 1969 *Lectures on Quantum Mechanics* (New York: Yeshiva Press)
[9] Bojowald M, Hossain G M, Kagan M and Shankaranarayanan S 2008 *Phys. Rev.* D **78** 063547
[10] Nicolai H, Peeters K and Zamaklar M 2005 *Class. Quantum Grav.* **22** R193
[11] Bojowald M, Hossain G M, Kagan M and Shankaranarayanan S 2009 *Phys. Rev.* D **79** 043505
Bojowald M, Hossain G M, Kagan M and Shankaranarayanan S 2010 *Phys. Rev.* D **82** 109903 (erratum)
[12] Bojowald M and Hossain G M 2007 *Class. Quantum Grav.* **24** 4801
[13] Bojowald M and Hossain G M 2008 *Phys. Rev.* D **77** 023508
[14] Bojowald M and Calcagni G 2011 *J. Cosmol. Astropart. Phys.* JCAP03(2011)32
[15] Bojowald M, Calcagni G and Tsujikawa S 2011 *Phys. Rev. Lett.* **107** 211302
[16] Mielczarek J, Cailleteau T, Barrau A and Grain J 2012 *Class. Quantum Grav.* **29** 085009
[17] Cailleteau T, Mielczarek J, Barrau A and Grain J 2012 *Class. Quantum Grav.* **29** 095010
[18] Wilson-Ewing E 2012 *Class. Quantum Grav.* **29** 215013
[19] Cailleteau T, Barrau A, Grain J and Vidotto F 2012 *Phys. Rev.* D **86** 087310
[20] Bojowald M and Paily G M 2013 *Phys. Rev.* D **87** 044044
[21] Tibrewala R 2013 *Class. Quantum Grav.* **31** 055010
[22] Agullo I, Ashtekar A and Nelson W 2013 *Phys. Rev.* D **87** 043507
[23] Rovelli C and Wilson-Ewing E 2013 arXiv:1310.8654 [gr-qc]
[24] Bojowald M 2001 *Phys. Rev.* D **64** 084018
[25] Linsefors L, Cailleteau T, Barrau A and Grain J 2013 *Phys. Rev.* D **87** 107503
[26] Mielczarek J 2013 arXiv:1311.1344 [gr-qc]
[27] Mielczarek J 2012 *AIP Conf. Proc.* **1514** 81
[28] Fernàndez-Méndez M, Marugàn G A M and Olmedo J 2012 *Phys. Rev.* D **86** 024003
Fernàndez-Méndez M, Marugàn G A M and Olmedo J 2013 *Phys. Rev.* D **88** 044013
[29] Ashtekar A, Fairhurst S and Willis J L 2001 *Class. Quantum Grav.* **20** 1031
Thirring W and Narnhofer N 1992 *Rev. Math. Phys.* **4** 197
Halvorson H 2004 *Stud. Hist. Phil. Mod. Phys.* **35** 45–56
[30] Giesel K and Thiemann T 2006 *Class. Quantum Grav.* **23** 5667
[31] Cailleteau T and Barrau A 2012 *Phys. Rev.* D **85** 123534
[32] Calcagni G and Hossain G M 2009 *Adv. Sci. Lett.* **2** 184
[33] Langlois D 1994 *Class. Quantum Grav.* **11** 389
[34] Hojman S A, Kuchar K and Teitelboim C 1976 *Ann. Phys.* **96** 88

5.2 Change of signature

When the density is greater than $\rho_c/2$, where ρ_c is of the order of the Planck density, the *Omega* factor introduced previously becomes negative and the Poisson bracket between scalar constraints becomes negative:

$$\left\{S^Q[M], S^Q[N]\right\} = \mathbf{\Omega} D\left[q^{ab}(M\partial_b N - N\partial_b M)\right]. \tag{5.1}$$

This can be interpreted as a change of signature of space-time. Interestingly, this has strong links with results often postulated (mostly for technical reasons, notably a better behavior of path integrals) in quantum cosmology, but it appears here as a real dynamical effect of the theory. It is not added by hands. In "historical" quantum cosmology, one usually deals with an amplitude

$$< \phi_2, t_2 | \phi_1, t_1 >= \int d[\phi] e^{I[\phi]}, \tag{5.2}$$

where $I[\phi]$ is the action of the field configuration $\phi(x,t)$, and $d[\phi]$ is a measure on the space of field configurations. The phase in the integrand of Eq.(5.2) is rapidly oscillating, and the path integral, in usual cases, does not converge. This is why time is rotated clockwise by $\pi/2$ so that $I[\phi] \to \tilde{I}[\phi] \equiv -iI[\phi]$. The integrand in the resulting Euclidean path integral is now exponentially damped, and the integral generically converges. On can then analytically continue the amplitude in the complex t-plane back to real values.

There are also relations with the so-called Hartle-Hawking no-boundary proposal [14]. But in our case the phenomenon is somehow inevitable for consistency reasons and not resulting from a boundary choice. Importantly, the appearance of an Euclidean phase was also independently derived from another approach to LQC where one relies on little "patches" of universes [15]. Many quantum gravity approaches seem to predict the existence of a silent surface ($\Omega = 0$) where light cones are completely squeezed, on each "side" of the Euclidean phase [16, 17].

Signature change might be an important consequence of holonomy modifications which had been overlooked so far, until spherically symmetric inhomogeneity and cosmological perturbations were studied in an anomaly-free framework. Without inhomogeneity, one indeed cannot determine the signature for two obvious reasons. First, one cannot see the relative sign between temporal and spatial derivatives. Second, the Poisson bracket between Hamiltonian constraints vanishes in homogeneous models. Nevertheless, it seems that the signature change is not a consequence of inhomogeneity, the latter rather being used as a test field. Signature change appears as a consequence of the strong modification one makes if one uses holonomy terms at high density, not of a small amount of perturbative inhomogeneity added to the system.

In the two articles presented hereafter, we make the assumption that it remains possible to evolve perturbations through the Euclidean bounce. We set initial conditions in the contracting Lorentzian branch and evolve the perturbations. The first article is devoted to tensor modes and the second one to scalar modes. The technical difficulties are due to the fact that the equations of propagation do have divergences, in particular at $\rho = \rho_c/2$. However thanks to different changes of variables, we were able to find regular solutions. At the level of the equation of propagation in Fourier space, the problem is well posed and well defined.

We also make the assumption that our calculations are physically valid even when the wavelength of the evolved perturbation shrinks below the Planck length. This causes no mathematical problem, but it could be questioned weather such short wavelengths are compatible with LQG. At the moment there is no consensus of what is the correct length operator in LQG, or weather it allows for a quasi-continuum below the Planck length.

In this section, we assume that it is possible to evolve the perturbations both through the Euclidean region and below the plank length. The opposite standpoint is explored in Section 5.4.

We find that, in the Euclidean region, the perturbations grow exponentially. However, the exponent is proportional to the wave number so that only short wave modes are noticeable effected by the signature change. For both scalar and tensor modes the resulting spectrum increase exponentially with k for $k > k_{UV}$, where k is the co-moving wave number normalized at the bounce and $k_{UV} \approx 2.3 m_{Pl}$. This is clearly not compatible with observations, however $k > k_{UV}$ is exactly the part of the spectrum that is mots questionable for theoretical reasons.

For the tensor modes, we get a flat spectrum in the IR-limit. This part of the spectrum is formed during the contraction of the universe, and the modes are frozen, out side the Hubble horizon, all though the bounce and following inflation. In the scalar mode case the situation is more complicated due to problem of imposing initial conditions for long wavelengths.

The spectrums for both for scalar and tensor modes exhibit oscillations in both UV-limits and intermediate regions. These oscillations are due to a similar effect as the autistic oscillations observed in the CMB.

PHYSICAL REVIEW D **87,** 107503 (2013)

Primordial tensor power spectrum in holonomy corrected Ω loop quantum cosmology

Linda Linsefors[*]
Laboratoire de Physique Subatomique et de Cosmologie, Université Joseph Fourier, INPG, CNRS, IN2P3 53, Avenue des Martyrs, 38026 Grenoble Cedex, France

Thomas Cailleteau[†]
Institute for Gravitation & the Cosmos, Pennsylvania State University, University Park, Pennsylvania 16802, USA

Aurelien Barrau[‡]
Laboratoire de Physique Subatomique et de Cosmologie, Université Joseph Fourier, INPG, CNRS, IN2P3 53, Avenue des Martyrs, 38026 Grenoble Cedex, France

Julien Grain[§]
Institut d'Astrophysique Spatiale, Université Paris-Sud 11, CNRS, UMR8617, F-91405 Orsay, France
(Received 13 December 2012; published 16 May 2013)

The holonomy correction is one of the main terms arising when implementing loop quantum gravity ideas at an effective level in cosmology. The recent construction of an anomaly-free algebra has shown that the formalism used, up to now, to derive the primordial spectrum of fluctuations was not correct. This paper aims at computing the tensor spectrum in a fully consistent way within this deformed and closed algebra.

DOI: 10.1103/PhysRevD.87.107503 PACS numbers: 04.60.−m, 98.80.Qc

I. INTRODUCTION

Nonperturbatively quantizing General Relativity (GR) in a background-invariant way is obviously an outstanding open problem of theoretical physics. Loop quantum gravity (LQG) is a promising framework in which to perform this program (see Ref. [1] for introductory reviews). Although this is still to be demonstrated, there is evidence that different approaches, based either on quantizations (covariant or canonical) of GR or on a formal quantization of geometry, lead to the same LQG theory. Experimental tests are, however, still missing. Trying to find possible observational signatures is a key challenge, and cosmological footprints are known for being one of the only possible paths toward a real experimental test of LQG. It is very hard to make clear predictions in loop quantum cosmology (LQC) using the full ''mother'' LQG theory. General introductions to LQC can be found in Ref. [2]. This study focuses on an effective treatment taking into account recent results on the correct algebra of constraints. We first review the theoretical framework. The spectrum is then derived. Some conclusions and consequences are finally underlined.

II. THEORETICAL FRAMEWORK

One of the fundamental quantum corrections expected from the Hamiltonian of LQG arises from the fact that loop quantization is based on holonomies, i.e., exponentials of the connection, rather than direct connection components. Based on a canonical approach, the theory uses Ashtekar variables, namely, SU(2) valued connections and conjugate densitized triads. The quantization is obtained through holonomies of the connections and fluxes of the densitized triads. This is the key ingredient of the effective approach. The cosmological equations are modified so as to account for the loop basis of the theory.

The main consequence of the holonomy correction on the cosmological background is to induce a bounce. The evolution is not singular anymore, and the big bang is replaced by a big bounce. The next step consists of studying the propagation of perturbations within this modified background. In cosmology, perturbations are of three different types: scalar, vector, and tensor. We focus here on the tensor modes that are directly gauge-invariant. Quite a lot of works have already been devoted to tensor modes in this framework [3]. Beyond that, the phenomenology of LQG is now a well-established field (see Ref. [4] for a review). Unfortunately, a recent study [5] has shown that the previously derived spectra are most probably incorrect.

The key issue relies in the closure of the algebra of constraints. Due to general covariance, the canonical Hamiltonian is a combination of constraints $\mathcal{C}_I$. Consistency requires that the constraints are preserved under the evolution they generate. This is ensured in the classical theory by the closure of the Poisson algebra of constraints,

$$\{\mathcal{C}_I, \mathcal{C}_J\} = f^K{}_{IJ}(A^j_b, E^a_i)\mathcal{C}_K, \tag{1}$$

where $\mathcal{C}_I$, $I = 1, 2, 3$, are the Gauss, diffeomorphism, and Hamiltonian constraints and $f^K{}_{IJ}(A^j_b, E^a_i)$ are structure functions, which, in general, depend on the phase space

[*]linsefors@lpsc.in2p3.fr
[†]thomas@gravity.psu.edu
[‡]Aurelien.Barrau@cern.ch
[§]julien.grain@ias.u-psud.fr

(Ashtekar) variables (A^j_b, E^a_i). They form a first class set. Otherwise stated, the gauge transformations and evolution generated by the constraints define vector fields that are tangent to the submanifold defined by the vanishing of constraints.

In LQC, quantum corrections are introduced as effective modifications of the Hamiltonian constraint. This generates anomalies: the modified constraints $\mathcal{C}^Q_I$ do not form a closed algebra anymore,

$$\{\mathcal{C}^Q_I, \mathcal{C}^Q_J\} = f^K{}_{IJ}(A^j_b, E^a_i)\mathcal{C}^Q_K + \mathcal{A}_{IJ}. \tag{2}$$

The anomalous terms $\mathcal{A}_{IJ}$ are removed by carefully adjusting the form of the quantum correction to the Hamiltonian constraint through the addition of suitable "counterterms" that vanish in the classical limit. This has been done in Ref. [5], following the approach of Ref. [6].

In the classical case, the Poisson brackets between the constraints read as

$$\{D_{(m+g)}[N^a_1], D_{(m+g)}[N^a_2]\} = 0, \tag{3}$$

$$\{H_{(m+g)}[N], D_{(m+g)}[N^a]\} = -H_{(m+g)}[\delta N^a \partial_a \delta N], \tag{4}$$

$$\{H_{(m+g)}[N_1], H_{(m+g)}[N_2]\} = D_{(m+g)}\left[\frac{\bar{N}}{\bar{p}}\partial^a(\delta N_2 - \delta N_1)\right], \tag{5}$$

where $(m + g)$ stands for gravity and matter. The quantum corrections are included at the effective level by replacing, as usual, in the Hamiltonian constraint

$$\bar{k} \to \frac{\sin(\bar{\mu}\gamma\bar{k})}{\bar{\mu}\gamma}. \tag{6}$$

The important result of Ref. [5] is that the quantum-corrected algebra is described by a single modification:

$$\{H_{(m+g)}[N_1], H_{(m+g)}[N_2]\} = \mathbf{\Omega} D_{(m+g)}\left[\frac{\bar{N}}{\bar{p}}\partial^a(\delta N_2 - \delta N_1)\right], \tag{7}$$

where

$$\mathbf{\Omega} = \cos(2\bar{\mu}\gamma\bar{k}) = 1 - 2\frac{\rho}{\rho_c}. \tag{8}$$

The $\mathbf{\Omega}$ factor encodes the quantum correction, $\bar{k}$ being the homogeneous Ashtekar connection and $\bar{\mu}$ being proportional to the ratio between the Planck length and the scale factor. The Mukhanov-Sasaki [7] equation of motion for gauge-invariant perturbations of scalar and tensor types $v_{S(T)}$ can be explicitly derived. In conformal time, the propagation of tensor modes is given by

$$v''_T - \mathbf{\Omega}\nabla^2 v_T - \frac{z''_T}{z_T}v_T = 0; \qquad z_T = \frac{a}{\sqrt{\mathbf{\Omega}}}, \tag{9}$$

where *prime* means differentiation with respect to conformal time. This leads to the following equation of motion for tensor perturbations, defined via $v_T = z_T \times h^i_a$:

$$h^{i\prime\prime}_a + h^{i\prime}_a\left(2\mathcal{H} - \frac{\mathbf{\Omega}'}{\mathbf{\Omega}}\right) - \mathbf{\Omega}\nabla^2 h^i_a = 0, \tag{10}$$

where $\mathcal{H} := a'/a$ is the conformal Hubble parameter.

III. POWER SPECTRUM

This equation being known, it is possible to investigate the associated primordial power spectrum. This is the fundamental ingredient for phenomenology. The background dynamics is not modified by the $\mathbf{\Omega}$ term. However, the perturbations will, of course, undergo a different evolution.

We use the Fourier transformed version of Eq. (10):

$$h'' + \left(2\mathcal{H} - \frac{\mathbf{\Omega}'}{\mathbf{\Omega}}\right)h' + \mathbf{\Omega}k^2 h = 0, \tag{11}$$

where the indices have been skipped for simplicity. The behavior of $\mathbf{\Omega}$ and $\mathbf{\Omega}'$ is displayed in Fig. 1. One can immediately see that $\mathbf{\Omega}$ vanishes for $\rho = \rho_c/2$, where

$$\rho_c = \frac{\sqrt{3}}{32\pi^2\gamma^3}m^4_{\mathrm{Pl}} \simeq 0.41 m^4_{\mathrm{Pl}}. \tag{12}$$

In addition, $\mathbf{\Omega}$ becomes negative-valued, leading to an effective change of signature of the metric (Euclidean phase) around the bounce. The interested reader will find a technical discussion in Ref. [8] and some qualitative speculations in Ref. [9]. Intuitively, this signature change can be straightforwardly interpreted as a change of sign of the Poisson bracket between Hamiltonian constraints. Equation (11) is apparently ill-defined as $\mathbf{\Omega}'/\mathbf{\Omega} \to \infty$ at $\eta = \eta^{(-)}$ and $\eta = \eta^{(+)}$, the values of conformal time when $\rho = \rho_c/2$ before and after the bounce, respectively. However, regular solutions do exist by rewriting Eq. (11) as:

$$h' = \mathbf{\Omega}g; \qquad g' = -2\mathcal{H}g - k^2 h, \tag{13}$$

which is regular.

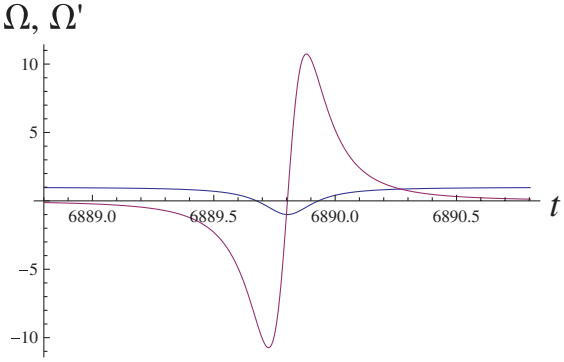

FIG. 1 (color online). Evolution of $\mathbf{\Omega}$ and its derivative with respect to conformal time. The density where $\mathbf{\Omega}$ vanishes is half the critical density, whereas $\mathbf{\Omega}'$ vanishes at the bounce.

The same set of equations in cosmic time is:

$$\dot{h} = \frac{\mathbf{\Omega}}{a} g; \qquad \dot{g} = -2Hg - \frac{k^2}{a} h, \tag{14}$$

where *dot* means differentiation with respect to cosmic time and H is the usual Hubble parameter. The dynamics can also be recast in a single second-order equation:

$$g'' + 2\mathcal{H} g' + (2\mathcal{H}' + \mathbf{\Omega} k^2) g = 0. \tag{15}$$

Whatever the chosen form, either Eq. (13), (14) or (15), the evolution can be computed numerically. Of course, the propagation of modes has to be coupled with the background evolution, which is drastically modified by the holonomy corrections that are at the origin of the bounce. The cosmological background evolution is basically driven by a single scalar massive matter field of mass m. We define

$$x := \frac{m\phi}{\sqrt{2\rho_c}} \quad \text{and} \quad y := \frac{\dot{\phi}}{\sqrt{2\rho_c}}, \tag{16}$$

which, respectively, represent the density of potential and kinetic energy normalized so that $x_B^2 + y_B^2 = 1$ at the bounce. The free parameters of the study are, therefore, m, x_B (the value of x at the bouce) and the relative sign of x_B and y_B. Interestingly, if the initial conditions for the background are specified at any time, long enough before the bounce, the probability of $|x_B|$ is strongly peaked around a given value of order m (in Planck units), with $\mathrm{sign}(x_B) = \mathrm{sign}(y_B)$ (the detailed probability distribution for x_B will be studied somewhere else [10]). For numerical reasons, it is better to specify computational initial conditions for the background before the bounce rather than at the bounce. Because of the peaked probability, the resulting x_B is always close to the same value.

It is also necessary to assign a numerical value to the scale factor a at some point. This choice has, of course, no physical consequences but has to be taken into account for the interpretation of the meaning of the wave vectors k, since they are expressed in the coordinate space and not in the physical space. The explicit choice made was $a = 1$ at the bounce, which is numerically easier than the usual normalization at the nowadays value.

In Fig. 2, the evolution of the scalar field and scale factor are shown for some typical parameters. As expected, the oscillations of the scalar field are amplified before the bounce because the negative Hubble parameter acts as an antifriction term. Then, just after the bounce, the Hubble parameter becomes positive and large, acting as a huge friction and, therefore, leading to slow-roll inflation.

The amplitudes of some Fourier modes of h are plotted in Fig. 3. They are obtained by choosing the Minkowski vacuum as the initial state, since $z''/z \to 0$ in the remote past.

Before the bounce, for $k^2 \gg z''/z$, $|h|^2 = 1/(2ka^2)$, when $z''/z \approx k^2$ or $z''/z > k^2$, $|h|^2$ grows more quickly. Since the amplitudes of smaller k start growing more quickly before the amplitudes of larger k, this adds up to a collecting effect that brings all modes up to a certain $k \approx \max_{t<t_B}(\sqrt{z''/z})$ up to the same amplitude. After the bounce, the amplitudes oscillate until $k^2 \gg z''/z$ when we

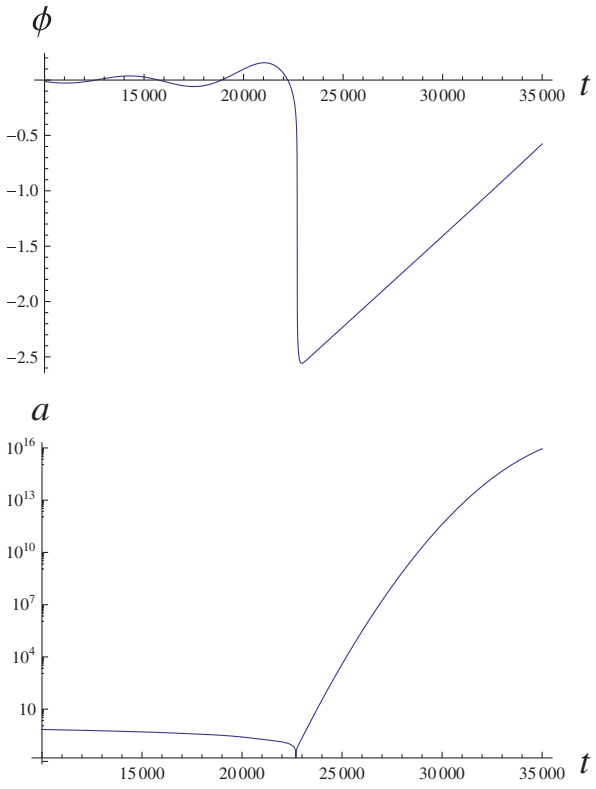

FIG. 2 (color online). Evolution of the scalar field (upper panel) and the scale factor (lower panel) as a function of cosmic time (the bounce corresponds to $t = 22693$). The parameters are $m = 10^{-3} M_{\mathrm{Pl}}$ and $x_B = -1.5 \times 10^{-3}$.

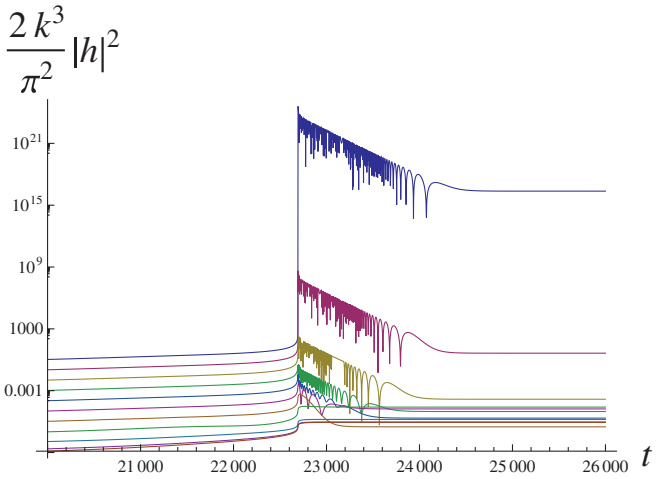

FIG. 3 (color online). Mode amplitudes as a function of time, corresponding (from top to bottom, at $t = 20000$) to $k = 10^2$, $10^{1.5}$, 10^1, $10^{0.5}$, 1, $10^{-0.5}$, 10^{-1}, $10^{-1.5}$, 10^{-2}, $10^{-2.5}$, and 10^{-3}. The parameters are $m = 10^{-3} M_{\mathrm{Pl}}$ and $x_B = -1.5 \times 10^{-3}$. It should be noted that the initial conditions for each mode are specified long before the time interval of this plot.

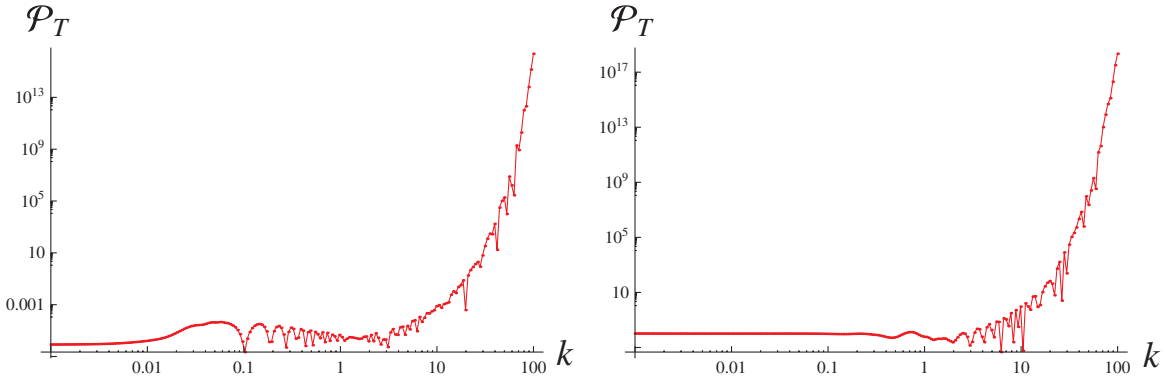

FIG. 4 (color online). Power spectrum of tensor perturbations after inflation for $m = 10^{-3}M_{\rm Pl}$ (left panel) and for $m = 10^{-1}M_{\rm Pl}$ (right panel).

get $v \propto a$ [as can bee seen from Eq. (9)] and, therefore, $h =$ constant.

Finally, the power spectra for different cases are presented in Fig. 4. The main features are the following:

(i) a flat (scale invariant) infrared limit,
(ii) an oscillating intermediary part,
(iii) an exponential behavior in the ultraviolet limit (starting around $k = 2$ independently of m).

This obviously exhibits important deviations, with respect both to the standard GR case and with respect to previous LQC computations without the $\mathbf{\Omega}$ term. Although surprising at first sight, the exponential divergence in the UV limit might not be catastrophic as physics at a very small scale is anyway not described by the primordial power spectrum.

Furthermore, this ultraviolet behavior can be checked analytically. In the large k limit of Eq. (9), the WKB conditions are satisfied in the Euclidean phase around the bounce. More precisely, those WKB conditions are met for $\eta \in [\eta^{(-)} + \epsilon_k^{(-)}, \eta^{(+)} - \epsilon_k^{(+)}]$ with $\epsilon_k^{(\pm)} \sim (k^2|\Omega'(\eta = \eta^{(\pm)}|)^{-1/3}$. The Mukhanov-Sasaki function can be approximated by

$$v_{\rm T} = v_+ e^{ik\int\sqrt{\mathbf{\Omega}}d\eta} + v_- e^{-ik\int\sqrt{\mathbf{\Omega}}d\eta}. \tag{17}$$

As $\mathbf{\Omega}$ is negative-valued during the Euclidean phase, the tensor mode is dominated by its exponentially growing solution

$$h \propto \exp\left(k\int_{\eta^{(-)}+\epsilon_k^{(-)}}^{\eta^{(+)}-\epsilon_k^{(+)}} \sqrt{|\mathbf{\Omega}|}d\eta\right). \tag{18}$$

This can also be seen in Fig. 3, where the amplitude of large k modes grows rapidly in the vicinity of the bounce, where $\mathbf{\Omega} < 0$.

IV. DISCUSSION

This study implements in a consistent way the modified algebra induced by holonomy corrections in the calculation of the primordial tensor power spectrum. Thanks to numerical calculations, it was possible to solve the equation of motion for gravitational waves. The resulting spectrum exhibits specific features. Of course, this raises important questions. First, the well-known problem of trans-Planckian modes in inflation (see, e.g., Ref. [11]) should be treated with a specific care in LQG in which the very meaning of a length smaller than the Planck length is dubious. If the number of e-folds of inflation is chosen (by appropriately setting a very small fraction of potential energy density at the bounce) to be just above the minimum required value, then modes relevant for the cosmic microwave background are still sub-Planckian, and the approach makes sense anyway. In other cases, the effective theory might just break down. With the normalization chosen in this work, the trans-Planckian window corresponds to $k > 1$. Second, the propagation of modes through the Euclidean phase is not straitghforward [8]. Strictly speaking, there is no "time" in that region, and the concept of evolution is not well-defined. In this work, we have deliberately chosen to withdraw the conceptual issues associated with the transition between hyperbolic and elliptic solutions and to focus on a well defined mathematical solution. An alternative approach, based on the BKL conjecture, will be studied later [12]. An analogous study should also be performed for scalar modes. The regularization trick used here, however, does not apply directly, and other methods have to be constructed. We stress that the case of scalar modes with holonomy corrections has been studied in Refs. [13,14] but in different settings for the background; for the study of Ref. [13] is restricted to superinflation while the study of Ref. [14] considered a dustlike bouncing Universe. Finally, those results will have to be compared with forthcoming studies based on other very recent approaches to LQC [15].

ACKNOWLEDGMENTS

We would like to thank Arnaud Demion with whom the first ideas were discussed. T. C. was supported by the NSF Grant No. PHY-1205388. This work was supported by the Labex ENIGMASS.

[1] P. Dona and S. Speziale, arXiv:1007.0402; A. Perez, arXiv:hep-th/0409061; R. Gambini and J. Pullin, *A First Course in Loop Quantum Gravity* (Oxford University, New York, 2011); C. Rovelli, Proc. Sci., QGQGS2011 (2011) 003; *Quantum Gravity* (Cambridge University Press, Cambridge, England, 2004); Living Rev. Relativity **1**, 1 (1998); L. Smolin, arXiv:hep-th/0408048; T. Thiemann, Lect. Notes Phys. **631**, 41 (2003); *Modern Canonical Quantum General Relativity* (Cambridge University Press, Cambridge, England, 2007).

[2] A. Ashtekar, M. Bojowald, and J. Lewandowski, Adv. Theor. Math. Phys. **7**, 233 (2003); A. Ashtekar, Gen. Relativ. Gravit. **41**, 707 (2009); A. Ashtekar and P. Singh, Classical Quantum Gravity **28**, 213001 (2011); M. Bojowald, Living Rev. Relativity **11**, 4 (2008); Classical Quantum Gravity **29**, 213001 (2012); I. Agullo and A. Corichi, arXiv:1302.3833.

[3] J. Mielczarek, J. Cosmol. Astropart. Phys. 11 (2008) 011; J. Grain and A. Barrau, Phys. Rev. Lett. **102**, 081301 (2009); J. Mielczarek, Phys. Rev. D **79**, 123520 (2009); J. Mielczarek, T. Cailleteau, J. Grain, and A. Barrau, Phys. Rev. D **81**, 104049 (2010); J. Grain, A. Barrau, T. Cailleteau, and J. Mielczarek, Phys. Rev. D **82**, 123520 (2010).

[4] F. Girelli, F. Hinterleitner, and S. Major, SIGMA **8**, 098 (2012).

[5] T. Cailleteau, A. Barrau, J. Grain, and F. Vidotto, Phys. Rev. D **86**, 087301 (2012).

[6] M. Bojowald, G. M. Hossain, M. Kagan, and S. Shankaranarayanan, Phys. Rev. D **78**, 063547 (2008); **79**, 043505 (2009); M. Bojowald and G. M. Hossain, Classical Quantum Gravity **24**, 4801 (2007); Phys. Rev. D **77**, 023508 (2008); Y. Li and J. Y. Zhu, Classical Quantum Gravity **28**, 045007 (2011); J. Mielczarek, T. Cailleteau, A. Barrau, and J. Grain, Classical Quantum Gravity **29**, 085009 (2012); T. Cailleteau, J. Mielczarek, A. Barrau, and J. Grain, Classical Quantum Gravity **29**, 095010 (2012).

[7] V. F. Mukhanov, H. A. Feldman, and R. H. Brandenberger, Phys. Rep. **215**, 203 (1992).

[8] M. Bojowald and G. M. Paily, Phys. Rev. D **86**, 104018 (2012).

[9] J. Mielczarek, AIP Conf. Proc. **1514**, 81 (2012).

[10] L. Linsefors, A. Barrau, arXiv:1301.1264.

[11] U. H. Danielsson, Phys. Rev. D **66**, 103514 (2002).

[12] J. Mielzcarek, AIP Conf. Proc. **1514**, 81 (2012).

[13] X.-J. Yue and J. Y. Zhu, Phys. Rev. D **87**, 063518 (2013).

[14] E. Wilson-Ewing, J. Cosmol. Astropart. Phys. 03 (2013) 026.

[15] I. Agullo, A. Ashtekar, and W. Nelson, Phys. Rev. D **87**, 043507 (2013); Phys. Rev. Lett. **109**, 251301 (2012); M. Bojowald, A. L. Chinchili, C. D. Dantas, M. Jaffe, and D. Simpson, Phys. Rev. D **86**, 124027 (2012).

Primordial scalar power spectrum from the Euclidean Big Bounce

Susanne Schander*
Technische Universität Kaiserslautern, D-67653 Kaiserslautern, Germany and
Laboratoire de Physique Subatomique et de Cosmologie, Université Grenoble-Alpes, CNRS-IN2P3
53, avenue des Martyrs, 38026 Grenoble cedex, France

Aurélien Barrau,† Boris Bolliet,‡ Linda Linsefors,§ and Jakub Mielczarek¶
Laboratoire de Physique Subatomique et de Cosmologie, Université Grenoble-Alpes, CNRS-IN2P3
53, avenue des Martyrs, 38026 Grenoble cedex, France

Julien Grain**
CNRS, Orsay, France, F-91405 and
Université Paris-Sud 11, Institut d'Astrophysique Spatiale, UMR8617, Orsay, France, F-91405
(Dated: October 8, 2015)

In effective models of loop quantum cosmology, the holonomy corrections are associated with deformations of space-time symmetries. The most evident manifestation of the deformations is the emergence of an Euclidean phase accompanying the non-singular bouncing dynamics of the scale factor. In this article, we compute the power spectrum of scalar perturbations generated in this model, with a massive scalar field as the matter content. Instantaneous and adiabatic vacuum-type initial conditions for scalar perturbations are imposed in the contracting phase. The evolution through the Euclidean region is calculated based on the extrapolation of the time direction pointed by the vectors normal to the Cauchy hypersurface in the Lorentzian domains. The obtained power spectrum is characterized by a suppression in the IR regime and oscillations in the intermediate energy range. Furthermore, the speculative extension of the analysis in the UV reveals a specific rise of the power.

PACS numbers: 98.80.Qc, 98.80.Jk

I. INTRODUCTION

Loop quantum gravity (LQG) is a simple, consistent, non-perturbative and background-independent quantization of general relativity. It uses Ashtekar variables, namely the SU(2)-valued connections and the conjugate densitized triads. The quantization is obtained through holonomies of the connections and fluxes of the densitized triads. No heavy hypothesis is required. Introductions can be found in Refs. [1].

Loop quantum cosmology (LQC) is an application of LQG-inspired quantization methods to a gravitational system with cosmological symmetries. In LQC, the big bang is generically replaced by a big bounce due to repulsive quantum geometrical effects when the density approaches the Planck density and interesting predictions can be made about the duration of inflation when a given matter content is assumed. It is, however, important to underline that LQC has not yet been rigorously derived from LQG and remains an attempt to use LQG-like methods in the cosmological sector. Introductions can be found in Refs. [2, 3].

The confrontation of LQG with available empirical data is crucial in order to check the physical validity of this approach to quantum gravity. The most promising option in this direction is currently given by the exploration of the cosmological sector of LQG. The present state of advancement, however, does not allow for a derivation of the cosmological dynamics directly from the full theory. Because of this, LQC models are considered to fill the existing gap. These models suffer from quantum ambiguities, which are believed to be fixed by the cosmological dynamics regained from LQG.

This study is based on the effective LQC dynamics, which allow to address various cosmological issues. In particular, numerous studies have been devoted to the computation of tensor power spectra and their significance in the light of the future observations (see, *e.g.*, Refs. [4–7]). In this work, we will focus on scalar modes, which are more relevant from the observational point of view but which are more demanding to deal with at the theoretical level because of subtle gauge-invariance issues and hypersurface deformation algebra closure conditions.

Two main types of quantum corrections are expected at the effective level of LQC. The first one comes from the fact that loop quantization is based on holonomies, *i.e.* using exponentials of the connection rather than direct connection components. The second type of corrections arises for inverse powers of the densitized triad, which, when quantized, becomes an operator without zero eigenvalue in its discrete spectrum, thus avoiding the divergence. As the status of "inverse volume" corrections is

* schander@lpsc.in2p3.fr
† Aurelien.Barrau@cern.ch
‡ boris.bolliet@ens-lyon.fr
§ linsefors@lpsc.in2p3.fr
¶ jakub.mielczarek@uj.edu.pl
** julien.grain@ias.u-psud.fr

not fully clear, due to the fiducial volume dependence, this work focuses on the holonomy term alone which has a major influence on the background equations and is better controlled [8]. In this framework, we will consider the Euclidean phase predicted by LQC [9, 10], and put, as advocated in Ref. [11], initial conditions in the remote past of the contracting branch of the universe (this choice can be questioned and other proposals have been considered [12, 13]).

It is worth noticing, that an alternative attempt regarding the cosmological perturbations in LQC have recently been presented (see Refs. [14]). In this approach, quantum fields are considered on a homogeneous quantum background, based on the methods developed in Ref. [15]. Because the gauge-invariant variables for perturbations are fixed to be the classical ones, the Euclidean phase characterized by the elliptic nature of the equations of motion does not occur. However, the consistency of the effective dynamics emerging from this formulation remains an open issue.

In the following section, we first remind the basis of the deformed algebra approach used in this study. In section III, we summarize some important features of the background dynamics in LQC. The equation of motion for scalar perturbations is derived in section IV. In section V, different ways of choosing initial conditions for perturbations are presented. Section VI is devoted to the analysis of the scalar power spectrum. Concluding remarks are given in section VII.

II. DEFORMED ALGEBRA

In the canonical formulation of general relativity, the Hamiltonian is a sum of three constraints,

$$H_{\rm G}[N^i, N^a, N] = \frac{1}{2\kappa}\int_\Sigma d^3x \left(N^i C_i + N^a C_a + NC\right) \approx 0,$$

where $\kappa = 8\pi G$, (N^i, N^a, N) are Lagrange multipliers, C_i is the Gauss constraint, C_a is the diffeomorphism constraint and C is the scalar constraint. The equality denoted as "$\approx$" is to be understood as an equality on the surface of constraints (*i.e.* a weak equality). It is convenient to define the corresponding smeared constraints,

$$\mathcal{C}_1 = G[N^i] = \frac{1}{2\kappa}\int_\Sigma d^3x\ N^i C_i, \tag{1}$$

$$\mathcal{C}_2 = D[N^a] = \frac{1}{2\kappa}\int_\Sigma d^3x\ N^a C_a, \tag{2}$$

$$\mathcal{C}_3 = S[N] = \frac{1}{2\kappa}\int_\Sigma d^3x\ NC, \tag{3}$$

such that $H_{\rm G}[N^i, N^a, N] = G[N^i] + D[N^a] + S[N]$. The Hamiltonian is a total constraint which vanishes for all multiplier functions (N^i, N^a, N). The time derivative of the Hamiltonian constraint vanishes also weakly and therefore the Hamilton equation, $\dot{f} = \{f, H_{\rm G}[M^i, M^a, M]\}$, leads to

$$\left\{H_{\rm G}[N^i, N^a, N], H_{\rm G}[M^i, M^a, M]\right\} \approx 0. \tag{4}$$

As the Poisson brackets are linear, the condition (4) is satisfied if the smeared constraints belong to a first class algebra,

$$\{\mathcal{C}_I, \mathcal{C}_J\} = f^K{}_{IJ}(A^j_b, E^a_i)\mathcal{C}_K, \tag{5}$$

where the $f^K{}_{IJ}(A^j_b, E^a_i)$ are structure functions which depend on the Ashtekar variables (A^j_b, E^a_i). The algebra closure is fulfilled at the classical level due to general covariance. The algebra must also be closed at the quantum level. Otherwise the system might escape from the surface of constraints, leading to an unphysical behavior. In addition, as shown in Ref. [16], the algebra of effective quantum constraints should be strongly closed (that is, *off shell* closure must be considered). This means that the relation (5) should hold in the whole kinematical phase space, and not only on the surface of constraints (corresponding to *on shell* closure). When the constraints are quantum-modified by the holonomy corrections, the resulting Poisson algebra might not be closed,

$$\{\mathcal{C}^Q_I, \mathcal{C}^Q_J\} = f^K{}_{IJ}(A^j_b, E^a_i)\mathcal{C}^Q_K + \mathcal{A}_{IJ}, \tag{6}$$

where $\mathcal{A}_{IJ}$ stands for the anomaly term which can appear due to the quantum modifications and the superscript 'Q' indicates that the constraints are quantum corrected. The consistency (closure of the algebra) requires that all $\mathcal{A}_{IJ}$ should vanish. Remarkably, the conditions, $\mathcal{A}_{IJ} = 0$, lead to restrictions on the form of the quantum corrections and determine them uniquely under natural assumptions.

The issue of anomaly freedom for the algebra of cosmological perturbations was extensively studied for inverse-triad corrections. It was demonstrated that this requirement can be fulfilled at first order in perturbations for scalar [17, 18], vector [19] and tensor perturbations [20]. Predictions for the power spectrum of cosmological perturbations were performed [21], leading to constraints on some parameters of the model by the use of observations of the cosmic microwave background radiation (CMB) [22]. It was also considered for holonomy corrections and vector modes in Ref. [23] and for scalar modes in Ref. [10] (the full analysis with inverse-triad and holonomy terms was performed in Ref. [24]). It was shown in Ref. [25] that there exists a single modification of the algebra structure that works for *all* kinds of modes, thus emphasizing the consistency of the theory. It is also important to underline that the matter content plays a role in removing degeneracies. Even if the calculations carried out in the above-mentioned articles are quite laborious, the guiding idea behind is very simple. Each time a $\bar{k}$ factor, defined as the mean value of the Ashtekar connection A^i_a, appears, it is replaced by

$$\bar{k} \to \frac{\sin(n\bar{\mu}\gamma\bar{k})}{n\bar{\mu}\gamma}, \tag{7}$$

where n is some unknown integer and $\bar{\mu}$ is the coordinate size of a loop. The full perturbations have to be calculated up to the desired order, the Poisson brackets are then explicitly calculated and the anomalies are cancelled by counter-terms required to vanish in the classical limit. The neat result is that the algebra of effective constraints is deformed with respect to its classical counterpart. It takes the following form:

$$\{D[M^a], D[N^a]\} = D[M^b\partial_b N^a - N^b\partial_b M^a],$$
$$\left\{D[M^a], S^Q[N]\right\} = S^Q[M^a\partial_b N - N\partial_a M^a],$$
$$\left\{S^Q[M], S^Q[N]\right\} = \Omega D\left[q^{ab}(M\partial_b N - N\partial_b M)\right],$$

where Ω is the deformation factor that plays a crucial role in the following. It is given by $\Omega = 1 - 2\rho/\rho_{\rm c}$ where ρ is the density of the Universe and $\rho_{\rm c}$ is the critical density expected to be close to the Planck density. In Lorentzian General Relativity $\Omega = 1$. When $\Omega < 0$ the structure of space-time becomes Euclidean. (Strictly speaking space-time is Lorentzian or Euclidean only if $\Omega = \pm 1$ but the most important properties regarding physical consequences, namely the existence of a causal structure and the general behavior of the solutions for wave equations, only depend on the sign of Ω and not on its precise value [13]. It therefore makes sense to speak of Lorentzian or Euclidean phases.)

Interestingly, this conclusion has strong links with results often postulated (for technical reasons, notably a better behavior of path integrals) in effective quantum cosmology, in particular in the Hartle-Hawking proposal, but it appears here as a real dynamical prediction of the theory. It was also independently derived from another approach to LQC in Ref. [26]. Quite a lot of quantum gravity approaches seem to predict the existence of a silent surface ($\Omega = 0$) where light cones are completely squeezed, on each "side" of the Euclidean phase. This is also a clear realization of the BKL conjecture (see, *e.g.* Ref. [27]). Arguments are given in Ref. [8] showing that the change from a hyperbolic to an elliptic type of equations in LQC should be understood as a true change of signature (that has been missed before because homogeneous models cannot probe it) and not just a tachyonic instability. It should also be emphasized that the deformed algebra approach is grounded in avoiding gauge issues. Many approaches make a gauge fixing. In most cases, gauge fixing before quantization is known to be harmless, but the situation is different in general relativity. The constraints we are considering are much more complicated functions than, for example, the Gauss constraint of Yang–Mills theories: it is therefore likely that the constraints receive significant quantum corrections. If the constraints are quantum corrected, the gauge transformations they generate are, as we have shown, not of the classical form. Gauge fixing before quantization might then be inconsistent because one would fix the gauge according to transformations which subsequently will be modified. In addition, in the present case, the dynamics is part of the gauge system. A consistent theory must therefore quantize gauge transformations and the dynamics at once. It is not correct to fix one part (the gauge) in order to derive the second part (the dynamics) in an unrestricted way. The subtle consistency conditions associated with the covariance of general relativity are encoded in the first class nature of its system of constraints. Here, great care is taken in not breaking this consistency.

The equations of motion derived in this framework are still covariant under the deformed algebra replacing classical coordinate transformations. The corresponding quantum space-time structure is obviously not Riemannian (there is no line element in the usual sense), but has a well-defined canonical formulation using hypersurface deformations.

III. BACKGROUND EVOLUTION

The evolution of the cosmological background is studied at the effective level with holonomy corrections. The background geometry is described by the homogeneous, isotropic and flat configuration parametrized by the scale factor a. The dynamics of the background is governed by the quantum-corrected Friedmann equation

$$H^2 = \frac{\kappa}{3}\rho\left(1 - \frac{\rho}{\rho_{\rm c}}\right), \tag{8}$$

derived in Ref. [28], where $H = \dot{a}/a$ is the Hubble rate in cosmic time, ρ is the energy density of the content of the universe and $\rho_{\rm c}$ denotes its maximal value attained at the bounce. The dot denotes a derivative w.r.t. cosmic time. Planck units are used throughout this article with $m_{\rm Pl} = 1/\sqrt{G} \approx 1.22\cdot 10^{19}$ GeV. Furthermore, we consider a single massive scalar field, ϕ, with a quadratic potential $V = m^2\phi^2/2$, as the matter content of the Universe. This choice is made for simplicity. It allows easy comparisons with other works and generates a phase of slow-roll inflation. Even if this potential is not favored by current observational data [29], it still serves as a valuable toy model for studying the phase of inflation in different frameworks. Moreover, taking into account more subtle effects, *e.*g. the quantum gravitational corrections considered here, might improve the status of the quadratic potential in the light of the observational data.

Splitting the field $\phi = \bar{\phi} + \delta\phi$ into a background part, $\bar{\phi}$, and a perturbed part, $\delta\phi$, the Klein-Gordon equation for the background reads

$$\ddot{\bar{\phi}} + 3H\dot{\bar{\phi}} + m^2\bar{\phi} = 0. \tag{9}$$

A first analysis of this model has already been studied in Ref. [30]; a detailed analysis of the background equations can be found in Ref. [31]. Here, we only summarize the main features of the background dynamics. The field evolution can be characterized by two dynamical parameters [6], the potential energy parameter, x, and the kinetic energy parameter, y, defined as

$$x := \frac{m\bar{\phi}}{\sqrt{2\rho_{\rm c}}}, \qquad y := \frac{\dot{\bar{\phi}}}{\sqrt{2\rho_{\rm c}}}. \tag{10}$$

Then the total energy density can be written as $\rho = \rho_{\rm c}(x^2+y^2)$. Eqs. (8) and (9) can then be recast as

$$\begin{cases} \dot{H} &= -\kappa\rho_{\rm c} y^2\left(1-2x^2-2y^2\right), \\ \dot{x} &= my, \\ \dot{y} &= -3Hy - mx, \end{cases} \tag{11}$$

showing that there are two timescales involved in this system: one is given by $1/m$ and corresponds to the classical evolution of the field, the other one is $1/\sqrt{3\kappa\rho_{\rm c}}$ and corresponds to the quantum regime of the evolution. The ratio of these two timescales is

$$\Gamma := \frac{m}{\sqrt{3\kappa\rho_{\rm c}}}. \tag{12}$$

According to standard assumptions of slow-roll inflation with a quadratic potential, the value of the mass $m \simeq 1.2\times10^{-6} m_{\rm Pl}$ is preferred in the light of the observational data from the Planck satellite (see Ref. [29]). The critical energy density at the bounce is given by $\rho_{\rm c} = 0.41\ m_{\rm Pl}^4$, which is exactly the upper bound of the spectrum of the energy density operator [3]. These values lead to $\Gamma \simeq 2\cdot10^{-7}$. Hence, one can safely assume that $\Gamma \ll 1$, ensuring that the evolution splits into three phases: (i) a classical pre-bounce contracting phase, (ii) the bouncing phase and (iii) a classical expanding phase after the bounce (slow-roll inflation), see Ref. [31] for details. Initial conditions, $\{a_0, x_0, y_0\}$, are set in the remote past of the contracting phase when the energy density is very small compared to the critical energy density, *i.e.*

$$\sqrt{\frac{\rho_0}{\rho_{\rm c}}} \ll \Gamma. \tag{13}$$

It is convenient to use polar coordinates for the potential and kinetic energy parameters

$$x(t) = \sqrt{\frac{\rho}{\rho_{\rm c}}}\sin(mt+\theta_0), \tag{14}$$

$$y(t) = \sqrt{\frac{\rho}{\rho_{\rm c}}}\cos(mt+\theta_0), \tag{15}$$

where θ_0 is the initial phase between the share of potential energy and kinetic energy. In order to select different background evolutions independently of the small oscillatory behavior of the solutions, the following parametrization shall be used:

$$\sqrt{\frac{\rho_0}{\rho_{\rm c}}} = \frac{\Gamma}{\alpha}\left(1-\frac{\sin(2\theta_0)}{4\alpha}\right)^{-1}, \tag{16}$$

where α is a number large enough such that (13) holds. To each phase, θ_0, corresponds a specific value of the potential energy parameter at the bounce $x_{\rm B}$. As shown in Ref. [32], for a mass $m = 1.21\times10^{-6}m_{\rm Pl}$, the favored value for $x_{\rm B}$ is 3.55×10^{-6}. This solution for the background dynamics features only a tiny amount of deflation before the bounce as shown in Fig. 1. In general, we will chose the normalization of the scale factor at the bounce as $a_{\rm B} = 1$. The plots and spectra are presented as functions of the number of e-folds $N := \pm\ln(a/a_{\rm B})$, that have to elapse until the bounce (negatively valued) and that have elapsed after the bounce (positively valued) respectively.

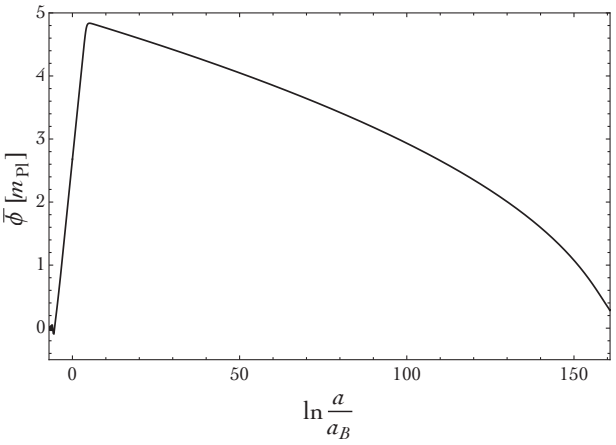

FIG. 1. Evolution of the scalar field as a function of the number of e-folds $N := \pm\ln a/a_{\rm B}$, with $m = 1.2\times10^{-6}m_{\rm Pl}$. The zero on the horizontal axis corresponds to the bounce when $a_{\rm B} = 1$. This solution is such that $x_{\rm B} = 3.55\times10^{-6}$ (obtained with $\alpha = 17\pi/4+1$ and $\theta_0 = 5.11$). The evolution is stopped at the end of inflation when $\phi = 1/\sqrt{4\pi}\ m_{\rm Pl}$.

IV. EQUATION OF MOTION FOR SCALAR MODES

The equation of motion for scalar modes in the deformed algebra approach is derived from the particular form of the Hamiltonian constraint. In Ref. [25], the gravitational part of the Hamiltonian constraint has been analyzed and reads (up to quadratic order)

$$H[N] = \int_\Sigma d^3x\left[\bar{N}\left(\mathcal{H}^{(0)}+\mathcal{H}^{(2)}\right)+\delta N\,\mathcal{H}^{(1)}\right], \tag{17}$$

where

$$2\kappa\,\mathcal{H}^{(0)} = -6\sqrt{\bar{p}}\bar{k}^2\ , \tag{18}$$

$$2\kappa\,\mathcal{H}^{(1)} = -4\sqrt{\bar{p}}\delta K_d^d - \frac{\bar{k}^2}{\sqrt{\bar{p}}}\delta E_d^d + \frac{2}{\sqrt{\bar{p}}}\partial^j\partial_c\delta E_j^c, \tag{19}$$

$$\begin{aligned} 2\kappa\,\mathcal{H}^{(2)} = &-2\frac{\bar{k}}{\sqrt{\bar{p}}}\delta K_a^i\delta E_i^a \\ &+\sqrt{\bar{p}}\left(\delta_i^b\delta K_a^i\delta_j^a\delta K_b^j - \delta_i^a\delta K_a^i\delta_j^b\delta K_b^j\right) \\ &+\frac{1}{4}\frac{\bar{k}^2}{\bar{p}^{\frac{3}{2}}}\left(\delta_a^i\delta E_i^a\delta_b^j\delta E_j^b - 2\delta_a^j\delta E_i^a\delta_b^i\delta E_j^b\right) \\ &+\frac{1}{\bar{p}^{\frac{3}{2}}}Y_{bdc}^{kjil}\ \epsilon_k^{ab}\ \partial_a\left(\delta E_j^d\partial_i\delta E_l^c\right) \\ &+\frac{1}{\bar{p}^{\frac{3}{2}}}Z_{ab}^{cidj}\ \left(\partial_c\delta E_i^a\right)\left(\partial_d\delta E_j^b\right). \end{aligned} \tag{20}$$

Here, $\bar{p}$ is the mean value of the densitized triad E^a_i and $\bar{k}$ was defined in Eq. (7). The term Z^{cidj}_{ab} depends on the kind of modes considered (scalar, vector or tensor):

$$Z^{cidj}_{ab} = \begin{cases} \delta_{ab}\delta^{ij}\delta^{cd} & \text{for tensor modes,} \\ 0 & \text{for vector modes,} \\ -\frac{1}{2}\delta^c_a\delta^d_b\delta^{ij} & \text{for vector modes.} \end{cases} \tag{21}$$

Lastly, Y^{kjil}_{bdc} is a complicated expression whose form is not relevant here. Based on this, the holonomy quantum corrections can be accounted for and the Mukhanov-Sasaki equation of motion for gauge-invariant perturbations can be calculated [10]. In conformal time it is given by

$$v_{\rm S}'' - \Omega\,\nabla^2 v_{\rm S} - \frac{z_{\rm S}''}{z_{\rm S}} v_{\rm S} = 0, \tag{22}$$

with

$$v_{\rm S} := \sqrt{\bar{p}}\left(\delta\phi + \frac{\bar{\phi}'}{\mathscr{H}}\Phi\right) \quad \text{and} \quad z_{\rm S} := \sqrt{\bar{p}}\,\frac{\bar{\phi}'}{\mathscr{H}}. \tag{23}$$

The variable Φ denotes the gauge invariant Bardeen potential taking into account the metric perturbations, whereas ϕ represents the massive scalar field. $\mathscr{H}$ is the conformal Hubble parameter. The Mukhanov equation of motion (22) reduces to the classical equation when $\Omega \to 1$. Note that for FLRW cosmologies, in conformal time, $\sqrt{\bar{p}} = a$. On the quantum-modified background discussed in the previous section, we can evaluate the evolution of the Mukhanov variable $v_{\rm S}$. For simplicity we will omit the index 'S' in the following, assuming that it is clear that v denotes the scalar perturbation variable. Using the Fourier space decomposition of the $v(\mathbf{x}, \eta)$ field,

$$v(\mathbf{x}, \eta) = \int \frac{d^3k}{(2\pi)^{3/2}} v_{\mathbf{k}}(\eta) e^{i\mathbf{k}\cdot\mathbf{x}}, \tag{24}$$

one gets a set of ordinary differential equations for the Fourier components $v_{\mathbf{k}}$. Due to the isotropy of space, the $\mathbf{k}$-vector of $v_{\mathbf{k}}$ might be simplified to the absolute value dependence v_k, where $k := \sqrt{\mathbf{k}\cdot\mathbf{k}}$. The v_k function is called a mode function. Instead of using the conformal time dependence, it is often (due to technical reasons) convenient to switch to cosmic time t in the numerical computations. With $t = \int a \cdot d\eta$, the Mukhanov equation of motion reads

$$\ddot{v}_k + H\dot{v}_k + f^{(v)}_k(t) v_k = 0, \tag{25}$$

with $z = a\frac{\dot{\bar{\phi}}}{H}$ and

$$f^{(v)}_k(t) := \Omega\frac{k^2}{a^2} - \frac{\dot{z}}{z}H - \frac{\ddot{z}}{z}, \tag{26}$$

being the effective frequency term. In order to derive the primordial power spectrum after inflation one would have to solve Eq. (25) for every mode k for all times from $t_{\rm init}$ until $t_{\rm end}$ where $t_{\rm init}$ is the initial starting point, set in the remote past as we will see later, and $t_{\rm end}$ denotes the time at the end of the inflationary phase. This requires a numerical integration. However, the Mukhanov variable v, cannot be used for the whole integration because of a non-physical singularity occurring at the bounce. Let us describe how to bypass this difficulty by using the change of variable. We introduce $h_k := v_k/a$ for every k, so that (25) becomes

$$\ddot{h}_k + 3H\dot{h}_k + f^{(h)}_k(t) h_k = 0 \tag{27}$$

with

$$f^{(h)}_k(t) := \Omega\frac{k^2}{a^2} - m^2 - m^2\kappa\,\Omega\frac{\dot{\bar{\phi}}\bar{\phi}}{H} + 2\left(\frac{\dot{H}}{H}\right)^2 - \frac{\ddot{H}}{H}. \tag{28}$$

In the numerical computation this second order differential equation is replaced by the following first order system:

$$\begin{cases} \dot{h}_k &= (1/a) g_k, \\ \dot{g}_k &= -2H g_k + f^{(h)}_k(t) a\; h_k. \end{cases} \tag{29}$$

The numerical integration of (29) is performed for $t \in [t_{\rm init}, t_{h\to\mathcal{R}}]$ where $t_{h\to\mathcal{R}}$ is before the bounce. Since the effective frequency terms, (28) or (26), depend on inverse powers of H, the differential equations have a generic singularity at the bounce, when the Hubble parameter vanishes. Nonetheless, this singularity is not physical, which can be seen by analyzing the physical scalar curvature,

$$\mathcal{R} := \frac{v}{z}. \tag{30}$$

Using this variable, one can rewrite Mukhanov's equation of motion in Fourier space as

$$\ddot{\mathcal{R}}_k - \left(3H + 2m^2\frac{\bar{\phi}}{\dot{\bar{\phi}}} + 2\frac{\dot{H}}{H}\right)\dot{\mathcal{R}}_k + \Omega\frac{k^2}{a^2}\mathcal{R}_k = 0. \tag{31}$$

When approaching the bounce, H tends to zero and Ω to minus one. Moreover, during the bouncing phase, $\dot{\bar{\phi}} \simeq \sqrt{2\rho_{\rm c}} \gg m\bar{\phi}$, so that the equation of motion reduces to

$$\ddot{\mathcal{R}}_k - 2\frac{\dot{H}}{H}\dot{\mathcal{R}}_k - \frac{k^2}{a^2}\mathcal{R}_k \simeq 0. \tag{32}$$

According to the analytical expression for $\bar{\phi}$ and $\dot{\bar{\phi}}$ around the bounce developed in Ref. [31], this gives

$$\ddot{\mathcal{R}}_k - \frac{2}{t - t_{\rm B}}\dot{\mathcal{R}}_k - k^2\mathcal{R}_k \simeq 0, \tag{33}$$

when we restrict ourselves to the first order in $(t - t_{\rm B})$. The space of solutions to this differential equation is spanned by the two independent functions,

$$\mathcal{R}^{(1)}_k = \left[\sinh\left(k(t - t_{\rm B})\right) - k(t - t_{\rm B})\cosh\left(k(t - t_{\rm B})\right)\right],$$
$$\mathcal{R}^{(2)}_k = \left[\cosh\left(k(t - t_{\rm B})\right) - k(t - t_{\rm B})\sinh\left(k(t - t_{\rm B})\right)\right].$$

These solutions show an obviously regular behavior at the bounce. But it should be noticed that (31) runs into trouble away from the bounce due to the time derivative of the potential $\dot{\bar{\phi}}$ appearing in the denominator of the friction term. During the classical contracting and expanding phases, $\dot{\bar{\phi}}$ oscillates around a null value, causing the break-down of the numerical integration of the differential equation (31) of $\mathcal{R}$. For this reason one has to switch twice between Eq. (29) and Eq. (31) during the numerical computations. For $t \in [t_{\rm init}, t_{h\to\mathcal{R}}]$ and $t \in [t_{\mathcal{R}\to h}, t_{\rm end}]$, where $t_{h\to\mathcal{R}} < t_{\rm B} < t_{\mathcal{R}\to h}$, the differential equation for h, namely (29), must be used. Whereas for $t \in [t_{h\to\mathcal{R}}, t_{\mathcal{R}\to h}]$, it is the equation for $\mathcal{R}$, Eq. (31), that has to be integrated. The exact choice of the transition points is irrelevant as long as they do not approach one of the singularity points.

V. INITIAL CONDITIONS

The considered equations of motion for the scalar perturbations (Eq. (22) or Eq. (25)) might be considered – at the effective level – as the quantum ones. This is due to the presence of the factor Ω, being a result of the quantum gravitational effects. The quantum effects taken into account here are, however, only those which modify the background degrees of freedom. The inhomogeneous degrees might be (and are), treated classically in the perturbative regime under consideration. In order to see it, let us consider the extrinsic curvature K_a^i which is exponentiated to the form of a holonomy operator in the quantum theory. In the perturbative treatment we have $K_a^i = \bar{k}\delta_a^i + \delta K_a^i$, together with the condition $|\delta K_a^i|/\bar{k} \ll 1$. Path integration of K_a^i leads to a factor of the form $\gamma\bar{\mu}\bar{k}$ for the homogeneous contribution, which is of the order of unity in vicinity of the bounce. Full exponentiation of the background contribution to K_a^i must be, therefore, kept over the evolution through the bounce. However, this is not necessary for sufficiently small perturbations, for which the condition $\gamma\bar{\mu}|\delta K_a^i| \ll 1$ might be satisfied even at the bounce. This allows for the expansion of the holonomy up to a linear contribution in δK_a^i and treating the perturbative degrees of freedom in a classical manner.

As the phase space of the perturbative degrees of freedom is approximated by the classical one, the canonical quantization procedure for the modes might be applied. The canonical quantization is an approximation, which is valid only for sufficiently small amplitudes of δK_a^i and sufficiently large wavelengths (roughly greater than the Planck length) in the mode expansion. If the conditions are satisfied, the Fourier mode $v_{\mathbf{k}}(\eta)$ can be promoted to be an operator, such that in the Heisenberg picture

$$\hat{v}_{\mathbf{k}}(\eta) = v_k(\eta)\hat{a}_{\mathbf{k}} + v_k^*(\eta)\hat{a}^\dagger_{-\mathbf{k}}, \tag{34}$$

where $v_k(\eta)$ are the so-called mode functions satisfying the classical equation (25). The $\hat{a}^\dagger_{\mathbf{k}}$ and $\hat{a}_{\mathbf{k}}$ are the creation and annihilation operators respectively, satisfying $[\hat{a}_{\mathbf{k}}, \hat{a}^\dagger_{\mathbf{q}}] = \delta^{(3)}(\mathbf{k}-\mathbf{q})$. Using this commutation relation, one may show that the following condition

$$v_k\frac{dv_k^*}{d\eta} - v_k^*\frac{dv_k}{d\eta} = i, \tag{35}$$

called Wronskian condition, has to be satisfied in order to preserve the standard canonical structure.

Based on the above, the two-point correlation function for the scalar curvature field $\hat{\mathcal{R}}(\mathbf{x},\eta)$ in the vacuum state $|0\rangle$ is given by

$$\langle 0|\hat{\mathcal{R}}(\mathbf{x},\eta)\hat{\mathcal{R}}(\mathbf{y},\eta)|0\rangle = \int_0^\infty \frac{dk}{k}\mathcal{P}_S(k,\eta)\frac{\sin kr}{kr}, \tag{36}$$

where $r = |\mathbf{x}-\mathbf{y}|$ and the scalar power spectrum reads

$$\mathcal{P}_S(k,\eta) := \frac{k^3}{2\pi^2}\frac{|v_k(\eta)|^2}{z^2}. \tag{37}$$

The power spectrum carries all statistical information about the Gaussian scalar curvature field under consideration (non-linear effects are neglected in our analysis) and its determination for the LQC model discussed in the previous sections is a main goal of this study.

The equations of motion for the scalar mode functions $v_k(\eta)$ can be solved numerically, following the procedure presented in the previous section. For this purpose initial conditions for perturbations have to be set for every wavenumber k. In standard cosmology, it is common to set Cauchy initial conditions at some moment in time after the big bang singularity. In the present work, we set initial conditions in the pre-bounce phase. This is the natural choice if the bounce is a phenomenon to be really understood as resulting from a causal evolution of the Universe, with time flowing in a unique direction. In addition, in the remote past of the contracting branch, the Universe is classical and quantum effects do not play any important role. This seems both technically more convenient (since the quantum dominated region still represents a quite unknown field of physics) and physically better motivated. In particular, as discussed in the previous sections, it has been shown in Ref. [10] that the geometry of the universe in its quantum stage ($\rho > \rho_c/2$) might become Euclidean instead of being Lorentzian (the very notion of time obviously looses here its meaning). The physical consequences are still not perfectly well understood and setting initial conditions in the Euclidean phase would be the worst possible choice: we therefore focus on the classical contracting phase. Note that another proposal, studied in Refs. [12, 13], is to set initial conditions at the surface of silence (or in a "hybrid" way as advocated by a careful study of the Tricomi problem). We do not consider this hypothesis here.

The most simple and natural way to set initial conditions for a quantum oscillator is provided by the vacuum state $|0\rangle_k$ for every mode k at some given moment in time. This sets a clear Cauchy initial value problem. However, it is well known that the notion of vacuum in an arbitrary curved spacetime is ambiguous since

the definition of the usual "instantaneous vacuum" is based on plane waves satisfying the differential equation of an harmonic oscillator with wavenumber k. In the case of scalar perturbations, as the effective frequency term depends non-trivially on time, it is more appropriate to use the Wentzel-Kramers-Brillouin (WKB) approximation and the so-called "adiabatic vacuum". In contrast with the ordinary instantaneous vacuum state, well known from quantum field theory, the adiabatic vacuum does not have to satisfy the differential equation of an harmonic oscillator in some limit. The instantaneous-vacuum state is recovered as the first term of the WKB expansion.

For scalar perturbations in LQC the equation of motion is given by Eq. (22). In conformal time, this equation resembles the differential equation of an oscillator,

$$v_k'' + k_{\rm eff}^2(\eta) v_{\rm k} = 0, \tag{38}$$

with a time-dependent wave number

$$k_{\rm eff}(\eta) := \sqrt{\Omega(\eta) k^2 - \frac{z''}{z}(\eta)}. \tag{39}$$

Recall that we set initial conditions in the remote past where $\Omega \sim 1$ is almost constant. Thus the Ω-factor actually plays no role when addressing the issue of initial conditions. The main idea of the WKB approximation is to use the following generic ansatz for the solutions to Eq. (38):

$$v_k(\eta) = c_1 \cdot e^{i(k_{\rm eff} T)\cdot W_k(\eta)} + c_2 \cdot e^{-i(k_{\rm eff} T)\cdot W_k(\eta)}, \tag{40}$$

where the values of constants c_1 and c_2 are constrained according to the Wronskian condition (35). In the WKB approximation the functions $W_k(\eta)$ are expanded in terms of some small parameter $(k_{\rm eff} T)^{-1}$ where T is the minimal time interval for which $k_{\rm eff}$, and its time derivatives, start to change substantially ($T \gg 1/k_{\rm eff}$). Then the WKB expansion reads

$$W_k(\eta) = \sum_{n=0}^{\infty} \left(\frac{i}{k_{\rm eff} T}\right)^n W_{k,n}(\eta). \tag{41}$$

Introducing this ansatz into Eq. (38), one gets the explicit expressions for the different orders, n, of $W_{k,n}$. The WKB approximation consists in truncating the series after the first order, leading to the approximated solution for the mode functions

$$v_k(\eta) = \frac{c_1}{\sqrt{k_{\rm eff}(\eta)}} e^{i\int^\eta k_{\rm eff}(\tilde\eta) d\tilde\eta} + \frac{c_2}{\sqrt{k_{\rm eff}(\eta)}} e^{-i\int^\eta k_{\rm eff}(\tilde\eta) d\tilde\eta}. \tag{42}$$

Using the Wronskian condition (35), we find $|c_2|^2 - |c_1|^2 = 1/2$ as a condition that the free parameters c_1 and c_2 have to fulfill. The most convenient choice is $c_1 = 0$ and $c_2 = 1/\sqrt{2}$ which corresponds to a wave propagating in positive time direction. For this choice the mode function reads

$$v_k(\eta) = \frac{1}{\sqrt{2k_{\rm eff}(\eta)}} e^{-i\int^\eta k_{\rm eff}(\tilde\eta) d\tilde\eta}. \tag{43}$$

This represents a suitable choice because the mode function reduces to the Bunch-Davies vacuum in the UV limit ($k \to \infty$).

In order to check that this approach is valid, we plug this solution into Eq. (38) and find that it is actually an exact solution to

$$v_k'' + \left(k_{\rm eff}^2 - \frac{3}{4}\frac{(k_{\rm eff}')^2}{k_{\rm eff}^2} + \frac{1}{2}\frac{k_{\rm eff}''}{k_{\rm eff}}\right) v_k = 0. \tag{44}$$

Therefore, the solution (42) is valid as long as

$$\left|\frac{1}{2}\frac{k_{\rm eff}''}{k_{\rm eff}^3} - \frac{3}{4}\frac{(k_{\rm eff}')^2}{k_{\rm eff}^4}\right| \ll 1, \tag{45}$$

when the effective wavenumber, $k_{\rm eff}$, varies slowly. The appropriate initial conditions are then

$$v_k(\eta_{\rm init}) = \frac{1}{\sqrt{2k_{\rm eff}(\eta_{\rm init})}}, \tag{46}$$

$$\left.\frac{dv_k}{d\eta}\right|_{\eta=\eta_{\rm init}} = -\left(ik_{\rm eff} + \frac{1}{2}\frac{k_{\rm eff}'}{k_{\rm eff}}\right) \left.\frac{1}{\sqrt{2k_{\rm eff}}}\right|_{\eta=\eta_{\rm init}}, \tag{47}$$

where the exponential term can be neglegted because it contributes only with an arbitrary phase. The initial moment $\eta_{\rm init}$ has to be chosen such that the WKB conditions are satisfied at this particular moment of time for all modes k. By analyzing $k_{\rm eff}(\eta)$ and its time derivatives, we can find an appropriate $\eta_{\rm init}$ in the remote past. For the numerical computations, the choice of $\eta_{\rm init}$ is therefore arbitrary as long as the condition (45) is fulfilled. The instantaneous vacuum can be used as well for setting initial conditions. The instantaneous vacuum choice relies on the minimal energy state of the system defined by the Hamiltonian. Therefore, the requirement

$$\left.\frac{k_{\rm eff}'}{(2k_{\rm eff})^{3/2}}\right|_{\eta=\eta_{\rm init}} = 0, \tag{48}$$

has to be satisfied (see Ref. [33] for instance). In fact, one can find that there exists $\eta_{\rm init}$ such that both conditions (45) and (48), are fulfilled. For reasons of comparability of the two approaches, we use this choice. In such a case, any difference between the two approaches is due to the higher order contribution to (47), which is present in case of the adiabatic vacuum-type normalization.

The conditions for the validity of both the instantaneous and WKB vacua depend strongly on the evolution of the cosmological term z''/z during the pre-bounce contracting phase. A direct calculation leads to

$$\frac{z''}{z} = -a^2\left(m^2 - 2H^2 + 2\kappa m^2 \frac{\bar\phi\dot{\bar\phi}}{H} + \frac{7}{2}\kappa\Omega\dot{\bar\phi}^2 - \kappa^2\Omega^2\frac{\dot{\bar\phi}^4}{2H^2} - 3\kappa\frac{\dot{\bar\phi}^4}{\rho_{\rm c}}\right). \tag{49}$$

This expression is valid at all times. In order to analyze the shape of the effective potential it is convenient to divide the evolution into three background phases as mentioned in Sec. III. Then, analytical approximations for every phase can be used respectively. During the pre-bounce classical contracting phase, when $\rho(t) \ll \rho_{\rm c}$, the scalar field undergoes an oscillatory behavior with an amplitude proportional to $\sqrt{\rho(t)}$. The Hubble parameter H is proportional to $\sqrt{\rho}$ as well, whereas $\Omega \simeq 1$. Inserting these solutions into Eq. (49) yield terms which are proportional to different orders of $\sqrt{\rho}$. Averaging over the oscillatory contributions, which all have a characteristic oscillation time of $1/m$, gives

$$\left\langle \frac{z''}{z} \right\rangle = -a^2 \left(m^2 - \alpha_1 \sqrt{\kappa} m \sqrt{\rho(t)} + \alpha_2 \kappa \rho(t) + \alpha_3 \kappa \rho_{\rm c} \left(\frac{\rho(t)}{\rho_{\rm c}} \right)^2 \right), \tag{50}$$

where the constants α_i are determined by the averaged oscillations. Since the energy density is increasing for all times in the remote past, $\rho(t)$ becomes sufficiently small in the remote past. Thus the m^2-term will dominate for early times and therefore $z''/z \propto -m^2 a^2$. On a logarithmic scale as a function of $\ln(a/a_{\rm B})$ like in Fig. 2 the absolute value of the effective potential is then given by a straight line with gradient -2 and with a $\ln(|z''/z|)$-intercept of $2\ln(a_{\rm B} m) = -27.26$. This result is obtained as well by a purely analytical analysis which is presented in Fig. 2. We use that the Hubble parameter H is approximated by $H(t) = H_0(1+\frac{3}{2}H_0 t)^{-1}$ for the pre-bounce phase when neglecting the fast oscillations, where H_0 denotes the initial Hubble parameter. H_0 is determined by the mass and the parameter α, namely $H_0 = -m/3\alpha$. Integration leads to the analytical solution of the scale factor in the pre-bounce phase

$$a(t) = a_* \left(2 - \frac{m}{\alpha} t \right)^{\frac{2}{3}}, \tag{51}$$

where the prefactor a_* is the scale factor for $t = \alpha/m$. With this expression the analytical solution for $\ln|(z''/z)| = \ln a(t)^2 m^2$ reads on the logarithmic scale

$$\ln\left|\frac{z''}{z}\right| = 2\ln a_* + \frac{4}{3}\ln\left(2 - \frac{m}{\alpha}t\right) + 2\ln m. \tag{52}$$

As a function of $\ln(a/a_{\rm B})$, one gets the red line on the left in Fig. 2. This analytic solution is valid until the energy density starts to dominate over the constant mass term in Eq. (50). The first term which is comparable to m^2 is proportional to $\sqrt{\rho}$. With the analytic solution of $\sqrt{\rho}$ in the pre-bounce phase,

$$\sqrt{\frac{\rho(t)}{\rho_{\rm c}}} = \frac{\Gamma\alpha^{-1}}{1 - \frac{1}{2\alpha}\left[mt + \frac{1}{2}\sin(2mt + 2\theta_0)\right]}, \tag{53}$$

we can compute the time when the $\sqrt{\rho}$-term crosses 'm^2' in its amplitude. The oscillation term in Eq. (53) is averaged over $T = 1/m$. This transition point is referred to $N_{\rm pre} := \ln(a_{\rm pre}/a_{\rm B}) = -5.38$ in the figure.

During the bouncing phase the potential energy parameter x, is very small compared to the kinetic potential parameter y, since we consider a kinetic bounce scenario. Then, in particular, $x^2 \ll y^2$ is satisfied during this phase and the Hubble parameter can be reduced to

$$H^2 \simeq \frac{\kappa\rho_{\rm c}}{3} y^2 \left(1 - y^2\right). \tag{54}$$

The analytic solution for y around the bounce is given by $y(t) = (1+3\kappa\rho_{\rm c}(t-t_{\rm B})^2)^{-1/2}$, as presented in Ref. [31] and the scale factor is related to y via $a = a_{\rm B}|y|^{-1/3}$. With these approximations the expression for z''/z reduces to

$$\frac{z''}{z} = \frac{\kappa\rho_{\rm c} a_{\rm B}^2}{3} \frac{\left(-\left(\frac{a}{a_{\rm B}}\right)^2 + 23\left(\frac{a}{a_{\rm B}}\right)^{-4} - 4\left(\frac{a}{a_{\rm B}}\right)^{-10} \right)}{\left(\frac{a}{a_{\rm B}}\right)^6 - 1}.$$

Note that this expression is negatively valued and diverges at the bounce. The absolute value of this expression on the logarithmic scale and as a function of $\ln(a/a_{\rm B})$ provides the red lines around the bounce in Fig. 2. These approximations are valid until x^2 becomes significant in comparison to y^2, let's say $x^2 > y^2/10$. The analytic solutions for x and y provide these transition points of validity respectively before and after the bounce, namely $N_{\rm preB} := \ln(a_{\rm preB}/a_{\rm B}) = -4.41$ and $N_{\rm postB} := \ln(a_{\rm postB}/a_{\rm B}) = 3.62$, as shown in Fig. 2.

During slow-roll inflation, $\Omega \simeq 1$ such that z''/z takes its classical expression. This leads to $z''/z = (2 + 6\epsilon_{\rm H} - 3\delta_{\rm H})/\eta^2$, with $\epsilon_{\rm H}$ and $\delta_{\rm H}$ the first and second Hubble flow functions, both much smaller than unity during inflation. Furthermore, $a \propto 1/\eta$ and therefore $\ln(z''/z) \propto 2\ln(a/a_{\rm B})$, see Fig. 2. In particular the effective potential is then given by $z''/z = \frac{1}{2}a^2H^2$. The curve can be approximated from the beginning of slow-roll inflation, *i.e.* when $t_{\rm i} = t_{\rm B} + f/m$ where f is an analytical expression related to the Lambert function and $t_{\rm B}$ is given analytically as well. For this time $a_{\rm i} = a_{\rm B}\Gamma^{-\frac{1}{3}}$ and the logarithm of the absolute value of the effective potential is given by $\ln|z''/z| = \ln(2/\eta^2) = \ln((1/2)a_{\rm i}^2 H_{\rm i}^2)$. The value of the Hubble parameter $H_{\rm i}$ is given analytically as well, see Ref. [31]. The approximation is valid starting from $N_{\rm post} := \ln(a_{\rm post}/a_{\rm B}) = 5.53$. For the approximation we use that

$$H(t) = H_{\rm i}\left|1 - \frac{\epsilon\Gamma}{x_{\rm i}} m(t - t_{\rm i})\right| \tag{55}$$

during slow-roll inflation, where ϵ is the sign of the cosine of the phase parameter between the potential and kinetic energy parameters at the transition point between the pre-bounce and bouncing phases, and $x_{\rm i}$ is the value of the potential energy parameter at $t_{\rm i}$. Furthermore, the scale factor undergoes an exponential growth with coordinate time, namely

$$a(t) = a_{\rm i} e^{-\frac{H_{\rm i}}{2x_{\rm i}}(t-t_{\rm i})(\epsilon\Gamma m(t-t_{\rm i}) - 2x_{\rm i})}. \tag{56}$$

The analytic fit given by these two functions is displayed by the red line on the right side in Fig. 2. as a function of $\ln(a/a_{\rm B})$ with a provided by Eq. (56). The slight difference between numerical results and the analytical solution during slow-roll inflation is due to the fact that the analytical approximations for this phase goes back on approximations even for the pre-bounce phase. Hence, small differences are propagated.

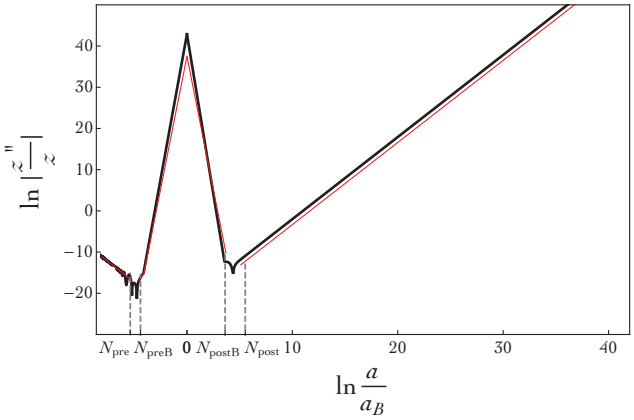

FIG. 2. Evolution of the cosmological term z''/z as a function of the number of e-folds $\ln(a/a_{\rm B})$, with $m = 1.2 \times 10^{-6} m_{\rm Pl}$. The parameters for the background are set as in Fig. 1. During the pre-bounce contracting phase and slow-roll inflation $\ln(z''/z) \propto \pm 2 \ln(a/a_{\rm B}) + const.$

VI. THE SCALAR POWER SPECTRUM

For scalar modes, the primordial power spectrum at the end of inflation is defined in terms of the mode functions by virtue of the definition (37). As we shall see in the next section, three ranges of wavenumbers can be identified, depending on how they compare to the effective potential z''/z: (i) the infrared regime, (ii) intermediate scales and (iii) the ultraviolet regime.

A. The infrared regime

The infrared limit (IR) of the primordial power spectrum corresponds to modes such that $k^2 \ll |z''/z|$ during the pre-bounce contracting phase. These modes are frozen during the bouncing phase and slow-roll inflation. The transition between the contracting phase and the bouncing phase occurs when $H \simeq -m/3$, as discussed in Ref. [31]. At the transition, the effective potential term z''/z is well approximated by a''/a, since $\dot{\bar{\phi}}/H$ remains nearly constant. This allows us to introduce the following IR scale (see Ref. [31]):

$$k_{\rm IR} := \frac{a_{\rm B}}{3\sqrt{2}} \left(m^2 \sqrt{3\kappa\rho_{\rm c}}\right)^{1/3} \approx 4.7 \times 10^{-5} m_{\rm Pl}, \qquad (57)$$

where the numerical value has been obtained for $m = 1.2 \times 10^{-6} m_{\rm Pl}$, $a_{\rm B} = 1$ and $\rho_{\rm c} = 0.41 m_{\rm Pl}^4$.
There is an important difference with respect to the case of tensor modes. For small enough values of k in the IR regime, the tensor power spectrum tends to be scale-invariant. This is due to the fact that initial conditions for tensor modes are set when *all* the modes of interest are sub-Hubble (or, more precisely, $k^2 \gg a''/a$). For the scalar modes, however, it is impossible to set appropriate initial conditions at a time when all relevant modes are such that $k^2 \gg |z''/z|$. Indeed, the conditions discussed in the previous section, (45) and (48), have to be satisfied as well respectively for the WKB and the instantaneous vacuum-type normalizations. In addition, the absolute value of the effective potential term keeps decreasing in the remote past of the contracting branch. It is possible to find a time $\eta_{\rm init}$, in the classical contracting phase, at which (i) the absolute value of the effective potential term z''/z is close to zero and (ii) the conditions of validity of the vacuum states are fulfilled. Nevertheless for the WKB vacuum, at this particular time, when $|z''/z|$ is minimal and condition (45) is satisfied, the effective potential does not strictly vanish, it is $|z''/z| = 2.1 \times 10^{-7} m_{\rm Pl}$, and therefore only the modes with $k > 4.5 \times 10^{-4} m_{\rm Pl}$ satisfy the condition $k^2 > |z''/z|$.

B. The ultraviolet regime

In the deformed algebra approach, the ultraviolet modes (UV) experience an exponential growth with increasing wavenumbers. This is due to the Ω-factor in front of the wavenumber in Eq. (31), which becomes negative near the bounce. When approaching the bounce, the friction term in Eq. (32), namely $\dot{H}/H = 1/(t - t_{\rm B})$, diverges. However, the approximate solution given in section IV shows that $\dot{\mathcal{R}}_k$ vanishes at the bounce, since its generic expression is given by

$$\dot{\mathcal{R}}_k = (t - t_{\rm B}) \left[c_1 {\rm ch}\left(k(t - t_{\rm B})\right) - c_2 {\rm sh}\left(k(t - t_{\rm B})\right)\right], \quad (58)$$

where c_1 and c_2 are numerical constants that have to be chosen in accordance to the initial state of the perturbations. Thus, the equation of motion (32) has no singularity, and $(\dot{H}/H)\dot{\mathcal{R}}_k \propto \sqrt{k}$. We are left with the differential equation of an harmonic oscillator, but with an imaginary frequency and a constant term, say $\beta\sqrt{k}$, such that $\ddot{\mathcal{R}}_k + \beta\sqrt{k} - k^2 \mathcal{R}_k = 0$. Close to the bounce the generic solution to this equation is

$$\mathcal{R}_k = \beta k^{-\frac{3}{2}} + \alpha_+ e^{kt} + \alpha_- e^{-kt}.$$

So, in the large k limit and close to the bounce the amplitude of scalar modes receives a real exponential contribution. A similar behavior for the tensor modes was already discussed in Refs. [11] and [31].
The characteristic energy scale $k_{\rm UV}$ at which the effect of the Euclidean nature of the bounce qualitatively affects the evolution of the modes can be determined from

an analysis of $k^2_{\rm eff}$ in Eq. (38). In vicinity of the bounce $\Omega \approx -1$ and $z''/z < 0$. Therefore, a given mode is affected by the Euclidean signature only if $k^2 \geq \frac{z''}{z}$. This is a necessary but not a sufficient condition. The second important quantity is the interval of conformal time $\Delta\eta(k)$ spend by the mode in the "$k^2_{\rm eff} < 0$"-regime. This leads to the following condition for the energy scale $k_{\rm UV}$:

$$k_{\rm UV}\Delta\eta(k_{\rm UV}) \approx 1. \tag{59}$$

A direct analytical analysis of this condition gives the following expression

$$k_{\rm UV} \simeq a_{\rm B}\sqrt{\frac{2}{3}}\sqrt{\frac{\sqrt{2}}{2\sqrt{2}-1}}\sqrt{\kappa\rho_{\rm c}} \approx 2.3\ m_{\rm Pl}, \tag{60}$$

where the numerical value is obtained with use of $a_{\rm B} = 1$ and $\rho_{\rm c} = 0.41\ m^4_{\rm Pl}$.

C. Numerical Results

The scalar power spectrum is obtained by numerical integration of the equation of motion for the mode functions, respectively for the variable h and $\mathcal{R}$ for different phases in the time evolution, and the solution of the background equations (11). Initial conditions for the perturbations can be set according to the WKB approximation referring to the adiabatic vacuum, or with the instantaneous vacuum as shown in Sec. V. The initial conditions for the cosmological background are set in the contracting phase, such that the preferred value of the potential energy parameter x at the bounce is obtained. Note that the dynamics of the background and subsequently the shape of the power spectrum $\mathcal{P}_{\rm S}(k)$ are determined by the mass m of the scalar field, the value of the critical energy density $\rho_{\rm c}$ and the phase θ_0.

Our numerical results are shown in Fig. 3 and Fig. 4 which display the primordial power spectra for the scalar modes, choosing the adiabatic (WKB) vacuum as initial conditions (Fig. 3) and the instantaneous vacuum as initial conditions (Fig. 4). The three regions mentioned in the previous section ($k < k_{\rm IR}, k_{\rm IR} < k < k_{\rm UV}, k > k_{\rm UV}$) can be well identified in the spectra.

In the intermediate region ($k_{\rm IR} < k < k_{\rm UV}$), the spectrum follows a characteristic oscillating behavior observed also in case of the tensor modes (see Ref. [31]). For the values of $k > k_{\rm UV}$, the power spectrum is characterized by the exponential growth. This behavior should, however, be considered with care. First, the UV regime ($k > k_{\rm UV}$) corresponds to the modes which are trans-Planckian at the bounce. For such modes the effective description based on the continuous equations of motion might not be reliable. Second, the observed amplification is due to an instability related to the elliptic type of the equation of motion for perturbations in the Euclidean regime. The Cauchy initial value problem might not be valid for the modes with $k > k_{\rm UV}$ which are strongly affected by the Euclidean nature of the deep quantum regime.

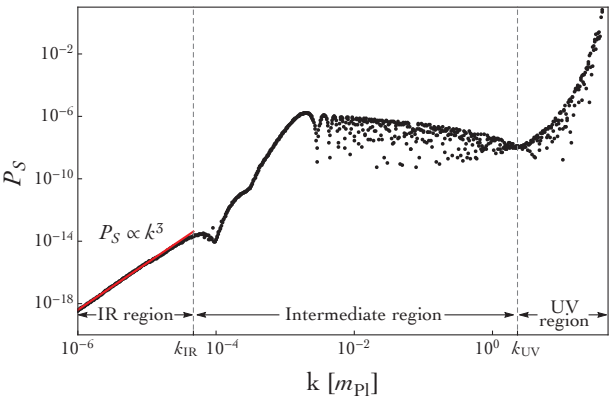

FIG. 3. Primordial power spectrum for scalar modes in the deformed algebra approach for $m = 1.2{\times}10^{-6} m_{\rm Pl}$ and the adiabatic vacuum for initial conditions in the pre-bounce (classical) contracting phase. The cosmological background is fixed such that $x_{\rm B} = 3.55 \times 10^{-6}$ and $a_{\rm B} = 1$ at the bounce.

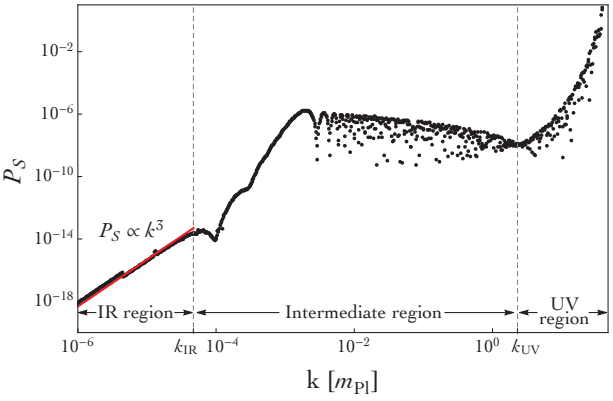

FIG. 4. Primordial power spectrum for scalar modes in the deformed algebra approach for $m = 1.2 \times 10^{-6} m_{\rm Pl}$ and the instantaneous vacuum for initial conditions in the pre-bounce (classical) contracting phase. The cosmological background is fixed such that $x_{\rm B} = 3.55 \times 10^{-6}$ and $a_{\rm B} = 1$ at the bounce.

The spectra for the adiabatic vacuum and the instantaneous vacuum choices are almost identical. The only difference is a slight enhancement in the IR region for the instantaneous vacuum-type normalization, in comparison to the adiabatic vacuum choice. This effect is due to the difference in $v'_k(\eta_{\rm init})$ for both types of initial conditions. At values of $k < k_{\rm IR}$, the shape of the spectra is mostly due to the initial super-Hubble vacuum normalization. In this limit $k_{\rm eff} \simeq \sqrt{k^2 - \frac{z''}{z}} \approx$ const, is almost the same for every mode at this particular initial time, because $k^2 \ll \left|\frac{z''}{z}\right|$. Therefore, $\mathcal{P}_{\rm S}(k) = \frac{k^3}{2\pi^2}\frac{1}{2k_{\rm eff}z^2} \propto k^3$. The initial $\mathcal{P}_{\rm S}(k) \propto k^3$ behavior is preserved in the further evolution due to the super-Hubble nature of the modes. Only the absolute amplitude changes, which is a result of the time dependence of the z parameter.

Furthermore, it is worth stressing that at scales $k < k_{\rm UV}$

the power spectra computed in this paper qualitatively agree with those obtained in the so-called "dressed metric" approach to perturbations in LQC [34]. In that case the Ω-factor does not appear in front of the Laplace operator and the instabilities related to the Euclidean phase do not arise. Therefore, the corresponding spectrum at $k > k_{\rm UV}$ becomes nearly-scale invariant in the "dressed metric" approach, as in the standard inflationary picture.

VII. DISCUSSION AND CONCLUSION

In this work, the primordial scalar power spectrum in the so-called "deformed algebra" approach to perturbations in loop quantum cosmology has been derived. Our considerations were focused on the model with a massive scalar field. The instantaneous and adiabatic vacuum-type initial conditions were imposed in the contracting phase. The non-trivial issue in the evolution of modes is their behavior in the Euclidean phase ($\Omega < 0$) surrounding the bounce. In this region, the equation of motion for the mode functions changes its type from hyperbolic to elliptic. In such a case, no preferred time direction exists. In this study, we have assumed that the time direction associated with the Cauchy surface of initial data is preserved across the Euclidean phase.

Even if the problem is not well-posed for the partial differential equation in that case, reliable predictions can still be obtained for sufficiently low values of k in the Fourier space representation. More precisely, a characteristic scale $k_{\rm UV}$ discriminates between the modes which are affected or not by the Euclidean nature of the bounce. For the modes satisfying $k > k_{\rm UV}$, the elliptic nature of the equations becomes important, leading to an abnormal amplification of the power spectrum. The effect is the same as the one observed earlier in case of the tensor perturbations [11]. In turn, for $k < k_{\rm UV}$, the cosmological contribution to the wave equation becomes dominant in the vicinity of the bounce, making the evolution almost unaffected by the signature change. In the regime $k_{\rm IR} < k < k_{\rm UV}$, a typical oscillatory behavior is observed. In the IR limit, the shape of the spectrum is determined by the initial vacuum normalization and scales as $\mathcal{P}_{\rm S}(k) \propto k^3$.This behavior is very different from the one observed in case of the tensor modes (see Ref. [31]), where the power spectrum becomes nearly-scale invariant while $k \to 0$. This is because the massive scalar field, oscillating in the contracting branch, effectively behaves as dust matter. As it is known, the freezing of massless modes during such an evolution leads to scale-invariance of the power spectrum, as for the case of tensor perturbations. For the scalar perturbations in a model with a massive scalar field the gauge-invariant degree of freedom $v_{\rm S}$ is explicitly massive leading to a breakdown of the scale-invariance.

Several points of the picture presented in this study still need to be addressed. First, the observational consequences of this calculations should be studied into the details [35]. Second, other proposals for setting initial conditions should also be considered. Here, the subtle issue of the very meaning of time in the Euclidean phase were deliberately ignored: modes were naively propagated through the Euclidean phase. A proper addressing of the well-posedness is crucial to obtain stable solutions in the $k > k_{\rm UV}$ regime (even if their physical meaning is not clear due to the breakdown of validity of the effective equations under considerations) [36]. Furthermore, the matter content considered in this paper is no more favored by the observations of the cosmic microwave background radiation. A caraful analysis of different inflationary potentials would therefore be desirable. In particular, the Colemen-Weinberg potential with an unstable state may lead to inflationary spectra being in agreement with the up-to-date observational data. Such a change of the potential function would unavoidably affect our predictions regarding the shape of the power spectra.

ACKNOWLEDGMENTS

BB is supported by a grant from ENS Lyon. JM is supported by the Grant DEC-2014/13/D/ST2/01895 of the Polish National Centre of Science.

[1] C. Rovelli & F. Vidotto, *Covariant Loop Quantum Gravity*, Cambridge University Press (2014);
R. Gambini & J. Pullin, *A First Course in Loop Quantum Gravity*, Oxford, Oxford University Press (2011);
T. Thiemann, *Lect. Notes Phys.*, **631**, 41 (2003);
T. Thiemann, *Modern Canonical Quantum General Relativity*, Cambridge, Cambridge University Press (2007);
C. Rovelli, *Quantum Gravity*, Cambridge, Cambridge University Press (2004);
C. Rovelli, *Living Rev. Relativity*, **1**, 1 (1998)

[2] A. Ashtekar and A. Barrau, arXiv:1504.07559;
A. Barrau, T. Cailleteau, J. Grain, J. Mielczarek, *Class. Quantum Grav.* **335**, 053001 (2014);
G. Calcagni, Annalen Phys. **525** (2013) 5, 323;
K. Banerjee, G. Calcagni, and M. Martin-Benito, *SIGMA*, **8**, 016 (2012);
M. Bojowald, *Quantum Cosmology*, Springer, New-York (2011);
A. Ashtekar, *Gen. Rel. Grav.* **41**, 707 (2009);
M. Bojowald, *Living Rev. Rel.* **11**, 4 (2008);
A. Ashtekar, M. Bojowald, & J. Lewandowski, *Adv. Theor. Math. Phys.* **7**, 233 (2003)

[3] A. Ashtekar, P. Singh, *Class. Quantum Grav.* **28**, 213001 (2011)

[4] J. Grain & A. Barrau, *Phys. Rev. Lett.* **102** 081301 (2009)

[5] J. Grain, T. Cailleteau, T. Cailleteau, & A. Gorecki, *Phys. Rev. D* **81** 024040 (2010)
[6] J. Mielczarek, T. Cailleteau, J. Grain, & A. Barrau, *Phys. Rev. D* **81** 104049 (2010)
[7] J. Grain, A. Barrau, T. Cailleteau, & J. Mielczarek, *Phys. Rev. D* **82** 123520 (2010)
[8] A. Barrau, M. Bojowald, G. Calcagni, J. Grain & M. Kagan, JCAP **1505** (2015) 05, 051
[9] M. Bojowald & G. M. Paily, Deformed General Relativity, *Phys. Rev. D* **87** 044044 (2013)
[10] T. Cailleteau, J. Mielczarek, A. Barrau & J. Grain, *Class. Quantum Grav.* 29 095010 (2012)
[11] L. Linsefors, T. Cailleteau, A. Barrau, & J. Grain, *Phys. Rev. D* **87** 107503 (2013)
[12] J. Mielczarek, L. Linsefors & A. Barrau, arXiv:1411.0272
[13] M. Bojowald & J. Mielczarek, JCAP **1508** (2015) 08, 052
[14] I. Agullo, A. Ashtekar, & W. Nelson, *Class. Quantum Grav.* **30**, 085014 (2013);
I. Agullo, A. Ashtekar, & W. Nelson, *Phys. Rev. D* **87**, 043507 (2013);
I. Agullo, A. Ashtekar, & W. Nelson, *Phys. Rev. Lett.* **109**, 251301 (2012)
[15] A. Ashtekar, W. Kaminski, & J. Lewandowski, *Phys. Rev. D* **79** 064030 (2009)
[16] H. Nicolai, K. Peeters & M. Zamaklar, *Class. Quantum Grav.* **22** R193 (2005)
[17] M. Bojowald, G. M. Hossain, M. Kagan & S. Shankaranarayanan, *Phys. Rev. D* **78** 063547 (2008)
[18] M. Bojowald, G. M. Hossain, M. Kagan & S. Shankaranarayanan, *Phys. Rev. D* **79** 043505 (2009)
[19] M. Bojowald & G. M. Hossain, *Class. Quantum Grav.* **24** 4801 (2007)
[20] M. Bojowald & G. M. Hossain, *Phys. Rev. D* **77** 023508 (2008)
[21] M. Bojowald & and G. Calcagni, *JCAP* 1103 032 (2011)
[22] M. Bojowald, G. Calcagni & S. Tsujikawa, *JCAP* 111 046 (2011)
[23] J. Mielczarek, T. Cailleteau, A. Barrau & J. Grain, *Class. Quantum Grav.* 29 085009 (2012)
[24] T. Cailleteau, L. Linsefors & A. Barrau *Class. Quantum Grav.* 31 125011 (2014)
[25] T. Cailleteau, A. Barrau, J. Grain, & F. Vidotto, *Phys. Rev. D* **86** 087301 (2012)
[26] E. Wilson-Ewing, *Class. Quantum Grav.* 29 085005 (2012)
[27] J. Mielczarek, *Europhys. Lett.* 108 4, 40003 (2014)
[28] A. Ashtekar, T. Pawlowski & P. Singh, *Phys. Rev. D* **74**, 084003 (2006)
[29] Planck Collaboration, arXiv:1502.01589 [astro-ph.CO]
[30] P. Singh, K. Vandersloot & G. V. Vereshchagin, *Phys. Rev. D* **74**, 043510 (2006)
[31] B. Bolliet, J. Grain, C. Stahl & A. Barrau, *Phys. Rev. D* **91** 084035 (2012)
[32] L. Linsefors & A. Barrau, arXiv:1301.1264v2 [gr-qc]
[33] V. F. Mukhanov & S. Winitzki, *Introduction to Quantum Effects in Gravity*, Cambridge University Press (2012);
S. A. Fulling, *Aspects of Quantum Field Theory in Curved Space-Time*, Cambridge Universtiy Press (1989);
[34] I. Agullo and N. A. Morris, arXiv:1509.05693 [gr-qc]
[35] B. Bolliet *et al.*, in preparation
[36] J. Mielczarek *et al.*, in preparation

5.3 Comparison of the different approaches

As explained previously, there are currently two main approached to LQC. One is the deformed algebra approach, which is the one considered for most of this thesis. The other one, described in Section 3.2, is the dressed metric one. They are grounded in deeply different hypotheses. However, in addition to those different assumptions, there is also a "contingent" difference which comes from the way both teams decide to set initial conditions. Here we choose the *same* initial conditions for both approaches to really compare their deep content, focusing on tensor modes. As initial cannot be set at the bounce time for the deformed algebra approach (as space-time is Euclidean), we have decided to put them in the contracting branch. In our opinion it makes more sense at both the technical and interpretational levels.

Although the dressed metric approach tries to deals with quantum fields in a quantum background in a profound way it is worth noticing that, at the end of the day, the equation of propagation one gets here (for highly peaked states) is exactly the one we would have obtained by simply taking the usual one on a LQC modified classical background.

The neat result of the simulations we have performed is that, not surprisingly, both spectrums are very similar for $k < k_{UV}$, exhibiting non-trivial universal (to LQC) features. This result also straightens the earlier conclusion, that $k < k_{UV}$ are not noticeable effected by the signature change in the deformed algebra approach.

We also took this opportunity to explicitly calculate quite a lot of background quantities that will be useful to future works.

PHYSICAL REVIEW D **91,** 084035 (2015)

Comparison of primordial tensor power spectra from the deformed algebra and dressed metric approaches in loop quantum cosmology

Boris Bolliet,[1,2,*] Julien Grain,[3,4,†] Clément Stahl,[4,3,‡] Linda Linsefors,[2,§] and Aurélien Barrau[5,‖]

[1]*École Normale Supérieure de Lyon, 46 Allée d'Italie, Lyon 69007, France*
[2]*Laboratoire de Physique Subatomique et de Cosmologie, Université Grenoble-Alpes, CNRS/IN2P3 53, avenue des Martyrs, 38026 Grenoble cedex, France*
[3]*CNRS, Orsay, France, F-91405*
[4]*Université Paris-Sud 11, Institut d'Astrophysique Spatiale, UMR8617, Orsay, France, F-91405*
[5]*Laboratoire de Physique Subatomique et de Cosmologie, Université Grenoble-Alpes, CNRS/IN2P3 53,avenue des Martyrs, 38026 Grenoble cedex, France*

(Received 10 February 2015; published 16 April 2015)

Loop quantum cosmology tries to capture the main ideas of loop quantum gravity and to apply them to the Universe as a whole. Two main approaches within this framework have been considered to date for the study of cosmological perturbations: the dressed metric approach and the deformed algebra approach. They both have advantages and drawbacks. In this article, we accurately compare their predictions. In particular, we compute the associated primordial tensor power spectra. We show—numerically and analytically—that the large scale behavior is similar for both approaches and compatible with the usual prediction of general relativity. The small scale behavior is, the other way round, drastically different. Most importantly, we show that in a range of wave numbers explicitly calculated, both approaches do agree on predictions that, in addition, differ from standard general relativity and do not depend on unknown parameters. These features of the power spectrum at intermediate scales might constitute a universal loop quantum cosmology prediction that can hopefully lead to observational tests and constraints. We also present a complete analytical study of the background evolution for the bouncing universe that can be used for other purposes.

DOI: 10.1103/PhysRevD.91.084035 PACS numbers: 04.60.Pp, 04.60.Bc, 98.80.Cq, 98.80.Qc

I. INTRODUCTION

Loop quantum gravity (LQG) is a consistent theory of quantum pseudo-Riemannian geometry that builds on both Einstein gravity and quantum physics, without requiring any fundamentally new principle (like, e.g., extra-dimensions or supersymmetry). Several introductory reviews can be found in [1]. Loop quantum cosmology (LQC) is a symmetry reduced version of LQG (see [2] for introductions) which accounts for the basic cosmological symmetries. At this stage, a fully rigorous derivation of LQC from the mother theory is not yet available. In fact, LQC imports the main techniques of LQG in the cosmological sector and uses a "LQG-like" quantization procedure. This so-called polymeric quantization relies on a kinematical Hilbert space that is different from the Wheeler-DeWitt one, and therefore evades the Von Neumann uniqueness theorem. Nonetheless, it has been shown to be well defined when the diffeomorphism invariance is rigorously imposed [3]. Since there is no operator associated with the Ashtekar connection but only with its holonomy, the basic variables of LQC are the holonomy of the Ashtekar connection and the flux of the densitized triad, its conjugate momentum. The main result of LQC is that the big bang singularity is removed and replaced by a big bounce smooth evolution, so that the total energy density cannot be greater than a critical energy density. Intuitively, for sharply peaked states of the background geometry, the Universe undergoes a quantum tunneling from a classical contracting solution to a classical expanding solution.

At the effective level, LQC can be modeled by two kinds of corrections. The inverse-volume corrections [4] (or inverse-triad, if one relaxes the isotropy hypothesis) are natural cutoff functions of divergences for factors containing inverse powers of densitized triads, arising because of spatial discreetness. The holonomy correction [5] is instead associated with higher powers of the intrinsic and extrinsic spatial curvature components, stemming from the appearance of holonomies of the Ashtekar connection. As the status of inverse-volume correction is less clear—in particular because of a fiducial-cell dependance—we only consider in this article the holonomy corrections.

Even when dealing with holonomy corrections only, there are two main ways of considering the effective theory, leading to a lively debate within the LQC community. This study aims at comparing the predictions for cosmological perturbations of both approaches, setting the initial conditions in the same way (that is at the same time and with the same vacuum), which has not been done to date.

*boris.bolliet@ens-lyon.fr
†julien.grain@ias.u-psud.fr
‡clement.stahl@icranet.org
§linsefors@lpsc.in2p3.fr
‖Aurelien.Barrau@cern.ch

The first approach has been developed in [6–8] and is referred to as the *dressed metric* approach. It relies on a minisuperspace strategy where the homogeneous and isotropic degrees of freedom as well as the inhomogoneous ones (considered as perturbations) are both quantized. The former quantization follows the loop approach whereas the latter is obtained from a Fock-like procedure on a quantum background. The physical inhomogeneous degrees of freedom are given by the Mukhanov-Sasaki variables derived from the linearized classical constraints. The second order Hamiltonian is promoted to be an operator and the quantization is performed using techniques suitable for the quantization of a test field evolving on a quantum background [9]. The Hilbert space is just the tensor product of a Hilbert space for the background degrees of freedom, with another for the perturbed ones. In the interaction picture, the Schrödinger equation for the perturbations was demonstrated to be formally identical to the Schrödinger equation for the quantized perturbations evolving on a classical background but using a *dressed* metric that encodes the quantum nature of this background.

The second approach, that we refer to as the *deformed algebra*, focuses on the well-known problem of the consistency of the effective theory. This basically means that the evolution produced by the model should be consistent with the theory itself. This translates into the requirement that the Poisson bracket between two corrected constraints should be proportional to another constraint. The coefficient of proportionality being a function of the fundamental variables, which makes the situation slightly more subtle than in usual field theories dealing with simple structure constants. The key point is that the closure of the algebra should also be considered off-shell [10]. Interestingly, this closure consistency condition is, after the holonomy correction implementation, basically enough to determine the structure of the quantum Poisson bracket algebra [11–13]. An essential result is that the spacetime structure eventually becomes Euclidean instead of Lorentzian around the bounce, when the total energy density is larger than half the critical energy density. This had been overlooked until spherically symmetric inhomogeneity and cosmological perturbations were studied in an anomaly-free way. Without inhomogeneity, one cannot determine the signature because (i) it is impossible to see the relative sign between temporal and spatial derivatives and (ii) the relevant Poisson bracket trivially equals zero in homogeneous models. The signature change is not a consequence of inhomogeneities, the latter rather being used as a test field. There are hints that in the present context, such an effect could really be interpreted as a deep signature change of space-time rather than a mere tachyonic instability [14].

In this specific study, we do not focus on a specific approach. Both have their advantages and drawbacks. The *dressed metric* approach certainly captures more quantum effects, as it deals with the full wave functions. But it faces a problem. In general relativity, there is in principle an infinite number of dynamical laws, all written with respect to different choices of time coordinates. They are all equivalent one to another because of the symmetries of the classical theory and it is legitimate to pick up an arbitrary choice. In the *dressed metric* approach, one is implicitly making use of several such choices, referred to as a background gauge. The mode dynamic is then written in terms of coordinate-invariant combinations of metric and matter perturbations. Only after these steps, one obtains a specific dynamic for the background variables and perturbations, which is written in a Hamiltonian way. Classically, the resulting dynamic does not depend on the coordinate choice and the procedure is valid. But as some degrees of freedom are quantized here, the equations are modified by quantum corrections of different kinds, and nothing still guarantees that the results do not depend on the arbitrary choices made before (that is, the theory may not be covariant or anomaly-free). What is important is the fact that the classical theory enjoys a strong symmetry which is often used in order to simplify the analysis. When one quantizes or modifies the theory, this symmetry must not be violated, or else one may obtain meaningless (gauge-dependent) results. When the dynamics (including dynamical equations and symmetries) is formulated as a constrained system, one gains access to powerful canonical methods by which the consistency of the theory can be easily analyzed. It is of course possible to use another formalism, but not to ignore the problem of potential violations of crucial symmetries [14]. The *deformed algebra* approach does not suffer from this problem and is certainly more obviously consistent. But it does suffer from other difficulties, namely the shape of the modifications is not strictly speaking entirely determined by the anomaly-free condition, there is a kind of tension with the Hojman, Kuchar and Teitelboim theorem [15] making the geometrical interpretation difficult, and the fact that the fields are normalized *after* the effective quantum corrections were applied to the background, leading to a kind of possibly artificial "requantization" of the theory.

We also take the opportunity of this study to clarify some points about the background dynamics, common to both approaches.

The first part of this article is devoted to analytical investigations of the background evolution that were already known but not expressed in such a systematic way. This material will also be very useful for the rest of the study, as the shape of the primordial tensor power spectrum depends mainly on the cosmic history. The second part is devoted to the calculation of the infrared and ultraviolet limits of the primordial tensor power spectrum for sharply peaked states in the dressed metric approach. The third part deals with the same issues in the deformed algebra model. In both cases, the initial conditions are set in the same way, in the contracting phase, in order to make a meaningful

comparison. The fourth part shows the results of the numerical computations of the full power spectra and some universal features are underlined. In the conclusion, we outline the main differences and similarities between both approaches before giving some perspectives toward observational tests and constraints.

II. BACKGROUND EVOLUTION: ANALYTICAL SOLUTIONS

In this section we study the background evolution at the effective level. Although this has already been studied (see [2]), our purpose here is to provide analytic solutions which are accurate approximations of the cosmic history over different regions. Our scope is twofold. First, this can give further insights on the effective dynamics of the background, potentially useful for further investigations. Second, these analytic results are developed in the scope of the forthcoming investigation of tensor perturbations since their equation of motion obviously involves background quantities such as the scale factor and the total energy density. Here we focus on the most probable dynamics as in [16,17].

A. Overview of the background dynamics

The background evolution of the quantum universe is described using the effective, semiclassical dynamics, as derived in loop quantum cosmology with holonomy corrections. In this article, the background geometry is described by the unperturbed metric tensor $\mathrm{g} = -\mathrm{dt} \otimes \mathrm{dt} + a^2 \delta_{ij} \mathrm{dx}^i \otimes \mathrm{dx}^j$, where a is the scale factor. Dots denote derivatives with respect to the cosmic time, $\dot{\mathrm{a}} \equiv \frac{\partial a}{\partial t}$, and primes denote derivatives with respect to conformal time, related to the cosmic time by $dt = a d\eta$. The content of the universe is modeled by a single massive scalar field, ϕ, with a quadratic potential, $V(\phi) = m^2\phi^2/2$. In order to characterize the field evolution we use two dynamical parameters, the potential energy parameter, x, and the kinetic energy parameter, y, defined by

$$x \equiv \frac{m\phi}{\sqrt{2\rho_\mathrm{c}}}, \qquad y \equiv \frac{\dot{\phi}}{\sqrt{2\rho_\mathrm{c}}}, \tag{1}$$

where ρ_c is the critical density, i.e., the maximum value of the total energy density that can be express as $\rho = \rho_\mathrm{c}(x^2 + y^2)$. The modified Friedmann equation, as predicted in LQC from the Hamiltonian constraint and the Hamilton equations, is

$$H^2 = \frac{8\pi G\rho}{3}\left(1 - \frac{\rho}{\rho_\mathrm{c}}\right), \tag{2}$$

where $H \equiv \frac{\dot{a}}{a}$ is the Hubble parameter. The Klein-Gordon equation for the scalar field is

$$\ddot{\phi} + 3H\dot{\phi} + m^2\phi = 0. \tag{3}$$

Equations (2) and (3) are recast into

$$\begin{cases} \dot{H} = -8\pi G\rho_\mathrm{c} y^2(1 - 2x^2 - 2y^2), \\ \dot{x} = my, \\ \dot{y} = -3Hy - mx. \end{cases} \tag{4}$$

There are two time scales involved in this system of equations. One is given by $1/m$ and corresponds to the classical evolution of the field. The other time scale is $1/\sqrt{G\rho_\mathrm{c}}$ and corresponds to the quantum regime of the evolution. Modulo a numerical factor, relevant for the following calculations, the ratio of these two time scales is

$$\Gamma \equiv \frac{m}{\sqrt{24\pi G\rho_\mathrm{c}}}. \tag{5}$$

If we assume $\Gamma \ll 1$, and start with a negative Hubble parameter (contracting universe), the background dynamics splits into three subsequent phases:

(i) Pre-bounce contracting phase,
(ii) Bouncing phase,
(iii) Slow-roll inflation.

In each phase, it is possible to get analytical expressions for all the background variables. Note that the value of the inflaton mass preferred by cosmic microwave background (CMB) observations is $m \simeq 10^{-6} m_\mathrm{Pl}$. Furthermore, calculations of the black hole entropy suggests $\rho_\mathrm{c} = 0.41 m_\mathrm{Pl}^4$, leading to $\Gamma \simeq 2 \times 10^{-7}$. Therefore, asserting $\Gamma \ll 1$ is not a strong assumption at all.

B. Initial conditions

The initial conditions $\{a_0, x_0, y_0\}$ are set in the remote past, when $H_0 < 0$ and

$$\sqrt{\frac{\rho_0}{\rho_\mathrm{c}}} \ll \Gamma. \tag{6}$$

The subscript "0" means that the variables are evaluated at $t = 0$. The condition (6) ensures that initially the dynamic is not dominated by the amplification due to the term "$3H$" in (3). We often use polar coordinates for x and y:

$$\begin{cases} x(t) = \sqrt{\frac{\rho(t)}{\rho_\mathrm{c}}} \sin(mt + \theta_0), \\ y(t) = \sqrt{\frac{\rho(t)}{\rho_\mathrm{c}}} \cos(mt + \theta_0). \end{cases} \tag{7}$$

The initial value of the energy density is specified with the two numbers α and θ_0:

$$\sqrt{\frac{\rho_0}{\rho_\mathrm{c}}} = \frac{\Gamma}{\alpha}\left\{1 - \frac{\sin(2\theta_0)}{4\alpha}\right\}^{-1}. \tag{8}$$

For a given $\alpha \gg 1$, such that (6) is valid, there is a one-to-one correspondence between the family of solutions to (4) and the interval $\{\theta_0 | 0 \leq \theta_0 < 2\pi\}$. The choice for this parametrization is clarified in the next section.

C. The pre-bounce classical contracting phase

As long as (6) holds for $\rho(t)$, the system (4) can be solved analytically. In the third line of (4), the term "$3Hy$" can be neglected, compared to "mx", as their ratio is of order $\mathcal{O}(1/\alpha)$ initially. Then, x and y behave simply as the phase variables of the harmonic oscillator [i.e., (7) with constant amplitude]. The solution for y can be injected into the equation for $\dot{H}$ in (4) where one neglects "$-2x^2 - 2y^2$" in comparison to unity in the bracket. The Hubble parameter is replaced by its expression in terms of the energy density (2) where the correction $\rho/\rho_c \ll 1$ is neglected. After these replacements, one is left with a first order differential equation over $\rho(t)$ which can be integrated into

$$\sqrt{\frac{\rho(t)}{\rho_c}} = \frac{\Gamma}{\alpha}\left\{1 - \frac{1}{2\alpha}\left[mt + \frac{1}{2}\sin(2mt + 2\theta_0)\right]\right\}^{-1}. \quad (9)$$

This solution exhibits an oscillatory behavior due to the sine function in the denominator. The oscillations have a period of order $1/m$, much smaller than the time scale of the growth, α/m. Moreover, their amplitude is also smaller than the averaged amplitude $\sqrt{\rho/\rho_c}$ by a factor α. When these small and fast oscillations are neglected, the Hubble parameter can be expressed as

$$H(t) = H_0\left(1 + \frac{3}{2}H_0 t\right)^{-1}, \quad (10)$$

where the initial Hubble parameter is $H_0 = -m/(3\alpha)$. With the parametrization (9), solutions with the same α but different θ_0's are all corresponding to the same averaged behavior (there is only a phase difference between them). From (10), the scale factor can be computed as a function of cosmic time, and as a function of conformal time after another integration. As the value of the initial conformal time η_0 can be set arbitrarily, we choose $\eta_0 = 2/(H_0 a_0)$. With such a choice, the expression for the scale factor simply reads

$$a(\eta) = \lambda_0 \eta^2 \quad \text{with} \quad \lambda_0 \equiv \frac{a_0^3 H_0^2}{4}, \quad (11)$$

so that the expression of the comoving Hubble radius during the contracting phase is

$$aH(\eta) = \frac{2}{\eta}. \quad (12)$$

This is the same behavior as with a universe filled with dust-like matter. When $H \simeq -m/3$, the amplification term $3H$ in (4) becomes dominant. It corresponds to the end of the pre-bounce contracting phase and the start of the bouncing phase. The contracting phase ends when $\rho_A = \Gamma^2 \rho_c$, so at this stage there are no significant quantum effects.

D. The bouncing phase

Let us define t_A, the time such that $H(t_A) = -m/3$. One finds $t_A = 2(\alpha - 1)/m$. Moreover, at t_A, if the small and fast oscillations of the field are neglected, the fractions of potential and kinetic energy are given by

$$x_A = \Gamma \sin\theta_A \quad \text{and} \quad y_A = \Gamma \cos\theta_A, \quad (13)$$

with $\theta_A \equiv 2(\alpha - 1) + \theta_0$. The Hubble parameter keeps increasing (in modulus) until it reaches a maximum, $H_{\max} \equiv \sqrt{24\pi G\rho_c}/6$. The inverse of $H_{\max}$ has the dimension of a time and gives an estimate of the time scale of this amplification. As a first analysis, in the second equation of the system (4), the time derivative can be replaced by a factor $H_{\max}$. Then, we find that the ratio between the fraction of potential and kinetic energy is of order $\sim 6\Gamma$, and therefore very small in comparison to unity. This suggests that at the start of the bouncing phase, the kinetic energy parameter grows very quickly, while the fraction of potential energy remains of order $\sim\Gamma$. When the kinetic energy is dominant, the system of equations (4) reduces to

$$\begin{cases} \dot{y} = \sqrt{24\pi G\rho_c}\, y^2\sqrt{1 - y^2}, \\ \dot{x} = my, \end{cases} \quad (14)$$

which can be solved analytically. The solutions to (14) shall be valid as long as the kinetic energy dominates over the potential energy. In particular, they are valid at the bounce when the energy density reaches ρ_c, or equivalently when $y(t_B) = 1$. For the time t_B, at which the bounce occurs, one finds $t_B = t_A + \frac{1}{m|\cos\theta_A|}$.

The fractions of kinetic and potential energy during the bouncing phase can be expressed as

$$y(t) = [1 + 24\pi G\rho_c (t - t_B)^2]^{-\frac{1}{2}}, \quad (15a)$$

$$x(t) = x_B + \varepsilon\Gamma \operatorname{arcsinh}(\sqrt{24\pi G\rho_c}(t - t_B)), \quad (15b)$$

where $\varepsilon \equiv \operatorname{sgn}(\cos\theta_A)$, and the value of the potential energy parameter at the bounce is given by

$$x_B = x_A - \varepsilon\Gamma \ln\left(\frac{1}{2}\Gamma|\cos\theta_A|\right). \quad (16)$$

The case $\cos\theta_A \ll 1$ may appear problematic. Actually it corresponds to a different evolution of the background,

with a phase of *deflation* before the bounce. Here we focus on cases—statistically much more frequent and therefore relevant for phenomenology [17]—where a sufficiently long phase of inflation is achieved. During the bouncing phase, the Hubble parameter and the scale factor take on a very simple form. The scale factor is related to the kinetic energy parameter by $a = a_{\rm B}|y|^{-\frac{1}{3}}$. Consequently, the expression for the scale factor at $t_{\rm A}$ is

$$a_{\rm A} = a_{\rm B}|\Gamma\cos\theta_{\rm A}|^{-\frac{1}{3}}. \tag{17}$$

Using (12), we can find the conformal time $\eta_{\rm A}$ that corresponds to $t_{\rm A}$. Then, we can use (17) and (11) in order to write $\eta_{\rm A}$ in terms of λ_0. We get

$$\eta_{\rm A} = -\left(\frac{6}{m\lambda_0}\right)^{1/3}. \tag{18}$$

After the bounce, the fraction of potential energy increases. Meanwhile, the fraction of kinetic energy decreases and eventually becomes smaller than the fraction of potential energy. This corresponds to the start of slow-roll inflation.

E. The classical slow-roll inflation

The total energy density $\rho = \rho_{\rm c}(x^2 + y^2)$, with $x(t)$ and $y(t)$ given by (15a) and (15b), reaches a minimum at time $t_{\rm i}$. According to these analytical expressions the total energy density increases for $t > t_{\rm i}$. Obviously, this is irrelevant in an expanding universe without energy sources: the total energy density must always decrease. The time $t_{\rm i}$ can be computed analytically by solving $\dot{\rho}(t_{\rm i}) = 0$. One gets $t_{\rm i} = t_{\rm B} + (f/m)$, where f is expressed in terms of the Lambert W function [defined as the solution to $z = W(z)e^{W(z)}$], and $x_{\rm B}$ is given by

$$f \equiv \sqrt{\frac{2}{W(z)}} \quad \text{with} \quad z = \frac{8}{\Gamma^2}\exp\left(\frac{2|x_{\rm B}|}{\Gamma}\right). \tag{19}$$

In general, f is of order $\mathcal{O}(1)$. For instance, when $\cos\theta_{\rm A} = 1$ and $\Gamma = 2\times10^{-7}$, one gets $f \simeq 0.18$. At $t_{\rm i}$, the fraction of potential energy is calculated with (15a), (15b) and (16). We find

$$x_{\rm i} = x_{\rm A} - 2\varepsilon\Gamma\ln\left(\frac{1}{2}\Gamma\sqrt{\frac{|\cos\theta_{\rm A}|}{f}}\right). \tag{20}$$

Shortly after $t_{\rm i}$ [in a time of order $1/(m\ln\Gamma)$], one can show that the fraction of kinetic energy ends up being almost constant. One then has $y_{\rm i} \equiv -\varepsilon\Gamma$ and the slow-roll conditions are fulfilled. Actually, for the quadratic potential it is enough to check that $\epsilon_{\rm H} \equiv -\dot{H}/H^2$ is small in comparison to unity for the slow-roll conditions to be valid. We find

$$\epsilon_{\rm H} = 3\left|\frac{\Gamma}{x_{\rm i}}\right|^2, \tag{21}$$

which is generally a small number. For $\cos\theta_{\rm A} = 1$ and $\Gamma = 2\times10^{-7}$ one gets $\epsilon_{\rm H} \simeq 0.003$. Slow-roll inflation can start, the system of equation (4) reduces to

$$\begin{cases} y = -\varepsilon\Gamma, \\ \dot{x} = my, \end{cases} \tag{22}$$

and the Hubble parameter becomes

$$H(t) = H_{\rm i}\left|1 - \varepsilon\frac{\Gamma}{x_{\rm i}}m(t - t_{\rm i})\right|. \tag{23}$$

where $H_{\rm i} = \sqrt{8\pi G\rho_{\rm c}/3}|x_{\rm i}|$. We can also use (23) to compute the scale factor at $t_{\rm i}$ with $|y_{\rm i}| = \Gamma$. We get

$$a_{\rm i} = a_{\rm B}\Gamma^{-\frac{1}{3}}. \tag{24}$$

Note that at the start of slow-roll inflation the total energy density is smaller than the critical energy density by a factor Γ^2. Therefore, when slow-roll inflation starts, the universe is already classical (since quantum corrections are negligible).

We stress that all the analytical approximations derived above have been checked against numerical integrations of Eq. (4). This has been done for each one of the three subsequent phases as well as for the matching between them.

III. POWER SPECTRUM IN THE DRESSED METRIC APPROACH

A. Preliminaries on the dressed metric approach

The dressed metric approach for both scalar and tensor cosmological perturbations in LQC has been developed in [6–8]. Focusing on the tensor modes, the primordial power spectrum at the end of inflation is defined in terms of the mode functions of the Mukhanov-Sasaki variables, denoted v_k, as[1]

$$\mathcal{P}_{\rm T}(k) = \frac{32Gk^3}{\pi}\left|\frac{v_k(\eta_{\rm e})}{a(\eta_{\rm e})}\right|^2, \tag{25}$$

with $\eta_{\rm e}$ standing for the end of inflation.

It is worth mentioning that the precise knowledge of $\eta_{\rm e}$ is not mandatory for the derivation of the primordial power spectrum in both the infrared (IR) and ultraviolet (UV) limits. For the IR limit, this is because infrared modes are

[1]This model is parity invariant and the two helicity states of the tensor mode are equally amplified. The summation over the helicity states is implicitly done in our definition of the primordial power spectrum.

(by definition) mainly amplified during the contraction and the contribution of inflation is suppressed as compared to the previous phases. In the UV, this is because we focus on modes that crossed the horizon during inflation, so that their amplitude has remained constant after a few e-folds.

In order to obtain the power spectrum, one has to solve the equation of motion for the mode functions, $v_k(\eta)$, with given initial conditions. In conformal time, this equation takes the form of a Schrödinger equation

$$v_k''(\eta) + \left(k^2 - \frac{\langle \tilde{a}'' \rangle}{\langle \tilde{a} \rangle}\right) v_k(\eta) = 0, \tag{26}$$

where $\tilde{a}$ is a *dressed* scale factor and $\langle . \rangle$ refers to the quantum expectation value on background states. This takes into account the width of the background wave function and has *a priori* no reason to be equal to the scale factor, $a(t)$, solution to the modified Friedmann equation (corresponding to the scale factor traced by the *peak* of the sharply peaked wave function). However, it is argued in [8] that for sharply peaked background states, the dressed effective potential term, $\langle \tilde{a}'' \rangle / \langle \tilde{a} \rangle$, is very well approximated by its peaked value, a''/a, from the bounce up to the entire expanding phase. We expect this approximation to be valid from the bounce down to the classical contracting phase since this also corresponds to a more and more classical universe when going backward in time from the bounce. With this approximation, (26) becomes

$$v_k''(\eta) + \left(k^2 - \frac{a''}{a}\right) v_k(\eta) = 0, \tag{27}$$

where the scale factor is now a solution to the modified Friedmann equation, and the analytical results derived in Sec. II can be used for the background variables.

B. Calculation of the IR limit

1. Definition of the IR regime

The IR limit of the primordial power spectrum is obtained by considering the modes which stopped oscillating with time and were frozen during the pre-bounce contracting phase. The freezing of a mode happens when its wave number becomes smaller than the effective potential, $\sqrt{a''/a}$. With the analytical expressions given in the previous section, one finds that during the contraction,

$$\frac{a''}{a} = \frac{2}{\eta^2}. \tag{28}$$

Thus, an infrared mode with a wave number k crosses the effective potential at a conformal time $|\eta_k| \equiv \sqrt{2}/k$. Its amplitude is frozen from that time up to the end of inflation, as k^2 remains smaller than a''/a. Since $-\infty < \eta < \eta_A$ (with $\eta_A < 0$), the modes that crossed the potential during the contracting phase are in the range $0 < k < k_{\rm IR}$, with $k_{\rm IR}$ defined by the mode that crossed the effective potential at the beginning of the bouncing phase. With (28), (17), (11) and (18) we find

$$k_{\rm IR} = \frac{a_{\rm B}}{3\sqrt{2}} \left(\frac{m^2 \sqrt{24\pi G \rho_{\rm c}}}{|\cos\theta_{\rm A}|}\right)^{1/3}. \tag{29}$$

The IR limit stands for the modes such that $k \ll k_{\rm IR}$.

2. Primordial power spectrum in the IR regime

For infrared modes, from the potential crossing η_k to the end of inflation $\eta_{\rm e}$, the solution to the equation of motion (27) is therefore well approximated by

$$v_k^{\rm IR}(\eta) = \alpha_k a(\eta) + \beta_k a(\eta) \int_{\eta_\star}^{\eta} \frac{d\eta'}{a^2(\eta')} + \mathcal{O}((k/k_{\rm IR})^2), \tag{30}$$

where α_k and β_k are two constants to be determined. The value of $\eta_\star$ can be conveniently set by requiring the term proportional to α_k to be solely decaying, and the term proportional to η_k to be solely growing. During the contracting phase, the term proportional to α_k is clearly decaying since $a(\eta)$ is decreasing. A convenient choice for $\eta_\star$ is such that the term proportional to β_k must be solely growing. Since $a(\eta) = \lambda_0 \eta^2$, the term proportional to β_k has a time dependance $\sim \eta^2(\eta^{-3} - \eta_\star^{-3})$, in which the part proportional to $\eta^2/\eta_\star^3$ is decaying ($\eta < 0$) and we send $\eta_\star$ to $(-\infty)$ to remove it.[2]

From (30) and (25), the expression of the IR limit of the spectrum reads

$$\mathcal{P}_{\rm T}(k)^{\rm IR} = \frac{32Gk^3}{\pi} |\alpha_k + \beta_k I(\eta_{\rm e})|^2, \tag{31}$$

where $I(\eta_{\rm e})$ is the integral defined as

$$I(\eta_{\rm e}) \equiv \int_{-\infty}^{\eta_{\rm e}} \frac{d\eta}{a^2}. \tag{32}$$

The calculation of the IR limit proceeds in two steps. First, we compute α_k and β_k by matching (30) to a set of solutions defined in the contracting phase. As we shall see, this determines the scale dependence of the primordial power spectrum in the infrared regime. The second step is the

[2]During the contracting phase, the identification of the growing and decaying modes differs from that identification during inflation. Because the Universe is expanding during inflation, the term $\alpha_k a(\eta)$ is solely growing (while it is solely decaying during contraction). Then the term $\beta_k \int_{\eta_\star}^{\eta} d\eta'/a^2(\eta')$ can be made solely decaying in an inflationary universe by setting $\eta_\star = \eta_{\rm e}$ (while it is made solely growing during contraction by setting $\eta_\star \to -\infty$).

calculation $I(\eta_e)$ using the analytical solutions for the background, obtained in Sec. II. This second step sets the amplitude of the power spectrum. The expression of the primordial spectrum is finally obtained by gathering the expressions of α_k, β_k and $I(\eta_e)$.

In order to derive the expressions of α_k and β_k, the approximate solution given in (30) (valid in the IR only but from η_k to η_e) has to be matched with a set of solutions to the equation (27), during the contracting phase. With $a''/a = 2/\eta^2$, this set of solutions corresponds to the linear combinations of the Hankel functions of order $\nu = 3/2$:

$$v_k^{\rm C}(\eta) = \sqrt{-k\eta}[A_k H_{3/2}(-k\eta) + B_k H^{\star}_{3/2}(-k\eta)], \quad (33)$$

where the superscript "C" recalls that (33) is valid only during the contracting phase. In order to specify A_k and B_k we match (33) with the Minkowski vacuum in the remote past, i.e., $v_k(\eta \to -\infty) = e^{-ik\eta}/\sqrt{2k}$. This requirement leads to

$$A_k = \sqrt{\frac{\pi}{4k}} \quad \text{and} \quad B_k = 0, \quad (34)$$

up to a phase which has no importance here.[3] A set of solutions valid in the range $-\infty < \eta < \eta_A$, and corresponding to the Minkowski vacuum, is thus

$$v_k^{\rm C}(\eta) = \frac{1}{2}\sqrt{-\pi\eta}H_{3/2}(-k\eta). \quad (35)$$

Since $\eta_k \ll \eta_{\rm A}$ for infrared modes, the IR limit of (35) has to coincide with (30) in the interval $\eta_k \lesssim \eta \lesssim \eta_{\rm A}$. At a given η in this interval, we calculate the asymptotic limit of the Hankel function when $k \to 0$. This leads to

$$\lim_{k\to 0} v_k^{\rm C}(\eta) = \frac{i}{\sqrt{2}k^{3/2}\eta} + \mathcal{O}(k^{3/2}). \quad (36)$$

The term of order $\mathcal{O}(k^{3/2})$ has a time dependence given by $a(\eta) \propto \eta^2$, and corresponds to the term proportional to α_k in (30).

Eventually, we have to match (36) with the explicit expression of (30) that one obtains with $a(\eta) = \lambda_0\eta^2$ and $\eta_\star = -\infty$:

$$v_k^{\rm IR}(\eta) = \alpha_k\lambda_0\eta^2 - \frac{\beta_k}{3\lambda_0\eta}. \quad (37)$$

By comparing (37) with (36), one finds

$$\alpha_k = \mathcal{O}(k^{3/2}) \quad \text{and} \quad \beta_k = (3i/\sqrt{2})\lambda_0 k^{-3/2}. \quad (38)$$

[3]This also fits with the appropriate Wronskian condition as required for the quantization *à la* Fock of the tensor perturbations field.

For infrared modes the contribution of α_k is negligible, so that (31) simplifies to

$$\mathcal{P}_{\rm T}(k)^{\rm IR} = \frac{144G}{\pi}\lambda_0^2|I(\eta_{\rm e})|^2. \quad (39)$$

Therefore, in the IR limit we expect the power spectrum to be *scale invariant* (at least at the order of validity of our approximations).

The amplitude of the power spectrum in the IR regime is obtained by evaluating the integral $I(\eta_{\rm e}) = \int_{-\infty}^{\eta_{\rm e}} d\eta/a^2$. In order to do this, we split the integral into three parts

$$I(\eta_{\rm e}) = I(-\infty, \eta_{\rm A}) + I(\eta_{\rm A}, \eta_{\rm i}) + I(\eta_{\rm i}, \eta_{\rm e}). \quad (40)$$

The first part corresponds to the contracting phase, the second part corresponds to the bouncing phase, and the last part gives the contribution of the inflationary phase. With $a(\eta) = \lambda_0\eta^2$ during the contracting phase, and recalling that $\eta_{\rm A} = -[6/(m\lambda_0)]^{1/3}$, the first part of the integral is easy to compute:

$$I(-\infty, \eta_{\rm A}) = \frac{m}{18\lambda_0}. \quad (41)$$

The second part of the integral is first written in cosmic time, $I(\eta_{\rm A}, \eta_{\rm i}) = \int_{t_{\rm A}}^{t_{\rm i}} a(t)^{-3}dt$. During the bouncing phase we have found that $a = a_{\rm B}|y|^{-\frac{1}{3}}$. Then, with $y = \dot{x}/m$, the integrand is proportional to $\dot{x}$ and the integral itself is proportional to the difference $|x_{\rm i} - x_{\rm A}|$ [which is given in Eq. (20)]. Eventually, one gets

$$I(\eta_{\rm A}, \eta_{\rm i}) = -\frac{m}{18\lambda_0}\frac{1}{|\cos\theta_{\rm A}|}\ln\left(\frac{1}{2}\Gamma\sqrt{\frac{|\cos\theta_{\rm A}|}{f}}\right). \quad (42)$$

The last part of the integral corresponds to the slow-roll inflation as obtained from a massive scalar field. The calculations are well known in this case, leading to

$$I(\eta_{\rm i}, \eta_{\rm e}) = \left(\frac{1}{3a_{\rm i}^3H_{\rm i}} - \frac{1}{3a_{\rm e}^3H_{\rm e}}\right)[1 + \mathcal{O}(\epsilon_{\rm H})], \quad (43)$$

where $\epsilon_{\rm H} \equiv -\dot{H}/H^2$ is the slow-roll parameter which remains small in comparison to unity (except in the neighborhood of $t_{\rm e}$). It will be neglected in the forthcoming calculations. During slow-roll inflation, the Hubble parameter decreases linearly with cosmic time while the scale factor grows exponentially. The second term, $1/(a_{\rm e}^3H_{\rm e})$, can be safely neglected as it is suppressed by a factor $\sim\exp(-3N_{\rm e})$, where $N_{\rm e}$ denotes the number of e-folds from $\eta_{\rm i}$ to $\eta_{\rm e}$. This also means that the detailed dynamic of inflation is not needed here, since its contribution is rapidly negligible after a few e-folds. With the expressions of $a_{\rm i}$ and $H_{\rm i}$ given in (23), $I(\eta_{\rm i}, \eta_{\rm e})$ evaluates to

$$I(\eta_{\rm i},\eta_{\rm e}) = \frac{m}{12\sqrt{3}\lambda_0}\frac{\Gamma}{|x_{\rm i}\cos\theta_{\rm A}|}, \tag{44}$$

with x_i given in (20).

Gathering the results (41), (42) and (44), the integral $I(\eta_{\rm e})$ can be written as $I(\eta_{\rm e}) = \frac{m}{18\lambda_0}(1+\mathcal{I}+\mathcal{J})$, so that the IR limit of the power spectrum (39) reads

$$\mathcal{P}_{\rm T}(k)^{\rm IR} = \frac{4G}{9\pi}m^2|1+\mathcal{I}+\mathcal{J}|^2, \tag{45}$$

where

$$\mathcal{I} \equiv -\frac{1}{|\cos\theta_{\rm A}|}\ln\left(\frac{1}{2}\Gamma\sqrt{\frac{|\cos\theta_{\rm A}|}{f}}\right), \tag{46}$$

$$\mathcal{J} \equiv \frac{\Gamma\sqrt{3}}{2|x_{\rm i}\cos\theta_{\rm A}|}. \tag{47}$$

In general, $\mathcal{J}$ is much smaller than $\mathcal{I}$, suggesting that the contribution to the amplitude of the spectrum in the IR that corresponds to inflation is negligible (for instance with $\cos\theta_{\rm A}=1$ and $\Gamma = 2\times10^{-7}$, one gets $\mathcal{J}/\mathcal{I}\simeq 0.002$).

The scale-invariance of the IR limit of the spectrum is a direct consequence of the fact that the infrared modes crossed the effective potential, a''/a, during the contracting phase whose dynamics is equivalent to that of a dust-like matter dominated era. No further assumption on the detailed dynamics of the bounce is needed to get the scale invariance (though the detailed dynamics is needed to get the amplitude of the power spectrum). The amplitude only depends on three parameters: the critical energy density, the mass of the scalar field, and the phase $\theta_{\rm A}$, between $x = m\phi/\sqrt{2\rho_{\rm c}}$ and $y = \dot{\phi}/\sqrt{2\rho_{\rm c}}$ at the start of the bouncing phase. The first two parameters are fundamental. The phase $\theta_{\rm A}$ depends on θ_0 which is a contingent parameter whose value sets the initial conditions (see [17] for a more detailed discussion). The case $\cos\theta_{\rm A}\ll 1$ may appear problematic (as it would lead to a divergent power spectrum), however in this case the dynamic of the background would be different (with *deflation* before the bounce) and our analytical results would not be valid.

C. Calculation of the UV limit

1. Definition of the UV regime

By definition, the ultraviolet modes have remained well inside the Hubble radius until the phase of slow-roll inflation. They are insensitive to the background curvature during the contracting and the bouncing phase. The effective potential a''/a can be written in terms of the Hubble parameter and its time derivative as $a''/a = a^2(\dot{H}+2H^2)$. During the bounce, this expression becomes

$$\frac{a''}{a} = \frac{8\pi G\rho_{\rm c}}{3}a_{\rm B}^2 y^{\frac{4}{3}}(4y^2-1). \tag{48}$$

It is clear in (48) that the effective potential reaches its maximum at the bounce, when $y=1$. This feature sets a scale, $k_{\rm UV}\equiv\max\sqrt{a''/a}$, which evaluates to

$$k_{\rm UV} = a_{\rm B}\sqrt{8\pi G\rho_{\rm c}}. \tag{49}$$

All modes with a wave number larger than $k_{\rm UV}$ crossed the potential during slow-roll inflation. The UV limit of the power spectrum is defined by the modes with a wave number $k\gg k_{\rm UV}$.

2. Primordial power spectrum in the UV regime

In the dressed metric approach, the calculation of the UV limit of the power spectrum is straightforward. As during the bouncing phase the mode functions do not feel the curvature of space-time, they are well approximated by

$$v_k^{\rm UV}(\eta) = \frac{1}{\sqrt{2k}}e^{ik\eta} \quad \text{for } \eta<\eta_{\rm i}. \tag{50}$$

Once the Universe enters inflation, the term a''/a cannot be neglected anymore and behaves as $(2+3\epsilon_{\rm H})/\eta^2$. The mode functions are now given by a linear combination of the Hankel functions of order $3/2+\epsilon_{\rm H}$. At this stage, the derivation of the primordial spectrum is simple: we have to match the Minkowski vacuum (well defined within the Hubble radius for $k\gg k_{\rm UV}$) with the mode functions commonly used in slow-roll inflation. The power spectrum in the UV regime is then given by the standard red-tilted power spectrum of slow-roll inflation (see [18–20]),

$$\mathcal{P}_{\rm T}(k)^{\rm UV} = \frac{16G}{\pi}H^2[1-2\epsilon_{\rm H}(2C+1)], \tag{51a}$$

$$\frac{{\rm d}\ln\mathcal{P}_{\rm T}(k)^{\rm UV}}{{\rm d}\ln k} = -2\epsilon_{\rm H}, \tag{51b}$$

where H is the Hubble parameter evaluated when $k=aH$, and $C\simeq -0.73$. At the order of validity of our approximation ($\Gamma\ll 1$) and neglecting $\epsilon_{\rm H}$ in the amplitude, these expressions become

$$\mathcal{P}_{\rm T}(k)^{\rm UV} = \frac{16G}{\pi}m^2\left|\frac{x_{\rm i}}{\Gamma}\right|^2, \tag{52a}$$

$$\frac{{\rm d}\ln\mathcal{P}_{\rm T}(k)^{\rm UV}}{{\rm d}\ln k} = -6\left|\frac{\Gamma}{x_{\rm i}}\right|^2, \tag{52b}$$

where $\Gamma\equiv m/\sqrt{24\pi G\rho_{\rm c}}$ and $x_{\rm i}$ is given by (20). This prediction of a slightly red tilted spectrum matches the standard inflationary model. The amplitude scales with m^2 and depends on the critical energy density in a nontrivial

way. With $\cos\theta_{\rm A}=1$ for simplicity, one gets $\mathcal{P}_{\rm T}(k)^{\rm UV}\propto m^2\ln^2(m/\sqrt{G\rho_{\rm c}})$. Moreover, with the standard value $\Gamma=2\times10^{-7}$ we find that the spectral index at the start of inflation, given by (52b), is $n_{\rm T}-1\simeq-0.007$.

IV. POWER SPECTRUM IN THE DEFORMED ALGEBRA APPROACH

A. The deformed algebra approach

The calculations presented above can be extended to the case of the tensor power spectrum in the deformed algebra approach [10–14]. The equation of motion for the mode functions of the Mukhanov-Sasaki variables also takes the form of a Schrödinger equation. However, the frequency term is time-dependent and the effective potential is different:

$$v_k''(\eta)+\left(\Omega k^2-\frac{z_{\rm T}''}{z_{\rm T}}\right)v_k(\eta)=0, \tag{53}$$

where

$$\Omega\equiv1-2\frac{\rho}{\rho_{\rm c}}\quad\text{and}\quad z_{\rm T}\equiv\frac{a}{\sqrt{\Omega}}. \tag{54}$$

The region with $\Omega>0$, corresponding to $\rho<\rho_{\rm c}/2$, is Lorentzian whereas the region with $\Omega<0$, corresponding to $\rho>\rho_{\rm c}/2$, is Euclidean. Here, the mode functions are related to the amplitude of the tensor modes of the metric perturbation, h_k, via $v_k=z_{\rm T}h_k/\sqrt{32\pi G}$, so that the power spectrum is now defined as

$$\mathcal{P}_{\rm T}(k)=\frac{32Gk^3}{\pi}\left|\frac{v_k(\eta_{\rm e})}{z_{\rm T}(\eta_{\rm e})}\right|^2, \tag{55}$$

where $\eta_{\rm e}$ denotes the conformal time at the end of slow-roll inflation. Actually, this definition is equivalent to (25) because during slow-inflation $z_{\rm T}\simeq a$ (as a consequence of $\rho_{\rm i}\ll\rho_{\rm c}$).

B. Calculation of the IR limit

The IR limit is defined exactly in the same way as in the dressed metric approach. From the expression of a and ρ as functions of conformal time, one easily notices that $\Omega k^2-z_{\rm T}''/z_{\rm T}\simeq k^2-2/\eta^2+\mathcal{O}(\Gamma^2/\eta^8)$. In the contracting phase, there is therefore no noticeable difference between the deformed algebra and the dressed metric approaches. The IR limit still corresponds to modes with $k\ll k_{\rm IR}$, where $k_{\rm IR}$ is given in (29).

The calculation of the IR limit of the spectrum proceeds in the same way as for the dressed metric approach. We first write the approximate solution to (53) in the infrared regime,

$$v_k^{\rm IR}(\eta)=\alpha_k z_{\rm T}(\eta)+\beta_k z_{\rm T}(\eta)\int_{-\infty}^{\eta}\frac{d\eta'}{z_{\rm T}^2(\eta')}+\mathcal{O}(k^2), \tag{56}$$

from which the general expression of the IR limit of the power spectrum directly follows:

$$\mathcal{P}_{\rm T}(k)^{\rm IR}=\frac{32Gk^3}{\pi}\left|\alpha_k+\beta_k\int_{-\infty}^{\eta_{\rm e}}\frac{d\eta}{z_{\rm T}^2}\right|^2. \tag{57}$$

With the definition of $z_{\rm T}$, the integral on the right-hand side is simply given by the sum of $I(\eta_{\rm e})+I_\Omega(\eta_{\rm e})$, with $I(\eta_{\rm e})$ defined in (32), and

$$I_\Omega(\eta_{\rm e})\equiv-2\int_{-\infty}^{\eta_{\rm e}}\frac{\rho}{\rho_{\rm c}}\frac{d\eta}{a^2}. \tag{58}$$

As before, the two constants α_k and β_k in (57) are obtained by matching the solution (56) with a set of solutions valid for any wave number k during the contracting phase. During the contracting phase the difference between $(\Omega k^2-z_{\rm T}''/z_{\rm T})$ and (k^2-a''/a) can be neglected. Consequently, the two constants α_k and β_k take the same value as before: $\alpha_k=\mathcal{O}(k^{3/2})$ and $\beta_k=(3i/\sqrt{2})\lambda_0k^{-3/2}$. With these expressions, the IR limit of the power spectrum becomes

$$\mathcal{P}_{\rm T}(k)^{\rm IR}=\frac{144G}{\pi}\lambda_0^2|I(\eta_{\rm e})+I_\Omega(\eta_{\rm e})|^2. \tag{59}$$

Note that all the differences between the deformed algebra and the dressed metric approach are encoded in the integral $I_\Omega(\eta_{\rm e})$.

Now, we will show that $I_\Omega(\eta_{\rm e})/I(\eta_{\rm e})=\mathcal{O}(\Gamma^2)$, so that the contribution of $I_\Omega(\eta_{\rm e})$ to the IR limit of the spectrum can be neglected. First, we split the integral into three parts: $I_\Omega(\eta_{\rm e})=I_\Omega(-\infty,\eta_{\rm A})+I_\Omega(\eta_{\rm A},\eta_{\rm i})+I_\Omega(\eta_{\rm i},\eta_{\rm e})$. The proof is straightforward for the first and the third parts of the integral. Indeed, recalling that before $\eta_{\rm A}$ the energy density remains smaller than $\rho_{\rm A}=\Gamma^2\rho_{\rm c}$, we have

$$I_\Omega(-\infty,\eta_{\rm A})\equiv-2\int_{-\infty}^{\eta_{\rm A}}\frac{\rho}{\rho_{\rm c}}\frac{d\eta}{a^2}\le-2\Gamma^2I(-\infty,\eta_{\rm A}). \tag{60}$$

The same holds for $I_\Omega(\eta_{\rm i},\eta_{\rm e})$, with $\rho_{\rm i}$ instead of $\rho_{\rm A}$. The remaining part of the integral is

$$I_\Omega(\eta_{\rm A},\eta_{\rm i})\equiv-2\int_{\eta_{\rm A}}^{\eta_{\rm i}}\frac{\rho}{\rho_{\rm c}}\frac{d\eta}{a^2}. \tag{61}$$

During the bouncing phase, $\rho=\rho_{\rm c}y^2$ and $a=a_{\rm B}|y|^{-\frac{1}{3}}$ so when we switch to cosmic time, the integral becomes

$$I_\Omega(\eta_{\rm A},\eta_{\rm i})=-(2/a_{\rm B}^2)\int_{t_{\rm A}}^{t_{\rm i}}|y(t)|^3dt. \tag{62}$$

The last step is to express dt in terms of dy with (14). Then the integration can be performed analytically and leads to

$$I_\Omega(\eta_A, \eta_i) = -\frac{m}{36\lambda_0}\frac{\sin^2\theta_A}{\cos\theta_A}\Gamma^2. \tag{63}$$

Therefore, at order $\mathcal{O}(\Gamma^2)$, we predict no difference for the IR limits of the power spectra in both approaches. The IR limit of the power spectrum in the deformed algebra approach is still given by (45).

C. Calculation of the UV limit

The UV limit of the power spectrum in the deformed algebra approach has already been discussed in [21], here we recall the conclusion of this previous work. Thanks to numerical integrations for the equation of motion as well as Wentzel-Kramers-Brillouin (WKB) based arguments, it is shown that the primordial power spectrum exponentially grows with the wave number k, for large values of k. Actually, oscillations are still superimposed to this exponential envelope. During the bouncing phase, the term z_T''/z_T reaches a maximum $|z_T''/z_T|_{t_B} = 40\pi G\rho_c$. This means that for modes such that $k^2 \gg 40\pi G\rho_c$, the time-dependent frequency in the equation of motion, $\Omega k^2 - z_T''/z_T$, is dominated by Ωk^2 during most of the cosmic history prior to inflation. The Euclidean phase around the bounce, $\Omega < 0$, leads to an instability in the equation of motion so the amplitude of tensor modes receives a real exponential contribution, i.e., $v_{k\to\infty} \propto \exp(k \times \int_{\Delta\eta}\sqrt{|\Omega|}d\eta)$, where the integration is performed over the interval $\Delta\eta$ corresponding to the Euclidean phase.

V. POWER SPECTRUM AT ALL SCALES: NUMERICAL RESULTS

Deriving the primordial power spectrum for tensor modes at all scales requires a numerical integration of *both* the equation of motion of the mode functions [(27) or (53) depending on the approach] *and* the equations of motion for the background [gathered in the system of equations (4)]. The numerical integration is performed starting in the contracting phase, when $\rho_0/\rho_c \ll \Gamma^2$. For the background, the initial conditions are set by choosing the value of θ_0, the initial phase between the share of potential energy and kinetic energy in the total energy density. For the perturbations, the initial conditions are set during the contracting phase when the modes are well inside the horizon. The initial state of the perturbation can then be identified with the usual Minkowski vacuum.

The detailed dynamics of the background (e.g., the value of x at the bounce, or the number of e-folds during inflation) and subsequently the detailed shape of $\mathcal{P}_T(k)$, are fully determined by two types of parameters: the mass of the scalar field and the critical energy density on one hand, and the phase θ_0 on the other hand.

The mass of the scalar field and the critical energy density can be seen as fundamental constants of the model. Though their values are not known, some particular values are favored by CMB observations and theoretical considerations. Even if the details of the calculation using the minimal area gap of LQG still need clarification, some dimensional arguments lead to believe that the value of ρ_c should not be far from the Planck scale. Note that ρ_c is the only parameter linked to LQG (via its dependence on the Immirzi parameter, γ). The value commonly accepted is $\rho_c = 0.41 m_{Pl}^4$, and we shall use it as the standard choice in our numerical simulation. The value of the mass of the scalar field, as deduced from the CMB observations, is generally chosen to be $m \simeq 1.2 \times 10^{-6} m_{Pl}$ [22].

The parameter θ_0 has a different status since it is totally *contingent*. Its value can vary between 0 and 2π (actually the range $0 < \theta_0 < \pi$ is enough as the equations remain unchanged under the transformation $\theta_0 \to \theta_0 + \pi$). As underlined in [17], most of the values of θ_0 lead to a universe with a phase of inflation shortly after the bounce (and no deflation before the bounce). We have restricted ourselves to these kinds of solutions since they are the most probable, and are more in line with our current knowledge of the cosmic history (believed to have undergone a phase of primordial inflation).

Qualitatively, we can already anticipate the global shape of the primordial power spectrum. Irrespective of any approach, its shape is driven by the background evolution through the functions a and Ω (in the deformed algebra approach) and their time derivatives. Our analysis is restricted to the wide range of cosmic histories that split into three main eras: a classical (dust-like) contracting phase, a bouncing phase where quantum effects are significant, and a classical inflationary phase. We anticipate the shape of the primordial power spectrum to be *qualitatively* unaffected by the values of m, ρ_c, and θ_0. (Obviously, the precise values of these parameters will affect the scales and amplitudes involved in the spectrum at a *quantitative* level). We can also anticipate three regimes in the power spectra, corresponding to: the modes that have left the horizon during the contracting phase (large scales); the modes that have left the horizon during the bouncing phase (intermediate scales); the modes that have remained within the horizon until the start of the inflationary phase (small scales). For the large and small scales, we should recover the IR and UV limit derived analytically in the previous sections.

In the next three sections we present the primordial power spectra obtained within each approach. We study the influence of the three parameters, m, ρ_c, and θ_0. For each varying parameter, we present the primordial power spectra as predicted by each approach, thus facilitating the comparison.

We use Planck units hereafter, with the following definition of the Planck mass, $m_{Pl} = 1/\sqrt{G}$. For simplicity,

we normalize the scale factor at the time of the bounce, setting $a_B = 1$. The power spectra are depicted as functions of the comoving wave number k.

A. Varying the mass of the scalar field

The primordial power spectrum for different values of the mass of the scalar field is presented in Fig. 1. The upper panel corresponds to the dressed metric approach and the lower panel to the deformed algebra approach. The mass takes three different values: $m = 10^{-3} m_{\rm Pl}$ (triangles), $m = 10^{-2.5} m_{\rm Pl}$ (open disks), and $m = 10^{-2} m_{\rm Pl}$ (black disks). For numerical convenience, these values are larger than the preferred value. However, the results can be extrapolated and the associated phenomenology shall be studied with values closer to $10^{-6} m_{\rm Pl}$ [23]. The critical energy density is set equal to $0.41 m_{\rm Pl}^4$ and $\cos\theta_A \simeq 1$.

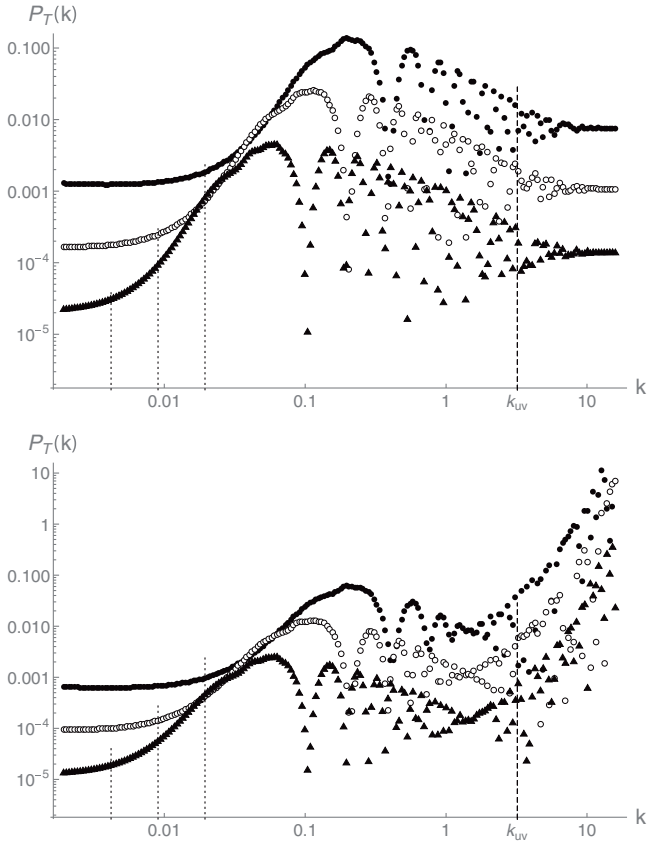

FIG. 1. Primordial power spectra for tensor modes in the dressed metric approach (upper panel) and in the deformed algebra approach (lower panel) for different values of the mass of the scalar field. The critical energy density is $\rho_c = 0.41 m_{\rm Pl}^4$ and $\cos\theta_A \simeq 1$. The mass of the scalar field takes three values: $m = 10^{-3} m_{\rm Pl}$ (triangles), $m = 10^{-2.5} m_{\rm Pl}$ (open disks), and $m = 10^{-2} m_{\rm Pl}$ (black disks). The dashed vertical line at large k, corresponds to $k_{\rm UV}$ (which does not depend on m). The dotted vertical lines at smaller k correspond to $k_{\rm IR}$ (which scales as $m^{2/3}$).

In the dressed metric approach (upper panel of Fig. 1), there are three regimes in the primordial power spectrum:

(i) At the largest scales, for $k < k_{\rm IR}$ with

$$k_{\rm IR} = \frac{1}{3\sqrt{2}} \left(\frac{m^2 \sqrt{24\pi G \rho_c}}{|\cos\theta_A|} \right)^{1/3},$$

the power spectrum is scale invariant in agreement with the analytical calculations of Sec. III. This corresponds to modes that were amplified mainly during the classical contracting phase. In Fig. 1, the scale corresponding to $k_{\rm IR}$ is depicted with vertical dotted lines. At this scale, there is a transition in the numerical results that is in perfect agreement with the analytical formula (especially its $m^{2/3}$ dependence). Moreover, it is clear on the figure that the numerical IR limit of the spectrum behaves as m^2, again in perfect agreement with (45).

(ii) For intermediate scales, such that $k_{\rm IR} < k < k_{\rm UV}$, with

$$k_{\rm UV} = \sqrt{8\pi G \rho_c},$$

the amplitude of the power spectrum is oscillating. This part of the spectrum corresponds to modes that were amplified during the bouncing phase. The first peak corresponds to a maximum of the power spectrum, that reaches $100 \times \mathcal{P}_T^{\rm IR}$ approximately. Then, the amplitude of the oscillations is damped for increasing values of the wave number. Intuitively, these oscillations can be understood as due to quasi-bound states in the effective Schrödinger equation. The second transition scale, $k_{\rm UV}$, is depicted in Fig. 1 as a vertical dashed line and is in agreement with the transition scale found numerically.

(iii) At the smallest scales, $k > k_{\rm UV}$, the power spectrum is a power law with a slightly red spectral index, just as predicted by the standard inflationary paradigm. This part of the power spectrum corresponds to modes that have remained inside the horizon until the start of the inflationary phase. The numerical results are in agreement with the UV limit derived analytically in Sec. III, see Fig. 3.

In the deformed algebra approach the primordial tensor power spectrum also features three different regimes (see the lower panel of Fig. 1). The first two regions (i.e., the large scales, $k < k_{\rm IR}$, and the intermediate scales, $k_{\rm IR} < k < k_{\rm UV}$), are almost identical to the power spectrum derived in the dressed metric approach. The scale-dependence of the power spectrum and the transition scales are the same. This is because the impact of Ω is subdominant for these modes. However, within these two regions the numerical results suggest that for $k < k_{\rm UV}$ the amplitude of the spectrum in the deformed algebra approach is slightly smaller than in the dressed metric approach (by less

than a factor 2). (This feature could not be explained by our analytics.)

At smaller scales, $k > k_{\mathrm{UV}}$, the primordial power spectrum in the deformed algebra approach strongly differs from the one predicted by the dressed metric approach. As already suggested by our analytical considerations (see Sec. IV), the power spectrum is exponentially increasing with the wave number (as a result of the instability generated by Ω which is negative-valued around the bounce), with superimposed oscillations. Note that the numerical results confirm once again that the scale defining the transition between the intermediate scales (oscillations) and the large scales (exponential growth) does not depend on m.

The UV behavior of the spectrum clearly raises questions. The first one is related to the fundamentally trans-Planckian nature of these modes. As demonstrated in [6], this is not a problem when considering the appropriate length operator in loop quantum gravity. A more serious issue is related to the use of the perturbation theory when the spectrum increases exponentially. Obviously, back-reaction should be taken into account in this regime and the results shown here are not fully reliable anymore. They just give a general trend and not the accurate shape of the spectrum. However, we believe that this is basically enough for the phenomenological purposes we are interested in. The most interesting region, that is the oscillatory one, is under control and the C_ℓ CMB spectrum can be safely calculated [23]. If the observational window of wave number was to fall on the exponentially rising part, this would anyway lead to a situation incompatible with data (as the tensor to scalar ratio is small). The perturbation theory breaks at a level where tensor modes are anyway excluded by current data.

B. Varying the critical energy density

The critical energy density depends on the Immirzi parameter, a fundamental parameter in LQG, whose value is traditionally deduced from a calculation of the black holes entropy. Nonetheless, it has been recently argued [24] that the formula for the entropy of black holes can be recovered, in the framework of LQG, without specifying the value of the Immirzi parameter. Recently, a quasi-local description of a black hole [25] was indeed shown to allow one to recover at the semiclassical limit the expected thermodynamical behaviors of a black hole for all values of γ [26], assuming the existence of a nontrivial chemical potential conjugate to the number of horizon punctures. A detailed microscopic mechanism was also put forward in [27] and [28] where the area degeneracy was analytically continued from real γ to complex γ and evaluated at the complex values $\gamma = \pm i$. This motivates us to consider other values for the critical energy density and discuss how it can affect the primordial tensor power spectrum.

In Fig. 2, we show the primordial tensor power spectra for different values of ρ_{c}. Here, the mass of the scalar field is set equal to $m = 10^{-3} m_{\mathrm{Pl}}$, and $\cos\theta_{\mathrm{A}} \simeq 1$. The upper panel corresponds to the dressed metric approach and the lower panel to the deformed algebra approach. The different values of the critical energy density are $\rho_{\mathrm{c}} = 0.0041 m_{\mathrm{Pl}}^4$ (triangles), $\rho_{\mathrm{c}} = 0.041 m_{\mathrm{Pl}}^4$ (open disks), and $\rho_{\mathrm{c}} = 0.41 m_{\mathrm{Pl}}^4$ (black disks) which is the theoretically favored value.

The global shape of the primordial power spectrum is recovered for both approaches, with three different regions. The positions of the transition scales, k_{IR} and k_{UV}, clearly depend on ρ_{c} irrespectively of the approach. The IR transition scale, k_{IR}, mildly decreases for smaller values of ρ_{c}, in agreement with the analytical calculations that led to $k_{\mathrm{IR}} \propto (G\rho_{\mathrm{c}})^{1/6}$. The UV transition scale, k_{UV}, is more strongly dependent on the value of the critical energy density, also in agreement with the scaling derived analytically, $k_{\mathrm{UV}} \propto \sqrt{G\rho_{\mathrm{c}}}$.

For the dressed metric approach, a decrease of ρ_{c} yields a slight decrease of the amplitude of the primordial power

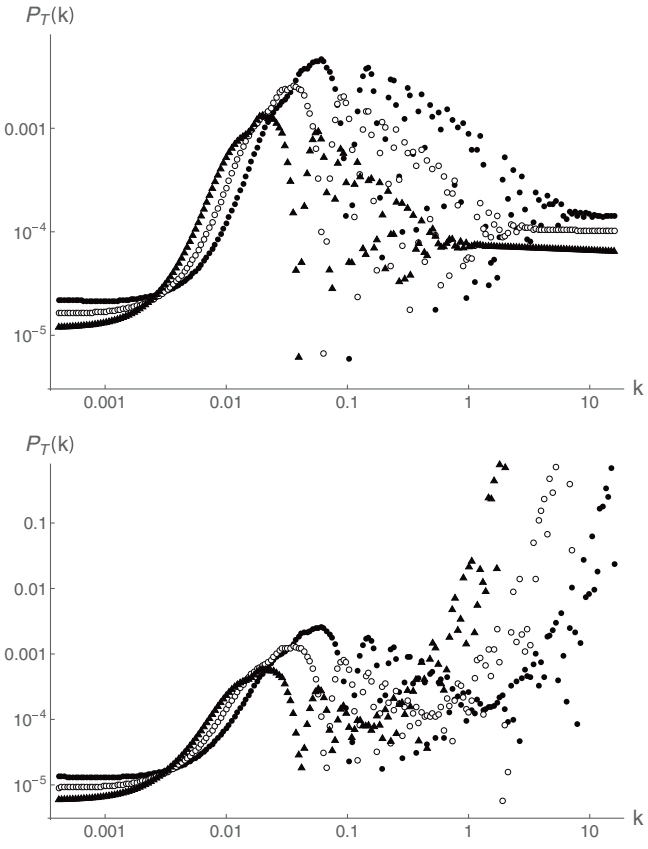

FIG. 2. Primordial power spectra for the tensor modes in the dressed metric approach (upper panel) and in the deformed algebra approach (lower panel) for different values of ρ_{c}. The mass of the scalar field is $m = 10^{-3} m_{\mathrm{Pl}}$ and $\cos\theta_{\mathrm{A}} \simeq 1$. The critical energy density is $\rho_{\mathrm{c}} = 0.0041 m_{\mathrm{Pl}}^4$ (triangles), $\rho_{\mathrm{c}} = 0.041 m_{\mathrm{Pl}}^4$ (open disks) and $\rho_{\mathrm{c}} = 0.41 m_{\mathrm{Pl}}^4$ (black disks).

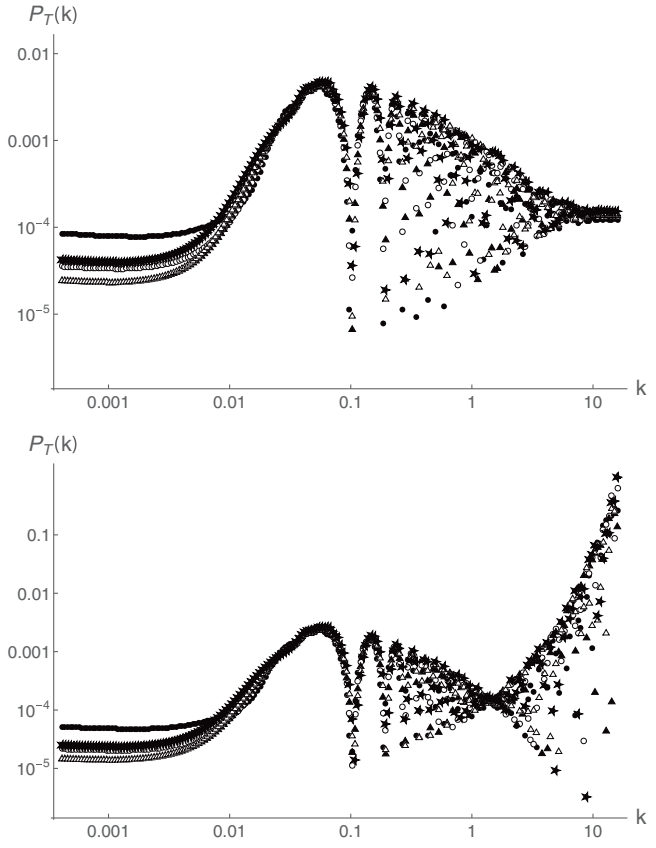

FIG. 3. Primordial power spectra for the tensor modes in the dressed metric approach (upper panel), and in the deformed algebra approach (lower panel). The parameter θ_0 varies from $(\pi/2-1) \simeq 0.18 \times \pi$ to $(\pi/2+1) \simeq 0.81 \times \pi$. The exact values are: plain disks for $\theta_0 = (\pi/2-1)$, open disks for $\theta_0 = (\pi/2-1/2)$, plain triangles for $\theta_0 = \pi/2$, open triangles for $\theta_0 = (\pi/2+1/2)$, and plain stars for $\theta_0 = (\pi/2+1)$. The mass of the field is $m = 10^{-3} m_{\rm Pl}$, and the critical energy density is $\rho_{\rm c} = 0.41 m_{\rm Pl}^4$.

spectrum at *all* scales. This feature is also suggested by the analytical results, as both formulas for the UV and IR limits depend on the critical energy density as $\sim \ln^2(m/\sqrt{G\rho_{\rm c}})$.

For the deformed algebra approach, a decrease of $\rho_{\rm c}$ leads to a slight decrease of the amplitude of the spectrum at large and intermediate scales as in the dressed metric approach. At smaller scales, $k > k_{\rm UV}$, the smallest value of $\rho_{\rm c}$ corresponds to the fastest divergence of the spectrum. Analytically, we expect this divergence to scale as $\propto \exp(k \int_{\Delta\eta} \sqrt{|\Omega|} d\eta)$, where the interval $\Delta\eta$ corresponds to the euclidean phase. Therefore we can define the rate of growth of the spectrum in the UV as $k_\Omega \equiv 1/\int_{\Delta\eta} \sqrt{|\Omega|} d\eta$. The integral can be computed, leading to

$$k_\Omega \simeq 0.8 \sqrt{24\pi G \rho_{\rm c}}. \tag{64}$$

So, small values of the critical energy density indeed correspond to a quicker divergence of the power spectrum in the UV.

C. Dependence on θ_0

The primordial power spectra for different choices of θ_0 are shown in Fig. 3, in the dressed metric approach (upper panel) and in the deformed algebra approach (lower panel). The mass of the scalar field is $m = 10^{-3} m_{\rm Pl}$, and the critical energy density is $\rho_{\rm c} = 0.41 m_{\rm Pl}^4$. We chose five values of θ_0, equally spaced between $(\pi/2-1)$ and $(\pi/2+1)$, ensuring that the background goes through a phase of inflation after the bounce. In the numerical simulations we have always set $\alpha = 17\pi/4 + 1$, so that $\cos\theta_{\rm A} = 0$ (with $\theta_{\rm A} = 2(\alpha-1) + \theta_0$) corresponds to $\theta_0 = 0$ and α is significantly larger than one.

The main impact of θ_0 is in the IR regime. Both the infrared transition scale $k_{\rm IR}$ (varying as $\sim |\cos(\theta_{\rm A})|^{-1/3}$) and the amplitude of the IR limit of the spectrum are significantly depending on θ_0. This is true in both approaches. At intermediate and smaller scales, the power spectra are nearly independent of the choice of θ_0, again irrespective of the considered approach. The numerical results confirm that the ultraviolet transition scale $k_{\rm UV}$ is independent of θ_0. Moreover, in the deformed algebra approach the growth rate of the spectrum in the UV appears to be independent on θ_0 too, in agreement with (64).

In order to highlight the dependence of the IR limit as a function of θ_0, Fig. 4 shows this limit in both approaches and for different choices of θ_0, with $m = 10^{-3} m_{\rm Pl}$, and

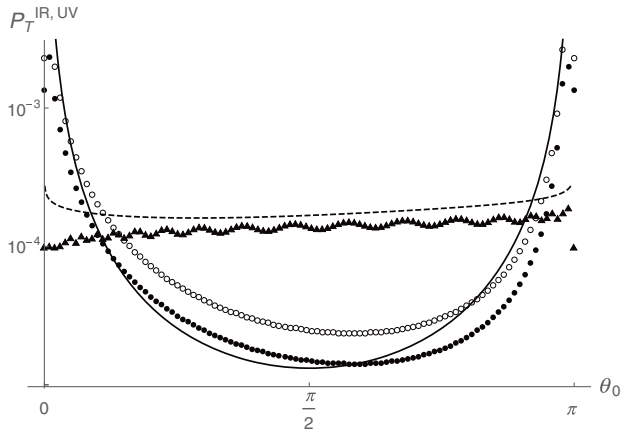

FIG. 4. The infrared limit (disks) and the ultraviolet limit (triangles) of the primordial power spectrum as a function of θ_0. The solid black curve corresponds to the analytical calculations for $\mathcal{P}_{\rm T}^{\rm IR}$, see (45). The IR limit from a numerical simulation is displayed with open disks for the dressed metric approach, and black disks in the deformed algebra approach. The dashed black curve stands for the analytical UV limit in the dressed metric approach, see (52a). The UV limit in the dressed metric approach, as derived from the numerics, corresponds to the black triangles. The mass of the scalar field is $m = 10^{-3} m_{\rm Pl}$, and the critical energy density is $\rho_{\rm c} = 0.41 m_{\rm Pl}^4$.

$\rho_c = 0.41 m_{\rm Pl}^4$. The solid black curve corresponds to the analytical calculation for $\mathcal{P}_{\rm T}^{\rm IR}$, see (45). This analytical curve is valid for both the dressed metric and the deformed algebra approaches at first order in $\Gamma \equiv m/\sqrt{24\pi G\rho_c}$. The numerical derivation of the IR limit is displayed as open disks for the dressed metric approach, and as black disks in the deformed algebra approach. We observe a fairly good agreement between analytical and numerical results. Although there are some differences in the amplitude of the IR limit,[4] the behavior as a function of θ_0 is consistent between the analytics and the numerics. This shows that $\mathcal{P}_{\rm T}^{\rm IR}$ strongly depends on θ_0, the former varying by more than one order of magnitude from its minimal value at $\theta_0 = \pi/2$ (thus giving $\cos\theta_{\rm A} = 1$), to its maximal value reached when θ_0 tends to 0 or π.

In the restricted case of the dressed metric approach, the UV limit as a function of θ_0 is also displayed in Fig. 4. The dashed black curve stands for the analytical calculation presented in (52a). The UV limit obtained from the numerical simulation is displayed with triangles. A good agreement is also observed here. Nonetheless, the remaining difference between the analytical and numerical results certainly comes from the approximations involved in the determination of $x_{\rm i}$, on which the UV limit depend.

VI. CONCLUSION AND DISCUSSION

In this work, we have compared the dressed metric and deformed algebra approaches to loop quantum cosmology. In order to compare them efficiently, we have set the initial conditions in the same way for both approaches (in the remote past of the classical contracting branch). This is consistent and arguably the most obvious choice if the word *initial* is to be taken literally. It is however fair to mention that this is not the only choice one could have made. As far as the dressed metric approach is concerned, the authors who developed the strategy have preferred to set the initial conditions at the bounce [6–8]. Then the initial state for tensor perturbations is given by a 4th-order WKB vacuum defined for $k \geq k_{\rm UV}$. In fact, their results seem to be very similar to ours (for the range of scales covered by both choices of initial conditions). As far as the deformed algebra approach is concerned, it should be underlined that it is also possible to set initial conditions at the surface of signature change. This has been investigated in [29] and leads to a different spectrum. If these issues are left for future considerations and if we focus on the comparison with similar initial conditions, several important conclusions can already be drawn.

First, it is remarkable that for both approaches the IR limit is the same and basically agrees with the prediction of standard general relativity. Therefore at the largest scales, the primordial tensor power spectrum cannot be used to probe quantum gravity (at least in this setting).

Second, there is a strong difference between the approaches in the ultraviolet regime. Whereas the dressed metric simply leads to the slightly red-tilted power spectrum, as predicted in standard inflationary cosmology, the deformed algebra leads to an exponentially increasing spectrum (modulated by oscillations).

Third, at intermediate scales, a very interesting behavior appears. Not only because it is substantially different from the predictions of the standard inflationary models but also because both predictions are in agreement with each other. This region seems to exhibit a *universal LQC effect* that has been searched for during the last decade. In addition, the phase of the oscillations that appear at these intermediate scales, does *not* depend on the unknown (and fundamentally random) phase parameter, θ_0. This opens an interesting avenue in the perspective of testing the predictions of effective LQC.

In the future, this work should be extended in two directions. One is to consider not only the tensor modes, that have not yet been observed, but also the well-known scalar modes. The relevant equations have already been derived for the dressed metric approach but are still to be investigated into more details in the deformed algebra approach. The reason for this difficulty is related to divergences (at the bounce and at the change of signature) that should be regularized. The difficulty is however more technical than conceptual and should be solved soon.

The second path to follow is naturally to go more deeply into the phenomenology of this comparison and calculate the corresponding cosmic microwave background C_ℓ spectra which are already constrained by observations. Two main tasks will have to be pursued. The first is related to the number of e-folds that the Universe underwent since the bounce. This number depends, among other parameters, on θ_0 and on the reheating temperature. Once the number of e-folds since the bounce will be specified, the range of wave numbers considered in this study that falls within our observable window will be completely determined. The second important task is to investigate how the oscillations at intermediate scales shall be washed out by the transfer phenomena that occur between the end of inflation and the decoupling.

[4]The discrepancy is not surprising. First of all, the analytic result is based on some approximations for the time dependence of a and Ω. Second, the numerical evaluation of $\mathcal{P}_{\rm T}^{\rm IR}$ cannot be exactly obtained for $k = 0$ since this would require to start the numerical integration at $\eta \to -\infty$ which is unfeasible. We believe that these features are at the origin of the disagreement between the numerics and the analytics.

ACKNOWLEDGMENTS

L.S. is supported by the Labex ENIGMASS, initiative d'excellence.

[1] P. Dona and S. Speziale, arXiv:1007.0402V1; A. Perez, arXiv:gr-qc/0409061v3; R. Gambini and J. Pullin, *A First Course in Loop Quantum Gravity* (Oxford University Press, New York, 2011); C. Rovelli, Living Rev. Relativity **1**, 1 (1998); *Quantum Gravity* (Cambridge University Press, Cambridge, England, 2004); *Proc. Sci.*, QGQGS2011 (2011) 003 [arXiv:1102.3660v5]; C. Rovelli and F. Vidotto, *Covariant Loop Quantum Gravity* (Cambridge University Press, Cambridge, England, 2014); L. Smolin, arXiv:hep-th/0408048v3; T. Thiemann, Lect. Notes Phys. **631**, 41 (2003); *Modern Canonical Quantum General Relativity* (Cambridge University Press, Cambridge, England, 2007).

[2] A. Ashtekar, M. Bojowald, and J. Lewandowski, Adv. Theor. Math. Phys. **7**, 233 (2003); A. Ashtekar, Gen. Relativ. Gravit. **41**, 707 (2009); A. Ashtekar and P. Singh, Classical Quantum Gravity **28**, 213001 (2011); M. Bojowald, Living Rev. Relativity **11**, 4 (2008); Classical Quantum Gravity **29**, 213001 (2012); K. Banerjee, G. Calcagni, and M. Martin-Benito, SIGMA **8**, 016 (2012); G. Calcagni, Ann. Phys. (Berlin) **525**, 323 (2013); I. Agullo and A. Corichi, in *The Springer Handbook of Spacetime*, edited by A. Ashtekar and V. Petkov (Springer-Verlag, Berlin, 2015); A. Barrau, T. Cailleteau, J. Grain, and J. Mielczarek, Classical Quantum Gravity **31**, 053001 (2014); A. Barrau and J. Grain, arXiv:1410.1714.

[3] A. Ashtekar and M. Campuglia, Classical Quantum Gravity **29**, 242001 (2012).

[4] T. Thiemann, Classical Quantum Gravity **15**, 839 (1998); C. Rovelli and L. Smolin, Phys. Rev. Lett. **72**, 446 (1994).

[5] T. Thiemann, Classical Quantum Gravity **15**, 1281 (1998).

[6] I. Agullo, A. Ashtekar, and W. Nelson, Phys. Rev. Lett. **109**, 251301 (2012).

[7] I. Agullo, A. Ashtekar, and W. Nelson, Phys. Rev. D **87**, 043507 (2013).

[8] I. Agullo, A. Ashtekar, and W. Nelson, Classical Quantum Gravity **30**, 085014 (2013).

[9] A. Ashtekar, W. Kaminski, and J. Lewandowski, Phys. Rev. D **79**, 064030 (2009).

[10] M. Bojowald, G. M. Hossain, M. Kagan, and S. Shankaranarayanan, Phys. Rev. D **78**, 063547 (2008).

[11] J. Mielczarek, T. Cailleteau, A. Barrau, and J. Grain, Classical Quantum Gravity **29**, 085009 (2012).

[12] T. Cailleteau, J. Mielczarek, A. Barrau, and J. Grain, Classical Quantum Gravity **29**, 095010 (2012).

[13] T. Cailleteau, A. Barrau, J. Grain, and F. Vidotto, Phys. Rev. D **86**, 087301 (2012).

[14] A. Barrau, M. Bojowald, G. Calcagni, J. Grain, and M. Kagan, arXiv:1404.1018.

[15] S. A. Hojman, K. Kuchar, and C. Teitelboim, Ann. Phys. (N.Y.) **96**, 88 (1976).

[16] A. Ashtekar and D. Sloan, Phys. Lett. B **694**, 108 (2010).

[17] L. Linsefors and A. Barrau, Phys. Rev. D **87**, 123509 (2013).

[18] D. Lyth and E. D. Stewart, Phys. Lett. B **302**, 171 (1993).

[19] E. D. Stewart and J.-O. Gong, Phys. Lett. B **510**, 1 (2001).

[20] J. Martin and D. Schwarz, Phys. Rev. D **62**, 103520 (2000).

[21] L. Linsefors, T. Cailleteau, A. Barrau, and J. Grain, Phys. Rev. D **87**, 107503 (2013).

[22] A. R. Liddle, P. Parsons, and J. D. Barrow, Phys. Rev. D **50**, 7222 (1994).

[23] B. Bolliet, A. Barrau, and J. Grain (to be published).

[24] E. Bianchi, arXiv:1204.5122.

[25] E. Frodden, A. Ghosh, and A. Perez, Phys. Rev. D **87**, 121503 (2013).

[26] A. Ghosh and A. Perez, Phys. Rev. Lett. **107**, 241301 (2011).

[27] E. Frodden, M. Geiller, K. Noui, and A. Perez, Europhys. Lett. **107**, 10005 (2014).

[28] J. B. Achour, A. Mouchet, and K. Noui, arXiv:1406.6021.

[29] J. Mielczarek, L. Linsefors, and A. Barrau, arXiv:1411.0272.

5.4 Initial conditions at the silent surface

If the Euclidean phase is taken seriously, it might not have any real meaning to propagate modes through the bounce. There is no time anymore and the causal structure is far from being clear at this stage: it might have completely disappeared. In this study, we therefore take another look of this same phenomenon. Starting from our current Universe, if we go backward in time, the "silent surface" (that is the surface where light cones are completely squeezed) is, in our model, reached when $\rho = \rho_c/2$. This surface is characterized by the fact that all the space points do decouple one from the other.

In this article, we assume that this silent surface is the natural "place" (or time, more accurately) where to impose the initial conditions. Indeed, the decorrelation of points naturally leads to a white noise initial spectrum. We therefore derive the equations of propagation for this spectrum itself and investigate how it can be turned into a (nearly) scale invariant power spectrum, as probed by observations.

In addition, we study the details the behavior of the $z"/z$ function entering the equation of propagation and the effect of the Ω-function now multiplying the k^2 term. We show that this changes quite substantially the usual picture, depending of the equation of state w of the barotropic fluid assumed to fill the Universe. The choice of the vacuum state is shown, depending on the valued of Ω to be highly non-trivial.

We also take this opportunity to face a well-known problem of cosmology: if the number of e-folds of inflation is slightly higher than its minimum value, then the modes that we currently see in the CMB were transplanckian before inflation. So, when going backward in time, depending on the duration of inflation, a mode will either first feel the Planckian density of the Universe, and the analysis presented here applies, or become Planckian in length and it should be treated in a appropriate manner. We deal with this issue by assuming dispersion relations that are inspired by LQC results in the sense that the generators of the Poincaré group are modified.

Finally, we investigate how successive periods of evolution with different equations of state can lead to a flat primordial spectrum without inflation. Although a solution – and even a family of solutions – is found, a high level of fine-tuning is required and it is honest to conclude that this specific hypothesis is not very convincing.

Silent initial conditions for cosmological perturbations with a change of space-time signature

Jakub Mielczarek[1,2], Linda Linsefors[3] and Aurelien Barrau[3]
1 Institute of Physics, Jagiellonian University, Łojasiewicza 11, 30-348 Cracow, Poland
2 Department of Fundamental Research, National Centre for Nuclear Research,
Hoża 69, 00-681 Warsaw, Poland
3 Laboratoire de Physique Subatomique et de Cosmologie, UJF, INPG,
CNRS, IN2P3 53, avenue des Martyrs, 38026 Grenoble cedex, France
(Dated: November 2, 2014)

Recent calculations in loop quantum cosmology suggest that a transition from a Lorentzian to an Euclidean space-time might take place in the very early Universe. The transition point leads to a state of silence, characterized by a vanishing speed of light. This behavior can be interpreted as a decoupling of different space points, similar to the one characterizing the BKL phase.

In this study, we address the issue of imposing initial conditions for the cosmological perturbations at the transition point between the Lorentzian and Euclidean phases. Motivated by the decoupling of space points, initial conditions characterized by a lack of correlations are investigated. We show that the "white noise" initial conditions are supported by the analysis of the vacuum state in the Euclidean regime adjacent to the state of silence.

Furthermore, the possibility of imposing the silent initial conditions at the trans-Planckian surface, characterized by a vanishing speed for the propagation of modes with wavelengths of the order of the Planck length, is studied. Such initial conditions might result from a loop-deformations of the Poincaré algebra. The conversion of the silent initial power spectrum to a scale-invariant one is also examined.

I. INTRODUCTION

A key issue in constructing any model describing the evolution of the Universe is the initial value problem. At the classical level, the Cauchy initial conditions have to be clearly specified. Imposed, *e.g.*, at the present epoch they allow for a (at least partial) reconstruction of the cosmic dynamics backward and forward in time. When dealing with the early Universe, the initial conditions may be also introduced *a priori* in the distant past. In this case, the consequences of a given assumption about the evolution of the Universe can be studied. In particular, the impact of the initial conditions on the properties of the inflationary stage has often been addressed. Many questions about why a given inflationary trajectory rather than another is realized in Nature remain open and the debate about the "naturalness" of inflation is going on. It is however widely believed that the answer should come from a detailed understanding of the pre-inflationary quantum era. One may hope that by taking into account the quantum aspects of gravity, some specific initial stages, leading to the proper inflationary evolution, will be naturally distinguished. An extreme example of such a state is given by the so-called Hartle-Hawking no-boundary proposal, which basically circumvent the problem of the initial conditions [1].

Recent results in loop quantum cosmology (LQC) provide a new opportunity to address the problem of initial conditions. Namely, it was shown that the signature of space-time can effectively change from Lorentzian to Euclidean at extremely high curvatures [2–4]. This effect is basically due to the requirement of anomaly freedom, that is to the necessity to have a closed algebra of quantum-corrected effective constraints when holonomy corrections from loop quantum gravity are included (the situation is less clear when inverse-triad terms are also added [5]). The beginning of the Lorentzian phase seems to be a natural place where initial conditions should be imposed. In this study, we follow this idea and investigate a possible choice of initial conditions on –or around– this surface. We address this issue in the case of cosmological perturbations.

In the considered model, the transition between the Lorentzian stage and the Euclidean stage is taking place at the energy density (see, *e.g.* [6])

$$\rho = \frac{\rho_c}{2}, \tag{1}$$

where ρ_c is the maximal allowed value of the energy density. In loop quantum cosmology, the value of ρ_c, reached at the bounce, is usually assumed to be given by the area gap of the area operator in loop quantum gravity, which gives $\rho_c \sim \rho_{\rm Pl}$, where $\rho_{\rm Pl}$ is the Planck energy density. Latest studies suggest that $\rho_c = 0.41\rho_{\rm Pl}$ but they require some extra assumptions. To remain quite generic, we assume in the following that $\rho_c = \rho_{\rm Pl}$, that is the naturally expected scale. Because of this, the numerical values obtained in this paper should be considered as orders of magnitudes rather than accurate results but the main conclusions do not depend on this.

The background geometry is assumed to be described by the Friedmann-Lemaitre-Robertson-Walker metric. In effective LQC, the dynamics of the scale factor a is governed by the modified Friedmann equation (see [7]

for introductory reviews):

$$H^2 = \frac{8\pi G}{3}\rho\left(1-\frac{\rho}{\rho_c}\right). \tag{2}$$

In this article, we fix the value of the scale factor to $a = 1$ at the beginning of the Lorentzian stage (that is when $\rho = \rho_c/2$). It is easy to show that for $\rho = \frac{\rho_c}{2}$, the value of the Hubble parameter is maximal and equal to

$$H_{\rm max} = \sqrt{\frac{8\pi G\rho_c}{12}}. \tag{3}$$

The equation of motion for scalar modes (using the Mukhanov variable v_S) reads as [2]:

$$\frac{d}{d\eta^2}v_S - \Omega\nabla^2 v_S - \frac{z_S''}{z_S}v_S = 0, \tag{4}$$

where $z_S = a\frac{\dot\varphi}{H}$ and

$$\Omega = 1 - 2\frac{\rho}{\rho_c}. \tag{5}$$

A prime indicates a derivative with respect to the conformal time η while a dot indicates a derivative with respect tothe cosmic time t. The conformal time related to the cosmic time by $\eta = \int \frac{dt}{a(t)}$. Based on the Mukhanov variable v_S, the scalar curvature $\mathcal{R} = \frac{v_S}{z_S}$ can be computed. Similarly, for tensor modes [8]:

$$\frac{d}{d\eta^2}v_T - \Omega\nabla^2 v_T - \frac{z_T''}{z_T}v_T = 0, \tag{6}$$

where $z_T = a/\sqrt{\Omega}$. The v_T variable relates to amplitude of the tensor modes h through $v_T = \frac{ah}{\sqrt{16\pi G}\sqrt{\Omega}}$. In what follows we will work mainly with the ϕ variable defined as $\phi := h\sqrt{16\pi G}$.

In both cases, there is a Ω factor in front of the Laplace operator, which is related with the speed of propagation c_s by $c_s^2 = \Omega$. When approaching the beginning of the Lorentzain stage the factor Ω tends to zero. Because the space dependence is suppressed, the different space points are decoupled and become independent one from another. This behavior agrees with the predictions of the Belinsky, Khalatnikov and Lifshitz (BKL) conjecture [9] which states, in particular, that near a classical space singularity, different points do decouple one from the other. When Ω becomes negative one enters the Euclidean regime. In the case of a symmetric bounce, the domains of positive and negative values of the parameter Ω are shown in Fig. 1.

In this article, for simplicity, we will only study tensor modes. However, because of the similarities between Eq. (4) and Eq. (6), it is reasonable to expect that most of the results will hold also for scalar modes.

The organization of the paper is as follows. In Sec. II, general considerations regarding the generation of quantum tensor perturbations in presence of holonomy corrections are presented. The evolution of the horizon as well as the dynamics of the modes are investigated. We also derive the equation of motion governing the evolution of the power spectrum. In Sec. III, a possibility of defining a proper vacuum state in both the Lorentzian and the Euclidean regions is investigated. In Sec. IV, the properties of the "silent surface", defined as the interface between the Lorentzian and Euclidean regions, are analyzed in details. In particular, the possibility of a "white noise"-type fluctuations at the surface is addressed. The solutions to EOMs in vicinity of the "silent surface" are presented as well. In Sec. V, we consider the possibility of imposing the initial conditions for $k < m_{\rm Pl}$ and $k > m_{\rm Pl}$ separately. Namely, for $k < m_{\rm Pl}$ the initial conditions are imposed at $\rho = \rho_c/2$ while for $k > m_{\rm Pl}$ the initial conditions are imposed at the trans-Planckian surface. We show that a flat power spectrum can be generated from the trans-Planckian initial conditions if an appropriate inflationary period takes place. In Sec. VI, we investigate a possible conversion of the $\mathcal{P} \propto k^3$ spectrum generated from modes with $k < m_{\rm Pl}$ at the initial surface to a scale-invariant shape. We find that it is indeed possible –but quite difficult– by combining two evolutions characterized by two different barotropic indices w_1 and w_2. The resulting spectrum is however modulated by acoustic oscillations due to the transitional sub-horizon evolution. Finally, in Sec. VII, results of the paper are summarized and conclusions are derived.

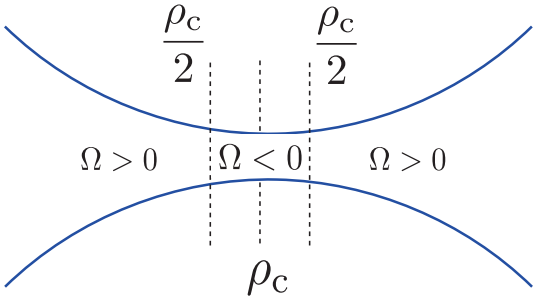

FIG. 1. Regions of the positive and negative values of the parameter Ω in a typical symmetric cosmic bounce. The silent initial conditions investigated in this paper are imposed at $\rho = \rho_c/2$.

II. QUANTUM GENERATION OF PERTURBATIONS

A. Horizon

In this paragraph, we study the general behavior of the horizon when the Universe, in its quantum regime (effectively described by the holonomy-corrected Hamiltonian), is filled with a barotropic fluid. This is relevant for setting the vacuum for perturbations.

The evolution of cosmological perturbations strictly depends on the length of the mode under considera-

tion. In particular, there are two regimes (super-Hubble and sub-Hubble) in which the evolution of perturbations qualitatively differs. The difference is transparent in the Fourier space, where an explicit wave-number dependence enters the equations of motion.

Performing the Fourier transform of the perturbation field $v = \int \frac{d^3k}{(2\pi)^3} v_{\mathbf{k}} e^{i\mathbf{k}\cdot\mathbf{x}}$, the equation of motion satisfied by the Fourier component $v_{\mathbf{k}}$ is

$$\frac{d}{d\eta^2} v_{\mathbf{k}} + \left(\Omega k^2 - \frac{z''}{z}\right) v_{\mathbf{k}} = 0. \tag{7}$$

Here, and in the rest of this work, for the sake of simplify, we denote $v := v_T$ and $z := z_T$.

Due to presence of the Ω factor in Eq. 7, the super-Hubble and sub-Hubble regimes are *not* the same as in the classical case (in the latter case, the borderline is approximately given by the Hubble radius $\sim 1/H$). In this new framework, the sub-Hubble modes are such that $\left|\Omega k^2\right| \gg \left|\frac{z''}{z}\right|$ while for, the super-Hubble ones, $\left|\Omega k^2\right| \ll \left|\frac{z''}{z}\right|$. The characteristic scale of the horizon

$$\lambda_H = \frac{a}{k_H}, \tag{8}$$

can be now defined by the following condition:

$$\left|\Omega k_H^2\right| = \left|\frac{z''}{z}\right|. \tag{9}$$

With this definition, the modes are called super-Hubble if $\lambda \gg \lambda_H$ and sub-Hubble if $\lambda \ll \lambda_H$. At the sub-Hubble scales the perturbations are decaying while at the super-Hubble scales, the amplitude of the perturbations is preserved (perturbations are "frozen"). This behavior has important consequences at the quantum level, where so-called mode functions (which parametrize the quantum evolution) satisfy the same equation as $v_{\mathbf{k}}$.

Let us now investigate the behavior of λ_H in the case of a universe filled with barotropic matter with a fixed ratio between pressure and density, that is $P = w\rho$, with $w = \text{const}$. In this case, it can be shown that

$$\frac{z''}{z} = \rho_c \kappa a^2 \frac{x}{\Omega^2}\left[\frac{1}{2}\left(\frac{1}{3} - w\right) + \left(\frac{9}{2} + 13w + \frac{9}{2}\right)x - (3 + 30w + 15w^2)x^2 + \left(\frac{11}{3} + 21w + 12w^2\right)x^3\right], \tag{10}$$

where $x := \rho/\rho_c$ and $\kappa = 8\pi G$. Because of the Ω^2 factor in the denominator, one may expect a divergence when the state of silence, $\Omega \to 0$, is reached. This is one of the issues studied in this article. Whether such a divergence affects drastically the evolution of modes across the $\Omega = 0$ surface will be analyzed deeply later in this study.

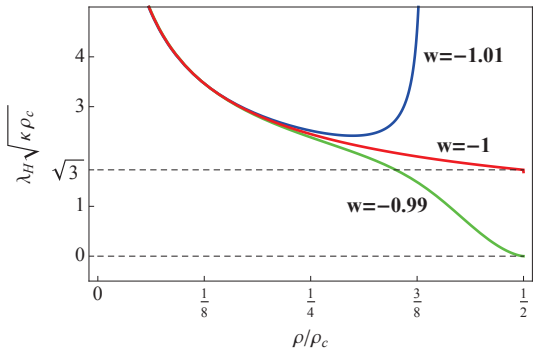

FIG. 2. Scale of the horizon λ_H as a function of ρ/ρ_c for different values of the barotropic index w. Only the Lorentzian domain ($\Omega > 0$) is considered.

The behavior of λ_H in the Lorentzian domain is plotted in Fig. 2.

For $w > -1$, that is for usual matter, all wavelengths are super-Hubble when $\Omega \to 0^+$ (corresponding to $\rho \to \frac{\rho_c}{2}^-$). The case $w = -1$ is the only possibility for which Eq. 10 is not divergent at $\Omega = 0$ and the corresponding $\lambda_H \to \sqrt{\frac{3}{\kappa\rho_c}}$ at this point. An interesting behavior is observed in the case of phantom matter ($w < -1$) for which all modes can be made sub-Hubble close to $\Omega = 0$.

B. Quantization of modes

In this subsection, we analyze the decomposition of perturbations for the mode functions when taking into account the specific structure of the holonomy-corrected algebra. This is fundamental for the quantum treatment of the problem.

The equations of motions (4) and (6) are the effective equations including quantum gravity effects. Although the quantum effects enter explicitly the equations of perturbations (through the factor Ω), only the background degrees of freedom were here quantized using the loop approach. The phase space of the perturbed variables remains classical but should, in principle, be modified by the quantization. A fully consistent procedure of quantization would require the application of the loop quantization to the perturbative degrees of freedom as well. However, for sufficiently large modes ($\lambda \gg l_{\rm Pl}$), loop quantization should reduce to the canonical one.

In this study, the Fourier modes $v_{\mathbf{k}}(\eta)$ are quantized following the standard canonical procedure. Promoting this quantity to be an operator, one performs the decomposition

$$\hat{v}_{\mathbf{k}}(\eta) = i^{\frac{1}{2}(1-\mathrm{sgn}\Omega)}(f_k(\eta)\hat{a}_{\mathbf{k}} + f_k^*(\eta)\hat{a}^\dagger_{-\mathbf{k}}), \tag{11}$$

where $f_k(\eta)$ is the so-called mode function which satisfies the same equation as $v_{\mathbf{k}}(\eta)$. Because we are working

in the Heisenberg picture, the operator $\hat{v}_{\mathbf{k}}(\eta)$ is time dependent, which is encoded in mode functions $f_k(\eta)$. The creation ($\hat{a}^\dagger_{\mathbf{k}}$) and annihilation ($\hat{a}_{\mathbf{k}}$) operators fulfill the commutation relation $[\hat{a}_{\mathbf{k}}, \hat{a}^\dagger_{\mathbf{q}}] = \delta^{(3)}(\mathbf{k}-\mathbf{q})$ and are defined at some initial time.

The new factor $i^{\frac{1}{2}(1-\mathrm{sgn}\Omega)}$ in Eq. (11) is due to reality condition for the field $\phi = v/z$, which leads to $\hat{\phi}^\dagger_{\mathbf{k}} = \hat{\phi}_{-\mathbf{k}}$. This does not translate into a similar condition for $\hat{v}_{\mathbf{k}}$ because $z = a/\sqrt{\Omega}$ can be both real and imaginary depending on the sign of Ω.

The mode functions are fulfilling the Wronskian condition

$$f_k (f_k')^* - f_k^* f_k' = i, \tag{12}$$

which was proven to keep its classical form [10].

As we deal with linear perturbations, which lead to Gaussian fluctuations, all the statistical information about the structure of the fluctuations is contained in the two-point correlation function. For the field $\phi = v/z$, the two-point correlation function is given by:

$$\begin{aligned} G(r) &:= \langle 0|\hat{\phi}(\mathbf{x},\eta)\hat{\phi}(\mathbf{y},\eta)|0\rangle \\ &= \int_0^\infty \frac{dk}{k}\mathcal{P}_\phi(k,\eta)\frac{\sin kr}{kr}, \end{aligned} \tag{13}$$

where the power spectrum is

$$\mathcal{P}_\phi(k,\eta) = \frac{k^3}{2\pi^2}\left|\frac{f_k}{z}\right|^2, \tag{14}$$

and $r = |\mathbf{x}-\mathbf{y}|$.

C. Equation of motion for the power spectra

In this subsection, we study how the spectrum, as defined in the previous section, can be propagated in time.

The idea is to derive the equation governing the evolution of the power spectrum defined by Eq. (14). Usually, the evolutions of v_k and z are calculated first and the power spectrum is derived subsequently. However, in some cases, it is possible and useful to obtain directly the evolution equation of $\mathcal{P}(k)$. In particular, this is relevant when initial conditions are determined by the form of the correlation function $G(r)$. This situation appears when imposing initial conditions at the "silent surface".

By using the equation of motion for v_k, as well as the Wronskian condition (12), one can show that the power spectrum fulfills the following nonlinear differential equation:

$$\frac{d^2\mathcal{P}}{d\eta^2} - \frac{1}{2\mathcal{P}}\left(\frac{d\mathcal{P}}{d\eta}\right)^2 + 2\Omega k^2\mathcal{P} + 2\frac{d\mathcal{P}}{d\eta}\frac{z'}{z} - \frac{1}{2z^4\mathcal{P}}\left(\frac{k^3}{2\pi^2}\right)^2 = 0. \tag{15}$$

After a change of variables, this equation can be reduced to an Ermakov equation.

Equation (15) can be written as a set of two first order differential equations. The advantage of this decomposition is that the obtained system of equations is free from the divergence at $\Omega = 0$. This leads to:

$$\frac{d\mathcal{P}}{d\eta} = \frac{\mathcal{G}}{a^2}\Omega, \tag{16}$$

$$\frac{d\mathcal{G}}{d\eta} = -2(ak)^2\mathcal{P} + \frac{\Omega}{2a^2\mathcal{P}}\left[\mathcal{G}^2 + \left(\frac{k^3}{2\pi^2}\right)^2\right]. \tag{17}$$

Importantly, the fixed point ($\mathcal{P}' = 0, \mathcal{G}' = 0$) of this set of equations is given by

$$\mathcal{G} = 0, \tag{18}$$

$$\mathcal{P} = \left(\frac{k}{2\pi}\right)^2\frac{\Omega}{a^2}, \tag{19}$$

which agrees with the Ω-corrected Minkowski vacuum (35).

III. VACUUM

In this section, we make some importants remarks on how one can define a vacuum state around the silence surface.

A first possibility to evaluate the spectrum in holonomy-corrected effective loop quantum cosmology (Ω-LQC) is to set initial conditions in the remote Lorentzian past (of the contracting branch) and calculate the resulting spectrum. This has been investigated in [11]. This is mathematically tantalizing and probably consistent but propagating perturbations through the Euclidean phase where there is, strictly speaking, no time anymore, is questionable. The main aim of this article is to investigate the possibility of imposing initial conditions at the interface between the Lorentzian and Euclidean regions. *A priori* nothing is know about the state of perturbations at this moment in time. This is the same difficulty as for initial conditions for the inflationary perturbations in the standard approach.

The usual assumption at this point is that the perturbations are initially in their vacuum state. Such an ansatz can be of course questioned. It is however a reasonable choice and it is worth investigating its consequences. In particular, within the standard inflationary evolution, the assumption of an initial vacuum state leads to a power spectrum in agreement with cosmological observations. It is also somehow nearly required by self-consistency conditions.

In principle, one could consider the perturbation fields classically and ignore quantization issues. However, in that case, no normalization of the modes would be available. Beyond it legitimacy, taking into quantum the evolution of perturbations is therefore heuristically

important.

We investigate the vacuum state for the holonomy-corrected case. To do so, the Hamiltonian for the considered type of perturbations has to be clearly defined. We adopt here observations made in [10], where it has been shown that the equation of motion (6) can be recovered by considering a wave equation on the effective metric

$$g^{eff}_{\mu\nu}dx^{\mu}dx^{\nu} = -\sqrt{\Omega}a^2 d\eta^2 + \frac{a^2}{\sqrt{\Omega}}\delta_{ab}da^a dx^b. \tag{20}$$

Based on this, the action for the massless field $\phi = v/z$ is given by

$$\begin{aligned} S &= -\frac{1}{2}\int d^4x\sqrt{-g}g^{\mu\nu}\partial_\mu\phi\partial_\nu\phi = \int d\eta L \\ &= \frac{1}{2}\int d\eta d^3x a^3\left[\frac{1}{\Omega}\left(\phi'\right)^2 - \left(\partial_i\phi\right)^2\right] \\ &= \frac{1}{2}\int d\eta d^3x\left[v'^2 - \Omega\left(\partial_i v\right)^2 + v^2\frac{z''}{z}\right], \end{aligned} \tag{21}$$

where an integration by parts was used in the second equality. Using the canonical momenta $\pi = \frac{\delta L}{\delta v'} = v'$, the Hamiltonian can be defined

$$\begin{aligned} H &= \int d^3x\pi v' - L \\ &= \int d^3x\left[\pi^2 + \Omega\left(\partial_i v\right)^2 - v^2\frac{z''}{z}\right]. \end{aligned} \tag{22}$$

The quantum version of this Hamiltonian can be written as

$$\begin{aligned} \hat{H} = \frac{1}{2}\int d^3k\Big[&\hat{a}_{\mathbf{k}}\hat{a}_{-\mathbf{k}}F_k + \hat{a}^{\dagger}_{\mathbf{k}}\hat{a}^{\dagger}_{-\mathbf{k}}F^*_k \\ &+ \left(2\hat{a}^{\dagger}_{\mathbf{k}}\hat{a}_{\mathbf{k}} + \delta^{(3)}(0)\right)E_k\Big], \end{aligned} \tag{23}$$

where

$$F_k = (f_k')^2 + \omega_k^2 f_k^2, \tag{24}$$
$$E_k = |f_k'|^2 + \omega_k^2|f_k|^2, \tag{25}$$

and

$$\omega_k^2 = \Omega k^2 - \frac{z''}{z}. \tag{26}$$

The vacuum expectation value is

$$\langle 0|\hat{H}|0\rangle = \delta^{(3)}(0)\frac{1}{2}\int d^3k E_k. \tag{27}$$

The ground state (vacuum) can be found by minimizing E_k while taking the Wronskian condition into account. This leads to the condition that the energy can be minimized if and only if $\omega_k^2 > 0$. Then, the interpretation of the excitations of the field as particles is also possible. In that case, the corresponding vacuum state is

$$f_k = \frac{e^{-i\omega_k\eta}}{\sqrt{2\omega_k}}. \tag{28}$$

This is rigorously satisfied only if $\omega_k = \text{const}$, which is not always the case. However, if ω_k is a slowly varying function of time, Eq. (28) remains a good approximation of the vacuum state.

The positivity of ω_k^2, required for a proper definition of the vacuum state, depends on both the sign of Ω and on the value of $\frac{z''}{z}$. In the Lorentzian regime ($\Omega > 0$) it is always possible to find values of k for which ω_k^2 is positive. If $\frac{z''}{z}$ is negative, this is the case for any k. If $\frac{z''}{z}$ is positive, this requires sufficiently large (sub-Hubble) k-valued mode.

The situation, however, changes in the Euclidean regime where $\Omega < 0$. Now, the k^2 term in the ω_k^2 function is multiplied by a negative number, and the positivity of ω_k^2 can be satisfied only if $\frac{z''}{z}$ takes a negative value.

In Fig. 3, we show $\frac{z''}{z}$ as a function of the energy density for some representative values of the barotropic index w.

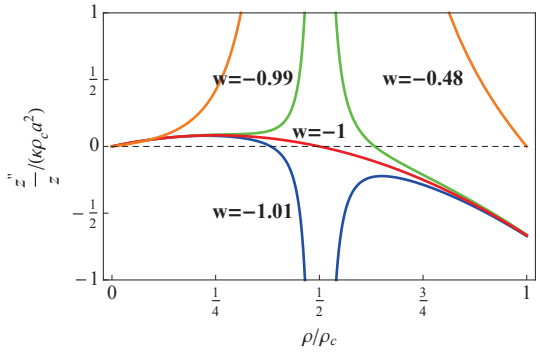

FIG. 3. The $\frac{z''}{z}$ as a function of ρ/ρ_c for different values of w.

One can show that for $w > \frac{1}{6}(-7+\sqrt{17}) \approx -0.48$, the $\frac{z''}{z}$ term is positive in the whole Euclidean domain. There is therefore no well defined vacuum state in this case. For, smaller values of w, it is possible to define the vacuum state in part of the Euclidean domain. An interesting special case is $w = -1$, for which the evolution of $\frac{z''}{z}$ across the surface of signature change is regular. Here, $\frac{z''}{z}$ is positive in the whole Lorentzian range and negative in the whole Euclidean range. The vacuum sate can be therefore defined for all values of the energy density but, of course, only for some values of k.

The range of wavelengths for which the vacuum state is well defined for $w = -1$ is shown in Fig. 4. In the Lorentzian domain, the vacuum state is well defined at the sub-Hubble scales. This reverses in the Euclidean regime where the vacuum state is defined for the super-Hubble modes.

The fact that the vacuum state can be well defined at

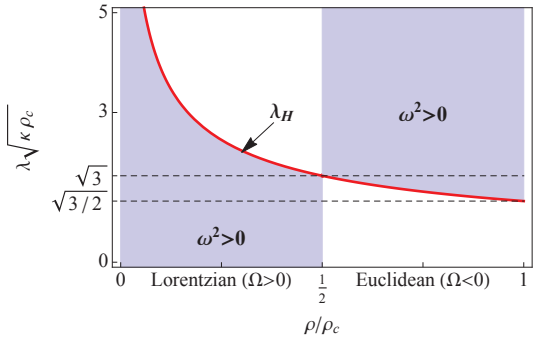

FIG. 4. The regions of $\omega_k^2 > 0$ for $w = -1$

super-Hubble scales is a new feature. It might be that the vacuum state can be used to impose initial conditions for the super-Hubble modes at the beginning of the Lorentzian regime, where the vacuum sate is not well defined. In particular, one may expect that through the quantum tunneling transition from the Euclidean to the Lorentzian phase, the structure of the Euclidean vacuum at the super-Hubble scales would define the configuration of the perturbations at the beginning of the Lorentzian regime. In this scenario, the super-Hubble power spectrum in vicinity of the silent surface would scale as k^3, as we shall demonstrate later.

A. Vacuum at $\Omega = -1$

As an example, let us consider the state of vacuum in the case $w = -1$ for $\Omega = -1$. The vacuum state is well defined for $\lambda \gg \lambda_H$ and is given by $|f_k|^2 = \frac{\sqrt{3}}{2\sqrt{2\kappa\rho_c}a}$. The corresponding power spectrum is

$$\mathcal{P}_\phi(k) \equiv \frac{k^3}{2\pi^2}\left|\frac{f_k}{z}\right|^2 = \frac{\sqrt{3}}{4\pi^2\sqrt{2\kappa\rho_c}}\left(\frac{k}{a}\right)^3 \propto k^3. \qquad (29)$$

This justifies (partly) the assertion presented at the end of the previous subsection. The power spectrum differs from the standard Bunch-Davies case, for which $\mathcal{P}_\phi \propto k^2$. Using the definition (13), one can show that the corresponding correlation function is vanishing $\langle 0|\hat{\phi}(\mathbf{x},\eta)\hat{\phi}(\mathbf{y},\eta)|0\rangle = 0$. In this case, fluctuations have a white noise spectrum. This is intuitively compatible with the idea that space points are indeed decorrelated.

B. Vacuum at $\Omega \approx 0$

This case is the most relevant one for the subject of this article. However, except for the very specific equation of state $w = -1$, ω_k^2 is divergent when $\Omega \to 0$ and this cannot lead to a proper definition of the vacuum state at the surface of silence.

In the case $w = -1$, the evolution of $\frac{z''}{z}$ across $\Omega = 0$ is regular and, in the vicinity of $\Omega = 0$, can be approximated as

$$\frac{z''}{z} \approx \frac{1}{3}\kappa\rho_c a^2\Omega, \qquad (30)$$

based on which

$$\omega_k^2 \approx \Omega\left(k^2 - \frac{1}{3}\kappa\rho_c a^2\right). \qquad (31)$$

One can then see that $\omega_k^2 > 0$ is satisfied either for $\Omega > 0$ and $k > \sqrt{\frac{1}{3}\kappa\rho_c a^2}$ or $\Omega < 0$ and $k < \sqrt{\frac{1}{3}\kappa\rho_c a^2}$.

For the positive values of ω_k^2 given by Eq. (31), the mode functions for the state of vacuum (28) are

$$|f_k|^2 = \frac{1}{2\sqrt{\Omega\left(k^2 - \frac{1}{3}\kappa\rho_c a^2\right)}}. \qquad (32)$$

Using this for the super-Hubble modes, that is $k < \sqrt{\frac{1}{3}\kappa\rho_c a^2}$, while approaching $\Omega \to 0^-$ the vacuum is characterized by the following spectrum

$$\mathcal{P}_\phi(k) = \frac{\sqrt{3}\sqrt{|\Omega|}}{4\pi^2\sqrt{\kappa\rho_c}}\left(\frac{k}{a}\right)^3 \propto \sqrt{|\Omega|}k^3. \qquad (33)$$

This is again a white noise spectrum. But it is modulated by Ω and therefore vanishes in the limit $\Omega \to 0^-$. There are no fluctuations strictly at the surface of silence in this case (but interesting features remain around this surface). The correlation function is therefore trivially vanishing $G(r) = 0$ exactly at $\Omega = 0$.

C. Vacuum at $\Omega > 0$

The $\Omega > 0$ region is where initial conditions for the quantum fluctuations are usually imposed. In this case, the vacuum sate is well defined for $\lambda \ll \lambda_H$, where $\omega_k^2 \approx \Omega k^2$. This, applied to Eq. (28), leads to the following expression for the vacuum normalization:

$$|f_k|^2 = \frac{1}{2k\sqrt{\Omega}}. \qquad (34)$$

This normalization has also been derived using independent arguments [10, 12]. The corresponding power spectrum is

$$\mathcal{P}_\phi(k) \equiv \frac{k^3}{2\pi^2}\left|\frac{f_k}{z}\right|^2 = \left(\frac{k}{2\pi}\right)^2\frac{\Omega}{a^2} \propto k^2. \qquad (35)$$

This is the $\Omega-$deformed Bunch-Davies vacuum. In that case the holonomy corrections change the normalization but do not modify the shape of the standard spectrum.

IV. PHYSICS AT THE SURFACE OF INITIAL CONDITIONS

In this section, we derive different relations useful for calculating the spectra. In particular, initial values for $\mathcal{P}$ and $\mathcal{G}$ governed by Eqs. (16) and (17) will be studied.

A. Solution for $\Omega \approx 0$

In the vicinity of the interface between the Euclidean and the Lorentzian regions (where $\Omega = 0$), the equation of motion for the ϕ variable,

$$\phi^{''} + \left(2\mathcal{H} - \frac{\Omega'}{\Omega}\right)\phi' - \Omega\Delta\phi = 0, \tag{36}$$

simplifies to

$$\phi^{''} + \left(2\mathcal{H} - \frac{\Omega'}{\Omega}\right)\phi' \approx 0. \tag{37}$$

Despite this approximation, the equation remains singular due to presence of the $\frac{\Omega'}{\Omega}$ factor. The solution across the silent surface is however regular. In order to find the solution, the equation (37) can be integrated to

$$\phi' = c_1 \frac{\Omega}{a^2}. \tag{38}$$

Further integration leads to the solution

$$\phi = c_2 + c_1 \int^{\eta} \frac{\Omega}{a^2} d\eta' = c_2 + c_1 \int^{\eta} \frac{d\eta'}{z^2}. \tag{39}$$

Because the Ω factor appears only in the numerator, no pathological behavior is to be expected. Using the above analysis, the solution to the simplified equation for the mode functions

$$\frac{d}{d\eta^2} f_k - \frac{z^{''}}{z} f_k = 0, \tag{40}$$

takes the following form:

$$f_k = z\left(A_k + B_k \int_{\eta_0}^{\eta} \frac{d\eta'}{z^2}\right). \tag{41}$$

It is worth stressing that evolution of the amplitude f_k/z is regular through the silent surface (when $\Omega = 0$) despite the fact that the $\frac{z^{''}}{z}$ factor present in the equation for f_k is generically divergent. The origin of this divergence is the $\sqrt{\Omega}$ factor occurring in definition of z. The $\sqrt{\Omega}$ factor is non-differentiable at $\Omega = 0$ leading to divergences occurring in equations governing the evolution of the mode functions. However, the $\sqrt{\Omega}$ factor does not appear in the equations for amplitudes (such as Eq. (36)), that have regular solutions.

The A_k and B_k in Eq. (41) are constants of integration and fulfill the following relation:

$$A_k B_k^* - A_k^* B_k = i, \tag{42}$$

due to the Wronskian condition. This leads to

$$\left|\frac{f_k}{z}\right|^2 = |A_k|^2 + |B_k|^2 \left(\int_{\eta_0}^{\eta} \frac{d\eta'}{z^2}\right)^2 + (A_k B_k^* + A_k^* B_k) \int_{\eta_0}^{\eta} \frac{d\eta'}{z^2}. \tag{43}$$

B. Initial conditions for the perturbations

One can now use Eq. (43) with $\eta_0 = 0$ corresponding to the transition point $\Omega = 0$ in order to impose initial conditions. The initial conditions for the fields $\mathcal{P}$ and $\mathcal{G}$ can then be written as follows:

$$\mathcal{P}|_{\eta=0} = \frac{k^3}{2\pi^2}|A_k|^2, \tag{44}$$

$$\mathcal{G}|_{\eta=0} = \frac{k^3}{2\pi^2}\left(A_k B_k^* + A_k^* B_k\right). \tag{45}$$

By expressing A_k and B_k in terms of amplitudes and phases

$$A_k = \tilde{A}_k e^{i\alpha}, \tag{46}$$

$$B_k = \tilde{B}_k e^{i\beta}, \tag{47}$$

the Wronskian condition (42) leads to

$$2\tilde{A}_k \tilde{B}_k \sin(\alpha - \beta) = 1, \tag{48}$$

and

$$A_k B_k^* + A_k^* B_k = 2\tilde{A}_k \tilde{B}_k \cos(\alpha - \beta) = \cot(\alpha - \beta). \tag{49}$$

The cotangent function has a period of π. Let us define the phase difference $X = \alpha - \beta \in (0, \pi)$. For the particular value $X = \pi/2$ we have

$$A_k B_k^* + A_k^* B_k = 0, \tag{50}$$

so $\mathcal{G}|_{\eta=0}$ is vanishing.

If we assume that the phase difference has a flat distribution

$$P(X) = \frac{1}{\pi}, \tag{51}$$

then the distribution of the values of

$$Y = \cot(X) \tag{52}$$

is given by a Cauchy distribution

$$P(Y) = \frac{1}{\pi}\frac{1}{(1+Y^2)}, \tag{53}$$

which is peaked at $Y = 0$. This might be seen as a probabilistic motivation for choosing $\mathcal{G}|_{\eta=0} = 0$. In other words, if the phase difference X is chosen randomly, then the most probable value of $\mathcal{G}|_{\eta=0}$ is zero. This is not a demonstration but rather an heuristic argument for this choice. We will use this value to perform numerical computations in the following.

C. Correlation functions

Here, we explicitly show that white noise initial conditions at the silent surface lead to a power spectrum

spectrum cubic in k.

The state of silence is characterized by the suppression of spatial derivatives, which leads to the decoupling of the evolution at different space points. As already explained before, and as shown in [13], this phase takes place in the vicinity of $\rho = \rho_c/2$. While approaching the state of silence, light cones collapse onto time lines, as pictorially presented in Fig. 5. Because the evolutions at different

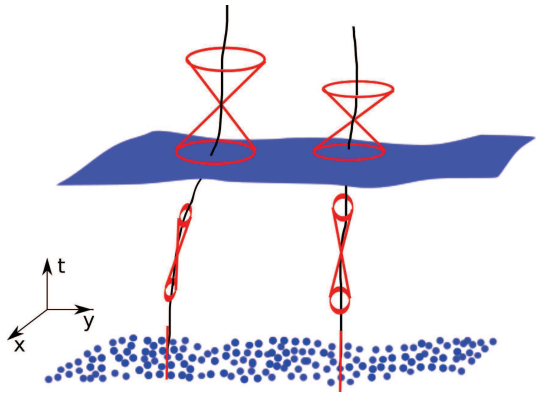

FIG. 5. Pictorial representation of the evolution of the light-cones towards the silence surface $\rho = \rho_c/2$, where space-time becomes a congruence of time lines.

space points are decoupled and run independently, one can expect that the correlations between physical quantities evaluated at different points are vanishing. More precisely, it is reasonable to expect that there are still some correlations but on very small scales, with a correlation length $\xi \sim l_{\rm Pl}$. This situation can be modeled by the following correlation function

$$G(r) = \begin{cases} G_0 & \text{for } \xi \geq r \geq 0, \\ 0 & \text{for } r > \xi. \end{cases} \tag{54}$$

Given a correlation function $G(r)$, the power spectrum can be straightforwardly found by using the relation

$$\mathcal{P}(k) = \frac{2}{\pi} k^3 \int_0^\infty dr\ G(r)\ r^2 \frac{\sin(kr)}{kr}. \tag{55}$$

For the considered model, using Eq. (55), we find:

$$\begin{aligned} \mathcal{P}(k) &= \frac{2}{\pi} k^3 G_0 \int_0^\xi dr\ r^2 \frac{\sin(kr)}{kr} \\ &= \frac{2}{\pi} G_0 \int_0^{\xi k} dx\ x\ \sin x \\ &= \frac{2G_0}{\pi} \left[-k\xi \cos k\xi + \sin k\xi\right]. \end{aligned} \tag{56}$$

In the limit $k\xi \ll 1$:

$$\mathcal{P}(k) = \frac{2}{3} \frac{G_0}{\pi} (k\xi)^3 + \mathcal{O}((k\xi)^5). \tag{57}$$

This shows that, at large scales, the power spectrum is of the k^3 form, as expected for white noise.

Importantly, $G(r) = 0$ in Eq. (55) corresponds to the trivial $\mathcal{P}(k) = 0$ case. However, from the definition Eq. (13) we know that $\mathcal{P}(k) \propto k^3$ also give $G(r) = 0$.

V. TRANS-PLANCKIAN MODES

The equations governing the evolution of both tensor and scalar perturbations are valid only for modes that are larger than the Planck scale. This is because at short scales the notion of continuity is expected to break down due to quantum gravity effects. However, some knowledge about how the so-called *trans-Planckian* modes behave can be gained by considering quantum deformations of space-time symmetries.

The relevant type of deformations can be inferred from the form of the algebra of quantum-corrected constraints. For the holonomy corrections considered in this article, the algebra of constraints takes the following form [2]:

$$\begin{aligned} \{D[M^a], D[N^a]\} &= D[M^b \partial_b N^a - N^b \partial_b M^a], \\ \{D[M^a], S^Q[N]\} &= S^Q[M^a \partial_a N - N \partial_a M^a], \\ \{S^Q[M], S^Q[N]\} &= \Omega D\left[q^{ab}(M\partial_b N - N\partial_b M)\right]. \end{aligned}$$

The D term is the diffeomorphism constraint and S^Q is the holonomy-corrected scalar constraint. The constraints play the role of generators of the symmetries and are parametrized by the laps function (N) and the shift vector (N^a). The Ω is a deformation factor (given by Eq. (5)), equal one in the classical limit while q^{ab} is the inverse of the spatial metric.

The algebra of constraints reduces to the Poincaré algebra, describing isometries of the Minkowski space, in the short scale limit. However, due to the deformation of the algebra of constraints, the Poincaré algebra is deformed as well [14, 15]. The deformation of the Poincaré algebra manifests itself through modifications of the dispersion relations. As discussed in [15], this leads to an energy dependent speed of propagation, such that the group velocity tends to zero when the energy of the modes approaches $m_{\rm Pl}$.

This effect can be introduced by considering a k-dependence in the Ω function. For phenomenological purposes, one can assume that the Ω factor in front of the k^2 term in the equations of motion is replaced by

$$\Omega = \left(1 - 2\frac{\rho}{\rho_c}\right)\left(1 - \frac{1}{m_{\rm Pl}^2}\left(\frac{k}{a}\right)^2\right). \tag{58}$$

Another way of introducing this effect is by performing the replacement $(k/a)^2 \to \Upsilon^2(k)$, as usually done when studying modified dispersion relations for the propagation of cosmological perturbations (See *e.g.* [16]). The $\Upsilon^2(k)$ function encodes deformation of the dispersion relation.

Eq. (58) can be studied in different regimes. When considering large scales ($\frac{k}{a} \ll m_{\rm Pl}$) the new factor in equation (58) can be neglected and $\Omega \approx 1 - 2\frac{\rho}{\rho_c}$. This

is, in particular, valid for the modes characterized by $k \ll m_{\rm Pl}$ at the surface of initial conditions. On the other hand, when we are far away from the initial surface ($\rho \ll \rho_{\rm c}$), the quantum effects are relevant only for short scale modes, then $\Omega \approx 1 - \frac{1}{m_{\rm Pl}^2}\left(\frac{k}{a}\right)^2$. Of course when $\rho \sim \rho_{\rm c}$ and $\frac{k}{a} \sim m_{\rm Pl}$ both effects should be taken into account simultaneously. In the classical domain, when $\rho \ll \rho_{\rm c}$ and $\frac{k}{a} \ll m_{\rm Pl}$, one naturally recovers $\Omega \approx 1$.

Initial condition for the modes can be imposed when

$$k \approx a\, m_{\rm Pl}. \tag{59}$$

At this time $\Omega \approx 0$ for $\rho \ll \rho_{\rm c}$ (perhaps also for $\rho \sim \rho_{\rm c}$ as the modification of the dispersion relation is here taking into account both effects basically independently). In this limit, the equation of motion simplifies to

$$\frac{d}{d\eta^2}v_k - \frac{z''}{z}v_k = 0, \tag{60}$$

as in the vicinity of $\rho = \rho_{\rm c}/2$. One can therefore expect that the state of asymptotic silence is realized also at the scales of the order of the Planck length.

Let us now compute the total power spectrum, including $k < m_{\rm Pl}$ and $k > m_{\rm Pl}$ regions. Initial conditions for the $k < m_{\rm Pl}$ modes will be imposed at the silence surface. In turn, initial conditions for the $k > m_{\rm Pl}$ are imposed at the Planckian surface, when $k \approx a\, m_{\rm Pl}$. In Fig. 6 the initial value surfaces are presented on the $\log\lambda - \log a$ plane.

A mode with a given k exits the Planckian surface when $k \approx a(t_e) m_{\rm Pl}$, (with $a(t_0) = 1$ at the beginning of the Lorentzian phase). For the modes being of the order of the Planck length ($k \approx a\, m_{\rm Pl}$), the equation of motion reduces to the k-independent form (60). Because at $k \approx a\, m_{\rm Pl}$ and for $\rho \ll \rho_c$ one has

$$\omega_k^2 = -\frac{z''}{z} \approx \rho\kappa a^2 \frac{1}{2}\left(-\frac{1}{3} + w\right), \tag{61}$$

the vacuum normalization (28) can be applied only if $w > \frac{1}{3}$. In this case, the spectrum at the Planckian surface is

$$\mathcal{P}(k = m_{\rm Pl}a) \approx \frac{m_{\rm Pl}^3 a^{\frac{3}{2}(1+w)}}{(2\pi)^2\sqrt{4\pi G\rho_0|w - 1/3|}}, \tag{62}$$

where ρ_0 is matter energy density at $a = 1$. In particular, for $w = 1$ this leads to $\mathcal{P}(k = m_{\rm Pl}a) \propto k^3$. This initial power spectrum cannot be, however, converted into a scale-invariant one in the same period, driven by the barotropic fluid with $w = 1$. A more relevant case for cosmology is the one with $\mathcal{P}(k = m_{\rm Pl}a) = $ const. This can be obtained from (62) for $w = -1$. However, in that case, $\omega_k^2 < 0$ and the spectrum (62) does not correspond to the initial vacuum state. Nevertheless, this initial state leads to predictions being in qualitative agreement with the cosmological observations. The state itself is, however, not distinguished at the purely theoretical ground.

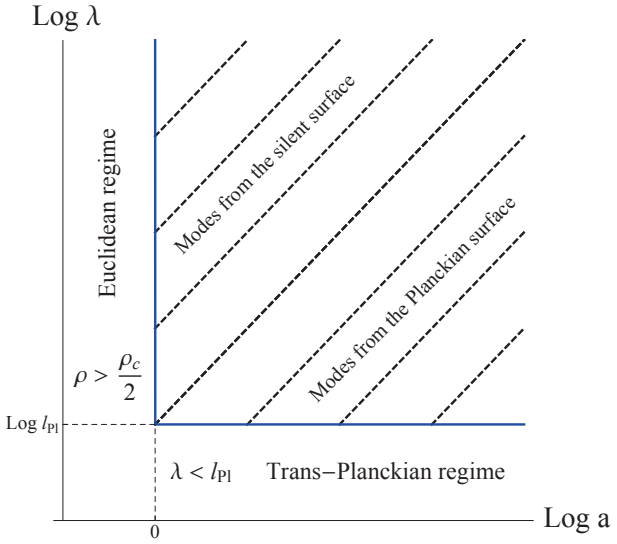

FIG. 6. The thick (blue) line represents the surface at which the initial conditions are imposed. For the modes with $k < m_{\rm Pl}$ at $a = 1$ this is the silent surface while for $k > m_{\rm Pl}$ it is the Planckian surface. The dashed lines represent the evolution of the different length scales $\lambda = \frac{a}{k}$. The wavelength $\lambda = l_{\rm Pl}a$ sets the limit between the different types of initial conditions.

The requirement $\mathcal{P}(k = m_{\rm Pl}a) = $ const at the Planckian surface in fact agrees with the standard vacuum-type normalization of modes. To see this explicitly, let us notice that the evolution of the amplitudes of perturbations can be approximated classically by $\phi_k = \frac{c_k}{a}$ (in the regime between the horizon and the Planckian surface). The power spectrum $\mathcal{P}(k) = \frac{k^3}{2\pi^2}\frac{|c_k|^2}{a^2}$ at the Planckian surface is therefore equal to

$$\mathcal{P}(k = m_{\rm Pl}a) = \frac{k\, m_{\rm Pl}^2}{2\pi^2}|c_k|^2. \tag{63}$$

It can be made constant by setting $c_k \sim \frac{1}{\sqrt{k}}$, which corresponds to the Bunch-Davies normalization of modes.

In order to illustrate the procedure, we have performed numerical computations of the power spectra with initial conditions:

$$\mathcal{P}|_{\Omega=0} = (k/m_{\rm Pl})^3, \tag{64}$$
$$\mathcal{G}|_{\Omega=0} = 0, \tag{65}$$

for $k < m_{\rm Pl}$ and

$$\mathcal{P}|_{k=m_{\rm Pl}a} = 1, \tag{66}$$
$$\mathcal{G}|_{k=m_{\rm Pl}a} = 0, \tag{67}$$

for $k > m_{\rm Pl}$.

Applying these initial condition to Eqs. (16) and (17), the evolution of the power spectrum can be computed.

The result is shown in Fig. 7. For $k < m_{\rm Pl}$, the shape of the power spectrum is preserved because of the "freezing" of modes at super-Hubble scales. The modes are initially super-Hubble and remain such demurring the whole evolution. The power spectrum for $k > m_{\rm Pl}$ is slightly red-tilted due to gradual increase of the Hubble radius during the evolution, as in usual cosmology.

The spectrum is characterized by a sharp transition between the k^3 IR behavior and the nearly scale-invariant UV part. The sharpness is obviously due to the naive matching between initial conditions at the silence surface and at the Planckian surface but the existence of two regimes is a specific prediction in this model. Some additional features are to be expected around $k \approx m_{\rm Pl}$ with a more sophisticated modeling.

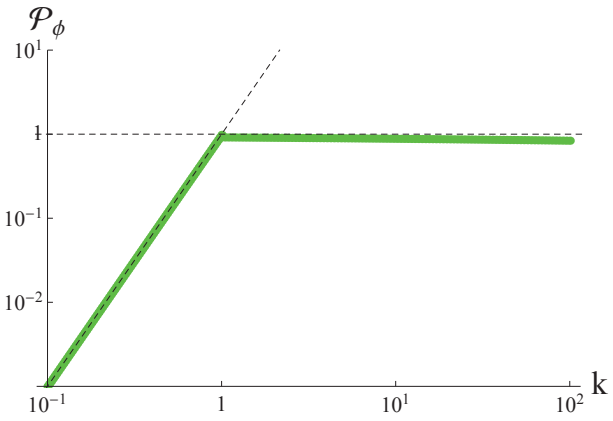

FIG. 7. Power spectrum at $t = 10\ t_{\rm Pl}$ with $w = -0.95$. The initial power spectrum was $\mathcal{P}(k) = k^3$ for $k < 1$ and $\mathcal{P}(k) = 1$ for the modes with $k > 1$, imposed at the trans-Planckian surface, as depicted by the dashed lines. The slight red-tilt appears due to decrease of the Hubble factor in time.

VI. FLAT POWER SPECTRUM WITHOUT TRANS-PLANCKIAN MODES

In this section, we study if it is possible to convert a pure "silent" initial power spectrum $\mathcal{P} \propto k^3$ to a flat one, in agreement with observational data. To this aim, we will consider two successive periods dominated by different types of barotropic matter. Here, the quantum effects will not be neglected in the dynamics. They will be used to determine initial conditions. It has, however, been numerically checked that the subtle corrections to the propagation equations do not play a significant role in the shape of the power spectrum.

Initially, the Hubble horizon is of the order of the Planck scale, that means that all the relevant modes (those with wavelengths much bigger than the Planck length) are frozen: they are outside the Hubble radius, and therefore (approximately) constant in time. If the amplitude of a mode is to evolve, so that a final spectrum (called primordial for the subsequent phenomenology) compatible with observations emerges, one needs the modes to first enter the Hubble horizon and then to exit again. To achieve this, one needs a background where the conformal Hubble factor $\mathcal{H} = \frac{a'}{a}$ is first decreasing and then, later on, growing. With barotropic matter, this means that at least two successive periods with different pressure to density ratios are required. Since entering and exiting the Hubble horizon is the key point here, and what happens to the background in-between is somehow irrelevant, there is no reason to include more than two different barotropic periods.

The important issue is to determine precisely the sufficient conditions for this specific evolution to indeed generate a scale-invariant spectrum. In order to answer this question let us consider the evolution of modes far from the surface of silence, where the $\Omega \approx 1$ approximation is valid. For a barotropic matter content, the solution to the mode equation (7) is

$$f_k = \frac{\sqrt{-k\eta}}{\sqrt{k}}\sqrt{\frac{\pi}{4}}\left(D_1 H^{(1)}_{|\nu|}(-k\eta) + D_2 H^{(2)}_{|\nu|}(-k\eta)\right), \tag{68}$$

where

$$|\nu| = \frac{3}{2}\left|\frac{1-w}{1+3w}\right|, \tag{69}$$

and D_1 and D_2 are constants which, based on the Wronskian condition, satisfy the following relation

$$|D_1|^2 - |D_2|^2 = 1. \tag{70}$$

Using the small value approximation of the Hankel function

$$H^{(1)}_{|\nu|}(x) \simeq -\frac{i}{\pi}\Gamma(|\nu|)\left(\frac{x}{2}\right)^{-|\nu|}, \tag{71}$$

the power spectrum at the super-Hubble scales is

$$\mathcal{P}_\phi(k) \propto |D_1 - D_2|^2\, k^{3-2|\nu|}. \tag{72}$$

Assuming the Bunch-Davies vacuum at short scales ($D_1 = 1$, $D_2 = 0$), a flat power spectrum is obtained for $|\nu| = \frac{3}{2}$. This, in the expanding universe, corresponds to $w = -1$. In this case, the power spectrum at the short scales is

$$\mathcal{P}_\phi(k) \propto k^2. \tag{73}$$

The quadratic sub-Hubble spectrum has to be produced from the initial cubic super-Hubble modes.

This can be achieved by considering a prior evolution driven by the barotropic matter. The evolution of the modes is described by Eq. (68). The initial cubic power spectrum at the super-Hubble scales can be obtained by taking $|\nu| = 0$ (which corresponds to $w = 1$) and requiring D_1 and D_2 to be independent on k. In that case, using the large value approximation,

$$H^{(1)}_{|\nu|}(x) \simeq \sqrt{\frac{2}{\pi x}}e^{i(x-|\nu|\pi/2-\pi/4)}, \tag{74}$$

the sub-Hubble spectrum is

$$\mathcal{P}_\phi(k) \propto k^2 \tag{75}$$

as required.

The transition between the phases characterized by $w = 1$ and $w = -1$ can be modeled by considering the following energy density:

$$\rho = \frac{\rho_0}{a^6} + \frac{\Lambda}{8\pi G}. \tag{76}$$

The first factor corresponds to matter with an equation of state $P = \rho$ while the second is the cosmological constant term with the equation of state $P = -\rho$. For such a setup together with initial conditions

$$\mathcal{P}|_{\Omega=0} = (k/m_{\rm Pl})^3, \tag{77}$$
$$\mathcal{G}|_{\Omega=0} = 0, \tag{78}$$

for $k < m_{\rm Pl}$, the equations of motion can be solved. In Fig. 8 we show the results of the numerical simulations with $\frac{\Lambda}{8\pi G\rho_c} = 10^{-7}$.

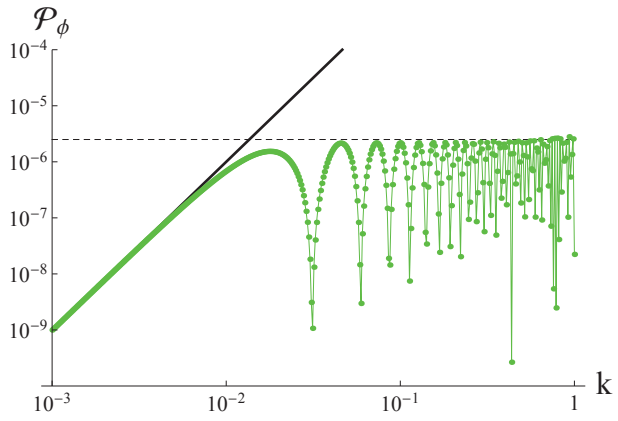

FIG. 8. Power spectrum converted to a rough scale invariance from the initial $\mathcal{P}(k) = (k/m_{\rm Pl})^3$. The spectrum was computed at $t = 6000 t_{\rm Pl}$ with $\frac{\Lambda}{8\pi G\rho_c} = 10^{-7}$.

As expected, the spectrum scales as k^3 in the IR limit and becomes quasi-flat for sufficiently large values of k. The flatness is however distorted by acoustic oscillations resulting from the sub-Hubble evolution of modes.

The above argument can be generalized. A cubic spectrum will be transformed to a flat spectrum under the following conditions: the relevant modes enters the Hubble horizon when $\omega = \omega_1 > -1/3$ and exits the Hubble horizon when $\omega = \omega_2 < -1/3$, where ω_1 and ω_2 fullfill

$$\frac{1}{1+3\omega_1} - \frac{1}{1+3\omega_2} = \frac{3}{4}. \tag{79}$$

If any case agreeing with the previous conditions, the final spectrum will be flat and modulated by acoustic oscillations.

VII. CONCLUSIONS

Loop quantum cosmology, together with other approaches to quantum gravity, might lead to a stage of asymptotic silence in the early Universe. This is in remarkable agreement with expectations from the purely classical BKL conjecture. In itself, the possible existence of this specific situation opens many windows to make links between primordial cosmology and phase transitions in solid state physics, not to mention the key question of "emergence" of time. In this work, we focused on more specific aspects, namely on the derivation of the tensor power spectrum of cosmological perturbations with initial conditions imposed around the state of silence.

The main results of the paper are the following:

- The state of silence provides a natural way to set initial conditions for the cosmological perturbations. This state is the beginning of the Lorentzian phase, and, in some sense, the beginning of time. This is qualitatively a new feature in cosmology.

- A cubic shape ($\mathcal{P} \propto k^3$) of the initial power spectrum at the "silent surface" is favored.

- In the pre-silent Euclidean regime, the sate of vacuum can be defined at large scales, which contrasts with the Lorentzain case. The vacuum is generically characterized by a $\mathcal{P} \propto k^3$ power spectrum (white noise).

- If the evolution of the universe was such that the modes of physical relevance were to become trans-Plackian when evolved backward in time up to the "silent surface", then initial conditions can be set at the "Planckian surface" (which is of course time dependent). The scale-invariant power spectrum of cosmological perturbations can be obtained if the power spectrum at the Planckian surface has a constant value.

- If the visible part of the power spectrum is due to modes that emerged from the silent surface without having been trans-Planckian, the white noise initial power spectrum can indeed be turned into a quasi-flat primordial power spectrum without inflation but this requires a quite high level of fine tuning. It this case the super-Hubble spectrum ($\mathcal{P} \propto k^3$) is converted to a $\mathcal{P} \propto k^2$ spectrum at sub-Hubble scales and the modes cross the horizon once again leading to a"final" $\mathcal{P} \approx$ const spectrum.

ACKNOWLEDGMENTS

The work was supported by Astro-PF and HECOLS programs, and by the Labex ENIGMASS.

[1] J. B. Hartle and S. W. Hawking, Phys. Rev. D **28** (1983) 2960.

[2] T. Cailleteau, J. Mielczarek, A. Barrau and J. Grain, Class. Quant. Grav. **29** (2012) 095010 [arXiv:1111.3535 [gr-qc]].

[3] M. Bojowald and G. M. Paily, Phys. Rev. D **86** (2012) 104018 [arXiv:1112.1899 [gr-qc]].

[4] J. Mielczarek, Springer Proceedings in Physics Volume **157** (2014) 555-562 arXiv:1207.4657 [gr-qc].

[5] T. Cailleteau, L. Linsefors, and A. Barrau, Class. Quant. Grav. **31** (2014) 125011 [arXiv:1307.5238 [gr-qc]].

[6] T. Cailleteau, A. Barrau, J. Grain, F. Vidotto, Phys. Rev. D **86** (2012) 087301 arXiv:1206.6736 [gr-qc].

[7] A. Ashtekar, M. Bojowald, and J. Lewandowski, Adv. Theor. Math. Phys. 7, 233, 2003;
A. Ashtekar, Gen. Rel. Grav. 41, 707, 2009;
A. Ashtekar, P. Singh, Class. Quantum Grav. 28, 213001, 2011;
A. Barrau, T. Cailleteau, J. Grain, and J. Mielczarek, Class. Quantum Grav. **31** (2014) 053001;
M. Bojowald, Living Rev. Rel. 11, 4, 2008;
M. Bojowald, Class. Quantum Grav. 29, 213001, 2012;
K. Banerjee, G. Calcagni, and M. Martn-Benito, SIGMA 8, 016, 2012;
G. Calcagni, Ann. Phys. (Berlin) 525, 323, 2013;
I. Agullo and A. Corichi, arXiv:1302.3833 [gr-qc]

[8] T. Cailleteau, A. Barrau, J. Grain and F. Vidotto, Phys. Rev. D **86** (2012) 087301 [arXiv:1206.6736 [gr-qc]].

[9] V. A. Belinskii, I. M. Khalatnikov and E. M. Lifshitz, *Adv. Phys.* **19** (1970) 525; **31** (1982) 639.

[10] J. Mielczarek, JCAP **1403** (2014) 048 [arXiv:1311.1344 [gr-qc]].

[11] L. Linsefors, T. Cailleteau, A. Barrau, and J. Grain, Phys. Rev. D **87** (2013) 10, 107503 [arXiv:1212.2852 [gr-qc]].

[12] A. Barrau, M. Bojowald, G. Calcagni, J. Grain, and M. Kagan, arXiv:1404.1018 [gr-qc].

[13] J. Mielczarek, AIP Conf. Proc. **1514** (2012) 81 [arXiv:1212.3527 [gr-qc]].

[14] M. Bojowald and G. M. Paily, Phys. Rev. D **87** (2013) 044044 [arXiv:1212.4773 [gr-qc]].

[15] J. Mielczarek, arXiv:1304.2208 [gr-qc].

[16] J. Kowalski-Glikman, Phys. Lett. B **499** (2001) 1 [astro-ph/0006250].

Chapter 6

LQC in Bianchi-I space time

Usually, anisotropies are neglected in cosmology. The reason for this is straightforward: in the Friedmann equation the shear term scales as $1/a^6$, it therefore decreases very fast and soon becomes sub-dominant. But, the other way round, during the contracting phase, this term will increase fast and might lead to a so-called "chaotic mixmaster behavior". For example, the ekpyrotic scenario was specifically designed to address this issue thanks to an equation of state $w > 1$.

In the following two articles, we specifically address the question of anisotropies in the framework of LQC. In the first paper, we derive a new effective Friedmann equation for the Bianchi-I LQC Universe that has not been derived before. We start by writing the classical Hamiltonian for a Bianchi-I univers and perform the usual holonomy modification. We then use the symmetries and obtain an equation of motion. We also investigate into the details and plot the Hubble parameters as a function of time for different situations.

Beyond the derivation of the anisotropic Friedmann equation for LQC, the main conclusion of this work is that there are infinitely many sets of solutions – with no possible evolution from one to the other – and only one of these sets are compatible with what we see. Putting initial conditions in the contracting branch, as advocated in the previous works, however automatically selects the set of preferred solutions. But this raises the important question of how to define natural initial conditions for the shear.

The second article on this topic basically consists in using the formalism developed in the first one. A Mathematica simulation was written to investigate many different situations. We address the question of understanding how is the duration of inflation affected by anisotropies that must be taken into account in any consistent bouncing approach. We find that a larger shear will in general lead to a lower energy density at the bounce. The growth of kinetic energy is stopped at a lower value than in the isotropic case, leading to a smaller boost of the potential energy, therefore implying less slow-roll inflation. Of course the unknown phase of the oscillating field in the contracting phase still has an influence on the results. The upper limit on the initial shear so as to have enough e-folds of inflation is explicitly calculated. The conclusion means that if the model is correct, the number of e-folds is probably not much larger that the lower bound required by observations. This is good for phenomenology as the quantum gravity effects may then not have been fully washed out by inflation. But, on the other hand, since there are no natural upper limit on the amount of shear, it is highly likely in this model that the shear completely out competes the matter energy density at the bounce, leading to no inflation at all.

IOP Publishing Classical and Quantum Gravity
Class. Quantum Grav. **31** (2014) 015018 (16pp) doi:10.1088/0264-9381/31/1/015018

Modified Friedmann equation and survey of solutions in effective Bianchi-I loop quantum cosmology

Linda Linsefors and Aurelien Barrau

Laboratoire de Physique Subatomique et de Cosmologie, UJF, INPG, CNRS, IN2P3
53, avenue des Martyrs, F-38026 Grenoble cedex, France

E-mail: linsefors@lpsc.in2p3.fr and Aurelien.Barrau@cern.ch

Received 20 May 2013, in final form 30 October 2013
Published 19 November 2013

Abstract
In this article, we study the equations driving the dynamics of a Bianchi-I universe described by holonomy-corrected effective loop quantum cosmology (LQC). We derive the LQC-modified generalized Friedmann equation, which is used as a guide to find different types of solutions. It turns out that, in this framework, most solutions never reach the classical behavior.

Communicated by P R L V Moniz

Keywords: quantum gravity, quantum cosmology, bouncing cosmology, anisotropic cosmology, Bianchi-I
PACS numbers: 04.60.−m, 98.80.Qc

1. Introduction

Loop quantum gravity (LQG) is a tentative nonperturbative and background-independent quantization of general relativity. It uses Ashtekar variables, namely SU(2) valued connections and conjugate densitized triads. The quantization is obtained through holonomies of the connections and fluxes of the densitized triads (see, e.g., [1] for introductions). Basically, loop quantum cosmology (LQC) is the symmetry reduced version of LQG. In LQC, the big bang is generically replaced by a big bounce due to huge repulsive quantum geometrical effects (see, e.g., [2] for reviews).

In bouncing cosmologies, the issue of anisotropies is however crucial for a simple reason: the shear term basically scales as $1/a^6$ where a is the scale factor of the universe. Therefore, when the universe is in its contraction phase, it is expected that the shear term eventually dominates and drives the dynamics. When spatial homogeneity is assumed, anisotropic hypersurfaces admit transitive groups of motion that must be three- or four-parameters isometry groups. The four-parameters groups admitting no simply transitive subgroups will not be considered here. There are nine algebraically inequivalent three-parameters simply transitive Lie groups, denoted Bianchi I through IX, with well known structure constants. The flat, closed and open generalizations of the FLRW model are respectively Bianchi-I, Bianchi-IX

and Bianchi-V. As the universe is nearly flat today and as the relative weight of the curvature term in the Friedmann equation is decreasing with decreasing values of the scale factor, it is reasonable to focus on the Bianchi-I model to study the dynamics around the bounce.

Many studies have already been devoted to Bianchi-I LQC [3–5]. In particular, it was shown that the bounce prediction is robust. As the main features of isotropic LQC are well captured by semi-classical effective equations, and it is a good guess that this remains true in the extended Bianchi-I case. The solutions of effective equations were studied into the details in [6]. In this work, we focus on slightly different aspects and derive the LQC-modified generalized Friedmann equation that was still missing. Thanks to this equation, we have systematically explored the full solution space in a way that has not been tired before.

2. Classical equations

The metric for a Bianchi-I spacetime reads as:

$$\mathrm{d}s := -N^2\,\mathrm{d}\tau^2 + a_1^2\,\mathrm{d}x^2 + a_2^2\,\mathrm{d}y^2 + a_3^2\,\mathrm{d}z^2, \tag{1}$$

where a_i denote the directional scale factors. A dot means derivation with respect to the cosmic time t, with $\mathrm{d}t = N\mathrm{d}\tau$.

Classically, the evolution of this metric is described by the Hamiltonian

$$\mathcal{H} = \mathcal{H}_G(c_i, p_i) + \mathcal{H}_M(p_i, \phi_n, \pi_n), \tag{2}$$

where

$$\mathcal{H}_G = \frac{N}{\kappa\gamma^2}\left(\sqrt{\frac{p_1p_2}{p_3}}c_1c_2 + \sqrt{\frac{p_2p_3}{p_1}}c_2c_2 + \sqrt{\frac{p_3p_1}{p_2}}c_2c_3\right), \tag{3}$$

and

$$\mathcal{H}_M = N\sqrt{p_1p_2p_3}\,\rho, \tag{4}$$

with the Poison brackets

$$\{c_i, p_j\} = \kappa\gamma\delta_{ij}, \quad \{\phi_n, \pi_m\} = \delta_{mn}, \tag{5}$$

where $i, j \in \{1, 2, 3\}$ and $n, m \in \{1, 2, \ldots, M\}$ for M matter fields. In the following, we have chosen to consider a comoving volume of size $1 \times 1 \times 1$. Since the universe is assumed to be homogenous, this will not affect the results. We denote by ϕ_n the matter fields, π_n their conjugate momentum, and ρ the total matter density. The c_i and p_i entering equation (3) are the diagonal elements of the Ashtekar variables (p_i is assumed to always be positive).

The directional scale factors can be written as

$$a_1 = \sqrt{\frac{p_2p_3}{p_1}} \quad \text{and cyclic expressions.} \tag{6}$$

The generalized Friedmann equation is

$$H^2 = \sigma^2 + \frac{\kappa}{3}\rho, \tag{7}$$

where

$$H := \frac{\dot{a}}{a} = \frac{1}{3}(H_1 + H_2 + H_3), \tag{8}$$

$$a := (a_1a_2a_3)^{1/3}, \tag{9}$$

$$H_1 := \frac{\dot{a}_1}{a_1} = -\frac{\dot{p}_1}{2p_1} + \frac{\dot{p}_3}{2p_3} + \frac{\dot{p}_3}{2p_3} \quad \text{and cyclic expressions,} \tag{10}$$

$$\sigma^2 := \frac{1}{18}[(H_1 - H_2)^2 + (H_2 - H_3)^2 + (H_3 - H_1)^2]. \tag{11}$$

It should be pointed out that the $1/18$ factor is not used in similar studies.

If we assume isotropic matter, that is

$$\mathcal{H}_M(p_i, \phi, \pi) = \mathcal{H}_M(\sqrt{p_1 p_2 p_3}, \phi, \pi), \tag{12}$$

then the equations of motion for H_i become

$$\dot{H}_1 = -H_1^2 + H_2 H_3 - \frac{\kappa}{2}(\rho + P) \quad \text{and cyclic terms,} \tag{13}$$

where P is defined to fulfil the equation $\dot{\rho} = 3H(\rho + P)$, that is

$$P := -\frac{\partial(\mathcal{H}_m/N)}{\partial\sqrt{p_1 p_2 p_3}}. \tag{14}$$

Several other relations will be useful:

$$\dot{H}_i - \dot{H}_j = -3H(H_i - H_j) \quad \Leftrightarrow \quad H_i - H_j \propto a^{-3}, \tag{15}$$

leading to

$$\sigma^2 \propto a^{-6} \quad \text{and} \quad \frac{H_i - H_j}{H_i - H_k} = \text{constant}. \tag{16}$$

Classically H_i can change sign, but H cannot. Many details about the classical behaviors of a Bianchi-I universe can be found, e.g., in [7].

3. Effective holonomy corrections

The holonomy correction in effective LQC is due to the fact that the Ashtekar connection cannot be promoted to be an operator but only its holonomy can. It is believed to capture most quantum effects at the semi-classical level. Following the usual prescription, we perform the substitution

$$c_i \to \frac{\sin(\bar{\mu}_i c_i)}{\bar{\mu}_i} \tag{17}$$

in the Hamiltonian given by equations (2) and (3). The $\bar{\mu}_i$ are given by

$$\bar{\mu}_1 = \lambda\sqrt{\frac{p_1}{p_2 p_3}} \quad \text{and cyclic expressions,} \tag{18}$$

where λ is the square root of the minimum area eigenvalue of the LQG area operator ($\lambda = \sqrt{\Delta}$). This was first proposed in [3], and later derived in [4].

The effective holonomy-corrected gravitational Hamiltonian is

$$\mathcal{H}_G = -\frac{N\sqrt{p_1 p_2 p_3}}{\kappa\,\gamma^2\lambda^2}[\sin(\bar{\mu}_1 c_1)\sin(\bar{\mu}_2 c_2) + \sin(\bar{\mu}_2 c_2)\sin(\bar{\mu}_3 c_3) + \sin(\bar{\mu}_3 c_3)\sin(\bar{\mu}_1 c_1)]. \tag{19}$$

The matter Hamiltonian $\mathcal{H}_M$ remains unchanged.

4. The LQC-modified generalized Friedmann equation

Various versions of the Friedmann equation—depending on the specific model considered—are used in cosmology. They allow to derive the key features of the dynamics in a simple way. The LQC-modified generalized Friedmann equation describing a holonomy-corrected Bianchi-I universe has so far been missing. It is derived in this section and, in more details, in the appendix.

The Friedmann equation is found by rewriting the constraint $\mathcal{H} = 0$ in terms of physical parameters. In our case, these parameters are: the total Hubble parameter, matter density and

shear. We start by finding the directional and total Hubble parameters as functions of c_i and p_i:

$$\dot{p}_1 = \frac{1}{N}\{p_1, \mathcal{H}\} = \frac{p_1}{\gamma\lambda}\cos(\bar{\mu}_1 c_1)[\sin(\bar{\mu}_2 c_2) + \sin(\bar{\mu}_3 c_3)] \quad \text{and cyclic expressions.} \tag{20}$$

From this, we get the directional Hubble parameters H_i and total Hubble parameter H:

$$H_1 = -\frac{\dot{p}_1}{2p_1} + \frac{\dot{p}_2}{2p_2} + \frac{\dot{p}_3}{2p_3} = \frac{1}{2\gamma\lambda}[\sin(\bar{\mu}_2 c_2 + \bar{\mu}_3 c_3) + \sin(\bar{\mu}_1 c_1 - \bar{\mu}_2 c_2) + \sin(\bar{\mu}_1 c_1 - \bar{\mu}_3 c_3)] \quad \text{and cyclic,} \tag{21}$$

$$H := \frac{1}{3}(H_1 + H_2 + H_3) = \frac{1}{6\gamma\lambda}[\sin(\bar{\mu}_1 c_1 + \bar{\mu}_2 c_2) + \sin(\bar{\mu}_2 c_2 + \bar{\mu}_3 c_3) + \sin(\bar{\mu}_3 c_3 + \bar{\mu}_1 c_1)]. \tag{22}$$

We also define the 'quantum shear' as:

$$\sigma_Q^2 := \frac{1}{3\lambda^2\gamma^2}\left(1 - \frac{1}{3}[\cos(\bar{\mu}_1 c_1 - \bar{\mu}_2 c_2) + \cos(\bar{\mu}_2 c_2 - \bar{\mu}_3 c_3) + \cos(\bar{\mu}_3 c_3 - \bar{\mu}_1 c_1)]\right). \tag{23}$$

Then, it is possible to derive the LQC-modified generalized Friedmann equation:

$$H^2 = \sigma_Q^2 + \frac{\kappa}{3}\rho - \lambda^2\gamma^2\left(\frac{3}{2}\sigma_Q^2 + \frac{\kappa}{3}\rho\right)^2. \tag{24}$$

The details of how to obtain this non-trivial equation are given in the appendix. It should be pointed out that

$$\lim_{\lambda\to 0}\sigma_Q^2 = \lim_{\lambda\to 0}\sigma^2, \tag{25}$$

so that in the limit $\lambda \to 0$ the classical Friedmann equation is recovered. On the other hand, in the limit $\sigma_Q^2 \to 0$, the isotropic holonomy-corrected Friedmann equation is recovered.

From equation (24), we can easily find the upper bounds for ρ and σ_Q^2:

$$\rho \leqslant \rho_c := \frac{3}{\kappa}\frac{1}{\lambda^2\gamma^2}, \tag{26}$$

$$\sigma_Q^2 \leqslant \sigma_{Q_c}^2 := \frac{4}{9}\frac{1}{\lambda^2\gamma^2}. \tag{27}$$

5. Equations of motion

In the gravitational sector, the information is contained in the combined objects h_i:

$$h_1 := \bar{\mu}_1 c_1 = \lambda\sqrt{\frac{p_1}{p_2 p_3}}c_1 \quad \text{and cyclic expressions.} \tag{28}$$

It is expected that the six gravitational degrees of freedom (c_i, p_i) account for only three physical degrees of freedom h_i. This is because three degrees of freedom are just rescaling of the scale factors which have no physical meaning.

Just as in the classical calculations, we assume isotropic matter. Then we can derive:

$$\dot{h}_1 = \frac{1}{N}\{h_1, \mathcal{H}\} = \frac{1}{2\gamma\lambda}[(h_2 - h_1)(\sin h_1 + \sin h_3)\cos h_2 + (h_3 - h_1)(\sin h_1 + \sin h_2)\cos h_3] - \frac{\kappa\gamma\lambda}{2}(\rho + P) \quad \text{and cyclic expressions,} \tag{29}$$

where we have used the constraint $\mathcal{H}_G + \mathcal{H}_M = 0$. Thus we have

$$(\dot{h}_i - \dot{h}_j) = -3H(h_i - h_j), \tag{30}$$

which means that

$$(h_i - h_j) \propto a^{-3} \quad \text{and} \quad \frac{h_i - h_j}{h_i - h_k} = \text{constant}. \tag{31}$$

This should be compared with the classical results given by equations (15) and (16).

6. Symmetries of the effective quantum equations

Equations (21)–(24) are invariant under the discrete symmetry

$$\begin{cases} h_1 \to h_1 + (2\tilde{n}_1 + \tilde{m})\pi \\ h_2 \to h_2 + (2\tilde{n}_2 + \tilde{m})\pi \\ h_3 \to h_3 + (2\tilde{n}_3 + \tilde{m})\pi \end{cases}, \quad \begin{array}{l} \forall \tilde{n}_1, \tilde{n}_2, \tilde{n}_3 \in \mathbf{Z} \\ \forall \tilde{m} \in \{0, 1\}. \end{array} \tag{32}$$

However, equation (29) is only invariant under the smaller symmetry

$$\begin{cases} h_1 \to h_1 + \tilde{n}\pi \\ h_2 \to h_2 + \tilde{n}\pi \\ h_3 \to h_3 + \tilde{n}\pi \end{cases}, \quad \forall \tilde{n} \in \mathbf{Z}. \tag{33}$$

Remember that $h_i = \bar{\mu}_i c_i$.

All observable quantities, and their evolution, are invariant under equation (33). This suggests that equation (33) is a gauge symmetry. However, this might not be the case, if more degrees of freedom are taken into account.

More consequences of these symmetries will be discussed later.

7. Classical limit

As one would expect, the classical equations are recovered in the limit $\lambda \to 0$. But one also expects to find a classical limit in the far future and in the remote past, far away from the bounce. We will therefore investigate for what values of h_i and ρ classical equations are recovered.

For $\sigma_Q^2 \ll \sigma_{Q_c}^2$ and $\rho \ll \rho_c$, equation (24) becomes

$$H^2 = \sigma_Q^2 + \frac{\kappa}{3}\rho, \tag{34}$$

to first order in σ_Q^2 and ρ. The above equation is equivalent to equation (7) if and only if $\sigma_Q^2 = \sigma^2$. It is trivial to check that this is the case, to lowest order in h_i if $h_i \ll 1$. But since σ_Q^2 and σ^2 are cyclic expressions of h_i, this is not the only region where equation (7) is recovered from (24).

Equation (7) is not enough to completely describe the classical system. To say that we have a classical limit, we also need to recover equation (13). The matter equations are assumed to be unaffected by the holomomy corrections.

The symmetries, equations (32) and (33), suggest the existence of more than one classical limit. And the knowledge of these symmetries could of course be used in the search for such limits. However, to be absolutely certain that we find all regions of classical behavior, we will search in the full parameter space.

We will try to recover the classical equations, equations (7) and (13), from the quantum modified equations (24), in the perturbative regime. But, instead of assuming, for example,

that h_i and ρ are small, an thus make an expansion around $(h_i, \rho) = (0, 0, 0, 0)$, we will expand around the more general point $(h_i, \rho) = (h_i^{(0)}, \rho^{(0)})$. We define

$$\begin{aligned} \delta h_i &:= h_i - h_i^{(0)}, \\ \delta\rho &:= \rho - \rho^{(0)}. \end{aligned} \tag{35}$$

In this section, we will find all points $(h_i^{(0)}, \rho^{(0)})$, such that, for $\delta h_i \ll 1$ and $\delta\rho \ll \rho_c$, equations (7) and (13) are recovered from the expressions given in sections 4 and 5.

All the following calculations in this section will be carried out to lowest order in δh_i and $\delta\rho$. We will also use the notations

$$\begin{aligned} \delta\sigma^2 &:= \sigma^2 - (\sigma^2)^{(0)} := \sigma^2(h_i) - \sigma^2\big(h_i^{(0)}\big), \\ \delta\sigma_Q^2 &:= \sigma_Q^2 - \big(\sigma_Q^2\big)^{(0)} := \sigma_Q^2(h_i) - \sigma_Q^2\big(h_i^{(0)}\big). \end{aligned} \tag{36}$$

It should be pointed out at this stage that, even though we assume $\delta\rho \ll \sigma_c$, and indirectly $\delta\sigma^2, \delta\sigma_Q^2 \ll \delta\sigma_{Q_c}^2$, this does not mean that the energy density and shear have to be small in a classical sense. This is because ρ_c and $\delta\sigma_{Q_c}^2$ have very large values.

Combining equations (7) and (24) we find that in the classical limit

$$\sigma^2 = \sigma_Q^2 - \lambda^2\gamma^2\left(\frac{3}{2}\sigma_Q^2 + \frac{\kappa}{3}\rho\right)^2. \tag{37}$$

Expanded, this becomes

$$\begin{aligned} (\sigma^2)^{(0)} + \delta\sigma^2 = \big(\sigma_Q^2\big)^{(0)} + \delta\sigma_Q^2 - \lambda^2\gamma^2\left(\frac{3}{2}\big(\sigma_Q^2\big)^{(0)} + \frac{\kappa}{3}\rho^{(0)}\right)^2 \\ -2\lambda^2\gamma^2\left(\frac{3}{2}\big(\sigma_Q^2\big)^{(0)} + \frac{\kappa}{3}\rho^{(0)}\right)\left(\frac{3}{2}\delta\sigma_Q^2 + \frac{\kappa}{3}\delta\rho\right). \end{aligned} \tag{38}$$

It should be noticed that $\delta\sigma$ and $\delta\sigma_Q^2$ are not independent variables since they both depend on δh_i. However, $\delta\rho$ is independent of $\delta\sigma$ and $\delta\sigma_Q^2$. The left-hand side of the above equation does not depend on $\delta\rho$, and since this equation has to be identically fulfilled in the classical limit, the pre-factor in front of $\delta\rho$ on the right-hand side must vanish,

$$\frac{3}{2}\big(\sigma_Q^2\big)^{(0)} + \frac{\kappa}{3}\rho^{(0)} = 0. \tag{39}$$

As $\sigma_Q^2 \geqslant 0$ and $\rho \geqslant 0$ at any time, the only solution is

$$\big(\sigma_Q^2\big)^{(0)} = \rho^{(0)} = 0. \tag{40}$$

Combing the above equation with the definition of σ_Q^2 in equation (23), we find:

$$\cos\big(h_i^{(0)} - h_j^{(0)}\big) = 1, \tag{41}$$

which can be translated into

$$\begin{aligned} h_2^{(0)} &= h_1^{(0)} + n_2 2\pi, \quad n_2 \in \mathbf{Z}, \\ h_3^{(0)} &= h_1^{(0)} + n_3 2\pi, \quad n_3 \in \mathbf{Z}. \end{aligned} \tag{42}$$

The other equation that has to be satisfied in the classical limit is equation (13). The left-hand side of equation (13) is calculated from $\dot{H}_i = \sum_j \frac{\partial H_i}{\partial h_j}\dot{h}_j$, where $\dot{h}_j$ is given by equation (29). The right-hand side is calculated by inserting expressions for H_i given by equation (21).

Equation (13) should be fulfilled for all $\delta h_i \ll 1$, and therefore also for $\delta h_i = 0$. Applying equation (42) and $\delta h_i = 0$ to equation (13), we get

$$\frac{\pi(n_2 + n_3)}{2\gamma^2\lambda^2}\big[3 - \cos\big(2h_1^{(0)}\big)\big]\sin\big(2h_1^{(0)}\big) - \cos\big(2h_1^{(0)}\big)\frac{\kappa}{2}(\rho + P) = -\frac{\kappa}{2}(\rho + P). \tag{43}$$

Since this equation has to be identically fulfilled for all matter states, the pre-factor in front of $(\rho + P)$ has to be the same on both sides. Therefore $\cos(2h_1^{(0)}) = 1$, which is equivalent to

$$h_1^{(0)} = n_1\pi, \quad n_1 \in \mathbf{Z}. \tag{44}$$

This also solves the rest of equation (43).

We also need to recover equation (13) for all $\delta h_i \ll 1$, not equal to zero. Expanding equation (13) to first order in δh_i and using equations (42) and (44) we get

$$\frac{\pi}{\gamma^2\lambda^2}[(n_2 + n_3)\delta h_1 + n_3\delta h_2 + n_2\delta h_3] = 0. \tag{45}$$

For this to be identically fulfilled for all $\delta h_i \ll 1$, we must have $n_2 = n_3 = 0$. Finally, we find that

$$h_1^{(0)} = h_2^{(0)} = h_3^{(0)} = n\pi, \quad n \in \mathbf{Z}. \tag{46}$$

In the classical limit, equation (21) becomes

$$H_i = \frac{\delta h_i}{\gamma\lambda} \ll \frac{1}{\gamma\lambda} \tag{47}$$

and

$$\begin{aligned} \sigma_Q^2 &= \sigma^2, \\ &= \frac{1}{18\gamma^2\lambda^2}[(h_1 - h_2)^2 + (h_2 - h_3)^2 + (h_3 - h_1)^2], \\ &\ll \sigma_{Q_c}^2. \end{aligned} \tag{48}$$

We also have

$$\rho = \rho^{(0)} + \delta\rho = \delta\rho \ll \rho_c. \tag{49}$$

This means that if we are in the classical limit, the Hubble parameters, the shear and the energy density, are small compared to the scale of quantum effects. We want to remind the reader that $\sigma_{Q_c}^2$ and ρ_c are of the order of Plank values, which are very large compared to anything expected during most of the evolution of the universe.

However, $\sigma_Q^2 \ll \sigma_{Q_c}^2$ and $\rho \ll \rho_c$ do not guarantee the classical behavior. This can be seen from the symmetries presented in section 6. A change of h_i belonging to the symmetry group equation (32) but not to equation (33) will give unchanged values of σ_Q^2 and ρ but will change the dynamics away from the classical one. For example, the evolutions in figures 7 and 8 have low energy density through the whole simulation, and passes trough regions of low share and Hubble rates, but never behaves classically.

From the symmetry, equation (33), we can also conclude that all classical limits are equivalent within this framework.

It should be noticed that we have not assumed anything about the pressure. That means that any pressure is allowed in the classical limit.

Finally, it should be stressed that this analysis does not claim that the shear cannot be large when compared to the other terms in the classical limit of the Friedmann equations. Usual Bianchi-I can appear as the classical limit of quantum Bianchi-I. Rather, the shear and density have to be small when compared to their maximum allowed values.

8. Allowed regions in parameter space

Figure 1 displays the parameter space projected down on to $(h_2 - h_1, h_3 - h_1)$. In this projection, the space is devised into allowed and forbidden regions by the requirement $\sigma_Q^2 \leqslant \sigma_{Q_c}^2$. The boundaries of those regions, e.g. when $\sigma_Q^2 = \sigma_{Q_c}^2$, correspond to

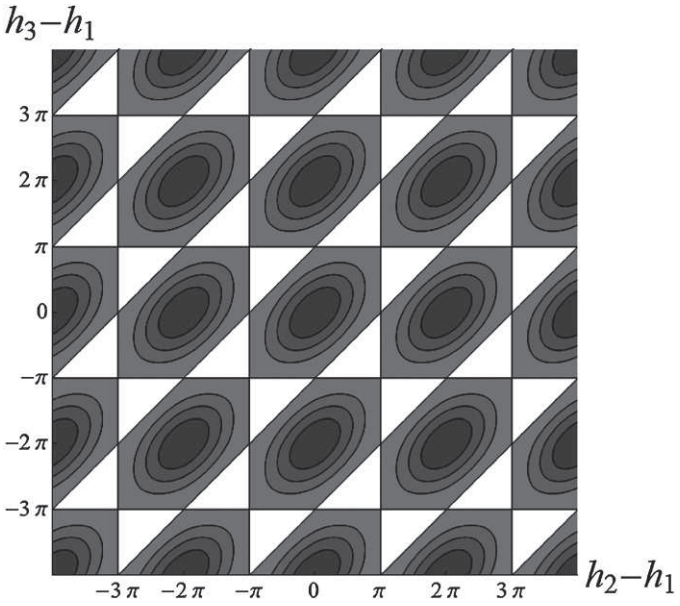

Figure 1. σ_Q^2 as a function of $h_2 - h_1$ (x-axis) and $h_3 - h_1$ (y-axis). The white areas correspond to $\sigma_Q^2 > \sigma_{Q_c}^2$, which is forbidden by the modified Friedman equation (24). The black lines are $\sigma_Q^2 = \frac{1}{4}\sigma_{Q_c}^2, \frac{1}{2}\sigma_{Q_c}^2, \frac{3}{4}\sigma_{Q_c}^2, \sigma_{Q_c}^2$.

$$h_i - h_j = (2m+1)\pi, \quad i \neq j\ ,\ m \in \mathbf{Z}. \tag{50}$$

The pattern showed in figure 1 goes on infinitely in all directions, which means that there is an infinite number of allowed regions. But, from equation (46), on can see that there is only one point in this projection near which it is possible to recover the classical limit, and that is $(h_2 - h_1, h_3 - h_1) = (0, 0)$.

An interesting question one can ask is: is it possible, within this framework, to dynamically pass between allowed region? The answers is no, as we shall show in this section.

The allowed regions are only connected by points, therefore any evolution between regions has to pass though these points, defined by:

$$\begin{matrix} h_j - h_i = (2m_1+1)\pi \\ h_k - h_i = (2m_2+1)\pi \end{matrix}, \begin{cases} i \neq j \neq k \neq i \\ m_1, m_2 \in \mathbf{Z} \end{cases}. \tag{51}$$

Any point on the boundary of the allowed regions, including the points connecting regions can only be reached when $\rho = 0$. But even without matter dynamical transitions between regions are impossible. The argument is as follow,

$$\rho = 0 \ \Leftrightarrow\ \mathcal{H}_M = 0 \ \Leftrightarrow\ \mathcal{H}_G = 0 \tag{52}$$

which is equivalent to

$$\sin h_1 \sin h_2 + \sin h_2 \sin h_3 + \sin h_3 \sin h_1 = 0. \tag{53}$$

Combining the above expression with equations (51) gives

$$0 = \sin h_i(-\sin h_i) + (-\sin h_i)\sin h_i + (-\sin h_i)(-\sin h_i) = -\sin^2 h_i. \tag{54}$$

By once again using equations (51) with the above relation, one gets:

$$\begin{matrix} h_i = (m_3 - 1)\pi \\ h_j = (2m_1 + m_3 + 1)\pi, \\ h_k = (2m_2 + m_3 + 1)\pi \end{matrix} \begin{cases} i \neq j \neq k \neq i \\ m_1, m_2, m_3 \in \mathbf{Z}. \end{cases} \tag{55}$$

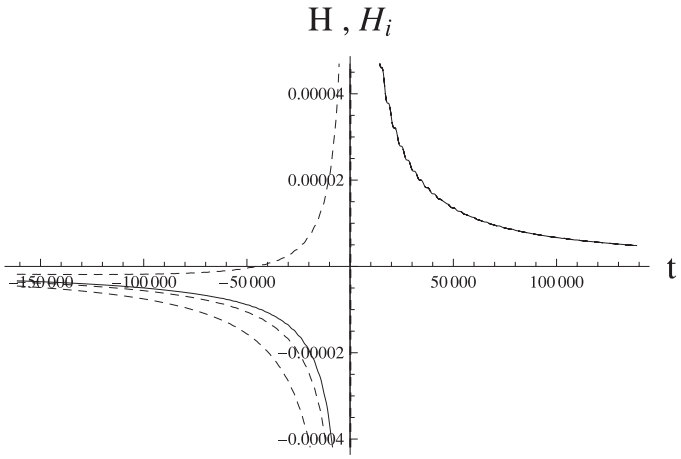

Figure 2. The full line is the total Hubble factor H and the tree dashed lines are the directional Hubble factors H_i, as a function of time.

Inserting this into equation (29), we obtain $\dot{h} = 0$ in all the connection points. Therefore those points can never be dynamically reached. Transitions between the allowed regions displayed in figure 1 are not possible, even without matter.

Whatever the region chosen by initial conditions, the solution will stay in that region. In other words, there are infinitely many solutions that never reach a classical limit. However if we assume that the universe starts out in the classical limit of a contracting universe, then the correct region is picked up from the beginning and the evolution will end up in the classical limit of an expanding universe.

It is however meaningful to wonder what happened to all the solutions that live in regions without classical limits. We find a clue in equation (31). Since in all the non-classical regions there is a lower bound for at least two of the differences $h_i - h_j$, there must also be an upper bound on a. This leaves two possibilities, either the solution approaches a constant a or the solution oscillates forever, leading to multiple bounces. Simulations favor the second hypothesis.

Equation (31) can be seen as an independent proof of the fact that there is no classical limit in regions not containing $h_i - h_j$ for all $i, j = 1, 2, 3$. Classically, a is unbounded, and this is only possible if $h_i - h_j$ is allowed to be arbitrarily close to zero.

9. Numerical solutions

In this section we present some typical examples of numerically generated solutions, both with and without classical limit. In all simulations the matter is taken to be a single massive scalar field, $V(\phi) = m^2\phi^2/2$, $m = 10^{-3}$. The equations used in the simulations are equations (29) and the matter equation

$$\ddot{\phi} + 3H\dot{\phi} + m^2\phi = 0, \tag{56}$$

with H expressed as a function of h_i.

Figures 2–5 are all plots from the same numerical simulations with parameters in the region containing the classical limit. In figure 2, we see that, initially, all the directional scale factors are negative but, still in the classical region, one of them changes sign. After the bounce $H_1 \approx H_2 \approx H_3 \approx H$. This is because the matter caused a short inflation—as

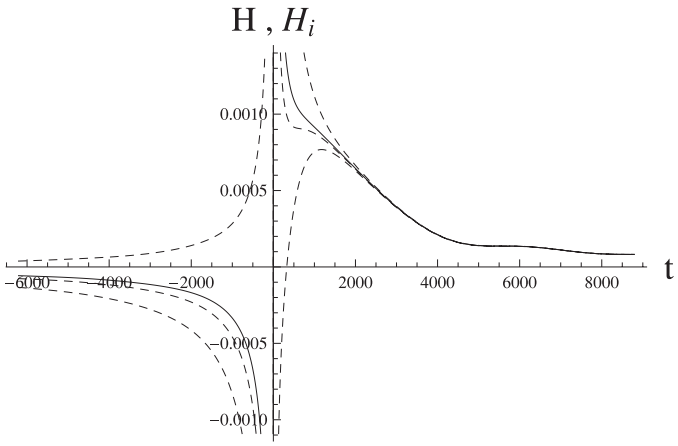

Figure 3. Zoom of figure 2 round the bounce. The full line is the total Hubble factor H and the tree dashed lines are the directional Hubble factors H_i, as a function of time.

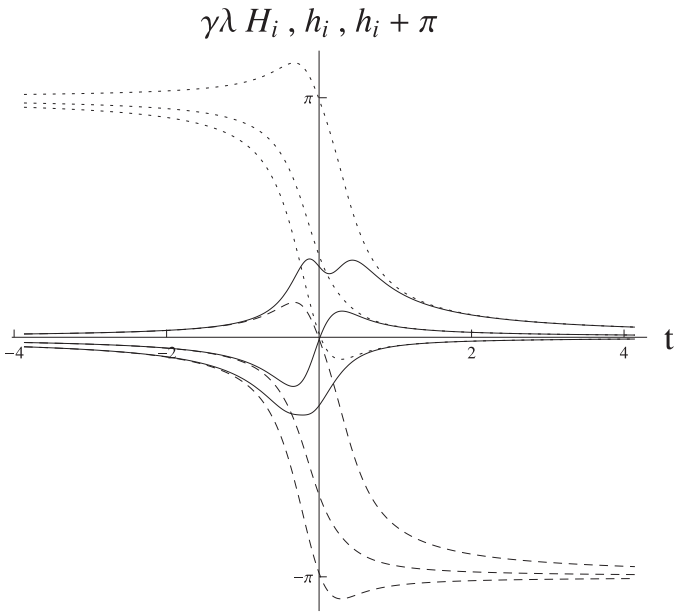

Figure 4. The full lines are $\gamma\lambda H_i$, the dashed lines are h_i and the dotted lines are $h_i + \pi$, as a function of time.

can be seen more clearly in figure 3 which is a zoom around the bounce. Figure 4 is an even closer zoom. Here the quantum effects can be seen. The classical equations are a good approximation until $h_i/(\gamma\lambda)$ deviates from H_i. The classical equations become a good approximation again when $H_i \approx (h_i - \pi)/(\gamma\lambda)$. During the bounce all the h_i are shifted by π compared to $\gamma\lambda H_i$. Simulations suggest that this shift always occurs. This specific solution exhibits a shear-dominated bounce. This can be seen in figure 5 since $\sigma_Q^2 \gg \frac{\kappa}{3}\rho$ at the bounce.

Simulations show that σ^2 is typically not symmetric around the bounce. For solutions with a classical limit, it appears to be the case that σ^2 is symmetric around the bounce if and only

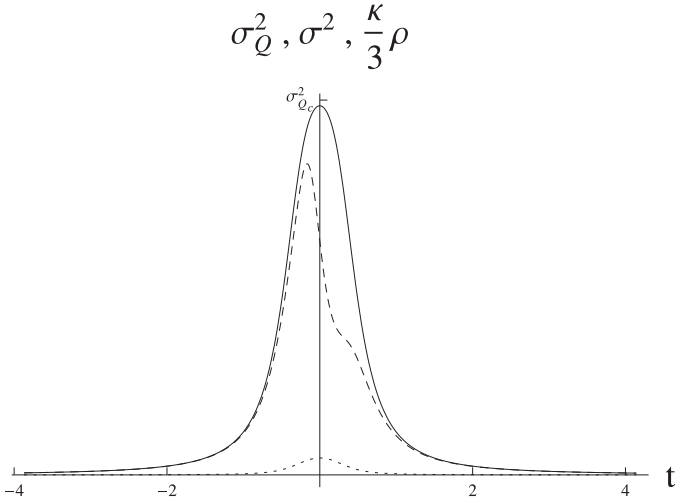

Figure 5. The full line is σ_Q^2, the dashed line is σ^2 and the dotted line is ρ, as a function of time.

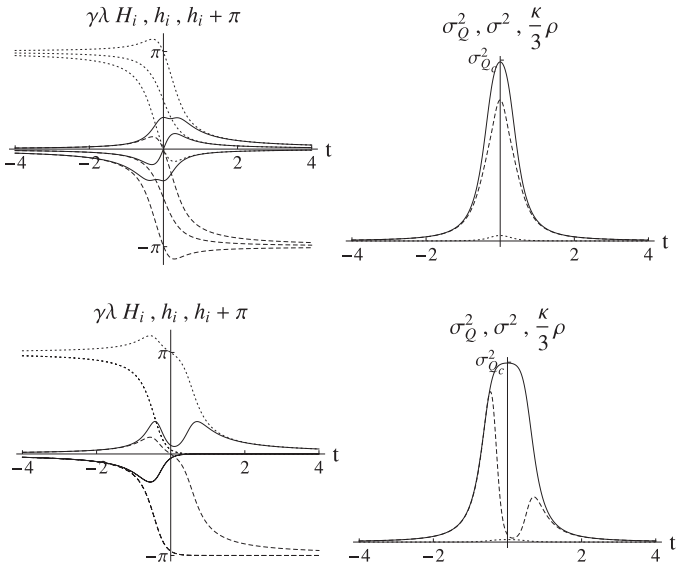

Figure 6. Upper: a solution with maximally symmetric anisotropy. Lower: a solution with maximally asymmetric anisotropy. Left: the full lines are $\gamma\lambda H_i$, the dashed lines are h_i and the dotted lines are $h_i + \pi$, as a function of time. Right: the full line is σ_Q^2, the dashed line is σ^2 and the dotted line is ρ, as a function of time.

if $h_i - h_j = h_j - h_k$ for some value of $i \neq j \neq k \neq i$. We therefore call this case maximally symmetric anisotropy. The opposite case is when $h_i = h_j \neq h_k$ for some $i \neq j \neq k \neq i$, and we call this maximally asymmetric anisotropy. Plots similar to figures 4 and 5, for the maximally symmetric and asymmetric cases are showed in figure 6.

Figures 7 and 8 are both plots from the same numerical simulations but with parameters in a region with no classical limit. One can see that the behavior is oscillatory and does not resemble anything classically expected.

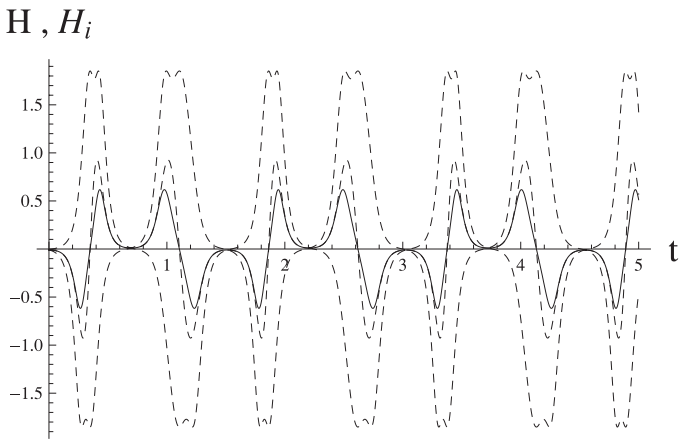

Figure 7. The full line is the total Hubble factor H and the tree dashed lines are the directional Hubble factors H_i, as a function of time.

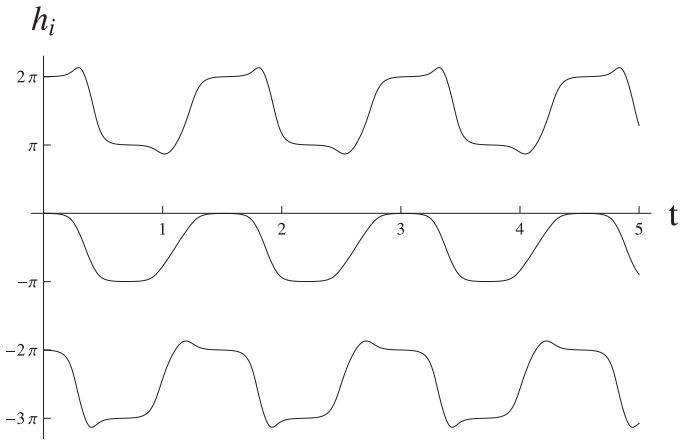

Figure 8. h_i as a function of time in a region without classical limit.

The simulation shown in figures 9–11 is generated by taking, as initial conditions, the values for h_i, ϕ and $\dot{\phi}$, as given by the solution shown in figure 2–5 at the bounce, with the only difference that $h_i \to h_i + 2\pi$ for $i = 1, 2, 3$ respectively.

Figures 9–11 all show oscillatory solutions with periods in the range 1–2 Plank times. These simulations clearly illustrate that equation (32) is not a symmetry of the full system. There are some similarities between figures 4 and 9, just around the bounce but the time scale is different by about a factor 4. The solutions in figures 10 and 11 are very different from anything classical.

10. Discussion

The results presented in this paper raise an important question for loop quantum cosmology. If the initial conditions are to be put at the bounce, as advocated e.g. in [8], we face a delicate problem: there are infinitely many more cases leading to universes that do not resemble ours than cases leading to a classically expanding universe. On the other hand, if we set the initial

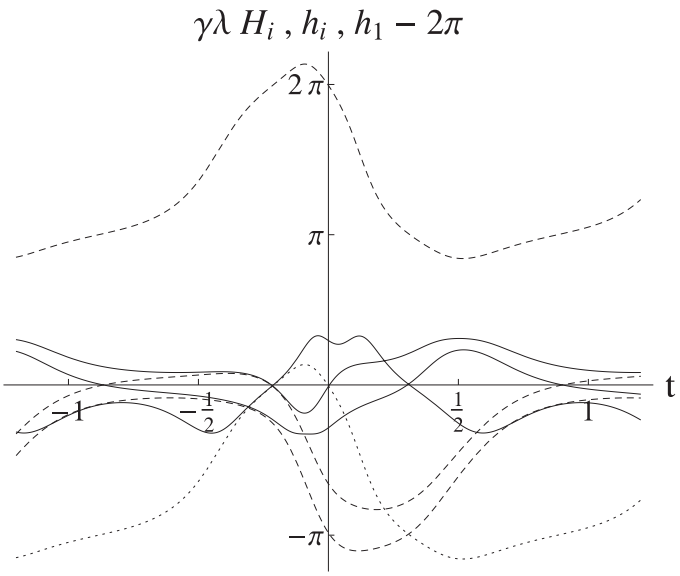

Figure 9. This solution is generated by taking the initial conditions at the bounce with the same values as the solution in figure 2–5 but adding 2π to h_1. The full line are $\gamma\lambda H_i$, the dashed lines are h_i and the dotted line is $h_1 - 2\pi$.

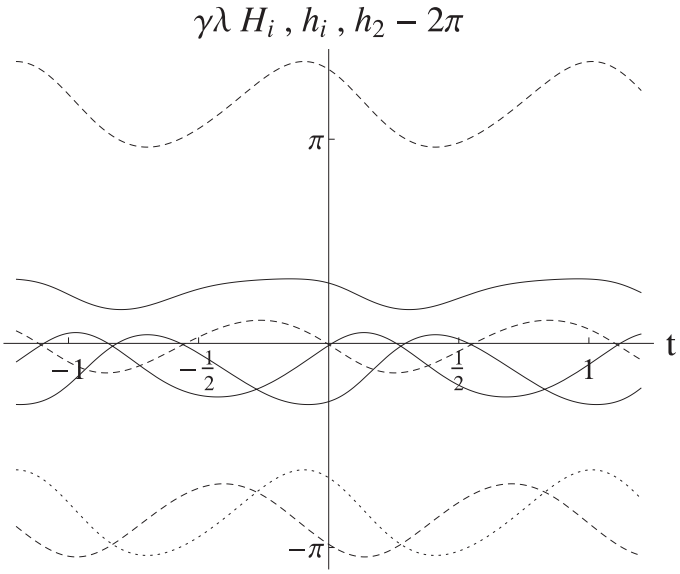

Figure 10. This solution is generated by taking the initial conditions at the bounce with the same values as the solution in figure 2–5 but adding 2π to h_2. The full line are $\gamma\lambda H_i$, the dashed lines are h_i and the dotted line is $h_2 - 2\pi$.

conditions in the classically contracting phase, as advocated in [9], we escape this problem. But we face another one: what is the 'natural' initial shear? Or, according to which measure—and at which time—should we assume a flat probability distribution function for variables quantifying the shear? In any case, this requires a deep rethinking of the initial conditions problem.

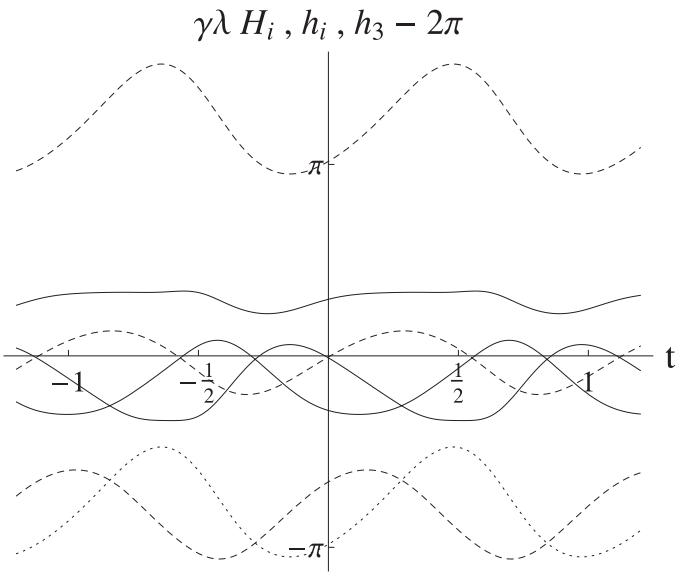

Figure 11. This solution is generated by taking the initial conditions at the bounce with the same values as the solution in figure 2–5 but adding 2π to h_3. The full line are $\gamma\lambda H_i$, the dashed lines are h_i and the dotted line is $h_3 - 2\pi$.

However, we do not yet know what is the physical meaning of the solutions without classical limit. To understand this better the results presented here, should be compared with, e.g., results found when quantizing this system.

It may also be the case that transitions between different regions in figure 1 are possible when including a non-zero curvature.

This work should also be extended so as to generalize the results presented in [9]: how will the prediction of the duration of inflation be modified by including anisotropies? This question has been partly addressed already in [6], however, only for a very narrow range of initial conditions.

Acknowledgments

We want to thank the referee for insightful discussions that have led to an important improvement in the formulation of this paper. This work was supported by the Labex ENIGMASS.

Appendix. Derivation of the modified generalized Friedmann equation

We define:

$$s_+ = \tfrac{1}{3}[\sin(h_1 + h_2) + \sin(h_2 + h_3) + \sin(h_3 + h_1)], \tag{A.1}$$

$$c_\pm = \tfrac{1}{3}[\cos(h_1 \pm h_2) + \cos(h_2 \pm h_3) + \cos(h_3 \pm h_1)]. \tag{A.2}$$

The average Hubble parameter can now be written as:

$$H = \frac{s_+}{2\gamma\lambda}. \tag{A.3}$$

By using elementary trigonometric relations $\sin(a)\sin(b) = (\cos(a-b) - \cos(a+b))/2$ and $\cos(a)\cos(b) = (\cos(a-b) + \cos(a+b))/2$, we find:

$$s_+^2 + c_+^2 = \frac{1 + 2c_-}{3}, \tag{A.4}$$

and

$$\mathcal{H}_G = \frac{3N\sqrt{p_1 p_2 p_3}}{2\kappa\gamma^2\lambda^2}(c_+ - c_-). \tag{A.5}$$

The constraint $\mathcal{H}_G + \mathcal{H}_M = 0$ then becomes

$$c_+ - c_- = -2\gamma^2\lambda^2\frac{\kappa}{3}\rho. \tag{A.6}$$

One can now use equations (A.4) and (A.6) to rewrite H^2 as a function of c_-. It will turn out to be useful to expand this expression in terms of $(1 - c_-)$. We re-express equations (A.4) and (A.6) as

$$s_+^2 = 1 - \tfrac{2}{3}(1 - c_-) - c_+^2, \tag{A.7}$$

$$c_+ = 1 - \left[(1 - c_-) + 2\gamma^2\lambda^2\frac{\kappa}{3}\rho\right]. \tag{A.8}$$

This allows us to write:

$$\begin{aligned} H^2 = \frac{s_+^2}{4\gamma^2\lambda^2} &= \frac{1}{4\gamma^2\lambda^2}\left(1 - \frac{2}{3}(1 - c_-) - c_+^2\right) \\ &= \frac{1}{4\gamma^2\lambda^2}\left(-\frac{2}{3}(1 - c_-) + 2\left[(1 - c_-) + 2\gamma^2\lambda^2\frac{\kappa}{3}\rho\right]\right. \\ &\quad \left. - \left[(1 - c_-) + 2\gamma^2\lambda^2\frac{\kappa}{3}\rho\right]^2\right) \\ &= \frac{1 - c_-}{3\gamma^2\lambda^2} + \frac{\kappa}{3}\rho - \gamma^2\lambda^2\left(\frac{1 - c_-}{2\gamma^2\lambda^2} + \frac{\kappa}{3}\rho\right)^2, \end{aligned} \tag{A.9}$$

where we have used equation (A.7) for the second equality, and equation (A.8) for the third equality.

It can now be seen that, to first order, $(1 - c_-)/(3\gamma^2\lambda^2)$ appears just like the shear in the classical equation (7). It can therefore be labeled the quantum shear

$$\sigma_Q^2 := \frac{1 - c_-}{3\gamma^2\lambda^2}, \tag{A.10}$$

which is exactly equation (23). Re-inserting this definition into equation (A.9), we find exactly equation (24).

References

[1] Dona P and Speziale S 2010 arXiv:1007.0402V1
Perez A 2004 arXiv:gr-qc/0409061v3
Gambini R and Pullin J 2011 *A First Course in Loop Quantum Gravity* (Oxford: Oxford University Press)
Rovelli C 2011 arXiv:1102.3660v5 [gr-qc]
Rovelli C 2004 *Quantum Gravity* (Cambridge: Cambridge University Press)
Rovelli C 1998 *Living Rev. Rel.* **1** 1
Smolin L 2004 arXiv:hep-th/0408048v3
Thiemann T 2003 *Lect. Notes Phys.* **631** 41
Thiemann T 2007 *Modern Canonical Quantum General Relativity* (Cambridge: Cambridge University Press)

[2] Ashtekar A, Bojowald M and Lewandowski J 2003 *Adv. Theor. Math. Phys.* **7** 233
Ashtekar A 2009 *Gen. Rel. Grav.* **41** 707
Ashtekar A and Singh P 2011 *Class. Quantum Grav.* **28** 213001
Bojowald M 2008 *Living Rev. Rel.* **11** 4
Bojowald M 2012 arXiv:1209.3403 [gr-qc]

Banerjee K, Calcagni G and Martin-Benito M 2012 *SIGMA* **8** 016
Calcagni G 2013 *Ann. Phys.* **525** 323
Agullo I and Corichi A 2013 arXiv:1302.3833 [gr-qc]
[3] Chiou D-W and Vandersloot K 2007 *Phys. Rev.* D **76** 084015
[4] Ashtekar A and Wilson-Ewing E 2009 *Phys. Rev.* D **79** 083535
[5] Cartin D and Khanna G 2005 *Phys. Rev. Lett.* **94** 111302
Date G 2005 *Phys. Rev.* D **72** 067301
Cartin D and Khanna G 2005 *Phys. Rev.* D **72** 084008
Chiou D-W 2007 *Phys. Rev.* D **75** 024029
Chiou D-W 2007 arXiv:gr-qc/0703010
Chiou D-W 2007 *Phys. Rev.* D **76** 124037
Szulc L 2008 *Phys. Rev.* D **78** 064035
Martin-Benito M, Marugan G A M and Pawlowski T 2008 *Phys. Rev.* D **78** 064008
Chiou D-W 2008 arXiv:0812.0921 [gr-qc]
Dzierzak P and Piechocki W 2009 *Phys. Rev.* D **80** 124033
Martin-Benito M, Marugan G A M and Pawlowski T 2009 *Phys. Rev.* D **80** 084038
Dzierzak P and Piechocki W 2012 *Ann. Phys.* **19** 290
Malkiewicz P, Piechocki W and Dzierzak P 2011 *Class. Quantum Grav.* **28** 085020
Martin-Benito M, Garay L J, Marugan G A Mena and Wilson-Ewing E 2012 *J. Phys.: Conf. Ser.* **360** 012031
Rikhvitsky V, Saha B and Visinescu M 2012 *Astrophys. Space Sci.* **339** 371
Singh P 2012 *Phys. Rev.* D **85** 104011
Cianfrani F, Marchini A and Montani G 2012 *Europhys. Lett.* **99** 10003
Fujio K and Futamase T 2012 *Phys. Rev.* D **85** 124002
Singh P 2012 *J. Phys.: Conf. Ser.* **360** 012008
Liu X, Huang F and Zhu J-Y 2013 *Class. Quantum Grav.* **30** 065010
Yue X-J and Zhu J-Y 2013 arXiv:1302.1014 [gr-qc]
[6] Gupt B and Singh P 2013 arXiv:1304.7686 [gr-qc]
[7] Jacobs K C 1969 Bianchi-I cosmological models *PhD Thesis* Caltech
[8] Ashtekar A and Sloan D 2012 *Phys. Lett.* B **694** 108
Ashtekar A and Sloan D 2011 *Gen. Rel. Grav.* **43** 3519
[9] Linsefors L and Barrau A 2013 arXiv:1301.1264 [gr-qc]

IOP Publishing Classical and Quantum Gravity
Class. Quantum Grav. **32** (2015) 035010 (15pp) doi:10.1088/0264-9381/32/3/035010

Exhaustive investigation of the duration of inflation in effective anisotropic loop quantum cosmology

Linda Linsefors and Aurelien Barrau

LPSC, Universit Grenoble-Alpes, CNRS/IN2P3 53, avenue des Martyrs, F-38026 Grenoble cedex, France

E-mail: linsefors@lpsc.in2p3.fr and Aurelien.Barrau@cern.ch

Received 27 August 2014, revised 27 October 2014
Accepted for publication 17 November 2014
Published 8 January 2015

Abstract

This article addresses the issue of estimating the duration in inflation in bouncing cosmology when anisotropies, inevitably playing an important role, are taken into account. It is shown that in Bianchi-I loop quantum cosmology, the higher the shear, the shorter the period of inflation. In a range of parameters, the probability distribution function of the duration of inflation is, however, peaked at values compatible with the data, but not much higher. This makes the whole bounce/inflationary scenario consistent and phenomenologically appealing as all the information from the bounce might then not have been fully washed out.

Keywords: loop quantum qosmology, inflation, Bianchi-I, loop quantum gravity, quantum cosmology, bouncing cosmology

(Some figures may appear in colour only in the online journal)

1. Introduction

Loop quantum gravity (LQG) is an attempt to derive a background-independent and non-perturbative quantization of general relativity. In the canonical formalism, it relies on Ashtekar variables, namely SU(2) valued connections and conjugate densitized triads. The quantization is basically obtained through holonomies of the connections and fluxes of the densitized triads. Quite a lot of impressive results were recently obtained, including an extensive covariant reformulation (see, e.g., [1] for introductions and reviews).

Loop quantum cosmology (LQC) tries to capture the main features of LQG in the highly symmetric situations relevant for cosmology. A generic and important result of LQC is that

the big bang is replaced by a big bounce due to strong repulsive quantum geometrical effects (see, e.g., [2] for reviews and [3] for a recent numerical test of the bounce robustness).

In all bouncing cosmologies (except ekpyrotic models built to avoid this problem), either from the loop approach or any other, the issue of anisotropies is crucial for a very clear reason: the shear term basically varies as $1/a^6$, where a is the 'mean' scale factor of the Universe. When the Universe is contracting, the shear term becomes more and more important and might drive the dynamics. The very reason why the shear can be safely neglected in standard inflationary cosmology is precisely the reason why it becomes essential in bouncing models. When one assumes spatial homogeneity, anisotropic hypersurfaces admit transitive groups of motion that must be three- or four-parameter isometry groups. The four-parameter groups have no simply transitive subgroups, and will not be considered here. There are nine algebraically nonequivalent three-parameter simply transitive Lie groups: Bianchi I through IX, all with well known structure constants. The flat, closed and open generalizations of the FLRW model are respectively called Bianchi-I, Bianchi-IX and Bianchi-V. In the following, we focus on the Bianchi-I model to study the dynamics around the bounce. This is meaningful as the Universe is nearly flat today and as the relative weight of the curvature term in the Friedmann equation is decreasing with increasing values of the density.

Different studies have already been devoted to Bianchi-I LQC [4, 5]. In particular, it was shown that the bounce prediction resists the introduction of anisotropies. As the main features of isotropic LQC are well captured by semi-classical effective equations [3], we will assume that this remains true when anisotropies are included.

In a previous work, we systematically explored the full solution space in a way that had not been considered before and derived the LQC-modified generalized Friedmann equation that was still missing [6]. In another work, we established that, if initial conditions are set in the contracting phase, the duration of inflation is not a free parameter anymore but becomes a highly peaked distribution in isotropic effective LQC [7]. In this article, we address both questions at the same time: how is the duration of inflation affected by anisotropies that *must* be taken into account in any consistent bouncing approach?

The solutions of effective equations of Bianchi-I LQC, and the effect of the shear on slow-roll inflation, were previously studied in [8]. The main difference between this article and [8] is that we set the initial conditions in the far past, well before the bounce, while [8] set their initial conditions at the bounce. This difference is further discussed in section 7.

2. Gravitational sector

Except the definition given in equation (22), this section is mostly a summary of the first half of [6].

The metric for a Bianchi-I spacetime is given by

$$\mathrm{d}s^2 = -N^2\mathrm{d}\tau^2 + a_1^2\mathrm{d}x^2 + a_2^2\mathrm{d}y^2 + a_3^2\mathrm{d}z^2, \tag{1}$$

where a_i denote the directional scale factors. The classical gravitational Hamiltonian is

$$\mathcal{H}_G = \frac{N}{\kappa\gamma^2}\left(\sqrt{\frac{p_1p_2}{p_3}}c_1c_2 + \sqrt{\frac{p_2p_3}{p_1}}c_2c_2 + \sqrt{\frac{p_3p_1}{p_2}}c_2c_3\right), \tag{2}$$

with Poisson brackets

$$\left\{ c_i, p_j \right\} = \kappa\gamma\delta_{ij}, \tag{3}$$

where γ is the Barbero–Immirzi parameter.

The classical directional scale factors can be calculated from p_i

$$a_1 = \sqrt{\frac{p_2 p_3}{p_1}} \qquad \text{and cyclic expressions.} \tag{4}$$

The generalized Friedmann equation is

$$H^2 = \sigma^2 + \frac{\kappa}{3}\rho, \tag{5}$$

where

$$H := \frac{\dot{a}}{a} = \frac{1}{3}\left(H_1 + H_2 + H_3\right),\ a := (a_1 a_2 a_3)^{1/3}, \tag{6}$$

$$\sigma^2 = \frac{1}{18}\left(\left(H_1 - H_2\right)^2 + \left(H_2 - H_3\right)^2 + \left(H_3 - H_1\right)^2\right), \tag{7}$$

$$H_1 := \frac{\dot{a}_1}{a_1} = -\frac{\dot{p}_1}{2p_1} + \frac{\dot{p}_3}{2p_3} + \frac{\dot{p}_3}{2p_3} \qquad \text{and cyclic expressions.} \tag{8}$$

To account for LQC effects, the holonomy correction has to be implemented. It is rooted in the fact that the Ashtekar connection cannot be promoted to be an operator whereas its holonomy can. It is assumed to capture relevant quantum effects at the semi-classical level. Following the usual prescription, one substitutes

$$c_i \to \frac{\sin\left(\bar{\mu}_i c_i\right)}{\bar{\mu}_i} \tag{9}$$

in the classical Hamiltonian. The $\bar{\mu}_i$ are given by

$$\bar{\mu}_1 = \lambda\sqrt{\frac{p_1}{p_2 p_3}} \qquad \text{and cyclic expressions,} \tag{10}$$

where λ is the square root of the minimum area eigenvalue of the LQG area operator ($\lambda = \sqrt{\Delta}$) [4]. The quantum corrected gravitational Hamiltonian is:

$$\begin{aligned}\mathcal{H}_G = -\frac{N\sqrt{p_1 p_2 p_3}}{\kappa\,\gamma^2\lambda^2}\Big[&\sin\left(\bar{\mu}_1 c_1\right)\sin\left(\bar{\mu}_2 c_2\right)\\ &+ \sin\left(\bar{\mu}_2 c_2\right)\sin\left(\bar{\mu}_3 c_3\right) + \sin\left(\bar{\mu}_3 c_3\right)\sin\left(\bar{\mu}_1 c_1\right)\Big].\end{aligned} \tag{11}$$

It can be shown that all gravitational observables are fully described by the h_i:

$$h_1 := \bar{\mu}_1 c_1 = \lambda\sqrt{\frac{p_1}{p_2 p_3}}\, c_1 \qquad \text{and cyclic expressions.} \tag{12}$$

As could be expected, the initial six degrees of freedom (c_i, p_i) reduce to only three physical degrees of freedom h_i. This is because only the H_i and not the a_i are observables. The a_i can indeed be changed by a rescaling of the corresponding coordinate, while H_i remains invariant under any coordinate transformation that preserves the form of the metric given by equation (1).

The equations of motion for the h_i are derived from equations (11) and (12):

$$\dot{h}_1 = \frac{1}{2\gamma\lambda}\Big[\big(h_2 - h_1\big)\big(\sin h_1 + \sin h_3\big)\cos h_2 + \big(h_3 - h_1\big)\big(\sin h_1 + \sin h_2\big)\cos h_3\Big] - \frac{\kappa\gamma\lambda}{2}(\rho + P) \text{ and cyclic expressions,} \tag{13}$$

where ρ is the total matter energy density and P is the total pressure.

The average and directional Hubble parameters can now be re-expressed in terms of h_i:

$$H_1 := \frac{\dot{a}_1}{a_1} = \frac{1}{2\gamma\lambda}\Big[\sin\big(h_1 - h_2\big) + \sin\big(h_1 - h_3\big) + \sin\big(h_2 + h_3\big)\Big] \text{ and cyclic expressions,} \tag{14}$$

and

$$H := \frac{\dot{a}}{a} = \frac{1}{3}\big(H_1 + H_2 + H_3\big) = \frac{1}{6\gamma\lambda}\Big[\sin\big(h_1 + h_2\big) + \sin\big(h_2 + h_3\big) + \sin\big(h_3 + h_1\big)\Big]. \tag{15}$$

The LQC-modified generalized Friedmann equation can now be written:

$$H^2 = \sigma_Q^2 + \frac{\kappa}{3}\rho - \lambda^2\gamma^2\left(\frac{3}{2}\sigma_Q^2 + \frac{\kappa}{3}\rho\right)^2, \tag{16}$$

where we define the quantum shear σ_Q^2 as

$$\sigma_Q^2 := \frac{1}{3\gamma^2\lambda^2}\left(1 - \frac{1}{3}\Big[\cos\big(h_1 - h_2\big) + \cos\big(h_2 - h_3\big) + \cos\big(h_3 - h_1\big)\Big]\right). \tag{17}$$

The LQC-modified generalized Friedman equation given by equation (16) puts upper limits on both σ_Q^2 and ρ

$$\sigma_Q^2 \leqslant \sigma_{Q_c}^2 := \frac{3}{2\lambda^2\gamma^2}, \quad \rho \leqslant \rho_c := \frac{\kappa}{3\lambda^2\gamma^2}. \tag{18}$$

It should be noticed that ρ_c is the same as in the isotropic case.

In the limit $h_i \to n\pi$ with the same integer n for all i, then $\sigma_Q^2 \approx \sigma^2$. A special case of this is of course $\lambda \to 0 \Rightarrow h_i \to 0$.

From equations (13) and (15), one finds that

$$\big(\dot{h}_i - \dot{h}_j\big) = -3H\big(h_i - h_j\big), \tag{19}$$

and from this, it follows that

$$\big(h_i - h_j\big) \propto a^{-3}. \tag{20}$$

Without any loss of generality, one can choose the labeling of the spatial dimensions such that initially

$$h_1 \leqslant h_2 \leqslant h_3. \tag{21}$$

Because of equation (20), we know that this inequality will hold at any time.

We now define a the symmetry variable for the anisotropy

$$S := \frac{\big(h_2 - h_1\big) - \big(h_3 - h_2\big)}{\big(h_3 - h_1\big)}. \tag{22}$$

It follows from equation (20), that S is a constant of motion, and it follows from its definition and equation (21) that $-1 \leqslant S \leqslant 1$.

The classical shear σ^2 can in principle be calculated from H, σ_Q^2 and S, since they contain all the physical information about the gravitational sector. However the exact relation is rather complicated and outside the scope of this article.

3. Matter

A matter field has to be introduced. It will of course play a crucial role in the inflationary phase. We will choose a simple massive scalar field with potential

$$V(\phi) = \frac{m^2\phi^2}{2}. \tag{23}$$

This is the simplest potential that will generate slow roll inflation, and therefore a good generic toy model.

Given this potential, the equation of motion for the scalar field is:

$$\ddot{\phi} = -3H\dot{\phi} - m^2\phi. \tag{24}$$

The above equation, together with equation (13), is the full set of equations of motion describing the system under study in this work.

4. Early evolution

As shown in [6], there are many solutions that never reach a classical limit, neither in the past nor in the future. However, in this study, we restrict ourselves to solutions that behave like a contracting classical Universe in the remote past. As was also found in [6], all these solutions, and only these solutions, will approach the behavior of a classical expanding Universe in the future.

For all the solutions of interest, there will therefore be a period in the far past where the solution behaves just like a classical contracting Universe. This gives

$$\sigma_Q^2 \propto a^{-6}. \tag{25}$$

The above relation can also be verified explicitly from equations (17) and (20) in the limit $h_i \to n\pi$. For the solutions of interest, equation (25) holds when $\sigma_Q^2 \ll 1$ in Planck units.

The matter content is slightly more complicated due to the oscillatory behavior of equation (24). Under the conditions

$$\rho \ll \rho_c, \quad H < 0, \quad H^2 \ll m^2, \quad \sigma_Q^2 \ll \frac{\kappa}{3}\rho, \tag{26}$$

the solutions to equation (24) are well approximated by [7]

$$\rho(t) = \rho_0\left(1 - \frac{1}{2}\sqrt{3\kappa\rho_0}\left(t + \frac{1}{2m}\sin(2mt + 2\delta)\right)\right)^{-2}, \tag{27}$$

$$m\phi(t) = \sqrt{2\rho(t)}\,\sin(mt + \delta), \tag{28}$$

and

$$\dot{\phi}(t) = \sqrt{2\rho(t)}\,\cos(mt + \delta), \tag{29}$$

for some parameters ρ_0 and δ. Note that $\rho(0)$ is approximately, but not exactly, equal to ρ_0.

For the solutions of interest, the conditions given by equation (26) will always be met at some early enough time. Equation (26) implies $\sigma_Q^2 \ll 1$ so that equation (25) is also true if the conditions of equation (26) are fulfilled.

If we average out the matter oscillations we find that

$$\langle \rho \rangle \propto a^{-3}, \tag{30}$$

where $\langle \cdot \rangle$ is the time average over one oscillation, or equivalently the average over all angles δ. At $t = 0$ we have $\langle \rho(0) \rangle = \rho_0$.

Combining the above with equation (25) gives

$$\sigma_Q^2 \propto \langle \rho \rangle^2. \tag{31}$$

5. Simulations

We have performed exhaustive numerical simulations (with control of the numerical errors) to investigate the duration of inflation as a function of the different variables entering the dynamics. All the simulations carried out is this work are started in the contracting phase, with a small energy density and shear, so that everything is well described by unmodified classical equations.

All simulations start from initial conditions fulfilling equation (26). As initial conditions for the matter sector, we use equations (27)–(29) with $t = 0$:

$$\rho(0) = \rho_0 \left(1 - \frac{1}{2} \sqrt{3\kappa\rho_0} \frac{1}{2m} \sin(2\delta) \right)^{-2}, \tag{32}$$

$$m\phi(0) = \sqrt{2\rho(0)} \sin(\delta), \tag{33}$$

and

$$\dot{\phi}(0) = \sqrt{2\rho(0)} \cos(\delta). \tag{34}$$

As demonstrated in [7], these initial conditions, together with a flat distribution of δ, give a natural distribution over solutions with different ratios of kinetic to potential energy. This is an important point for this study.

Since everything is initially very small in Planck units, we can approximate:

$$H(0) \approx \frac{1}{3\gamma\lambda} \left[h_1(0) + h_2(0) + h_3(0) \right], \tag{35}$$

$$\sigma_Q^2(0) \approx \frac{1}{18\gamma^2\lambda^2} \Big[\big(h_1(0) - h_2(0) \big)^2 + \big(h_2(0) - h_3(0) \big)^2 + \big(h_3(0) - h_1(0) \big)^2 \Big]. \tag{36}$$

Solving the above equations together with equation (22) gives for $h_1(0)$, $h_2(0)$ and $h_3(0)$:

$$h_1(0) \approx \gamma\lambda H(0) + \gamma\lambda \frac{-3 - S}{\sqrt{3 + S^2}} \sqrt{\sigma_Q^2(0)}, \tag{37}$$

$$h_2(0) \approx \gamma\lambda H(0) + \gamma\lambda \frac{2S}{\sqrt{3 + S^2}} \sqrt{\sigma_Q^2(0)}, \tag{38}$$

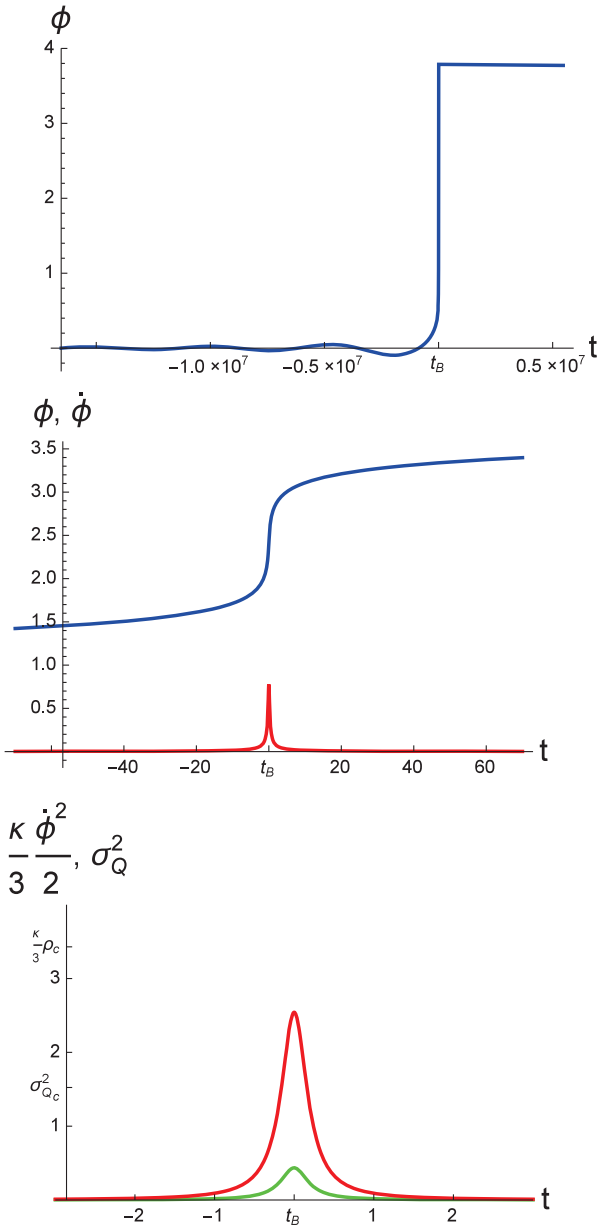

Figure 1. Typical evolution of ϕ, $\dot{\phi}$, and σ_Q^2 as a function of time. t_B is the time of the bounce, when $H = 0$. The blue line is ϕ, the red is $\dot{\phi}$ or $\frac{\kappa}{3}\frac{\dot{\phi}^2}{2}$, and the green is σ_Q^2. All the above plots are from the same simulation. Note that the kinetic energy is always completely dominating over the potential energy at the bounce $\frac{\dot{\phi}_B^2}{2} \gg \frac{m^2\phi_B^2}{2}$. The fraction of shear and potential energy at the bounce varies, depending on the initial conditions. The initial conditions are $\sigma_Q^2(0) = 10^{-3}\frac{\kappa}{3}\rho_0$, $S = 0$ and $\delta = 0$.

$$h_3(0) \approx \gamma\lambda H(0) + \gamma\lambda \frac{3-S}{\sqrt{3+S^2}} \sqrt{\sigma_Q^2(0)}\,. \tag{39}$$

Finally, the initial conditions have to fulfill equation (16), and since we are in the contracting branch we get the negative solution for $H(0)$

$$H(0) = -\sqrt{\sigma_Q^2(0) + \frac{\kappa}{3}\rho(0) - \lambda^2\gamma^2\left(\frac{3}{2}\sigma_Q^2(0) + \frac{\kappa}{3}\rho(0)\right)^2}\,. \tag{40}$$

The initial conditions of the simulations are now fully specified by equations (32)–(34) and (37)–(40), and the parameters ρ_0, δ, $\sigma_Q^2(0)$ and S.

To make sure that the approximations used for the initial conditions hold, the parameters must fulfill:

$$\sigma_Q^2(0) \ll \frac{\kappa}{3}\rho_0 \ll m^2 \tag{41}$$

in Planck units, together with

$$-1 \leqslant S \leqslant 1 \quad \text{and} \quad 0 \leqslant \delta < 2\pi, \tag{42}$$

which follows from the definitions.

For all the simulations in this work, we have used $m = 1.21 \times 10^{-6}$, as favored by observation [9]. In addition, we have used $\gamma = 0.2375$ and $\lambda = \sqrt{4\sqrt{3}\pi\gamma}$ [1] which gives $\rho_c = 0.41$ and $\sigma_{Q_c}^2 = 1.52$. In all simulations $\frac{\kappa}{3}\rho_0 = 10^{-3}m^2$, and $\sigma_Q^2(0) \in [0,\, 10^{-5}m^2]$.

6. Results

It is important to stress that our results are model dependent. The results presented in this section are only true for the specific matter content described in section 3 with $m = 1.21 \times 10^{-6}$. Any more general statement would require further investigations.

Figure 1 shows a typical evolution around the bounce (the bounce being defined as the point in time when $H = 0$). At the bounce, the Universe is completely dominated by the kinetic energy and the shear. The kinetic energy is very large for a very short time. This gives the scalar field a boost, and lifts it up to create the initial conditions for slow-roll inflation.

The evolution of the scalar field ϕ, shown in the upper panel of figure 1, is not at all time symmetric around the bounce. After the bounce one can see the beginning of slow-roll inflation, with a high and almost constant value of ϕ. But there is, in general, no analog slow-roll deflation before the bounce. This is very typical of solutions for which the initial conditions are specified in the contraction phase before the bounce. The reason for this is that in forward time evolution, slow-roll deflation is a repellant, while slow-roll inflation is an attractor. This behavior has been thoroughly studied for the isotropic case in [7].

As confirmed by the results given later in this section, if there is a lot of shear, the bounce happens at a lower value of the kinetic energy, and the scalar field is not lifted as high as in the isotropic case, which leads to less slow-roll inflation.

The number of e-folds of slow-roll inflation, N, can be calculated from the value of the scalar field at the beginning of the slow-roll phase ϕ_{infl}:

$$N = 2\pi\phi_{\text{infl}}^2, \tag{43}$$

where the field is expressed in Planck units. The simulations confirm that slow-roll inflation starts when $|\phi|$ reaches its maximum value after the bounce.

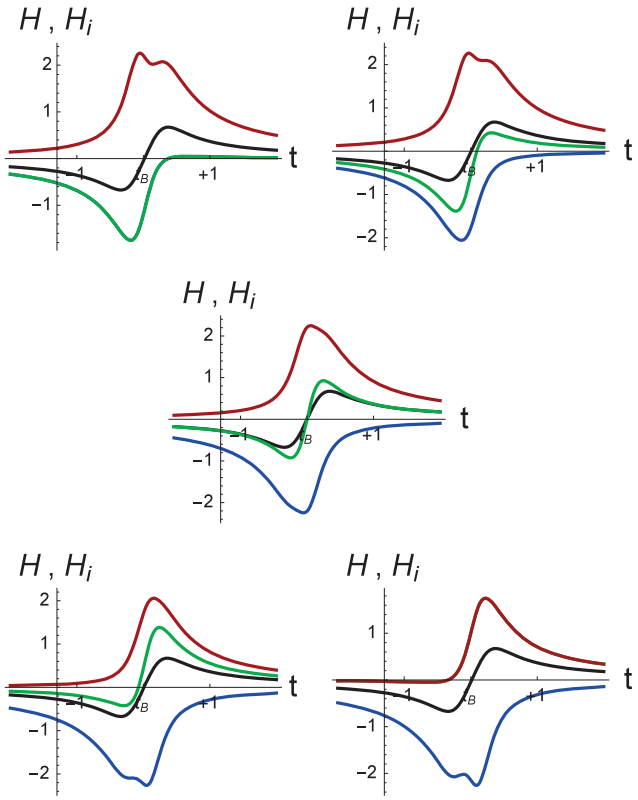

Figure 2. Details of the bounce shown for different values of the symmetry factor S. Upper left: $S = -1$. Upper right: $S = -0.5$. Center: $S = 0$. Lower left: $S = 0.5$. Lower right: $S = 1$. Black is H, red is H_3, green is H_2 and blue is H_1. $\sigma_Q^2(0) = 10^{-2}\frac{\kappa}{3}\rho_0$ and $\delta = 0$ for all the above plots. In the upper left plot, the blue line is hidden by the green one. In the lower right plot, the green line is hidden by the red one.

6.1. Symmetry

Classically (i.e. with no quantum corrections), the value of S does not influence the evolution of the total Hubble parameter H and therefore does not have any impact on the inflation in this scenario. In effective LQC, however, the situation is different. A large asymmetry (i.e. $|S|$ close to one) will stretch out the bounce. This can be seen in figure 6 of [6] and in figure 11 of [8].

It should be noticed that in [8] the variables used for the shear are not the same as the ones chosen here. However, in [8], the initial conditions are given at the bounce, i.e. $H(0) = 0$, so that $\sigma_Q^2(0)$ becomes completely fixed by equation (16) together with the initial values for the matter fields $\phi(0)$, $\dot{\phi}(0)$. Therefore, varying σ^2 in the setting of [8] is equivalent to varying S in the setting of this paper.

The more dominant the shear is at the bounce, the stronger this stretching effect becomes, and vice versa. A longer bounce epoch might influence the outcome of ϕ_{infl} and thereby the duration of slow-roll inflation. We will therefore investigate how strong this effect is for the range of initial conditions studied in this article.

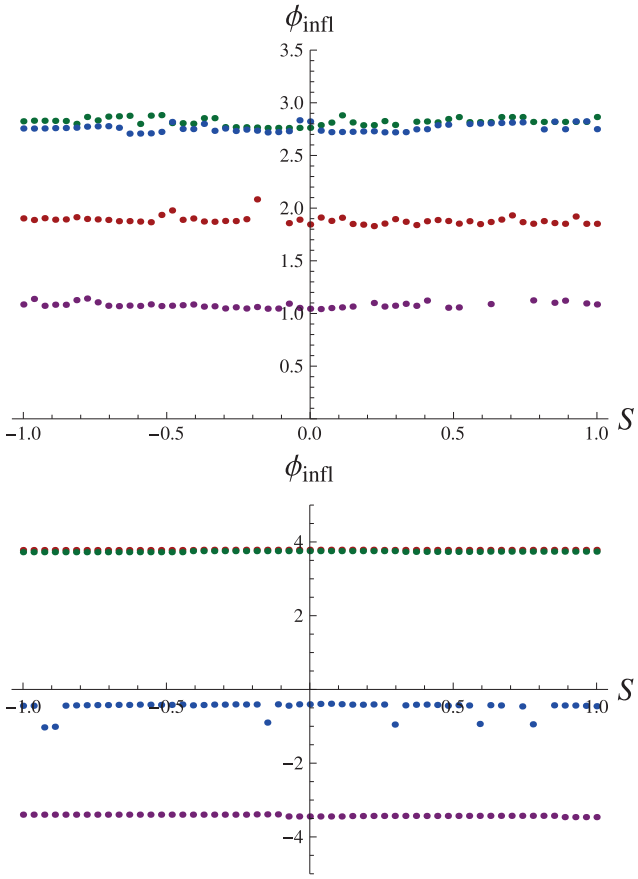

Figure 3. Scalar field at the beginning of inflation as a function of S. Upper: $\sigma_Q^2(0) = 10^{-2}\frac{\kappa}{3}\rho_0$. Lower: $\sigma_Q^2(0) = 10^{-3}\frac{\kappa}{3}\rho_0$. Red is $\delta = 0$, green is $\delta = \frac{\pi}{4}$, blue is $\delta = \frac{\pi}{2}$ and purple is $\delta = \frac{3\pi}{4}$. Note that in the lower plot, the green points are right on top of the red ones and are therefore hard to be seen.

Figure 2 shows the evolution of H and H_i just around the bounce for $\sigma_Q^2(0) = 10^{-2}\frac{\kappa}{3}\rho_0$, $\delta = 0$ and some values of S. One can see that in this case the evolution of H is very similar for all choices of S.

Figure 3 shows the resulting ϕ_{infl}, as an output of simulations for different values of $\sigma_Q^2(0)$, δ and S. One sees that, up to numerical errors, there is no dependence on S. We conclude that the symmetry variable has no effect on the duration of slow-roll inflation in the parameter range of this article. Therefore, $S = 0$ is chosen for the rest of this study.

6.2. Shear

In this section we vary $\sigma_Q^2(0)$ and δ to see how this affects the length of slow-roll inflation.

Figure 4 shows the results of extensive simulations carried out by varying both parameters. It can be concluded that, in general, the number of e-folds goes down when the shear

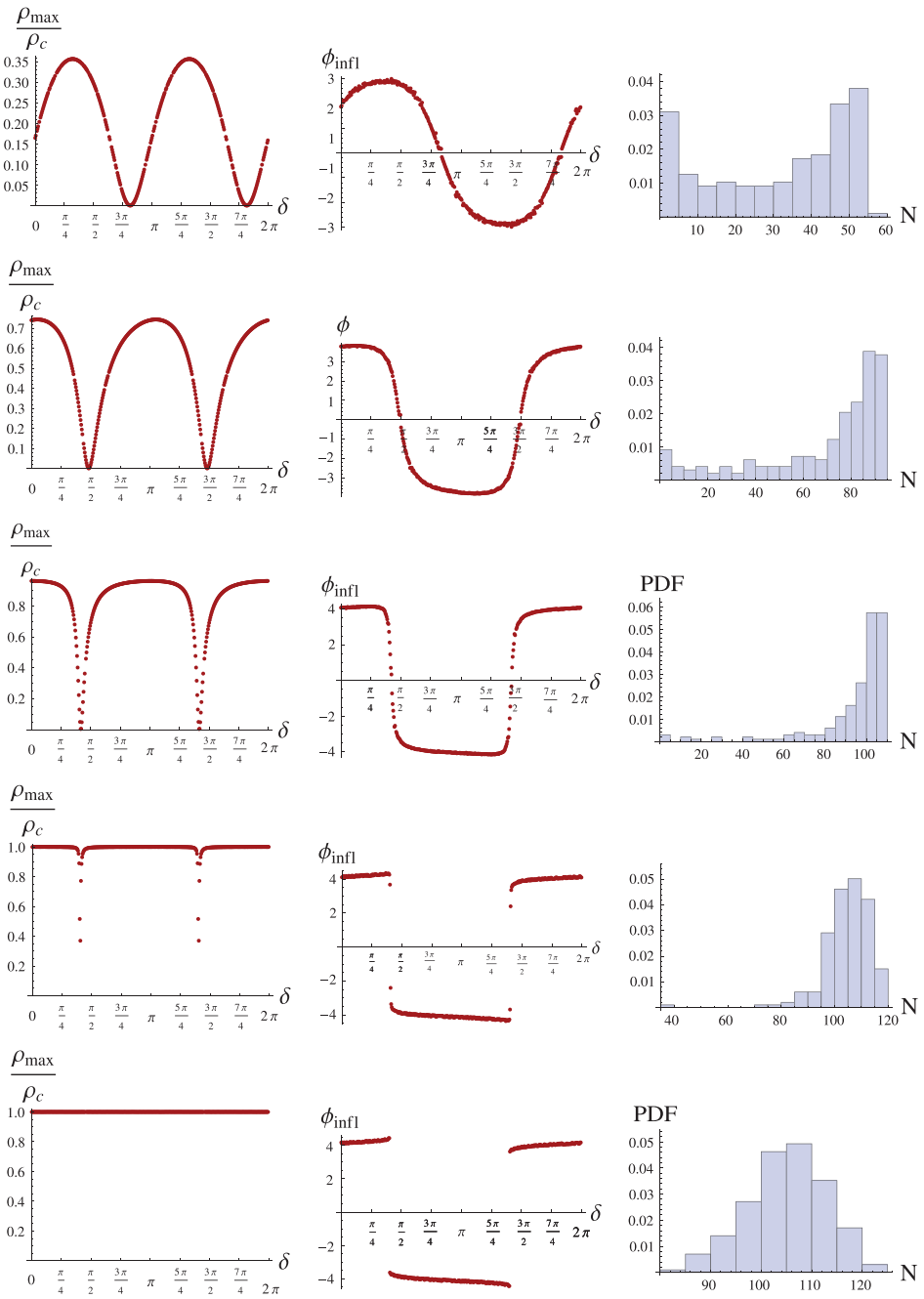

Figure 4. Results of the simulations, for each row, starting from the top $\sigma^2_{\hat{Q}}(0) = \{10^{-2}\frac{\kappa}{3}\rho_0,\ 10^{-3}\frac{\kappa}{3}\rho_0,\ 10^{-4}\frac{\kappa}{3}\rho_0,\ 10^{-6}\frac{\kappa}{3}\rho_0,\ 0\}$. First column: the maximum value of ρ (which is the value of ρ at the bounce) normalized to ρ_c. Second column: ϕ at the start of slow-roll inflation. Third column: numerically calculated probability distribution function of the number of e-folds of slow-roll inflation, given that all δ have an equal probability.

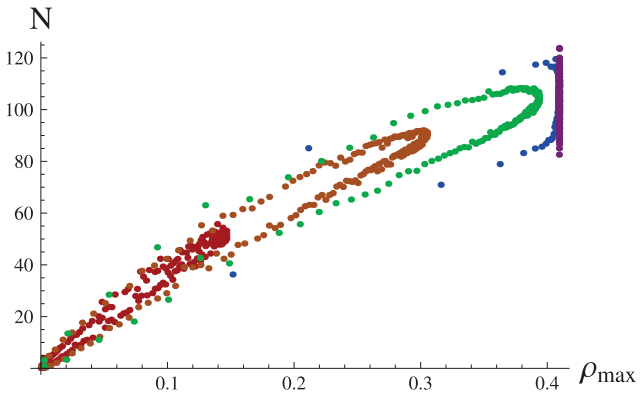

Figure 5. Number of e-folds as a function of ρ at the bounce. Red: $\sigma_Q^2(0) = 10^{-2}\frac{\kappa}{3}\rho_0$. Orange: $\sigma_Q^2(0) = 10^{-3}\frac{\kappa}{3}\rho_0$. Green: $\sigma_Q^2(0) = 10^{-4}\frac{\kappa}{3}\rho_0$. Blue: $\sigma_Q^2(0) = 10^{-6}\frac{\kappa}{3}\rho_0$. Purple: $\sigma_Q^2(0) = 0$. Different points of the same color correspond to different values of delta.

increases. But a greater shear will also lead to a bigger spread in the number of e-folds, depending on the initial angle δ.

We stress that our results are complementary to those of [8] and cannot be directly compared because the initial conditions are set in two very different manners. In this article we chose to assume that the natural place to put initial conditions in the classical contracting past is as far away as possible from the highly quantum bounce region, and in agreement with usual causality.

For a model to be compatible with the observations, about 60 e-folds or more of slow-roll inflation are needed [9]. In figure 4, one can see that for the given parameters, this bound goes somewhere between $\sigma_Q^2 = 10^{-2}\frac{\kappa}{3}\rho_0$ and $\sigma_Q^2 = 10^{-3}\frac{\kappa}{3}\rho_0$. With the help of equation (31), one can express this in a slightly more general way. As long as equation (26) holds

$$\sigma_Q^2(t) = \frac{\sigma_Q^2(0)}{\rho_0^2}\langle\rho(t)\rangle^2. \tag{44}$$

To have a long enough slow-roll inflation period we need $\sigma_Q^2(0) \lesssim 5 * 10^{-3}\frac{\kappa}{3}\rho_0$ for $\frac{\kappa}{3}\rho_0 = 10^{-3}m^2$, which is equivalent to

$$\begin{aligned}\sigma_Q^2(t) &\lesssim \frac{\left(5 * 10^{-3}\right)\left(10^{-3}m^2\right)}{\left(\frac{3}{\kappa}10^{-3}m^2\right)^2}\langle\rho(t)\rangle^2 \\ &= \frac{5}{m^2}\left(\frac{\kappa}{3}\langle\rho(t)\rangle\right)^2\end{aligned} \tag{45}$$

during the early evolution.

Figure 5 shows the same data as figure 4 but in a different way. Here one can clearly see that the number of e-folds of slow-roll inflation depends strongly on $\rho_{\max}$, which is of course not surprising. When the shear vanishes, $\rho_{\max}$ becomes fixed, otherwise it can vary between zero and the associated maximum value.

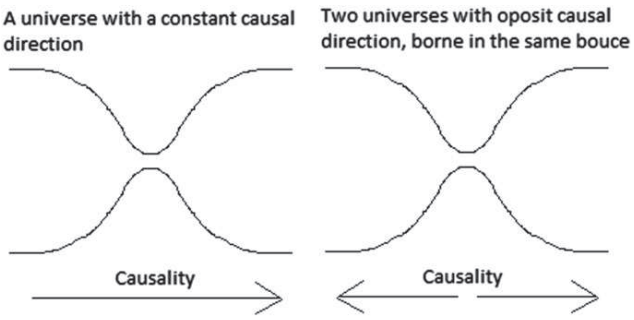

Figure 6. Two possibilities for the causal structure of a bouncing Universe.

From figure 5 one can read that to get more than 60 e-folds of inflation, $\rho_{\max} \gtrsim 0.18$ is required. However, this result is highly dependent on the fact that the initial conditions are set in the past, long enough before the bounce. As pointed out earlier, using initial conditions in the contracting phase promotes a certain kind of solution. This is precisely the spirit of this study and of the previous ones [6, 7] that we intend to generalize here.

7. Discussion

In this work we have investigated how the amount of shear affects the duration of slow-roll inflation in effective LQC, when the initial conditions are set in the far past. We have found that a larger shear will in general lead to a lower energy density at the bounce.

At the bounce, the energy density is dominated by the kinetic energy. For a very short time around the bounce, of the order of a Planck time, the kinetic energy is of the order of the Planck energy. This peak of kinetic energy will lift the potential energy up to a value of the order m^2. When the peak of kinetic energy has died down, only the potential energy remains, and the slow-roll inflation starts.

However, the bounce will occur when ρ together with σ_Q^2 are large enough so that the left hand side of equation (16) vanishes. Naturally, more shear will leave less room for the energy density. The growth of kinetic energy is interrupted at a lower value than in the isotropic case, leading to a smaller boost of the potential energy, leading to less slow-roll inflation. It should also be noticed that the initial parameter δ, relating the amount of initial kinetic and potential energy, has an impact on the duration of slow-roll inflation. However, δ should be seen as a truly random parameter, and we should therefore consider the results for a flat statistical distribution of δ.

We conclude that to have a good probability for at least 60-efolds of inflation in this model, the initial conditions must fullfill: $\sigma_Q^2 \lesssim \frac{5}{m^2}\left(\frac{\kappa}{3}\rho_0\right)^2$.

There are two major schools on how to set initial conditions in LQC. One is, as in this study, to set the initial conditions in the remote past. The other direction is to set the initial conditions at the bounce. Which way is correct is a rather philosophical question. Causality in our Universe seems to be running in a certain direction, which we call forward in time. When simulating almost any epoch in the Universe, physicists always run the simulations in the forward time direction, even though the laws of physics are time symmetric. The reason for this is because we are not actually interested by *all* possibilities, we are only interested in the most probable ones. The direction of causality is important for probabilities, e.g. an attractor

in one time direction will be a repellant in the opposite time direction. The question of when to set the initial conditions in the simulation is an important one.

What is then the correct initial time in LQC? Well, it depends on how one thinks about the bounce. If one believes in a constant causal direction, as in the left panel of figure 6, it is natural to set the initial conditions well before the bounce. However, we do not know how time behaves in quantum gravity, so this might not be the case. An alternative history is sketched in the right panel of figure 6, where two universes with opposite causal direction are borne from the same 'bounce'. In this case, it would be natural to assign initial conditions at the bounce. We do not know which, if any, of these two cases is correct. It is therefore reasonable to consider both paths. Anyway, each of them has its own problem with anisotropies.

In this article, we investigated the case of initial conditions set well before the bounce. We found that if the shear is too large when compared to the energy density, we will not have enough inflation to explain the known Universe. This means that the shear 'decreases' the amount of solutions that are compatible with data, and therefore the 'naturalness' of the model. But on the other hand, this means that if the model is correct, the number of e-folds is probably not much larger that the lower bound required by observations. This is good for phenomenology as the quantum gravity effects may then not have been fully washed out by inflation.

The case of initial conditions set at the bounce was investigated in [8] where it was found that the anisotropies are not a problem for inflation. However, only solutions leading to a classical limit in the future were considered. But the vast majority of solutions never lead to anything remotely like a classical Universe at all [6]. When starting from a classical contracting Universe, the nice solutions (i.e. the ones leading to a classical expanding Universe after the bounce) are automatically singled out. But if initial conditions are put at the bounce, something else is needed to play this role.

References

[1] Dona P and Speziale S 2010 (arXiv:1007.0402V1)
Perez A 2004 (arXiv:0409061v3[gr-qc])
Gambini R and Pullin J 2011 *A First Course in Loop Quantum Gravity* (Oxford: Oxford University Press)
Rovelli C 2011 (arXiv:1102.3660v5[gr-qc])
Rovelli C 2004 *Quantum Gravity* (Cambridge: Cambridge University Press)
Rovelli C 1998 *Living Rev. Relativ.* **1** 1
Smolin L 2004 (arXiv:0408048v3[hep-th])
Thiemann T 2003 *Lecture Notes Phys.* **631** 41
Thiemann T 2007 *Modern Canonical Quantum General Relativity* (Cambridge: Cambridge University Press)

[2] Ashtekar A, Bojowald M and Lewandowski J 2003 *Adv. Theor. Math. Phys.* **7** 233
Ashtekar A 2009 *Gen. Relativ. Gravit.* **41** 707
Ashtekar A and Singh P 2011 *Class. Quantum Grav.* **28** 213001
Bojowald M 2008 *Living Rev. Relativ.* **11** 4
Bojowald M 2012 (arXiv:1209.3403[gr-qc])
Banerjee K, Calcagni G and Martin-Benito M 2012 *SIGMA* **8** 016
Calcagni G 2013 *Ann. Phys.* **525** 323
Agullo I and Corichi A 2013 *The Springer Handbook of Spacetime* ed A Ashtekar and V Petkov (Berlin: Springer) (arXiv:1302.3833[gr-qc])
Barrau A *et al* 2014 *Class. Quantum Grav.* **31** 053001

[3] Diener P, Gupt B and Singh P 2014 (arXiv:1402.6613)

[4] Ashtekar A and Wilson-Ewing E 2009 *Phys. Rev.* D **79** 083535

[5] Cartin D and Khanna G 2005 *Phys. Rev. Lett.* **94** 111302
Date G 2005 *Phys. Rev.* D **72** 067301
Cartin D and Khanna G 2005 *Phys. Rev.* D **72** 084008
Chiou D-W 2007 *Phys. Rev.* D **75** 024029
Chiou D-W 2007 (arXiv:0703010[gr-qc])
Chiou D-W and Vandersloot Kevin 2007 *Phys. Rev.* D **76** 084015
Chiou D-W 2007 *Phys. Rev.* D **76** 124037
Szulc L 2008 *Phys. Rev.* D **78** 064035
Martin-Benito M, Mena Marugan G A and Pawlowski T 2008 *Phys. Rev.* D **78** 064008
Chiou D-W 2008 (arXiv:0812.0921[gr-qc])
Dzierzak P and Piechocki W 2009 *Phys. Rev.* D **80** 124033
Martin-Benito M, Mena Marugan G A and Pawlowski T 2009 *Phys. Rev.* D **80** 084038
Dzierzak P and Piechocki W 2012 *Ann. Phys.* **19** 290
Malkiewicz P, Piechocki W and Dzierzak P 2011 *Class. Quantum Grav.* **28** 085020
Martin-Benito M, Garay L J, Mena Marugan G A and Wilson-Ewing E 2012 *J. Phys. Conf. Ser.* **360** 012031
Rikhvitsky V, Saha B and Visinescu M 2012 *Astrophys. Space Sci.* **339** 371
Singh P 2012 *Phys. Rev.* D **85** 104011
Cianfrani F, Marchini A and Montani G 2012 *Europhys. Lett.* **99** 10003
Fujio K and Futamase T 2012 *Phys. Rev.* D **85** 124002
Singh P 2012 *J. Phys. Conf. Ser.* **360** 012008
Liu X, Huang F and Zhu J-Y 2013 *Class. Quantum Grav.* **30** 065010
Yue X-J and Zhu J-Y 2013 (arXiv:1302.1014[gr-qc])
[6] Linsefors L and Barrau A 2014 *Class. Quantum Grav.* **31** 015018
[7] Linsefors L and Barrau A 2013 *Phys. Rev.* D **87** 123509
[8] Gupt B and Singh P 2013 *Class. Quantum Grav.* **30** 145013
[9] Linde A 2014 (arXiv:1402.0526)

Chapter 7

Taking into account coordinate transformations

7.1 Spatially Curved FLRW spacetime

In this article we try to put general restrictions on possible forms of Friedmann equations in modified gravity. The key assumption is that there is still a line element in the usual sense.

This work is deeply grounded in the symmetry properties of de Sitter space. De Sitter space is the maximally symmetric solution of Einstein's equations with a positive cosmological constant. By choosing a specific situation where the density of the Universe is constant in time, which is always possible, we get an extra symmetry of the system. This has direct consequences for possibles shapes of the modified Friedmann equation that are investigated into the details. We have shown that under very general assumptions, for any metric modified cosmology or modified gravity, the Friedmann equation for curved space can be non-ambiguously deduced from the Firedmann equation for a flat space.

When applying his result to LQC, we find that there is a conflict between this work and previous results. It might be interpreted as a new insight in favor of the fact that, as suggested by the deformed algebra approach, we deal here with a non-metric theory.

Physics Letters B 748 (2015) 295–300

Contents lists available at ScienceDirect

Physics Letters B

www.elsevier.com/locate/physletb

Restrictions on curved cosmologies in modified gravity from metric considerations

Linda Linsefors *, Aurelien Barrau

Laboratoire de Physique Subatomique et de Cosmologie, Universite Grenoble-Alpes, CNRS-IN2P3, 53, avenue des Martyrs, 38026 Grenoble cedex, France

ARTICLE INFO

Article history:
Received 8 January 2015
Received in revised form 14 June 2015
Accepted 18 June 2015
Available online 22 June 2015
Editor: M. Trodden

ABSTRACT

This study uses very simple symmetry and consistency considerations to put constraints on possible Friedmann equations for modified gravity models in curved spaces. As an example, it is applied to loop quantum cosmology.

1. Introduction

From the mathematical perspective, the equations governing the background cosmological evolution can be seen as is a symmetry reduced version of the gravity field equations. As well as being successful in describing the evolution of the Universe, cosmology can be seen as an interesting testing ground for new theories of gravity, in particular motivated for being effective models (or low-energy limits) of quantum gravity.

In this article, we will study a general class of modified cosmologies that will be defined by a number of assumptions. We will find how these theories are constrained by the coordinate freedom that is fundamentally encoded in the metric, whatever the considered theory. Beyond constraints on the modified Friedmann equations, an interesting result will be to show how the Hamiltonian can also be constrained for consistency reasons.

Our study is rooted in the symmetries of de Sitter and Minkowski spaces. Intuitively speaking, the idea is to consider a de Sitter phase and use its maximal symmetry.

As a fruitful example, the conclusions previously derived will be applied to loop quantum cosmology (LQC), see [1] for general introductions. In itself, LQC is a symmetry reduced version of loop quantum gravity, see [2] for introductory reviews. Basically, in kinetic-dominated models of LQC, the Big Bang is shown to be replaced by a Big Bounce. The question of whether sharply peaked states assumed for effective equations can be used close to the Big Bounce is still open.

* Corresponding author.
E-mail addresses: linsefors@lpsc.in2p3.fr (L. Linsefors), Aurelien.Barrau@cern.ch (A. Barrau).

2. FLRW metric

The FLRW metric reads as

$$ds^2 = -dt^2 + a(t)^2\left(\frac{dr^2}{1-kr^2} + r^2 d\Omega^2\right). \tag{1}$$

This is the most general homogenous and isotropic metric one can write down. More precisely, this is the interval written in a coordinate system where the symmetries of the Universe are clearly manifest. The only way to preserve the homogeneity and isotropy of space and yet incorporate time evolution is to allow the curvature scale, characterized by a, to be time-dependent. At this stage, only symmetries are involved and nothing is assumed about the details of the considered gravitational theory. In this expression, k is a constant and $a(t)$ is the scale factor. The evolution of $a(t)$ is determined by Einstein's equations or, alternatively, by some modified gravity or modified cosmology theory.

In general, there are two possible coordinate transformations witch leave the FLRW formalism invariant. The first one is a rescaling of the radial coordinate by a constant $b > 0$. Such a transformation affects both a and k, but keeps the FLRW expression unchanged:

$$r' = r/b, \tag{2}$$

$$a'(t) = b\,a(t), \tag{3}$$

$$k' = b^2\,k. \tag{4}$$

The other possibility is a time translation, which is of no interest in this study.

It is common in the literature to fix this coordinate freedom by choosing $k \pm 1$ whenever $k \neq 0$. We will not do so in this article.

http://dx.doi.org/10.1016/j.physletb.2015.06.046

3. (Modified) Friedmann equation

Classically, the evolution of $a(t)$ is given by the first Friedmann equation,

$$H^2 = -\frac{k}{a^2} + \frac{\kappa}{3}\rho + \frac{\Lambda}{3}, \tag{5}$$

where $H := \frac{\dot{a}}{a}$ is the Hubble parameter, $\kappa = 8\pi G$, ρ is the matter energy density, and Λ is the cosmological constant. This equation is correct for any type of homogenous matter. By homogenous we mean that ρ is constant over space-like slices defined by a constant value to the time variable t.

The first Friedmann equation is directly derived from general relativity (GR) field equations, or alternatively from the Hamiltonian constraint. A modified theory of gravity (that may or may not come out from some version of quantum gravity) will most probably give rise to a modified Friedmann equation.

It should be noticed that the Friedmann Eq. (5) is invariant under the rescalings given by Eqs. (2)–(4). Any modified Friedmann equation must have this property. Otherwise, the theory would be inconsistent, or alternatively Eq. (1) would not describe a metric.

The first Friedmann equation (that we are interested in for this study) is a reformulation of the Hamiltonian constraint, this is why it only involves first order derivatives. We assume that this will also be the case for the equation of motion of a in the modified cosmology considered here. Since we are restricted to first order derivatives of a in Eq. (5), there are only three independent gravitational variables as far as this specific equation in concerned: a, $\dot{a}$ and k. From these, we can construct two independent gravitational quantities that are invariant under Eqs. (2)–(4): H and $\frac{k}{a^2}$. The equation of motion for H^2 can in principle always be solved and the result has to be a function of $\frac{k}{a^2}$ and matter variables.

3.1. Main assumptions and their consequences

The assumptions so far for the modified cosmology or modified gravity theory considered are:

1. If the Universe starts out homogenous and isotropic, it remains homogenous and isotropic. This is certainly not true at all scales as any consistent theory should lead to a growth of inhomogeneities. But this is very reasonable at the background order.
2. The theory allows for a metric interpretation, i.e. all physical equations must be invariant under metric coordinate transformations.
3. Given the metric, Eq. (1), the equation of motion for the scale factor $a(t)$ is given by the first Friedmann equation or its analogous in the modified theory considered, which is first order in the time derivative of $a(t)$.
4. There are no hidden gravitational degrees of freedom apart from the metric.

Any theory of modified gravity or modified cosmology that fulfills the above assumptions will have a (modified) Friedmann equation of the form

$$H^2 = \tilde{f}\left(\frac{k}{a^2}, \text{matter}\right), \tag{6}$$

where $\tilde{f}$ is a function of $\frac{k}{a^2}$ and of any set of homogenous coordinate-independent matter variables. This is grounded in the symmetries.

It can be noticed that in the flat case, $k = 0$, the modified Friedmann equation is not allowed to depend explicitly on a. This is of course true in GR.

3.2. Additional assumptions

It is now necessary add two more assumptions to go ahead in the study.

5. The total energy density is the only matter variable that enters the first modified Friedmann equation.

By combining the above assumption with Eq. (6), one gets

$$H^2 = f\left(\frac{k}{a^2}, \rho\right), \tag{7}$$

where f is a function of $\frac{k}{a^2}$ and ρ.

6. Given an arbitrary constant ρ_1 such that $f\left(\frac{k}{a^2}, \rho_1\right) \geq 0$, the theory has a solution with $\rho = \rho_1$ for a non-vanishing amount of time. The keypoint is that the theory has a portion of de Sitter or Minkowski space–time as a semiclassical solution.

A situation with a constant energy density could for example be realized by a scalar field temporarily trapped in a false vacuum, or by a vacuum quantum-fluctuations domination stage. It is important to stress that we don't need this specific stage to have been explicitly realized in the history of the Universe, we just need the theory to be able to account for such a stage. This is obviously the case for GR and for all the most discussed theories beyond GR.

In the analysis performed so far, the possibility of a cosmological constant and/or dark energy has not been left out. If the acceleration of the Universe is due to some exotic matter content (dark energy), then this will be included in ρ. If, on the other hand, the acceleration of the Universe is due to a true cosmological constant Λ, this will be included directly in the function f by the relation $\frac{\Lambda}{3} = f(0,0)$.

3.3. de Sitter/Minkowski space–time

Let us choose a situation where $k = 0$ and $\rho = \rho_1$ such that $f(0,\rho_1) \geq 0$ for some time. Then we have:

$$H^2 = f(0,\rho_1) = \text{constant}, \tag{8}$$

for a non-vanishing amount of time. The above equation together with the FLRW metric, Eq. (1), describes exactly the de Sitter space–time for $f(0,\rho_1) > 0$, and Minkowski space–time for $f(0,\rho_1) = 0$.

By choosing a specific situation where ρ is constant in time, we get an extra symmetry of the system. In the general case, Eqs. (2)–(4) are the only coordinate transformations that preserve the FLRW formulation. However, due to the time symmetry of Minkowski and de Sitter space–times, more coordinate transformations are available still within the FLRW metric formulation.

Using the coordinate transformation described in Appendix A, one finds that

$$H^2 = -\frac{k}{a^2} + f(0,\rho_1)\,, \quad \forall k \leq a^2 f(0,\rho_1), \tag{9}$$

describes exactly the same space–time as Eq. (8). Therefore, if Eq. (8) is correct then Eq. (9) must be correct too.

For any theory of modified gravity or cosmology that fulfill Assumptions (1)–(6), the modified Friedmann equation must therefore be of the form:

$$H^2 = -\frac{k}{a^2} + f_0(\rho), \tag{10}$$

where f_0 is a function of ρ related to previous expressions by $f_0(\rho) = f(0,\rho)$.

3.4. Preliminary conclusion

For a wide large class of modified cosmology models, it was shown that the modified Friedmann equation for curved (i.e. $k \neq 0$) FLRW space–times, can be immediately derived from the modified Friedmann equation for flat a (i.e. $k = 0$) FLRW space–time by Eq. (10). This basically relies on the symmetries and should be considered as a ground before going ahead.

4. Hamiltonian

In this section, the Hamiltonian that leads to Eq. (10) will be derived, as far as it is possible without assuming an explicit expression for $f_0(\rho)$. We somehow follow the reverse path when compared to the one usually considered: we begin by finding the Friedmann equation where the constraints can easily be put and the physical meaning of all terms is clear and use it to infer the Hamiltonian.

To avoid infinities we consider a finite region of space defined by a fiducial volume $\mathcal{V}$, given by some fixed region in coordinate space. It follows from the metric that $\mathcal{V}$ has the volume $V = vV_0$, where $v := a^3$ and V_0 is a constant. We choose v and α to be the canonical coordinates describing the gravitational degree of freedom. The coordinate α is defined by the Poisson bracket

$$\{\alpha, v\} = \frac{1}{V_0}. \tag{11}$$

This choice can be made without any loss of generality as it is always possible to change to another pair after the Hamiltonian constraint has been found.

The total Hamiltonian is written as

$$\mathcal{H}_{tot} = \mathcal{H}_G(v, \alpha) + V\rho, \tag{12}$$

which defines ρ.

We now derive the expression of the gravitational part of the Hamiltonian $\mathcal{H}_G(v, \alpha)$, using Eqs. (10)–(12).

From the Hamiltonian constraint, $\mathcal{H}_{tot} = 0$, we get

$$\rho = \frac{-\mathcal{H}_G}{vV_0}. \tag{13}$$

We also have:

$$H = \frac{\dot{v}}{3v} = \frac{1}{3v}\{v, \mathcal{H}\} = \frac{1}{3vV_0}\frac{\partial(-\mathcal{H}_G)}{\partial\alpha}. \tag{14}$$

Combining Eq. (13) and Eq. (14) with Eq. (10), one gets

$$\frac{\partial(-\mathcal{H}_G)}{\partial\alpha} = \pm 3vV_0\sqrt{-\frac{k}{v^{2/3}} + f_0\left(\frac{-\mathcal{H}_G}{vV_0}\right)}. \tag{15}$$

Since the RHS of the above equation does not depend explicitly on α, one can separate the variables and integrate:

$$\int d\alpha = \pm\int \frac{d\left(\frac{-\mathcal{H}_G}{vV_0}\right)}{3\sqrt{-\frac{k}{v^{2/3}} + f_0\left(\frac{-\mathcal{H}_G}{vV_0}\right)}} \tag{16}$$

where v is held constant during the integration.

When f_0 is known, the integration can in principle be performed. Finally, one has to solve for $\mathcal{H}_G$ to obtain the expression for the gravitational part of the Hamiltonian constraint.

5. Effective LQC

We now focus on effective loop quantum cosmology as an example of modified cosmology grounded in quantum gravity consideration. In LQC, for kinetic-dominated matter systems or for states assumed to be sharply peaked at high density, the Friedmann equation for $k = 0$ is known to be [1]:

$$H^2 = \frac{\kappa}{3}\rho\left(1 - \frac{\rho}{\rho_c}\right). \tag{17}$$

This is the effective description of the bounce believed to replace the Big Bang: the density is bounded from above at the value $\rho_c \sim \rho_{Pl}$ and the Hubble parameter vanishes when this density is reached. This result is not yet firmly established, in particular when backreaction becomes important, and the following results are therefore not fully generic. According to the previously given arguments, the Friedmann equation for a general k must be

$$H^2 = -\frac{k}{a^2} + \frac{\kappa}{3}\rho\left(1 - \frac{\rho}{\rho_c}\right). \tag{18}$$

This is in conflict with earlier results, as it will be discussed in the next section.

5.1. Hamiltonian

It is now possible to use results from Section 4 to calculate the Hamiltonian that leads to Eq. (18). In this case,

$$f_0(\rho) = \frac{\kappa}{3}\rho\left(1 - \frac{\rho}{\rho_c}\right). \tag{19}$$

Inserting this in Eq. (16) gives

$$\int d\alpha = \pm\int \frac{d\left(\frac{-\mathcal{H}_G}{V_0}\right)}{\sqrt{-9kv^{1/3} + 3\kappa v\frac{-\mathcal{H}_G}{V_0}\left(1 - \frac{1}{3v\rho_c}\frac{-\mathcal{H}_G}{V_0}\right)}}. \tag{20}$$

This can be solved to:

$$\mathcal{H}_G = -vV_0\frac{\rho_c}{2} \times\left(1 - \sqrt{1 - \frac{12}{\kappa\rho_c}\frac{k}{v^{2/3}}}\cos\left(\sqrt{\frac{3\kappa}{\rho_c}}[\alpha - \alpha_1(v)]\right)\right), \tag{21}$$

where α_1 is an integration 'constant'. Since v was kept fixed during the integration, α_1 can be any function of v. It is easy to check that this Hamiltonian indeed gives the correct modified Friedmann equation.

In the derivation of Eq. (21) no other assumption or ansatz than the one given by the modified Friedmann equation, together with Eq. (12), was assumed. Because of this, Eq. (21) gives all the solutions to $\mathcal{H}_G$, given Eq. (18) and Eq. (12).

In this study we have chosen to work with the variables v and α for simplicity, and to clarify the dependence upon ρ_c which, together with the coupling constant $\kappa = 8\pi G$, is the only parameter entering the dynamics. However, Eq. (21) can be re-expressed using more familiar variables often used in the literature. In the effective formulation, the choice of canonical variables is just a matter of taste. The Hamiltonian can as well be expressed as

$$\mathcal{H}_G = -vV_0\frac{\rho_c}{2} \times\left(1 - \sqrt{1 - \frac{12}{\kappa\rho_c}\frac{k}{v^{2/3}}}\cos\left(2\lambda[\beta - \beta_1(v)]\right)\right), \tag{22}$$

where $\{\beta, v\} = \frac{\gamma\kappa}{2V_0}$, or

$$\mathcal{H}_G = -p^{3/2}V_0\frac{\rho_c}{2} \times \left(1 - \sqrt{1 - \frac{12}{\kappa\rho_c}\frac{k}{p}}\cos\left(2\frac{\lambda}{\sqrt{p}}[c - c_1(p)]\right)\right), \tag{23}$$

where $p = a^2 = v^{2/3}$, and $\{c, p\} = \frac{\gamma\kappa}{3V_0}$.

6. Previous LQC models with $k \neq 0$

Prior to this work, two different curved LQC models were considered for $k > 0$ and one for $k < 0$. We briefly review the results in this section.

As mentioned earlier, usually $k > 0$ is referred to as $k = 1$ and $k < 0$ as $k = -1$, since one often chooses coordinates so that $|k| = 1$ using the coordinate freedom of Eqs. (2)–(4).

6.1. $k > 0$, *first model: the homology way*

This model was developed independently in both [3] and [4]. The effective equations from this Hamiltonian were first calculated in [5], and later in [6].

The effective Hamiltonian in this model is

$$\mathcal{H}_{tot} = -V\rho_c\left[\sin^2(\lambda\beta - D) - \sin^2 D + \left(1 + \gamma^2\right)D^2\right] + V\rho, \tag{24}$$

where V is the total volume of the Universe, which makes sense since the Universe is closed, $\{\beta, V\} = \frac{\kappa\gamma}{2}$ and $D = \lambda\left(\frac{2\pi^3}{V}\right)^{1/3} = \lambda\sqrt{\frac{k}{a^2}}$.

The modified Friedmann equation in this model is

$$H^2 = \frac{\kappa}{3}(\rho - \rho_1)\left(1 - \frac{\rho - \rho_1}{\rho_c}\right), \tag{25}$$

where

$$\rho_1 := \frac{3}{\kappa}\left[\left(1 + \frac{1}{\gamma^2}\right)\frac{k}{a^2} - \frac{1}{\gamma^2\lambda^2}\sin^2\left(\lambda\sqrt{\frac{k}{a^2}}\right)\right]. \tag{26}$$

6.2. $k > 0$, *second model: the connection way*

This model was first suggested in [7], and further studied in [8]. The effective equations were first derived in [6].

The effective Hamiltonian in this model is

$$\mathcal{H}_{tot} = -V\rho_c\left[(\sin\lambda\beta - D)^2 + \gamma^2 D^2\right] + V\rho, \tag{27}$$

where V, β and D are the same as in the previous model.

The modified Friedmann equation in this model is

$$H^2 = \left(\frac{\kappa}{3}\rho - \frac{k}{a^2}\right)\left(1 - \frac{\rho - \rho_2}{\rho_c}\right), \tag{28}$$

where

$$\rho_2 = \frac{3}{\kappa}\left[\left(1 - \frac{1}{\gamma^2}\right)\frac{k}{a^2} \mp \frac{1}{\gamma}\sqrt{\frac{k}{a^2}\left(\frac{\kappa}{3}\rho - \frac{k}{a^2}\right)}\right] \tag{29}$$

and

$$(\mp) = -\text{sign}\left(\sin\lambda\beta - \lambda\sqrt{\frac{k}{a^2}}\right). \tag{30}$$

6.3. $k < 0$

The effective Hamiltonian in this model, proposed in [9], is

$$\mathcal{H}_{tot} = -\frac{3V_0p^{3/2}}{\kappa\gamma^2\lambda^2}\sin^2\left(\frac{\lambda c}{\sqrt{p}}\right) + \frac{3V_0\sqrt{p}}{\kappa} + V_0p^{3/2}\rho, \tag{31}$$

where $\{c, p\} = \frac{\gamma\kappa}{3V_0}$ and $k = -1$. Changing canonical variables, and un-freezing k we get an equivalent expression:

$$\mathcal{H}_{tot} = -vV_0\rho_c\left[\sin^2\lambda\beta + \gamma^2\lambda^2\frac{k}{v^{2/3}}\right] + vV_0\rho, \tag{32}$$

where $\{\beta, v\} = \frac{\gamma\kappa}{2V_0}$.

The modified Friedmann equation in this case is

$$H^2 = \left(\frac{\kappa}{3}\rho - \frac{k}{a^2}\right)\left(1 + \gamma^2\lambda^2\frac{k}{a^2} - \frac{\rho}{\rho_c}\right). \tag{33}$$

7. Discussion

We have shown that under very general and conservative assumptions, for any modified cosmology or modified gravity, the Friedmann equation for curved space can be immediately deduced from the Friedmann equation for a flat space. We have applied this result to effective LQC. In reviewing previous models for effective LQC on curved space, we find that there is a conflict between this work and previous results.

The source of this tension might come from the fact the holonomy corrections are in some approaches expected to lead to a deformed algebra of constraints that is known to lead to a non-metric theory. In that sense, the mismatch observed could be taken as an independent indication that holonomy modifications should lead to non-classical space–time structures, or deformed constraint algebras in the canonical formulation.

These works anyway suggest to more carefully consider the consistency conditions required for modified cosmologies. Even if there are good theoretical reasons to consider a given Hamiltonian and related modified Friedmann equation, symmetry considerations should not be forgotten if the theory is to be interpreted as a metric theory.

Acknowledgements

We would like to thank Martin Bojowald and Jakub Mielczarek for interesting comments.

L.S. is supported by the Labex ENIGMAS.

Appendix A. Different FLRW coordinates for de Sitter and Minkowski spaces

In this appendix we show by construction that in de Sitter and Minkowski spaces, there is always a coordinate transformation that leads to a FLRW coordinate representation, with the intrinsic curvature of any choice, only limited by $\frac{k}{a^2} \leq \frac{1}{\alpha^2}$, where α is a parameter of the manifold to be defined below.

Intuitively we use the fact that in de Sitter space, curvature is pure gauge.

A.1. de Sitter space

An N dimensional de Sitter space can be embedded in an N + 1 dimensional Minkowski space. Specifically for N = 4, the embedding is given by

$$-x_0^2+\sum_{i=1}^{4}x_i^2=\alpha^2, \tag{A.1}$$

and the metric is directly inherited,

$$ds^2=-dx_0^2+\sum_{i=1}^{4}dx_i^2, \tag{A.2}$$

where α is defined by Eq. (A.1) and $\alpha\geq 0$. Actually, α should be viewed as a property of the manifold rather than one of the coordinates.

Both the above equations are invariant under a Lorentz transformation of the $N+1$ dimensional Minkowski space. By such a coordinate transformation, any point P in the de Sitter space can be rotated so as to have the coordinates $(x_0,x_1,x_2,x_3,x_4)=(0,\alpha,0,0,0)$.

Given a plane in the larger Minkowski space,

$$b_0x_0+b_1x_1=c, \tag{A.3}$$

for some constants b_0, b_1 and c; the intersection between Eq. (A.1) and Eq. (A.3) will be a homogenous, 3 dimensional (possibly disconnected) surface. This intersection will be space-like if and only if the plane is intersected by the line $-x_0^2+x_1^2=\alpha^2$ at least once, and light-like if it is tangent to this line.

One can use the intersection with such planes to find FLRW coordinates for the de Sitter space. We start from the ansatz

$$x_0(t,r)=\alpha\left[\sinh\left(\frac{t}{\alpha}\right)+\sin(\theta)g(r,t)\right], \tag{A.4}$$

$$x_1(t,r)=\alpha\left[\cosh\left(\frac{t}{\alpha}\right)-\cos(\theta)g(r,t)\right], \tag{A.5}$$

$$\sqrt{x_2^2+x_3^2+x_4^2}=a(t)r, \tag{A.6}$$

where

$$g(0,t)=0\,,\quad \theta\in[-\frac{\pi}{2},-\frac{\pi}{2}], \tag{A.7}$$

and t, r and $a(t)$ are the same as in Eq. (1).

The ansatz is chosen so that t is the proper time along $r=0$, and points at constant t belong to a plane at an angle θ which is defined by Fig. 1.

The remaining step is, for every $\theta\in[-\frac{\pi}{2},\frac{\pi}{2}]$, to find $g(t,r)$, $a(t)$ and k, so that Eq. (A.1) is fulfilled, and Eq. (A.2) together with Eqs. (A.4)–(A.7) yield the FLRW metric.

In the case $\sin^2(\theta)\neq\cos^2(\theta)$, it is straightforward to show that the above requirements are fulfilled by

$$g(t,r)=\frac{\sin(\theta)\sinh\left(\frac{t}{\alpha}\right)+\cos(\theta)\cosh\left(\frac{t}{\alpha}\right)}{\sin^2(\theta)-\cos^2(\theta)}\times\left(-1+\sqrt{1-kr^2}\right), \tag{A.8}$$

and

$$a(t)=\alpha\sqrt{k}\,\frac{\left|\sin(\theta)\sinh\left(\frac{t}{\alpha}\right)+\cos(\theta)\cosh\left(\frac{t}{\alpha}\right)\right|}{\sqrt{\cos^2(\theta)-\sin^2(\theta)}}. \tag{A.9}$$

In the case $\theta=\frac{\pi}{4}$, one has:

$$g(t,r)=\frac{a_0^2r^2}{\sqrt{2}\,\alpha^2}e^{t/\alpha}\,,\quad a(t)=a_0e^{t/\alpha}\,,\quad k=0. \tag{A.10}$$

In the case $\theta=-\frac{\pi}{4}$, one has:

$$g(t,r)=\frac{a_0^2r^2}{\sqrt{2}\,\alpha^2}e^{-t/\alpha}\,,\quad a(t)=a_0e^{-t/\alpha}\,,\quad k=0. \tag{A.11}$$

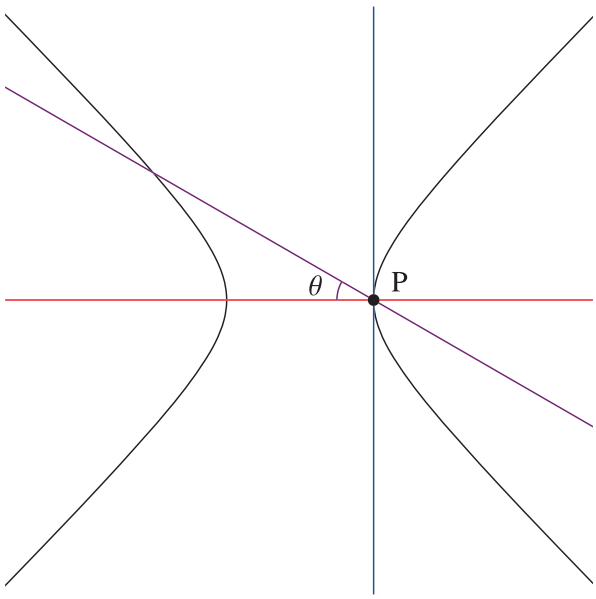

Fig. 1. The x_0,x_1-plane of Minkowski space. The black lines are the embedding of de Sitter space for R = 0. The straight lines represent different FLRW coordinate choices of de Sitter. There is one for each $\theta\in[-\frac{\pi}{2},\frac{\pi}{2}]$.

In all the above cases, we find that

$$H^2=\frac{1}{\alpha^2}-\frac{k}{a^2}, \tag{A.12}$$

and

$$\left.\frac{k}{a^2}\right|_{t=0}=\frac{1}{\alpha^2}\left(1-\tan^2(\theta)\right). \tag{A.13}$$

From the above equation, it is clear that $\frac{k}{a^2}\leq\frac{1}{\alpha^2}$, but other than that, it is a pure coordinate choice. It should be kept in mind that any point can be moved to $t=0$ by a Lorentz transformation of Eq. (A.1). Therefore, if one considers a FLRW metric with a Friedmann equation on the form Eq. (A.13), one can always move to some other FLRW coordinates with a different value of $\frac{k}{a^2}$ for some given time. Then, Eq. (A.13) will still be true for the new coordinates, with the same value of α.

A special case of this is when $k=0$ in the first set of coordinates: given a FLRW metric and a Friedmann equation that looks like

$$H^2=\text{constant}, \tag{A.14}$$

it is always possible to do a coordinate transformation to a system with

$$\left(H'\right)^2=\text{constant}-\frac{k'}{(a')^2}, \tag{A.15}$$

for $\frac{k'}{a'^2}\leq\text{constant}$.

A.2. Minkowski space

Let us start from the flat spherical coordinates (T,R,θ,ϕ) with the metric

$$ds^2=-dT^2+dR^2+R^2d\Omega^2. \tag{A.16}$$

We now define the hyperbolic coordinates (t,r) from the relations

$$R=\sqrt{-k}\,tr\,,\quad T^2-R^2=t^2\,,\quad k<0. \tag{A.17}$$

We leave the angular coordinates (θ,ϕ) as they are. See Fig. 2.

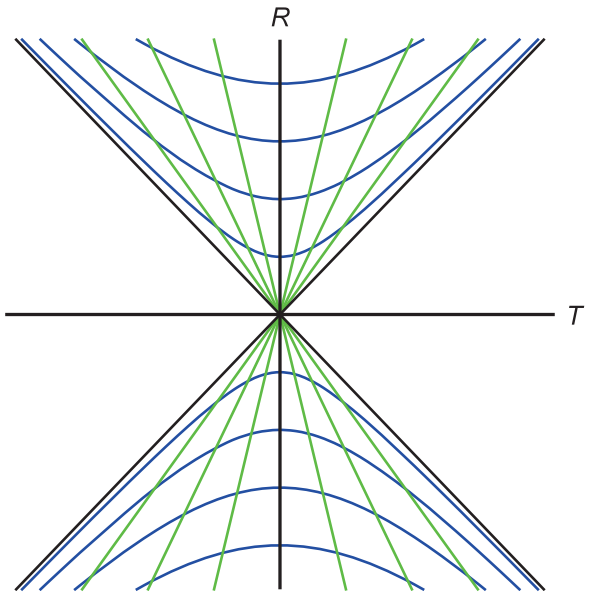

Fig. 2. Hyperbolic coordinates of Minkowski space. Green lines are $r =$ constant, and blue lines are $t =$ constant. (For interpretation of the references to color in this figure legend, the reader is referred to the web version of this article.)

It is straightforward to show that in the hyperbolic coordinates, the metric becomes

$$ds^2 = -dt + a(t)^2 \left(\frac{dr^2}{1 - kr^2} + r^2 d\Omega \right), \tag{A.18}$$

where

$$a(t) = \sqrt{-k}\, t. \tag{A.19}$$

Minkowski space can therefore be described by FLRW coordinates for any $k \leq 0$. The scale factor of these coordinates will be

$$a(t) = \begin{cases} \text{constant} & \text{for } k = 0, \\ \sqrt{-k}\,(t - t_0) & \text{for } k < 0, \end{cases} \tag{A.20}$$

where t_0 is an arbitrary time translation.

For both $k = 0$ and $k < 0$, we find that

$$H^2 = -\frac{k}{a^2}. \tag{A.21}$$

Given a FLRW metric together with $k = 0$ and $H^2 = 0$, it is always possible to do a coordinate transformation to some other FLRW coordinates with

$$\left(H'\right)^2 = -\frac{k'}{(a')^2}, \tag{A.22}$$

with $k' \leq 0$.

References

[1] I. Agullo, A. Corichi, in: A. Ashtekar, V. Petkov (Eds.), The Springer Handbook of Spacetime, Springer-Verlag, 2013, arXiv:1302.3833 [gr-qc];
A. Ashtekar, M. Bojowald, J. Lewandowski, Adv. Theor. Math. Phys. 7 (2003) 233;
A. Ashtekar, Gen. Relativ. Gravit. 41 (2009) 707;
A. Ashtekar, P. Singh, Class. Quantum Gravity 28 (2011) 213001;
K. Banerjee, G. Calcagni, M. Martin-Benito, SIGMA 8 (2012) 016;
A. Barrau, T. Cailleteau, J. Grain, J. Mielczarek, Class. Quantum Gravity 31 (2014) 053001;
A. Barrau, J. Grain, in: A. Ashtekar, J. Pullin (Eds.), 100 Years of General Relativity, World Scientific, 2015, arXiv:1410.1714;
M. Bojowald, Living Rev. Relativ. 11 (2008) 4;
M. Bojowald, Class. Quantum Gravity 29 (2012) 213001;
G. Calcagni, Ann. Phys. (Berlin) 525 (2013) 323.
[2] P. Dona, S. Speziale, arXiv:1007.0402v1;
A. Perez, arXiv:gr-qc/0409061v3;
R. Gambini, J. Pullin, A First Course in Loop Quantum Gravity, Oxford University Press, Oxford, 2011;
C. Rovelli, arXiv:1102.3660v5 [gr-qc];
C. Rovelli, Quantum Gravity, Cambridge University Press, Cambridge, 2004;
C. Rovelli, Living Rev. Relativ. 1 (1998) 1;
L. Smolin, arXiv:hep-th/0408048v3;
T. Thiemann, Lect. Notes Phys. 631 (2003) 41;
T. Thiemann, Modern Canonical Quantum General Relativity, Cambridge University Press, Cambridge, 2007.
[3] L. Szulc, W. Kaminski, J. Lewandowski, Class. Quantum Gravity 24 (2007) 2621.
[4] A. Ashtekar, T. Pawlowski, P. Singh, K. Vandersloot, Phys. Rev. D 75 (2007) 024035.
[5] J. Mielczarek, O. Hrycyna, M. Szydlowski, J. Cosmol. Astropart. Phys. 0911 (2009) 014.
[6] A. Corichi, A. Karami, Phys. Rev. D 84 (2011) 044003.
[7] A. Ashtekar, E. Wilson-Ewing, Phys. Rev. D 80 (2009) 123532.
[8] E. Wilson-Ewing, Phys. Rev. D 82 (2010) 043508.
[9] K. Vandersloot, Phys. Rev. D 75 (2007) 023523.

7.2 Possible re-birth of the Universe

This article is probably the most speculative of this manuscript. It addresses the question of a possible fundamental role played by the cosmological constant in the remote past. The idea is the following: if one assumes that the Universe is currently dominated by a true cosmological constant, as advocated in [18], and if this cosmological constant is taken as a fundamental parameter of LQG – that might, in addition, play the role of an infrared regulator – it should also be present before the bounce. So, when going far enough backward in time in the contracting branch, the Universe should also be Λ-dominated. It would then be in the contracting solution of de-Sitter space: $H = -\sqrt{\Lambda/3}$.

But de-Sitter space is known to exhibit thermodynamical properties close to those of a black hole. Here, we consider the emission of radiation by the de-Sitter horizon and evaluate explicitly the time it would take for this radiation content to reach the Planck density and therefore trigger the bounce. This is a proposal for a geometrical origin of the content of the Universe.

Interestingly this hypothesis also has interesting features for the far future of the Universe. After a finite amount of time a given Hubble patch will become fully empty because of the expansion. It will then be pure de Sitter. But in pure de-Sitter space, being expanding, contracting or static is not physical: it is just a matter of coordinate choice. But when a photon is emitted at a typical energy $(1/2\pi)\sqrt{\Lambda/3}$ it will inevitably induce a symmetry breaking by imposing a preferred time direction. If this symmetry breaking is such that the Universe is expanding, the radiation will be red-shifted and after some time we get back to an empty universe. The other way round, if this symmetry breaking is such that the Universe is contracting (and this will inevitably happen sooner or later), the radiation will be blue-shifted and the density of the Universe increases. This leads to a cyclic model whose origin is purely geometrical.

We have also checked that the homogeneous hypothesis is consistent and that it offers a graceful exit to the problem of growth of inhomogeneities in a contracting universe.

Journal of Cosmology and Astroparticle Physics
An IOP and SISSA journal

Our Universe from the cosmological constant

Aurélien Barrau and Linda Linsefors

Laboratoire de Physique Subatomique et de Cosmologie,
Université Grenoble-Alpes, CNRS-IN2P3,
53, avenue des Martyrs, 38026 Grenoble Cedex, France

E-mail: Aurelien.Barrau@cern.ch, linda.linsefors@lpsc.in2p3.fr

Received October 15, 2014
Revised November 10, 2014
Accepted December 3, 2014
Published December 17, 2014

Abstract. The issue of the origin of the Universe and of its contents is addressed in the framework of bouncing cosmologies, as described for example by loop quantum gravity. If the current acceleration is due to a true cosmological constant, this constant is naturally conserved through the bounce and the Universe should also be in a (contracting) de Sitter phase in the remote past. We investigate here the possibility that the de Sitter temperature in the contracting branch fills the Universe with radiation that causes the bounce and the subsequent inflation and reheating. We also consider the possibility that this gives rise to a cyclic model of the Universe and suggest some possible tests.

Keywords: initial conditions and eternal universe, physics of the early universe, quantum cosmology

ArXiv ePrint: 1406.3706v2

doi:10.1088/1475-7516/2014/12/037

JCAP12(2014)037

Contents

1 Basic hypothesis of the model

The scenario presented in this article deals with the question of the origin of the Universe and of its contents in models were a bounce replaces the Big Bang, with a specific emphasis on the loop quantum gravity theory. It does not provide a new model of the high-density universe and relies on successful existing scenarios for the UV behavior. But it does suggest an original geometric understanding of the remote past (in the contracting branch), of the far future (in the expanding branch) and of the origin of matter and radiation. When a bounce replaces the original singularity, those questions become fundamental.

There are many attempts to account for the current acceleration of the Universe (see, e.g., [1] for a pedagogical review). In this work, we will follow the most simple and — in our opinion — most natural one: a pure cosmological constant. It should be reminded that in itself the cosmological constant has no link with quantum fluctuations of the vacuum as it is part of standard general relativity. The most general low-energy second order action for the gravitational field, invariant under the diffeomorphisms symmetry is

$$S[g] = \frac{1}{16\pi G}\int (R[g] - 2\Lambda)\sqrt{g}, \tag{1.1}$$

which leads to the Einstein equations with a cosmological constant. Otherwise stated, in a metric theory of gravity in d dimensions, the generic local Lagrange density which leads to equations of motion containing at most second order derivatives of the metric is [2, 3]:

$$\begin{aligned} L &= \sum_{n=0}^{[d/2]} c_n L_n \\ &\equiv \sum_{n=0}^{[d/2]} c_n 2^{-n} \delta^{\alpha_1\cdots\alpha_{2n}}_{\beta_1\cdots\beta_{2n}} R_{\alpha_1\alpha_2}{}^{\beta_1\beta_2} \ldots R_{\alpha_{2n-1}\alpha_{2n}}{}^{\beta_{2n-1}\beta_{2n}}, \end{aligned} \tag{1.2}$$

where $\delta^{\alpha_1\cdots\alpha_k}_{\beta_1\cdots\beta_k}$ is the generalized Kronecker delta symbol, $[d/2]$ is $d/2$ rounded up to the nearest integer and c_n are constants ($L_0 \equiv 1$). The first term is the cosmological constant, the second is the Einstein-Hilbert Lagrange density, and next terms correspond to Lovelock gravity. In $d = 4$, Einstein gravity with a cosmological constant is therefore the natural general solution.

JCAP12(2014)037

Nothing here is added "by hands" to fit the observations. In the spirit of [4], we assume that the observed acceleration is caused by this $\Lambda-$term and that the quantum fluctuations do not gravitate at all. It is highly probable as the "suppression" factor required to account for the acceleration by the vacuum energy would need to be huge and extremely fine-tuned. And the problem of understanding why the true cosmological constant is exactly zero — which is not a value favored by general relativity — would remain. Several solutions to avoid the coupling of quantum fluctuations to gravity are already known, for exemple through deriving gravity by maximizing a suitable entropy functional without using the metric tensor as a dynamical variable [5], or by considering the trace-free version of Einstein equations which is essentially equivalent to unimodular gravity [6].

The second hypothesis of this article is that, as quite generically expected in quantum gravity, a bounce replaces the Big Bang singularity. Bounces are present in different classes of models, e.g. in the Pre-Big Bang approach [7] or in the ekpyrotic model [8]. This may even happen in classical gravity [9–12]. To remain specific and precise, we however focus in the following on the particular case of the bounce induced by loop quantum gravity (LQG) as this provides a simple, well defined and intensively studied example where a fundamental cosmological contant fits the theory and where the bounce conditions are triggered by the density. It should be made clear that our proposal just requires two assumptions: that the cosmological contant is basically conserved at the bounce and that the bounce itself happens when the density reaches a given critical value. LQG is a non-perturbative and background-invariant quantization of gravity [13–21] and loop quantum cosmology (LQC) is its symmetry-reduced version [22–29]. Using the Chern-Simons theory in d=3 (that is a topological quantum field theory), successful attempts to account for a cosmological constant through a quantum group structure in d=4 were recently presented [30], based on the fact that the Turaev-Viro spinfoam model is also defined in terms of quantum groups. In the framework of LQC, it was shown that a simple modification of the amplitude describing the dynamics, corresponding to the introduction of the cosmological constant (and related to the $\mathrm{SL}(2,\mathbb{C})q$ extension of the theory considered in [31]), yields the standard classical de Sitter (dS) cosmological solution [32] in the low energy limit.

In LQC, the Big Bang singularity is resolved in a very precise manner due to repulsive quantum geometrical effects (see [33] and references therein), the theory being inequivalent to the Wheeler-deWitt approach already at the kinematical level. Holonomy corrections lead to modified Friedmann equations reading (in the high density limit, where the cosmological constant and curvature can be neglected) [22–29]:

$$H^2 = \frac{8\pi G}{3}\rho\left(1-\frac{\rho}{\rho_{\mathrm{c}}}\right), \tag{1.3}$$

where ρ_{c} is of order of the Planck density. This equation clearly shows that the Big Bang singularity is solved and replaced by a Big Bounce: when $\rho=\rho_{\mathrm{c}}$, the Hubble parameter vanishes and changes sign. There is a contracting branch before our current expanding branch. In the remote past, the Universe was necessarily dominated by the cosmological constant: it was just in exponential contraction instead of being in exponential expansion as in the remote future. As the Friedmann equation reads, for a flat $\Lambda-$dominated universe, $H^2=\frac{\Lambda}{3}$, there are indeed positive H and negative H solutions, even for a positive cosmological constant.

In the following, we heavily use the properties of those dS contracting and expanding banches of the Universe.

JCAP12(2014)037

2 The de Sitter horizon

De Sitter space is the maximally symmetric solution of the vacuum Einstein equations with a positive cosmological constant. It is positively curved with a characteristic length $l = \sqrt{3/\Lambda}$. A key feature is that there are now particle horizons. Each observer is surrounded by a horizon of area $A = 4\pi l^2$. In static coordinates, the metric reads

$$ds^2 = -\left(1 - r^2\right) dt^2 + \left(1 - r^2\right)^{-1} dr^2 + r^2 d\Omega_{n-2}^2 \,. \tag{2.1}$$

It was shown that the close connection between event horizons and thermodynamics found in the case of black holes can be extended to dS spaces [34]. Any observer perceives a temperature T given by

$$T = \frac{H}{2\pi} = \frac{1}{2\pi l} = \frac{1}{2\pi}\sqrt{\frac{\Lambda}{3}} \,. \tag{2.2}$$

Many articles were devoted to the thermodynamics of dS spaces [35–45]. The current situation is not fully clear. It might be argued that due to the dS temperature the mean value of the stress-energy tensor receives a correction that appears as a modified cosmological constant [46, 47]. But those results are obtained using standard methods of quantum field theory in curved spaces at vanishing temperature. The stability of the contracting dS phase was studied in the framework of effective theories and some hints were found in favor of an instability [48, 49]. However those analysis were not based on the $< in|in >$ formalism [50], which is more relevant in this case and reaches different conclusions [51–54]. For generic consideration on this issue, see [55] and references therein.

The status of particles created by the dS horizon is therefore highly debated (see, e.g., [56–58]). There is no clear consensus. In this work, and this can be considered as our third hypothesis, we assume that they behave as standard radiation that can be considered as a source term in the Friedmann equation, continuously fed by the dS horizon. This is a reasonable and conservative hypothesis supported by the deep analogy between the dS temperature and the Hawking temperature of a black hole. This is in agreement with (if not required by) all studies of the dS thermal properties (see, e.g., [59] and references therein). Otherwise stated, backreaction has to be taken into account to go beyond QFT on a curved background and this is mandatory in this case. The universe is in the Bunch Davies vacuum in the remote past. So, either the symmetries are taken seriously and the quantum state is maximally symmetric, just like the dS space, which leads to a correction of the cosmological constant, or the matter and radiation contents are taken seriously and the quantum state then looks like a thermal bath. This second option is the path we follow here as it is — as explained in the previously quoted articles — more consistent and arguably more conservative.

We therefore consider that particles in the dS Universe are, in the spirit of [34] and as supported by more recent works [60], continuously created by the horizon, in thermal equilibrium at the temperature given by eq. (2.2). Since it is very low, $T = 2 \times 10^{-34}\,\mathrm{eV}$, we focus on massless particles. As for any gas of thermal bosons the energy and number density are

$$\rho = \frac{\pi^2}{30} g T^4 = \frac{g\Lambda^2}{4320\pi^2} \,, \quad n = \frac{\zeta(3)}{\pi^2} g T^3 \,, \tag{2.3}$$

where g is the number of species and ζ is Riemann zeta function. The average total number of particles inside the Hubble horizon will be $N = \frac{4\pi l^3}{3} n = \frac{\zeta(3)}{6\pi^4} g = 0.0021 g$, where g is equal to 2 or 4 depending on whether gravitons are included or not. In any case $N \ll 1$, so that most of the time, the space is truly empty.

JCAP12(2014)037

3 Origin of the Universe

This empty dS space is maximally symmetric: all space-time points are the same, even points in the future and in the past. However, depending on the choice of coordinates, the dS space might appear to either contract or expand. In a pure dS space the difference between expansion and contraction is just a coordinate transformation. The amount of spatial curvature is also just a coordinate choice, but with an upper bound $\frac{k}{a^2} \leq \frac{\Lambda}{3}$ (this can be derived from the Friedmann equation which, in this case, is $H^2 = \frac{\Lambda}{3} - \frac{k}{a^2}$). When $\frac{k}{a^2} = \frac{\Lambda}{3}$, the universe will appear to bounce in the considered coordinates. But for any coordinate-invariant observable, a dS universe always remains the same for all times. If, however, standard fields, e.g. radiation coming from the dS horizon itself, are introduced, the time symmetry will be broken. In the simplest case, we end up with a homogenous universe that evolves in time. We focus on this specific case to get qualitative ideas of what this implies.

We suggest a scenario where the radiation from the dS horizon spontaneously breaks the symmetry of the dS structure. Out of this, one gets a universe with a tiny amount of radiation, an arbitrary curvature, and a Hubble factor with arbitrary sign. This is fully determined by the emitted radiation which depends on a random quantum process. If the Universe happens to be put in an expanding state by this quantum emission, the radiation will be diluted away and one gets back to an empty dS space until the next radiation is emitted. But if the Universe happens to be contracting, the radiation gets blues-shifted and the energy density of the Universe will increase.

Let us start with the Friedmann equation (without quantum correction as we here deal with the IR behavior)

$$H^2 = \frac{\Lambda}{3} - \frac{k}{a^2} + \frac{\kappa}{3}\rho. \tag{3.1}$$

By choosing an appropriate integration constant, the equation of motion for the contracting solution reads

$$-2\sqrt{\frac{\Lambda}{3}}t = \ln\left(-K + \sqrt{\frac{\Lambda}{\kappa\rho}} + \sqrt{1 - 2K\sqrt{\frac{\Lambda}{\kappa\rho}} + \frac{\Lambda}{\kappa\rho}}\right), \tag{3.2}$$

where K is a constant of motion defined as $K := \frac{3k}{2a^2\sqrt{\Lambda\kappa\rho}}$. There are tree types of solutions:

$$K > 1 \quad \text{bounce at} \qquad -2\sqrt{\frac{\Lambda}{3}}t_B = \ln\left(\sqrt{K^2 - 1}\right), \tag{3.3}$$

$$K = 1 \quad \text{eternal contraction,} \tag{3.4}$$

$$K < 1 \quad \text{crunch at} \qquad -2\sqrt{\frac{\Lambda}{3}}t_C = \ln(-K + 1). \tag{3.5}$$

One of those cases will be randomly selected by the emission of radiation out of the empty dS space. If the case $K > 1$ is selected, a bounce will happen at the energy density $\rho_B = \frac{\Lambda}{\kappa}\left(K + \sqrt{K^2 - 1}\right)^{-2} < \frac{\Lambda}{\kappa} = 1.1 \times 10^{-123}$ which is way to small to be the "origin" of the expanding Universe that we observe today. In this case, the radiation will just dilute away. We conclude that if the dS symmetry is broken so that $H \geq 0$ or $H < 0$ and $K > 1$, the radiation will just be diluted away. In both those cases, one gets back to an empty dS space and the process can start again. Another emission will select another case. The probability of ending up with exactly $K = 1$ is vanishing.

JCAP12(2014)037

Therefore, sooner or later, the Universe will end up with $H \leq 0$ and $K < 1$. Here, the energy density will grow to arbitrary large values due to the blue-shift. If we now combine this picture with a quantum bounce, e.g. from LQC, this sets a suitable origin for our expanding universe.

4 Quantum bounce

Classically, if $K < 1$, which will inevitably happen in this scenario, the Universe ends up in a crunch. But if quantum gravity effets are taken into account, the crunch will be replaced by a bounce. Contrary to the kurvature bounce (which happens when $K > 1$), the quantum bounce happens at a high enough energy ($\rho_c \approx 0.41$) to be a possible beginning for our expanding universe. At this energy density, the curvature will be

$$\left(\frac{k}{a^2}\right)_{\rm QB} = \sqrt{\frac{\rho_c}{\rho_0}}\,\frac{k}{a_0^2} \approx -3.3\times 10^{123}\,\frac{k}{a_0^2}. \tag{4.1}$$

Since $K < 1$ for the quantum bounce to happen, $\left(\frac{k}{a^2}\right)_{\rm QB} < \frac{2}{3}\sqrt{\Lambda\kappa\rho_c} \approx 3.6\times 10^{-61}$. This sould be compared with $\frac{\kappa}{3}\rho_c \approx 3.4$. Therefore, any positive curvature can be safely ignored at the quantum bounce. However there is no similar limit for the negative curvature, which, in principe, can be large. (Interestingly, the LQC bounce has also been studied in the case of negative curvatures [64–66]).

The time between the initial symmetry breaking of the dS space and the quantum bounce can be estimated to be

$$(t_{\rm QB}-t_0) \approx \frac{1}{2}\sqrt{\frac{3}{\Lambda}}\ln\left[\frac{1}{1-K}\left(-K+\sqrt{\frac{\Lambda}{\kappa\rho_0}}+\sqrt{1-2K\sqrt{\frac{\Lambda}{\kappa\rho_0}}+\frac{\Lambda}{\kappa\rho_0}}\right)\right], \tag{4.2}$$

with interesting limits:

$$\left|\frac{k}{a_0^2}\right| \ll \Lambda \quad\Rightarrow\quad (t_{\rm QB}-t_0) \approx \frac{1}{2}\sqrt{\frac{3}{\Lambda}}\ln\left(2\sqrt{\frac{\Lambda}{\kappa\rho_0}}\right) = 1.3\times 10^{12}\ \text{years}, \tag{4.3}$$

$$-\frac{k}{a_0^2} \gg \Lambda \quad\Rightarrow\quad (t_{\rm QB}-t_0) \approx \left(-\frac{k}{a_0^2}\right)^{-1/2}. \tag{4.4}$$

The duration of the contraction phase can be, depending on the curvature, anything between the Planck time and 1.3×10^{12} years.

When the energy density approaches the critical density, quantum gravity effects enter the game and the bounce takes place. For the specific framework of LQC, we refer the reader to [22–29] and references therein for details. Basically, the Wheel-DeWitt equation is replaced by a difference equation: $\partial_\varphi^2\Psi(\nu,\varphi) = \frac{3\pi G}{4\lambda^2}\nu\left[(\nu+2\lambda)\Psi(\nu+4\lambda)-2\nu\tilde{\Psi}(\nu)+(\nu-2\lambda)\Psi(\nu-4\lambda)\right]$ where Ψ is the wave function of the Universe and λ is the square root of the minimum area gap. Our scenario elegantly matches the usual LQC view (among others) by providing an explicit mechanism for the origin of the contents that triggers the bounce. The Universe does not need anymore to be arbitrary assumed to be filled by some matter whose origin is mysterious. Here, the origin of the contents is only provided by the quantum geometrical properties of the dS space.

JCAP12(2014)037

It is natural — or at least possible — to assume that during the contraction, the contents of the Universe gets dominated by a scalar field (either fundamental or effective) which would automatically lead to inflation [61–63] and to the usual evolution of the Universe. The new scenario presented here does *not* replace the usual early Universe evolution and does *not* depend on the details on this mechanism. The bounce is a very generic feature of quantum geometry (see, e.g., [67] and references therein) and the detailed contents of the Universe at the bounce time, either a massive scalar field or something else, does not play a significant role in this model. It is of course relevant for the generation of perturbations and the details of the UV behavior but not for the new input of this article which does not deal with particle physics at (or near) the Planck scale.

The question addressed here is the origin of the content of the Universe and its remote past and future behavior.

5 Inhomogeneities

Throughout this article, we have assumed a homogeneous and isotropic universe. This is certainly not true at all times.

By construction of the model, the "initial" state is indeed homogenous and isotropic as it results from the total dilution of any matter contents in the previous expanding branch (the model anyway starts from dS which is by definition homogeneous). It is therefore legitimate to use standard Friedmann equations at this starting point.

As soon as a photon is emitted by the horizon and begins to fill the Universe, the homogeneity is broken. Both time and space symmetry are broken. Space symmetry is therefore only assumed at this stage of the development of the model to keep the calculations simple. This assumption should be relaxed in future works. However, some qualitative arguments might lead to think that the main conclusions or this work should remain true. The wavelength of the radiation is indeed initially comparable with the Hubble radius and homogeneity can therefore be assumed to be a reasonable approximation. Spatial homogeneity is not strongly violated. As time goes on, the wavelength gets blue-shifted and the photon is more and more localized. But, in the meanwhile, other photons have been emitted and the Universe remains quite homogeneous when averaged on large enough scales. It is easy to show using Stefan's law that the mean time between two emissions from the horizon is, in Planck units, of order $1/T$. This is precisely the time it takes for the scale factor to change by a sizable amount (that is for the radiation to be substancially blue-shifted). The time needed for the scale factor to vary by a factor x is indeed $\ln(x)/\sqrt{\Lambda} \sim 1/T$. The precise estimate of the inhomogeneities is beyond the scope of this article and should be studied in a future work but using Friedmann equations to describe the basics of the background seems at this stage quite reasonable.

The issue of anisotropies is less severe as, even if they develop and if the shear eventually dominates near the bounce — which is expected, — the main characteristics of the bounce have been already shown to survive.

This also raises an interesting feature of this model. In usual LQC, or more generically in bouncing cosmologies, the remote past of the contracting branch (after a possible Λ-dominated stage) is implicitly assumed to be matter dominated for time-symmetry reasons (the expanding branch is matter-dominated up to the cosmological constant domination phase). This raises a problem. In an expanding matter-dominated universe, it is well known that inhomogeneities grow linearly with the scale factor a. Gravity is in competition with

JCAP12(2014)037

the expansion. However, in a contracting universe, both play in the same direction — that is help the growth of inhomogeneities — and it can easily be shown that perturbations grow (the scale factor is now decreasing) as $1/a^{\frac{3}{2}}$ that is (as expected) faster. Matter inhomogeneities are therefore expected to eventually become very important. On the other hand, in our model, the Universe is only filled by radiation and radiation does not cluster. The initial dS temperature is obviously way too small to lead to the emission of any matter field. As the universe contracts, it will always remain radiation dominated (up to a possible scalar field transition around, e.g., the GUT scale). Even after the mean temperature became high enough to create matter particles by scattering, radiation will anyway dominate because of its scale-factor dependance. This circumvents the previously mentioned problem and makes a point for this model.

6 Rebirth of the Universe and tests of the model

Up to now, we have shown how the remote past Universe should be filled with dS radiation due to the cosmological constant which should cause the bounce and the standard evolution. The question of the far future and fundamental origin of the remote past state must now be addressed. In the future, huge patches of our Universe, with radii larger than the Hubble scale, will be completely empty. They will be pure dS spaces. If the model suggested in this work is correct, these empty spaces will undergo the very same process as described previously (as there is no distinction between an expanding and a contracting pure empty dS space). Radiation will be emitted until one photon randomly leads to a contracting foliation. This makes the model cyclic and solves the question of the origin: the contracting branch emerges from a symmetry breaking of the previous expanding branch (which is neither really expanding or contracting when it becomes pure empty dS). It should be emphasized that time always exist in this scenario in the sense of a light cone structure.

Is it possible to test this scenario? First, it should be pointed out that no new "theory" is suggested here. We just link together all the consequences of already accepted or assumed models. The two main ingredients of our proposal are the bounce and the cosmological constant. Both can be tested and, in principle, if both are validated the suggest scenario comes somehow automatically. As far as the bounce in concerned, different observational footprints can be expected, even beyond LQC (see, e.g., [68, 69] and references therein). As far as the interpretation of the acceleration of the Universe by a cosmological constant (or not) is concerned, many experiments are devoted to this issue, in particular the LSST telescope and the Euclid satellite.

One step further, this specific scenario of filling the Universe with dS radiation (beyond the bounce and cosmological constant ingredients) can be falsified. Let us consider an example. If our suggestion is correct, one does not expect complex structures in the contracting branch because radiation always dominates. In particular, there is no simple way to form stars and subsequent black holes. However, coalescence of black holes in the contracting phase have been shown to be detectable [70]. If such circles were to be seen in data, this would disproof our proposal. This statement should be readdressed when inhomogeneities are taken into account.

A third insight might come from analog systems. The strong mathematical links between the dS radiation and the Hawking radiation of black holes pointed out in [71] could lead to indirect tests of the existence of the dS radiation, as seen in static coordinates.

JCAP12(2014)037

This simple model builds on the specific properties of dS spaces and bouncing cosmologies to suggest an original new scenario which does not require any assumption about the initial matter contents of the Universe. Everything happens because of the cosmological constant and quantum effects. Particle physics enters the game for the details of the dynamics around the bounce, but the main picture just relies on "vacuum" properties. There are no divergences, no origin of time, and no problem of initial values for the contents of the Universe. The issue of inhomogeneities and the explicit construction of a global spacetime structure will be studied in future works.

Acknowledgments

L.L. is supported by the Labex ENIGMASS.

References

[1] P. Brax, *Gif Lectures on Cosmic Acceleration*, arXiv:0912.3610 [INSPIRE].

[2] D. Lovelock, *The Einstein tensor and its generalizations*, *J. Math. Phys.* **12** (1971) 498 [INSPIRE].

[3] F. Ferrer and S. Rasanen, *Lovelock inflation and the number of large dimensions*, *JHEP* **11** (2007) 003 [arXiv:0707.0499] [INSPIRE].

[4] E. Bianchi and C. Rovelli, *Why all these prejudices against a constant?*, arXiv:1002.3966 [INSPIRE].

[5] T. Padmanabhan, *A dialogue on the nature of gravity*, in *Foundations of Space and Time*, J. Murugan, A. Weltman and G. ellis eds., Cambridge University Press, Cambridge, U.K (2012), pg. 8–49.

[6] G.F.R. Ellis, *The Trace-Free Einstein Equations and inflation*, *Gen. Rel. Grav.* **46** (2014) 1619 [arXiv:1306.3021] [INSPIRE].

[7] M. Gasperini and G. Veneziano, *The pre-big bang scenario in string cosmology*, *Phys. Rept.* **373** (2003) 1 [hep-th/0207130] [INSPIRE].

[8] P.J. Steinhardt and N. Turok, *Cosmic evolution in a cyclic universe*, *Phys. Rev.* **D 65** (2002) 126003 [hep-th/0111098] [INSPIRE].

[9] P. Peter and N. Pinto-Neto, *Primordial perturbations in a non singular bouncing universe model*, *Phys. Rev.* **D 66** (2002) 063509 [hep-th/0203013] [INSPIRE].

[10] F.T. Falciano, M. Lilley and P. Peter, *A classical bounce: Constraints and consequences*, *Phys. Rev.* **D 77** (2008) 083513 [arXiv:0802.1196] [INSPIRE].

[11] L.R. Abramo, I. Yasuda and P. Peter, *Non singular bounce in modified gravity*, *Phys. Rev.* **D 81** (2010) 023511 [arXiv:0910.3422] [INSPIRE].

[12] D. Battefeld and P. Peter, *A Critical Review of Classical Bouncing Cosmologies*, arXiv:1406.2790 [INSPIRE].

[13] P. Dona and S. Speziale, *Introductory lectures to loop quantum gravity*, arXiv:1007.0402 [INSPIRE].

[14] A. Perez, *Introduction to loop quantum gravity and spin foams*, gr-qc/0409061 [INSPIRE].

[15] R. Gambini and J. Pullin, *A First Course in Loop Quantum Gravity*, Oxford University Press, Oxford, U.K. (2011).

[16] C. Rovelli, *Zakopane lectures on loop gravity*, PoS(QGQGS 2011)003 [arXiv:1102.3660] [INSPIRE].

JCAP12(2014)037

[17] C. Rovelli, *Quantum Gravity*, Cambridge University Press, Cambridge U.K. (2004).

[18] C. Rovelli, *Loop Quantum Gravity*, *Living Rev. Rel.* **1** (1998) 1.

[19] L. Smolin, *An invitation to loop quantum gravity*, *Rev. Mod. Phys.* (2004) 655 [hep-th/0408048] [INSPIRE].

[20] T. Thiemann, *Lectures on loop quantum gravity*, *Lect. Notes Phys.* **631** (2003) 41 [gr-qc/0210094] [INSPIRE].

[21] T. Thiemann, *Modern Canonical Quantum General Relativity*, Cambridge University Press, Cambridge U.K. (2007).

[22] A. Ashtekar, M. Bojowald and J. Lewandowski, *Mathematical structure of loop quantum cosmology*, *Adv. Theor. Math. Phys.* **7** (2003) 233 [gr-qc/0304074] [INSPIRE].

[23] A. Ashtekar, *Loop Quantum Cosmology: An Overview*, *Gen. Rel. Grav.* **41** (2009) 707 [arXiv:0812.0177] [INSPIRE].

[24] A. Ashtekar and P. Singh, *Loop Quantum Cosmology: A Status Report*, *Class. Quant. Grav.* **28** (2011) 213001 [arXiv:1108.0893] [INSPIRE].

[25] M. Bojowald, *Loop Quantum Cosmology*, *Living Rev. Rel.* **11** (2008) 4.

[26] M. Bojowald, *Quantum Cosmology: Effective Theory*, *Class. Quant. Grav.* **29** (2012) 213001 [arXiv:1209.3403] [INSPIRE].

[27] K. Banerjee, G. Calcagni and M. Martin-Benito, *Introduction to loop quantum cosmology*, *SIGMA* **8** (2012) 016 [arXiv:1109.6801] [INSPIRE].

[28] G. Calcagni, *Observational effects from quantum cosmology*, *Annalen Phys.* **525** (2013) 323.

[29] I. Agullo and A. Corichi, *Loop Quantum Cosmology*, arXiv:1302.3833 [INSPIRE].

[30] M. Dupuis and F. Girelli, *Observables in Loop Quantum Gravity with a cosmological constant*, *Phys. Rev.* **D 90** (2014) 104037 [arXiv:1311.6841] [INSPIRE].

[31] W.J. Fairbairn and C. Meusburger, *Quantum deformation of two four-dimensional spin foam models*, *J. Math. Phys.* **53** (2012) 022501 [arXiv:1012.4784] [INSPIRE].

[32] E. Bianchi, T. Krajewski, C. Rovelli and F. Vidotto, *Cosmological constant in spinfoam cosmology*, *Phys. Rev.* **D 83** (2011) 104015 [arXiv:1101.4049] [INSPIRE].

[33] A. Ashtekar, *Singularity Resolution in Loop Quantum Cosmology: A Brief Overview*, *J. Phys. Conf. Ser.* **189** (2009) 012003 [arXiv:0812.4703] [INSPIRE].

[34] G.W. Gibbons and S.W. Hawking, *Cosmological Event Horizons, Thermodynamics and Particle Creation*, *Phys. Rev.* **D 15** (1977) 2738 [INSPIRE].

[35] M.D. Pollock and T.P. Singh, *On the thermodynamics of de Sitter space-time and quasi-de Sitter space-time*, *Class. Quant. Grav.* **6** (1989) 901 [INSPIRE].

[36] B.B. Wang and C.G. Huang, *Thermodynamics of de Sitter space-time in York's formalism*, *Mod. Phys. Lett.* **A 16** (2001) 1487 [INSPIRE].

[37] T. Padmanabhan, *Thermodynamics and/of horizons: A Comparison of Schwarzschild, Rindler and de Sitter space-times*, *Mod. Phys. Lett.* **A 17** (2002) 923 [gr-qc/0202078] [INSPIRE].

[38] C.-G. Huang, L. Liu and B. Wang, *Thermodynamics of de Sitter universes*, *Phys. Rev.* **D 65** (2002) 083501 [INSPIRE].

[39] M.R. Setare and R. Mansouri, *Holographic thermodynamic on the brane in topological Reissner-Nordstrom de Sitter space*, *Int. J. Mod. Phys.* **A 18** (2003) 4443 [hep-th/0210252] [INSPIRE].

[40] A.V. Frolov and L. Kofman, *Inflation and de Sitter thermodynamics*, *JCAP* **05** (2003) 009 [hep-th/0212327] [INSPIRE].

JCAP12(2014)037

[41] G. Calcagni, *De Sitter thermodynamics and the braneworld*, *JHEP* **09** (2005) 060 [hep-th/0507125] [INSPIRE].

[42] R. Aros, *De Sitter Thermodynamics: A glimpse into non equilibrium*, *Phys. Rev.* **D 77** (2008) 104013 [arXiv:0801.4591] [INSPIRE].

[43] H. Saida, *De Sitter thermodynamics in the canonical ensemble*, *Prog. Theor. Phys.* **122** (2010) 1239 [arXiv:0908.3041] [INSPIRE].

[44] A. Farmany, *Generalized thermodynamics uncertainty and (anti) de Sitter space*, *Astrophys. Space Sci.* **338** (2012) 401 [INSPIRE].

[45] X. Busch and R. Parentani, *Dispersive fields in de Sitter space and event horizon thermodynamics*, *Phys. Rev.* **D 86** (2012) 104033 [arXiv:1207.5961] [INSPIRE].

[46] J.S. Dowker and R. Critchley, *Effective Lagrangian and Energy Momentum Tensor in de Sitter Space*, *Phys. Rev.* **D 13** (1976) 3224 [INSPIRE].

[47] M.B. Fröb, A. Roura and E. Verdaguer, *One-loop gravitational wave spectrum in de Sitter spacetime*, *JCAP* **08** (2012) 009 [arXiv:1205.3097] [INSPIRE].

[48] P.R. Anderson, W. Eaker, S. Habib, C. Molina-Paris and E. Mottola, *Attractor states and quantum instabilities in de Sitter space*, *Int. J. Theor. Phys.* **40** (2001) 2217 [INSPIRE].

[49] P.R. Anderson and E. Mottola, *On the Instability of Global de Sitter Space to Particle Creation*, *Phys. Rev.* **D 89** (2014) 104038 [arXiv:1310.0030] [INSPIRE].

[50] A. Higuchi and Y.C. Lee, *Conformally-coupled massive scalar field in de Sitter expanding universe with the mass term treated as a perturbation*, *Class. Quant. Grav.* **26** (2009) 135019 [arXiv:0903.3881] [INSPIRE].

[51] D. Krotov and A.M. Polyakov, *Infrared Sensitivity of Unstable Vacua*, *Nucl. Phys.* **B 849** (2011) 410 [arXiv:1012.2107] [INSPIRE].

[52] D. Marolf and I.A. Morrison, *The IR stability of de Sitter: Loop corrections to scalar propagators*, *Phys. Rev.* **D 82** (2010) 105032 [arXiv:1006.0035] [INSPIRE].

[53] D. Marolf and I.A. Morrison, *The IR stability of de Sitter QFT: Physical initial conditions*, *Gen. Rel. Grav.* **43** (2011) 3497 [arXiv:1104.4343] [INSPIRE].

[54] D. Marolf, I.A. Morrison and M. Srednicki, *Perturbative S-matrix for massive scalar fields in global de Sitter space*, *Class. Quant. Grav.* **30** (2013) 155023 [arXiv:1209.6039] [INSPIRE].

[55] R. Bousso, *Adventures in de Sitter space*, in *The Future of Theoretical Physics and Cosmology*, G. Gibbons, P. Shellard and S. Rankin eds., Cambridge University Press, Cambridge, U.K. (2003), pg. 539–569.

[56] T. Mishima and A. Nakayama, *Notes on the Hawking Effect in de Sitter Space*, *Phys. Rev.* **D 37** (1988) 348 [INSPIRE].

[57] A. Nakayama, *Notes on the Hawking Effect in de Sitter Space. II*, *Phys. Rev.* **D 37** (1988) 354 [INSPIRE].

[58] G.E. Volovik, *On de Sitter radiation via quantum tunneling*, *Int. J. Mod. Phys.* **D 18** (2009) 1227 [arXiv:0803.3367] [INSPIRE].

[59] U.H. Danielsson and M.E. Olsson, *On thermalization in de Sitter space*, *JHEP* **03** (2004) 036 [hep-th/0309163] [INSPIRE].

[60] Y. Tian, *De Sitter thermodynamics from diamonds's temperature*, *JHEP* **06** (2005) 045 [gr-qc/0504040] [INSPIRE].

[61] A. Ashtekar and D. Sloan, *Probability of Inflation in Loop Quantum Cosmology*, *Gen. Rel. Grav.* **43** (2011) 3619 [arXiv:1103.2475] [INSPIRE].

JCAP12(2014)037

Part III

Conclusions

Loop quantum gravity is more than 25 years old. It is now a mature theory. Historically, it was based on the Ashtekar's formulation of general relativity. It has since be demonstrated that the theory can be derived in three different ways: canonical quantization of general relativity, covariant quantization of general relativity on a lattice, and a formal quantization of geometrical "shapes". Quite surprisingly, these very different techniques and philosophies converge towards the very same formalism [2]. This is a good point in favor of the reliability and consistency of the model. Of course it also has problems, in particular concerning the way radiative corrections should be handled. In our opinion, the key point is, however, linked with observations and this thesis was therefore devoted to this line of research, in the cosmological sector.

We have first studied the background dynamics. We have shown that inflation not only occurs generically (when the appropriate matter content in assumed) but, more importantly, that the duration of inflation is a product of the model. The bounce lifts up the potential energy to a very precise value, which then determines the length of inflation. In the specific case of a homogenous isotropic universe, with a square potential inflation field, the predicted length of in inflation is around 145 e-folds, which is in agreement with data.

Then, we have considered perturbations. In particular we have focused on the *deformed algebra* approach. We have derived the detailed structure of the algebra of constraints including the two main corrections from loop quantum gravity, *i.e.* the holonomy correction and the inverse-volume correction. From these adjusted constraints the gauge invariant equations of motion for perturbations were obtained.

We then focused on a very important possible consequence of the holonomy correction: the appearance of an Euclidean phase at very high density. We have considered different ways to take this into account. One is to propagate perturbations through this Euclidean period. To this aim, we have regularized the solutions (both for the scalar and for the tensor modes) to the equation of motion in Fourier space. We have also compared these predictions with the ones from a competing approach to loop quantum cosmology called *dressed metric*. Another possibility, that we also investigated, is to put the initial conditions at the silent surface between the Euclidean and Lorentzian passes.

In the case where the perturbations are propagated through the Euclidean region, we get an exponential UV behavior in both tensor and scalar spectrums. This is clearly not compatible with observations. However, this behavior arises exactly when the wavelengths are shorter than the plank length, and we do not know if our model is valid in this regime. This exponential behavior is a result of the Euclidean structure and does therefore, only arise in the deformed algebra approach, and not in the competing dressed metric approach. The signature change causes the amplitudes to increase exponentially instead of oscillating. These results indicate that either our model is not valid for these short wavelengths, or we should not propagate the wave modes through the Euclidean phase in this manner, or possibly both.

In the IR limit, on the other hand, the spectrum is completely frozen during and after the bounce. Here we see the spectrum that was formed during the contraction. All that happens at the bounce, including the signature change, has no effect. For the tensor spectrum this means a flat spectrum, as is expected from a matter dominated contraction. The scalar spectrum, on the other hand, is more complicated due to problems with defining vacuum initial conditions in this model. The resulting IR spectrum for scalar modes are proportional to k^3. However, this part of the spectrum is most probably outside our Hubble horizon now and is therefore unobservable.

There is also an intermediate region which gets its overall shape from slow-roll inflation. However these modes are frozen for a short time at the bounce, then unfrozen and eventually

re-frozen during slow-roll inflation. This freezing and releasing of wave modes causes the amplitudes to oscillate. The resulting spectrum for the intermediate region is therefore the almost flat spectrum of slow-roll inflation modulated with oscillations.

We have also investigated the scenario when initial conditions for the spectrum is placed at the end of the Euclidean region, after the bounce. We call this the silent surface, since the speed of light is zero at this time. At the silent surface every position is decoupled which suggest that the natural initial conditions here are white noise. However this does not naturally lead to the almost flat spectrum necessary to match observations. Because the wave modes are not propagated through the Euclidean in this scenario, the resulting spectrum does not share the problem in the IR limit described above.

In the same paper we also considered an alternative treatment of wavelengths shorter than the plank length. The correct interpretation of LQG might be that there is no quasi-continuum below the Plank length. If we assume that wave modes appear from the quantum foam as the universe grows, and combine this with slow-roll inflation, we do, indeed, get a nice, almost flat, red-tilted spectrum. However, it should be pointed out that having wave modes appearing continuously when they reach plank length, is not a new idea and not specifically tied to LQC [19]. In addition, the specific effects of LQC disappear very quickly after the bounce. If indeed the cosmic structures we observe today where produced in such a way, the bounce is now most likely completely invisible. However, there might be some other observable LQG signatures caused by the exact mechanism of how the perturbations are formed. This needs to be investigated in the future.

Next we have taken into account anisotropies that should play a crucial role at the time of the bounce. We have derived the effective Friedmann equation for Bianci-I LQC and investigated in detail how the amount of cosmic shear affects inflation. We found that higher shear will trigger a bounce at lower matter energy density, which in turn will lead to shorter inflation since there are less potential energy to drive the inflation. This result is problematic, because, on the one hand, we know of no natural upper limit for the amount of shear in a contracting universe and, on the other hand, inflation cannot be too short if it is to explain the observed features of CMB.

In a bouncing cosmology slow-roll inflation is not necessary to solve the horizon problem. However, inflation is the best known theory that produces the observed CMB spectrum. Since there has previously not been any conflict between LQC and inflation, it has been a natural choice to include inflation in our models. However our recent results with anisotropic LQC suggest that the theories might not fit together as well as was previously believed.

What would be the consequence of removing slow-roll inflation from LQC? As we have seen, just including slow-roll inflation in the model does not automatically give the correct observed spectrum. However in some settings LQC does give a spectrum that is compatible with observations (*e.g.* wave modes appearing when they reach plank length and/or dressed metric approach), and in these cases, the resulting spectrums are almost entirely the result of inflation. If these results are to stand we need to find some mechanism to limit the shear.

So far in the the discussion about the anisotropic universe, we have assumed that the initial conditions, for the homogenous variables, should be defined at some time in the far past, in the contracting universe. However one could argue that the initial conditions should be put at the bounce. This could, for example, be motivated by proposing that the bounce is the first moment of the universe from which the universe evolves causally in both directions. In this scenario we don't get growing shear as we approach the bounce, since we never evolve in this direction. This, in a way, solves the inflation problem since it was ultimately caused by the fact that shear

increases in a contracting universe.

However this view results in another problem. If one assigns arbitrary initial conditions at the bounce, the probability that this universe will ever evolve to anything similar to ours is literally infinitesimal. This is, on the other hand, not a problem the far-in-the-past initial condition model, since a classical limit in the contracting past guarantees a classical limit in the expanding future.

We have also considered the implication of invariance under coordinate transformation for a general class of modified gravity. More specifically, we have considered the case of of a homogenous and isotropic, but spatially curved universe. We have found that under some very general assumptions – the most important being: limiting the number gravitational degrees of freedom, allowing for a matter content with constant energy density during a finite amount of time, and that the theory in question should be coordinate independent – the dynamics of a spatially curved universe can be derived from just the dynamics of a spatially flat universe.

This result is of interest for LQC for two reasons. Firstly, it is not obvious how to generalize the scheme used to derive LQC in flat space, to curved space. Secondly, there are several attempts to do this, starting from the loops dynamics, but none of them agrees with our result. This means that either someone is wrong, or LQC does not fulfill the assumptions we used in this investigation.

These conflicting results, together with the strange change of signature found in the deformed algebra approach may suggest that we are not dealing with a metric theory in the way we are used to.

Finally, we have considered an original hypothesis about the possible role played by the cosmological constant for filling the Universe with matter, based on the thermodynamical properties of de Sitter horizons. This may even lead to a cyclic model of geometrical origin.

If we assume that the the acceleration of the expansion of the universe is caused by a true cosmological constant, and if we then follow the dynamics of LQC backwards in time, we will eventually approach a state of de Sitter space, with nothing but the cosmological constant. We propose that once the universe was truly empty (all quantum fields were in their vacuum states) and that all the matter that exists today appeared though the process of horizon radiation. Contraction then compressed this matter until the matter reached approximately plank density, at which time the Universe bounced. We propose that this is the origin of the extremely dense universe which then continued to expand to produce what we see today.

Further, current observations implies that our universe is evolving towards de Sitter space. We believe that in the far future there will be Hubble volume sized patches of the universe that are completely devoid of all matter. In those Hubble volumes there will nothing that physically distinguish expansion from contraction. However, eventually, new matter will be introduced from horizon radiation. We want to point out here that the horizon radiation at this curvature is extremely slow, which is what makes it possible to have a completely empty Hubble volume in the first place. We suggest that this introduction of matter in to void de Sitter space will cause a spontaneous symmetry breaking in to either contraction or expansion. When contraction occurs this will raise the matter density until eventually there is a new big bounce and a new expanding universe is born. And the process goes on.

Of course, many things remain to be done. The Euclidean phase needs to be better understood. The appearance of the Euclidean phase in our model comes ultimately from requiring a closed constraint algebra, which we believe is necessary for consistency. Mathematically the situation is, by now, quite clear, however we do not know how to interpret it physically. Our fist

naive approach was to assume that causality in the Euclidean region could be borrowed from the surrounding regions, however, our results showed that this was probably not the right approach here. Further investigation is needed.

Our results considering anisotropic LQC suggests that the cosmic shear might be a serious problem here. However, the shear will also affect the perturbations more directly. To get a complete picture of the effects of shear in LQC, the evolution of the perturbations need to be explicitly calculated in this setting.

However, I believe that the most important challenge for LQC right now is the treatment of wavelengths close to the plank length. Any version of LQC hinges on this question. We might need to take into account possible modified dispersion relations to account not only for Planck density but also for Planck length effects. Or we might need to abandon our model of Fourier modes all together at this scale. New input from LQG will be needed to solve this problem.

Beyond cosmology there are two other directions in which contact between LQG and observations could be made. One is astroparticle physics. It has been advocated for quite a long time that the discrete structure of space-time should lead to Lorentz invariance violations [20]. Counter-arguments were then given [21]. The situation is currently not very clear and should be investigated in more detail.

Another path is related to black holes. The entropy of black holes seems to be well derived in loop quantum gravity, possibly without fixing the Immirzi parameter [22]. General (loop) quantum gravity arguments tend to suggest that black holes are not really black holes but are bouncing objects [23, 24]. If correct, this new idea might lead to observational signatures that are just at the beginning of being investigated [25, 26, 27].

We remind the reader that the bibliography at the end of this manuscript is quite brief as most useful references are cited directly within the articles where they are used.

Bibliography

[1] M. Bojowald, *Loop quantum cosmology*, *Living Rev. Rel.* **8** (2005) 11, [gr-qc/0601085].

[2] C. Rovelli, *Zakopane lectures on loop gravity*, *PoS* **QGQGS2011** (2011) 003, [arXiv:1102.3660].

[3] F. Cianfrani, J. Kowalski-Glikman, and G. Rosati, *Cyclic universe from Loop Quantum Gravity*, [arXiv:1507.00226].

[4] M. Bojowald, *Absence of singularity in loop quantum cosmology*, *Phys.Rev.Lett.* **86** (2001) 5227–5230, [gr-qc/0102069].

[5] A. Ashtekar, T. Pawlowski, and P. Singh, *Quantum Nature of the Big Bang: Improved dynamics*, *Phys. Rev.* **D74** (2006) 084003, [gr-qc/0607039].

[6] C. Rovelli and E. Wilson-Ewing, *Why are the effective equations of loop quantum cosmology so accurate?*, *Phys. Rev.* **D90** (2014), no. 2 023538, [arXiv:1310.8654].

[7] I. Agullo, A. Ashtekar, and W. Nelson, *The pre-inflationary dynamics of loop quantum cosmology: Confronting quantum gravity with observations*, *Class.Quant.Grav.* **30** (2013) 085014, [arXiv:1302.0254].

[8] I. Agullo, A. Ashtekar, and W. Nelson, *A Quantum Gravity Extension of the Inflationary Scenario*, *Phys. Rev. Lett.* **109** (2012) 251301, [arXiv:1209.1609].

[9] I. Agullo, A. Ashtekar, and W. Nelson, *Extension of the quantum theory of cosmological perturbations to the Planck era*, *Phys. Rev.* **D87** (2013), no. 4 043507, [arXiv:1211.1354].

[10] A. Ashtekar, W. Kaminski, and J. Lewandowski, *Quantum field theory on a cosmological, quantum space-time*, *Phys. Rev.* **D79** (2009) 064030, [arXiv:0901.0933].

[11] A. Ashtekar and P. Singh, *Loop Quantum Cosmology: A Status Report*, *Class. Quant. Grav.* **28** (2011) 213001, [arXiv:1108.0893].

[12] P. Diener, B. Gupt, M. Megevand, and P. Singh, *Numerical evolution of squeezed and non-Gaussian states in loop quantum cosmology*, *Class. Quant. Grav.* **31** (2014) 165006, [arXiv:1406.1486].

[13] A. Ashtekar and D. Sloan, *Probability of Inflation in Loop Quantum Cosmology*, *Gen. Rel. Grav.* **43** (2011) 3619–3655, [arXiv:1103.2475].

[14] J. B. Hartle and S. W. Hawking, *Wave function of the universe*, *Phys. Rev. D* **28** (Dec, 1983) 2960–2975.

[15] E. Wilson-Ewing, *Lattice loop quantum cosmology: scalar perturbations*, *Class. Quant. Grav.* **29** (2012) 215013, [arXiv:1205.3370].

[16] J. Mielczarek, *Signature change in loop quantum cosmology*, *Springer Proc. Phys.* **157** (2014) 555–562, [arXiv:1207.4657].

[17] J. Mielczarek, *Asymptotic silence in loop quantum cosmology*, AIP Conf. Proc.1514,81(2012), [arXiv:1212.3527].

[18] E. Bianchi and C. Rovelli, *Why all these prejudices against a constant?*, [arXiv:1002.3966].

[19] U. H. Danielsson, *A Note on inflation and transPlanckian physics*, *Phys. Rev.* **D66** (2002) 023511, [hep-th/0203198].

[20] G. Amelino-Camelia and T. Piran, *Planck scale deformation of Lorentz symmetry as a solution to the UHECR and the TeV gamma paradoxes*, *Phys. Rev.* **D64** (2001) 036005, [astro-ph/0008107].

[21] C. Rovelli and S. Speziale, *Reconcile Planck scale discreteness and the Lorentz-Fitzgerald contraction*, *Phys. Rev.* **D67** (2003) 064019, [gr-qc/0205108].

[22] D. Oriti, D. Pranzetti, and L. Sindoni, *Horizon entropy from quantum gravity condensates*, [arXiv:1510.06991].

[23] C. Rovelli and F. Vidotto, *Planck stars*, *Int. J. Mod. Phys.* **D23** (2014), no. 12 1442026, [arXiv:1401.6562].

[24] H. M. Haggard and C. Rovelli, *Quantum-gravity effects outside the horizon spark black to white hole tunneling*, *Phys. Rev.* **D92** (2015), no. 10 104020, [arXiv:1407.0989].

[25] A. Barrau and C. Rovelli, *Planck star phenomenology*, *Phys. Lett.* **B739** (2014) 405–409, [arXiv:1404.5821].

[26] A. Barrau, C. Rovelli, and F. Vidotto, *Fast Radio Bursts and White Hole Signals*, *Phys. Rev.* **D90** (2014), no. 12 127503, [arXiv:1409.4031].

[27] A. Barrau, B. Bolliet, F. Vidotto, and C. Weimer, *Phenomenology of bouncing black holes in quantum gravity: a closer look*, [arXiv:1507.05424].

Abstract

Loop quantum gravity (LQG) is an attempt to solve the problem of quantum gravity. Loop quantum cosmology (LQC) is an attempt to apply LQG to early cosmology. The purpose of LQC is to connect LQG with observations. It is very hard to observe any quantum gravity effects because enormous energy density is most likely required. This is exactly why the early Universe is chosen as a stage to search for quantum gravity phenomena.

The central result of LQC is that the big bang singularity is replaced by a big bounce. However this is not something that is possible to observe today. For this reason, we have investigated how cosmic perturbations are affected by LQC. We have used the so called *deformed algebra* approach, and have calculated the resulting spectrums for both scalar and tensor perturbations.

We have also studied the background dynamics (the homogenous part of the equations) of LQC. Since slow-roll inflation is essential in explaining many features of the universe, including the CMB, we want to know if slow-roll inflation is compatible with LQC. We have found that, indeed, it is. If a square potential inflation field is added to the theory, the bounce will lift the potential energy enough to provide around 145 e-folds of slow-roll inflation. However, when anisotropies are taken into account, the amount of inflation decreases, and can even disappear completely if there is too much shear at the time of the bounce.

We have derived the modified Friedman equation for anisotropic LQC. This has allowed us to study anisotropic LQC not just numerically, but also analytically, which has given us a much more comprehensive understanding of the situation than what was known before.

Finally, we have studied some geometric aspects of de Sitter space, which has resulted in two very different considerations. Firstly we found that we can, for a general theory of modified cosmology and under some quite conservative assumptions, derive the dynamics for a spatially curved universe, given the dynamics of a spatially flat one. This is relevant in theories such as LQC, where it is easier to find the flat solution than the curved one. Secondly, we propose a possible mechanism for the origin and rebirth of the Universe.